

REPORT DOCUMENTATION PAGE

Form Approved
OMB No. 0704-0188

Public reporting burden for this collection of information is estimated to average 1 hour per response, including the time for reviewing instructions, searching existing data sources, gathering and maintaining the data needed, and completing and reviewing the collection of information. Send comments regarding this burden estimate or any other aspect of this collection of information, including suggestions for reducing this burden, to Washington Headquarters Services, Directorate for Information Operations and Reports, 1215 Jefferson Davis Highway, Suite 1204, Arlington, VA 22202-4302, and to the Office of Management and Budget, Paperwork Reduction Project (0704-0188), Washington, DC 20503.

1. AGENCY USE ONLY (Leave blank)	2. REPORT DATE 7 July 1995	3. REPORT TYPE AND DATES COVERED Annual, 1 July 94 - 30 June 95
----------------------------------	-------------------------------	--

4. TITLE AND SUBTITLE Stochastic Nonlinear Dynamics of Floating Structures	5. FUNDING NUMBERS G - N0014 - 93 - 1 - 0763
---	---

6. AUTHOR(S) H. Benaroya	
-----------------------------	--

7. PERFORMING ORGANIZATION NAME(S) AND ADDRESS(ES) Rutgers University Dept. of Mechanical and Aerospace Engineering PO Box 909 Piscataway, NJ 08855-0909	8. PERFORMING ORGANIZATION REPORT NUMBER
--	--

9. SPONSORING / MONITORING AGENCY NAME(S) AND ADDRESS(ES) Office of Naval Research Ballston Tower One 800 North Quincy Street Arlington, VA 22217-5660	10. SPONSORING / MONITORING AGENCY REPORT NUMBER
--	--

11. SUPPLEMENTARY NOTES

12a. DISTRIBUTION / AVAILABILITY STATEMENT Approved for public release; distribution is unlimited.	12b. DISTRIBUTION CODE
---	------------------------

13. ABSTRACT (Maximum 200 words)

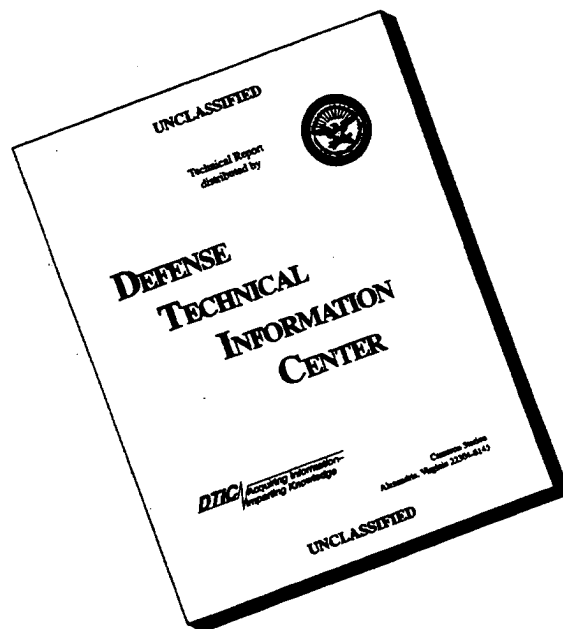
A nonlinear stochastic dynamic model is developed using a variational mechanics formulation for an articulated tower in the ocean. Forcing is due to waves, current and wind. Various response cases are included, such as beating and chaotic.

19960913 112

14. SUBJECT TERMS nonlinear dynamics, offshore structures	15. NUMBER OF PAGES 237
	16. PRICE CODE

17. SECURITY CLASSIFICATION OF REPORT UL	18. SECURITY CLASSIFICATION OF THIS PAGE UL	19. SECURITY CLASSIFICATION OF ABSTRACT UL	20. LIMITATION OF ABSTRACT UL
---	--	---	----------------------------------

DISCLAIMER NOTICE



THIS DOCUMENT IS BEST QUALITY AVAILABLE. THE COPY FURNISHED TO DTIC CONTAINED A SIGNIFICANT NUMBER OF PAGES WHICH DO NOT REPRODUCE LEGIBLY.

THE STATE UNIVERSITY OF NEW JERSEY
RUTGERS
CAMPUS at NEW BRUNSWICK

College of Engineering, Department of Mechanical and Aerospace Engineering
P.O. Box 909, Piscataway, New Jersey 08855-0909
(908) 445-4408 FAX (908) 445-5313 e-mail: benaroya@zodiac.rutgers.edu

Haym Benaroya, Associate Professor
Mechanical and Aerospace Engineering

7 July 1995

Dr. Thomas F. Swean
CODE 3212
Office of Naval Research
Ballston Tower One
800 North Quincy Street
Arlington, Virginia 22217-5660

Dear Tom:

Attached to this letter is the report of our second year's efforts under Grant No: N00014-93-1-0763, entitled: "Stochastic Nonlinear Dynamics of Floating Structures". This work was carried out by me and ONR Grant-supported Graduate Assistant, Patrick Bar-Avi.

Following up on two papers submitted for publication:

1. *Nonlinear Dynamics of an Articulated Tower in the Ocean*, has been accepted for publication by the **Journal of Sound and Vibration**.
2. *The van Kampen Expansion for a Linked Fokker-Planck Equation of a Duffing Oscillator Excited by Colored Noise*, has been accepted for publication by the **Journal of Sound and Vibration**.

Both papers will appear in 1996.

Manuscripts attached to this letter are the following:

1. *Stochastic Response of a Two DOF Articulated Tower*. This was presented at the Puerto Rico Stochastic Dynamics Symposium in January 1995, and is under review for publication in the **Int.J. Nonlinear Mechanics**.

DTIC QUALITY INSPECTED 5

19950710 085

2. *Dynamic Response of an Articulated Tower to Random Wave and Current Loads.* This is a briefer and slightly different version of the above, to be published in the Puerto Rico Proceedings.
3. *Dynamic Response of Offshore Articulated Towers.* This state-of-the-art paper has been submitted for publication to **Applied Mechanics Reviews**.
4. *Response of an Articulated Tower to Loads due to Slamming, Wind, and Coriolis Acceleration.* This paper considers new forces, and was presented at the AIAA Structures and Dynamics Conference (New Orleans Apr 1995). It appeared in a Conference Special Volume. Attached are copies of the overheads used in the presentation.
5. *Response of a Two DOF Articulated Tower to Different Environmental Conditions.* This is the substance of the presentation I made by invitation at the EUROMECH Symposium on Nonlinear Stochastic Dynamics, April 1995. It has been submitted for review for publication in the **Int.J. Nonlinear Mechanics**.

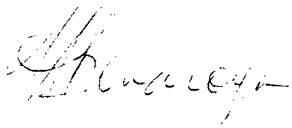
As before our approach to the problem has been, and continues to be, based on an examination of the physics of the environment and its interaction with the structure. This allows us to proceed along a research path that best examines the importance of each force component, each nonlinearity, and helps us decide which terms in our analytical model can be ignored or must be retained. In addition, by going back and forth between analytical model and simulation, we are able to estimate the loss in accuracy resulting from any particular approximation.

It is in this manner that we have proceeded with the work you see before you on the articulated tower. We have explored various behavior regimes, including a chaotic one and a friction damping effect. New forcing has been considered in the second year of our work. I am very pleased with our progress and the level of the analytical modeling that has been achieved. We continue to utilize commercial codes: MAPLE, ACSL, and MATLAB. Patrick is an exceptional graduate student who has worked very hard and very capably. He will complete his doctoral studies next academic year.

As usual, I would be pleased to visit you to provide you with more details, and you are welcome here for a working visit.

Thank you for your interest in our work. Your support is appreciated. Best regards.

Sincerely yours,



Haym Benaroya

cc: Administrative Grants Officer

Director, Naval Research Laboratory

DTIC

Stochastic Response of a Two DOF Articulated Tower

P. Bar-Avi and H. Benaroya

Department of Mechanical and Aerospace Engineering, Rutgers University

Piscataway, N.J. 08855

January 2, 1995

Abstract

In a previous paper [1], the response of an articulated tower in the ocean subjected to deterministic and random wave loading was investigated. The tower was modeled as an upright rigid pendulum with a concentrated mass at the top and having one angular degree of freedom about a hinge with coulomb damping. In this paper, which is an extension of the previous one, the tower is modeled as a spherical pendulum having two angular degrees of freedom. The tower is subjected to wave, current, and vortex shedding loads. Geometrical nonlinearities as well as non-

linearities due to wave drag force, which is assumed be proportional to the square of the relative velocity between the tower and the waves, were considered. The governing coupled differential equations of motion are highly nonlinear, and have time-dependent coefficients. The tower's average response is evaluated for uniformly distributed random fluid constants C_D, C_M, C_L , friction coefficient μ and current direction α . This accomplished computationally via Monte-Carlo simulations with the use of 'ACSL' software. The influence on the tower's response of different parameter values is investigated.

Key words : Articulated tower, Dynamics, Random

1 Introduction

Compliant platforms such as articulated towers are economically attractive for deep water conditions because of their reduced structural weight compared to conventional platforms. The foundation of the tower does not resist lateral forces due to wind, waves and currents; instead, restoring moments are provided by a large buoyancy force, a set of guylines or a combination of both. These structures

have a fundamental frequency well below the wave lower-bound frequency. As a result of the relatively large displacements, geometric nonlinearity is an important consideration in the analysis of such a structure. The analysis and investigation of these kinds of problems can be divided into two major groups: deterministic and random wave and/or current loading. Most workers have considered the tower to be an upright rigid pendulum attached to the sea floor via a pivot having one or two degrees of freedom.

Bar-Avi and Benaroya (1994) [1] investigated the nonlinear response of a single degree of freedom articulated tower. The equation of motion was derived via Lagrange's equation. Nonlinearities due to geometry and wave drag force are considered. A combined wave and current field, coulomb friction force, and vortex shedding force are included in the analysis. The influences on the response of current velocity and direction, significant wave height and frequency, and damping mechanism were analyzed. The response to sub/superharmonics and harmonic excitation demonstrate beating, and for certain excitation frequencies a chaotic behavior was observed. Current has a large influence on the response and on the

equilibrium position of the tower.

Other studies of the response of a single degree of freedom were performed by Chakrabarti and Cotter [2], Gottlieb et al. [7], Muhuri [8], Datta and Jain [9], [10], [11]. Two degree of freedom models were analyzed by Chakrabarti and Cotter [3] and Jain and Kirk (1981) [4]. A detailed description of these studies is given in [1].

Vortex induced oscillation of tension leg platform tethers was analyzed by Dong and Lou 1991 [5], and Dong et. al. 1992 [6]. The tether was modeled as a uniform tension beam under combined action of wave and current. Only the response normal to the direction of the wave and current was considered. A numerical solution was obtained to find the response and to perform stability analysis. They found out that for small drag and lift coefficients the system may become unstable. For moderate drag and lift coefficients multiple equilibrium positions occur, one of them is unstable. The region of multiple solutions, where the response can jump from one branch to the other, is reduced as the drag and/or lift coefficient are increased. When the frequency of excitation was not exactly the fundamental frequency, beating phenomenon was observed, however chaotic mo-

frequency, beating phenomenon was observed, however chaotic motion was not detected.

1.1 New Study

In this paper, the stochastic response of a two degree of freedom articulated tower submerged in the ocean is analyzed. The nonlinear differential equations of motion are derived, including Non-linearities due to geometry, coulomb damping, drag force, added mass, and buoyancy. All forces/moments are evaluated at the instantaneous position of the tower and, therefore, they are not only time-dependent, but also highly nonlinear. The equations are then numerically integrated and Monte-Carlo simulations are performed to evaluate the tower's average response and scatter. Effects of various parameters such as the fluid constants, significant wave height, coulomb and structural damping coefficient, and current direction are then investigated.

2 Problem Description

A schematic of the structure under consideration is shown in Fig. 1. It consists of a tower submerged in the ocean having a concentrated mass at the top and two degrees of freedom; θ about the z axis and ϕ about the x axis. The tower is subjected to wave, current, and vortex shedding loads. As can be seen from Fig. 1, two coordinate systems are used: one fixed x,y,z and the second attached to the tower x',y',z' . All forces/moments, velocities, and accelerations are derived in the fixed coordinate system.

This problem has similarities to that of an inverted spherical pendulum with additional considerations;

- Buoyancy force is included.
- Drag forces proportional to the square of the relative velocity between the fluid and the tower need to be considered.
- Fluid inertia and added mass forces due to fluid and tower acceleration are part of the loading environment.
- Current and vortex shedding forces are considered.

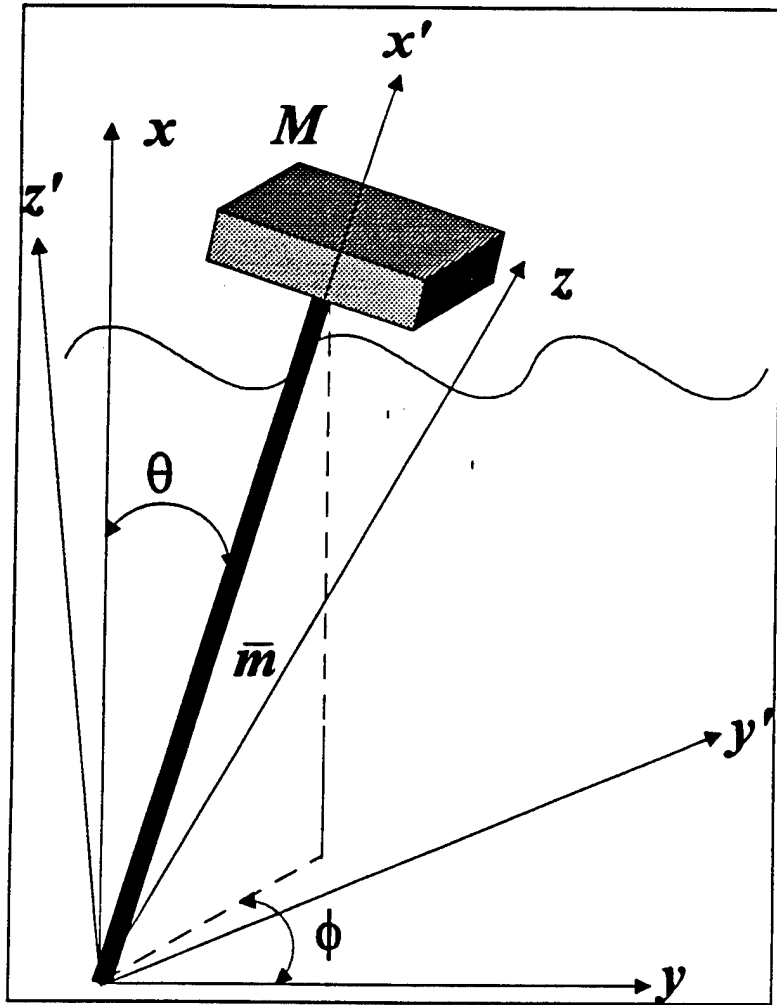


Figure 1: Model and Coordinate Systems

3 Equations of Motion

The equations of motion are derived using Lagrange's equation for large displacements. Certain assumptions have been made and they are listed below.

3.1 Assumption

- The tower stiffness is infinite: $EI = \infty$.
- The hinge consists of coulomb friction.
- The tower has a uniform mass per unit length, \bar{m} and is of length l and diameter D .
- The tower diameter is much smaller than its length, $D \ll l$.
- The tower is a slender smooth structure with uniform cross section.
- The end mass M is considered to be concentrated at the end of the tower.

- The structure is at static stable position due to the buoyancy force.
- The waves are linear having random height.
- Morison's fluid force coefficients C_D , C_M , and C_L are random uniformly distributed parameters.

3.2 Lagrange's Equations

The general form of the Lagrange's equations is

$$\frac{d}{dt} \left(\frac{\partial K_E}{\partial \dot{q}_i} \right) - \frac{\partial K_E}{\partial q_i} + \frac{\partial P_E}{\partial q_i} + \frac{\partial D_E}{\partial \dot{q}_i} = Q_{q_i}, \quad (1)$$

where K_E is the kinetic energy, P_E is the potential energy, D_E is the dissipative energy and Q_{q_i} is the generalized force related to the q_i generalized coordinate.

The model consists of two degrees of freedom, thus, we have two generalized coordinates; θ and ϕ . The generalized forces in the relevant direction are derived using the principle of virtual work. We first derive the general form for the forces assuming an external force per unit length having three components,

$$\mathbf{F}_e = F_x \hat{x} + F_y \hat{y} + F_z \hat{z}. \quad (2)$$

From Fig. 2 we can find the virtual work done by \mathbf{F}_e due to a virtual displacement $\delta\theta$,

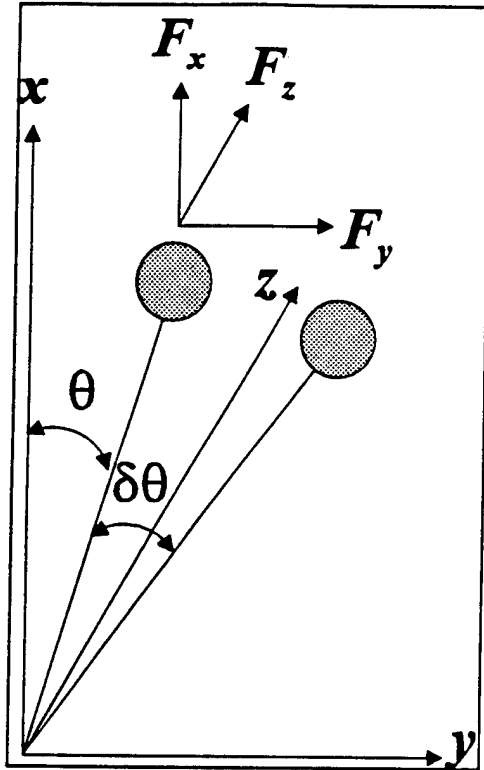


Figure 2: Generalized Force for θ

$$\begin{aligned}
 F_{\theta}\delta\theta &= F_x x' [\cos(\theta + \delta\theta) - \cos\theta] + \\
 &F_y x' \cos\phi [\sin(\theta + \delta\theta) - \sin\theta] + \\
 &F_z x' \sin\phi [\sin(\theta + \delta\theta) - \sin\theta], \quad (3)
 \end{aligned}$$

and using appropriate trigonometric identities we find

$$\begin{aligned}
 F_\theta \delta\theta &= F_x x' [\cos\theta \cos\delta\theta - \sin\theta \sin\delta\theta - \cos\theta] + \\
 &\quad F_y x' \cos\phi [\sin\theta \cos\delta\theta + \cos\theta \sin\delta\theta - \sin\theta] + \\
 &\quad F_z x' \sin\phi [\sin\theta \cos\delta\theta + \cos\theta \sin\delta\theta - \sin\theta], \quad (4)
 \end{aligned}$$

Since we deal with virtual work, we set the virtual displacement $\delta\theta \ll 1$, and replace $x' = \frac{x}{\cos\theta}$, thus, the generalized force per unit length for the θ coordinate is

$$F_\theta = -F_x x \tan\theta + F_y x \cos\phi + F_z x \sin\phi. \quad (5)$$

From Fig. 3 we can find the virtual work done by \mathbf{F}_e due to a virtual displacement $\delta\phi$,

$$\begin{aligned}
 F_\phi \delta\phi &= F_y x' \sin\theta [\cos(\phi + \delta\phi) - \cos\phi] + \\
 &\quad F_z x' \sin\theta [\sin(\phi + \delta\phi) - \sin\phi], \quad (6)
 \end{aligned}$$

and going through the same procedure described for F_θ , we find the generalized force per unit length to be

$$F_\phi = -F_y x \tan\theta \sin\phi + F_z x \tan\theta \cos\phi. \quad (7)$$

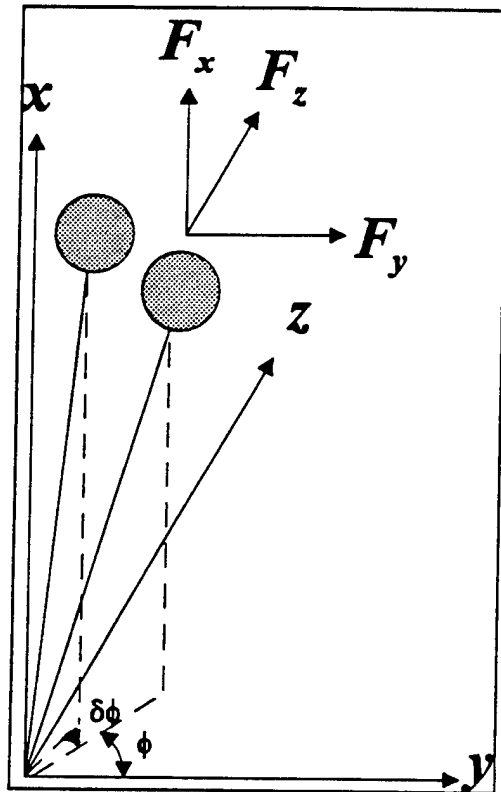


Figure 3: Generalized Force for ϕ

Finally, the generalized moments are evaluated by integrating F_θ and F_ϕ ,

$$M_\theta = \int_0^L (-F_x \tan \theta + F_y \cos \phi + F_z \sin \phi) x dx, \quad (8)$$

and

$$M_\phi = \int_0^L (-F_y \tan \theta \sin \phi + F_z \tan \theta \cos \phi) x dx. \quad (9)$$

where L is the projection in the x direction of the submerged part of the tower. It depends on the angle θ as follows :

$$L = \begin{cases} l \cos \theta & \text{if } d > l \cos \theta \\ d + \eta(y, t) & \text{if } d < l \cos \theta, \end{cases} \quad (10)$$

and $\eta(y, t)$ is the wave height elevation to be defined later.

3.3 Tower, Wave and Current Kinematics

To derive the equations of motion using Lagrange's equations, the kinetic, dissipative, and potential energies need to be evaluated, as well as the generalized forces. In this subsection, the tower's linear and angular absolute velocities and accelerations are determined in the fixed coordinate system x, y, z .

3.3.1 Tower Kinematics

The tower is assumed to be oriented along a unit vector \mathbf{l} with the following directional cosines (see Fig. (1))

$$\mathbf{l} = \cos \theta \hat{x} + \sin \theta \cos \phi \hat{y} + \sin \theta \sin \phi \hat{z} \quad (11)$$

so that the tower's the radius vector \mathbf{R} is

$$\mathbf{R} = x'\mathbf{l} = x' \cos \theta \hat{x} + x' \sin \theta \cos \phi \hat{y} + x' \sin \theta \sin \phi \hat{z}. \quad (12)$$

Its velocity \mathbf{V} , relative to the wave's velocity, is found by taking the time-derivative of the radius vector

$$\begin{aligned} \frac{d\mathbf{R}}{dt} = \mathbf{V} = & -x'\dot{\theta} \sin \theta \hat{x} + x'(\dot{\theta} \cos \theta \cos \phi - \dot{\phi} \sin \theta \sin \phi) \hat{y} + \\ & x'(\dot{\theta} \cos \theta \sin \phi - \dot{\phi} \sin \theta \cos \phi) \hat{z}, \end{aligned} \quad (13)$$

and the acceleration $\dot{\mathbf{V}}$ by taking the time-derivative of the velocity,

$$\begin{aligned} \frac{d\mathbf{V}}{dt} = \dot{\mathbf{V}} = & -x'(\ddot{\theta} \sin \theta + \dot{\theta}^2 \cos \theta) \hat{x} + \\ & x'[\ddot{\theta} \cos \theta \cos \phi - \ddot{\phi} \sin \theta \sin \phi - (\dot{\theta}^2 + \dot{\phi}^2) \sin \theta \cos \phi - 2\dot{\theta}\dot{\phi} \cos \theta \sin \phi] \hat{y} + \\ & x'[\ddot{\theta} \cos \theta \sin \phi + \ddot{\phi} \sin \theta \cos \phi - (\dot{\theta}^2 + \dot{\phi}^2) \sin \theta \sin \phi + 2\dot{\theta}\dot{\phi} \cos \theta \cos \phi] \hat{z}. \end{aligned} \quad (14)$$

Since the equations are derived in the fixed coordinate system x , y , z , we replace $x' = \frac{x}{\cos \theta}$ to find,

$$\mathbf{R} = x \hat{x} + x \tan \theta \cos \phi \hat{y} + x \tan \theta \sin \phi \hat{z}$$

$$\begin{aligned}
\mathbf{V} &= -x\dot{\theta}\tan\theta\hat{x} + x(\dot{\theta}\cos\phi - \dot{\phi}\tan\theta\sin\phi)\hat{y} + x(\dot{\theta}\sin\phi + \dot{\phi}\tan\theta\cos\phi)\hat{z} \\
\dot{\mathbf{V}} &= -x(\ddot{\theta}\tan\theta + \dot{\theta}^2)\hat{x} + \\
&\quad x[\ddot{\theta}\cos\phi - \ddot{\phi}\tan\theta\sin\phi - (\dot{\theta}^2 + \dot{\phi}^2)\tan\theta\cos\phi - 2\dot{\theta}\dot{\phi}\sin\phi]\hat{y} + \\
&\quad x[\ddot{\theta}\sin\phi + \ddot{\phi}\tan\theta\cos\phi - (\dot{\theta}^2 + \dot{\phi}^2)\tan\theta\sin\phi + 2\dot{\theta}\dot{\phi}\cos\phi]\hat{z}. \quad (15)
\end{aligned}$$

Finally, the tower's angular velocity is

$$\Omega = \dot{\phi}\hat{x} + \dot{\theta}\hat{z}. \quad (16)$$

3.3.2 Wave and Current Kinematics

In this study linear wave theory is assumed, therefore, the wave vertical and horizontal velocities are (Wilson [12] pp. 84):

$$\begin{aligned}
w_w &= \frac{1}{2}H\omega\frac{\sinh kx}{\sinh kd}\sin(ky - \omega t) \\
u_w &= \frac{1}{2}H\omega\frac{\cosh kx}{\sinh kd}\cos(ky - \omega t), \quad (17)
\end{aligned}$$

and the respective accelerations:

$$\begin{aligned}
\dot{w}_w &= -\frac{1}{2}H\omega^2\frac{\sinh kx}{\sinh kd}\cos(ky - \omega t) \\
\dot{u}_w &= \frac{1}{2}H\omega^2\frac{\cosh kx}{\sinh kd}\sin(ky - \omega t), \quad (18)
\end{aligned}$$

where H is the significant wave height, ω the wave frequency, k the wave number, and d the mean water level, which are related by

$$\omega^2 = gk \tanh(kd). \quad (19)$$

Without losing generality we assume that the wave propagates in the y direction so that the horizontal velocity u is in that direction, and w is in the x direction. We are aware of the fact that random waves are not unidirectional, but this consideration is out of the scope of this study.

Current velocity magnitude is calculated assuming that the current is made up of two different components (Issacson (1988) [13]): the tidal component, U_c^t , and the wind-induced current U_c^w . If both components are known at the water surface, the vertical distribution of the current velocity $U_c(x)$ may be taken as

$$U_c(x) = U_c^t \left(\frac{x}{d}\right)^{\frac{1}{2}} + U_c^w \left(\frac{x}{d}\right). \quad (20)$$

The tidal current U_c^t at the surface can be obtained directly from the tide table, and the wind-driven current U_c^w at the surface is generally taken as 1 to 5 % of the mean wind speed at 10 m above the surface.

When current and wave coexist, the combined flow field should

be used to determine the wave loads. The influence of an assumed uniform current on the wave field is treated by applying wave theory in a reference frame which is fixed relative to the current. For a current of magnitude U_c propagating in a direction α relative to the direction of the wave propagation, the wave velocity, $c_0 = \frac{\omega n}{k}$ for no current, is modified and becomes

$$\begin{aligned} c &= c_0 + U_c \cos \alpha, \\ \omega &= ck. \end{aligned} \tag{21}$$

The velocities then used to determine the wave loads are the vectorial sum of the wave and current velocities

$$\begin{aligned} w &= w_w \\ u &= u_w + U_c \cos \alpha \\ v &= U_c \sin \alpha, \end{aligned} \tag{22}$$

where u , v and w are the total velocities in x , y and z directions, respectively.

To consider geometric nonlinearities, the velocities and accelerations are evaluated at the instantaneous position of the tower. Replacing $y = x \tan \theta \cos \phi$ in the velocity and acceleration expressions

(equations (22) and (18)) yields velocities,

$$\begin{aligned}
 w &= \frac{1}{2} H \omega \frac{\sinh kx}{\sinh kd} \sin(kx \tan \theta \cos \phi - \omega t) \\
 u &= \frac{1}{2} H \omega \frac{\cosh kx}{\sinh kd} \cos(kx \tan \theta \cos \phi - \omega t) + U_c \cos \alpha \\
 v &= U_c \sin \alpha,
 \end{aligned} \tag{23}$$

and the accelerations

$$\begin{aligned}
 \dot{w} &= \frac{1}{2} H \omega \left(-\omega + \dot{\theta} \frac{kx \cos \phi}{\cos^2 \theta} - \dot{\phi} kx \tan \theta \sin \phi \right) \frac{\sinh kx}{\sinh kd} \cos(kx \tan \theta \cos \phi - \omega t) \\
 \dot{u} &= -\frac{1}{2} H \omega \left(-\omega + \dot{\theta} \frac{kx \cos \phi}{\cos^2 \theta} - \dot{\phi} kx \tan \theta \sin \phi \right) \frac{\cosh kx}{\sinh kd} \sin(kx \tan \theta \cos \phi - \omega t) \\
 \dot{v} &= 0.
 \end{aligned} \tag{24}$$

The influence of current on the wave height depends on the manner in which the waves propagate onto the current field. An approximation to the wave height in the presence of current is given by Isaacson (1988) [13],

$$H = H_0 \sqrt{\frac{2}{\gamma + \gamma^2}}, \tag{25}$$

where H_0 , H are the significant wave heights in the absence and presence of current, respectively, and γ is

$$\gamma = \sqrt{1 + \frac{4U_c}{c_0} \cos \alpha} \quad \text{for} \quad \frac{4U_c}{c_0} \cos \alpha > -1. \tag{26}$$

3.4 Fluid Forces and Moments Acting on the Tower

Fig. 4 depicts the external forces acting on the tower:

1. T_0 is a vertical buoyancy force.
2. F_{ji} are the vertical and horizontal fluid forces due to drag, inertia, added mass and vortex shedding.
3. Mg , $\bar{m}lg$ are the forces due gravity.

We next describe and develop explicit expressions for these forces and moments.

3.4.1 Buoyancy Moment

The buoyancy force provides the restoring moment,

$$M_b = T_0 l_b. \quad (27)$$

T_0 is the buoyancy force, and l_b is its moment arm; both are time-dependent, where

$$T_0 = \rho g V_0 = \rho g \pi \frac{D^2}{4} L_s. \quad (28)$$

V_0 is the volume of the submerged part of the tower, ρ is the fluid density and L_s , which is the length of the submerged part of the tower, is

$$L_s = \frac{d + \eta(y, t)}{\cos \theta}, \quad (29)$$

where $\eta(y, t)$ is the wave height elevation evaluated at the instantaneous position of the tower and at $x = d$ with $y = d \tan \theta$,

$$\eta(\theta, t) = \frac{1}{2} H \cos(kd \tan \theta - \omega t + \varepsilon). \quad (30)$$

The buoyant force acts at the center of mass of the submerged part of the tower. If we consider the tower to be of cylindrical cross-section then the center of mass in the x', y', z' coordinates is

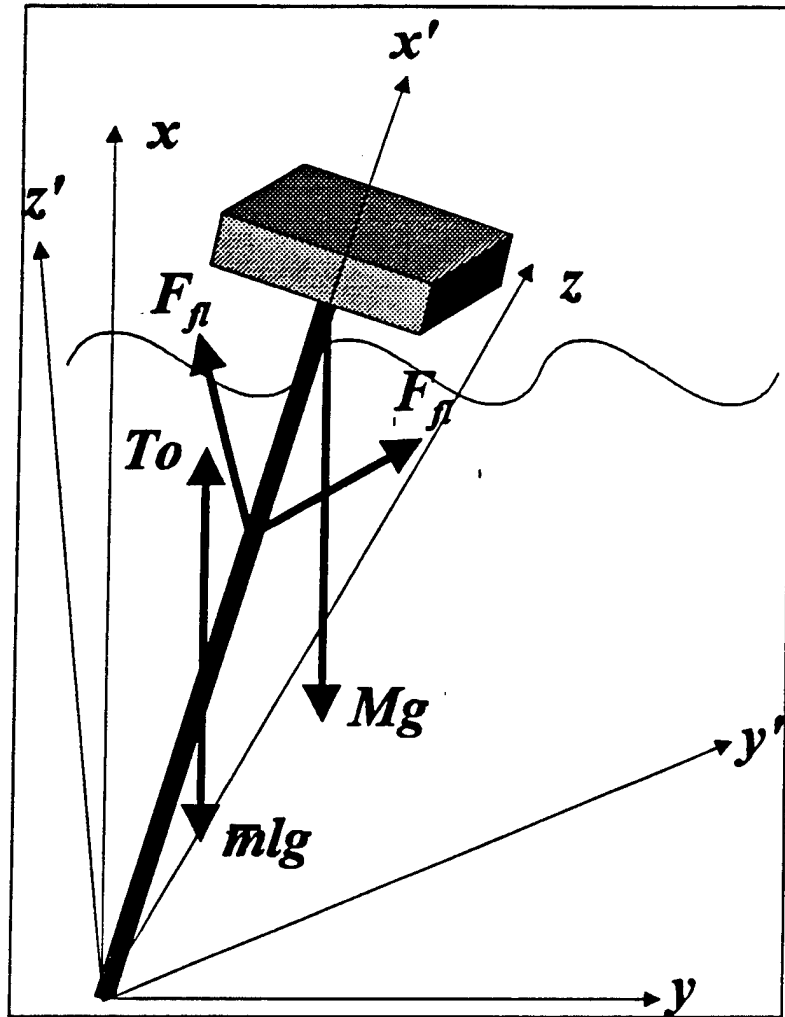


Figure 4: External Forces Acting on the Tower

$$\begin{aligned}
 l_b^{y'} &= \frac{D^2}{16L_s} \tan^2 \theta \\
 l_b^{z'} &= \frac{1}{2}L_s + \frac{D^2}{32L_s} \tan^2 \theta
 \end{aligned}
 \tag{31}$$

Transforming to x, y, z coordinates, we find the moment arm l_b

$$l_b = \frac{D^2}{16L_s} \tan^2 \theta \cos \theta + \left(\frac{1}{2}L_s + \frac{D^2}{32L_s} \tan^2 \theta \right) \sin \theta, \tag{32}$$

and finally the buoyancy generalized moment is then

$$M_b^\theta = \rho g \pi \frac{D^2}{4} \left[\frac{D^2}{32} \tan^2 \theta (2 \cos \theta + \sin \theta) + \frac{1}{2} \left(\frac{d + \eta(y, t)}{\cos \theta} \right)^2 \sin \theta \right]. \tag{33}$$

3.4.2 Wave Forces/Moments

In general, the fluid forces acting on a slender smooth tower are of three types: drag, inertia, and vortex-shedding. In this section these forces are derived.

Drag and Inertia Forces - Morison's Equation The drag and inertia forces per unit length are approximated by Morison's equation. The drag force is proportional to the square of the relative velocity between the fluid and the tower, and the inertia force is proportional

to the fluid acceleration,

$$\mathbf{F}_{fl} = C_D \rho \frac{D}{2} |\mathbf{V}_{rel}| \mathbf{V}_{rel} + C_M \rho \pi \frac{D^2}{4} \dot{\mathbf{U}}_w, \quad (34)$$

where \mathbf{F}_{fl} is the fluid force per unit length normal to the tower. \mathbf{V}_{rel} is the vector of the relative velocity between the fluid and the tower in a direction normal to the tower, and $\dot{\mathbf{U}}_w$ is the fluid acceleration normal to the tower. C_D and C_M are the drag and inertia coefficients, respectively. The relative velocity and fluid acceleration normal to the tower can be decomposed to their components as follows,

$$\begin{bmatrix} V_{rel}^x \\ V_{rel}^y \\ V_{rel}^z \end{bmatrix} = \mathbf{1} \times (\mathbf{U}_w - \mathbf{V}) \times \mathbf{1}$$

$$\begin{bmatrix} \dot{U}_w^x \\ \dot{U}_w^y \\ \dot{U}_w^z \end{bmatrix} = \mathbf{1} \times \dot{\mathbf{U}}_w \times \mathbf{1}. \quad (35)$$

Using Morison's equation (34), the tower velocity equation (15), and fluid velocity and acceleration equations (23), (24), the fluid

force components are the drag force

$$\begin{bmatrix} F_D^x \\ F_D^y \\ F_D^z \end{bmatrix} = C_D \rho \frac{D}{2} \sqrt{(V_{rel}^x)^2 + (V_{rel}^y)^2 + (V_{rel}^z)^2} \begin{bmatrix} V_{rel}^x \\ V_{rel}^y \\ V_{rel}^z \end{bmatrix}, \quad (36)$$

and the inertia force,

$$\begin{bmatrix} F_I^x \\ F_I^y \end{bmatrix} = C_M \rho \pi \frac{D^2}{4} \begin{bmatrix} \dot{w} \\ \dot{u} \end{bmatrix}. \quad (37)$$

Vortex Shedding Moments The lift force F_L due to vortex shedding is acting in a direction normal to the wave velocity vector and normal to the tower. Different models of lift force exist in the literature; see especially Billah (1989) [14]. We will initially use a simple model given in a paper by Dong (1991) [5]

$$\mathbf{F}_L = C_L \rho \frac{D}{2} \cos \omega_s t | \mathbf{1} \times \mathbf{U}_T | (\mathbf{1} \times \mathbf{U}_T), \quad (38)$$

where \mathbf{U}_T , the vector of the maximum fluid velocity along the tower, is

$$\begin{bmatrix} U_T^x \\ U_T^y \\ U_T^z \end{bmatrix} = \begin{bmatrix} \frac{1}{2} H \omega \frac{\sinh kx}{\sinh kd} \\ \frac{1}{2} H \omega \frac{\cosh kx}{\sinh kd} + U_c \cos \alpha \\ U_c \sin \alpha \end{bmatrix}, \quad (39)$$

C_L is the lift coefficient, and ω_s is the vortex shedding frequency (Issacson (1988) [13])

$$C_L = 0.6 \text{ to } 2, \quad \omega_s = 2\omega. \quad (40)$$

Total Fluid Moment The moment due to fluid forces (drag, inertia, and lift) is evaluated by substituting the sum of all fluid forces, defined by equation (41),

$$\begin{aligned} F_{x_{fl}} &= F_D^x + F_I^x + F_L^x \\ F_{y_{fl}} &= F_D^y + F_I^y + F_L^y \\ F_{z_{fl}} &= F_D^z + F_I^z + F_L^z \end{aligned} \quad (41)$$

into equations (8) and (9). Therefore the moments M_{fl}^θ and M_{fl}^ϕ are

$$\begin{aligned} M_{fl}^\theta &= \int_0^L (-F_{fl_x} \tan \theta + F_{fl_y} \cos \phi + F_{fl_z} \sin \phi) x dx \\ M_{fl}^\phi &= \int_0^L (-F_{fl_y} \tan \theta \sin \phi + F_{fl_z} \tan \theta \cos \phi) x dx. \end{aligned} \quad (42)$$

3.4.3 Added Mass Moment

The fluid added mass force per unit length F_{ad} is

$$F_{ad} = C_A \rho \pi \frac{D^2}{4} \dot{V} \quad (43)$$

where $C_A = C_M - 1$ is the added mass coefficient. Substituting the expression for the tower acceleration, equation (15) into equation (43) leads to the expressions for the forces in the x, y, z directions,

$$\begin{aligned} F_{ad}^x &= C_A \rho \pi \frac{D^2}{4} (-x(\ddot{\theta} \tan \theta + \dot{\theta}^2)) \\ F_{ad}^y &= C_A \rho \pi \frac{D^2}{4} (x[\ddot{\theta} \cos \phi - \ddot{\phi} \tan \theta \sin \phi - (\dot{\theta}^2 + \dot{\phi}^2) \tan \theta \cos \phi - 2\dot{\theta}\dot{\phi} \sin \phi]) \\ F_{ad}^z &= C_A \rho \pi \frac{D^2}{4} (x[\ddot{\theta} \sin \phi + \ddot{\phi} \tan \theta \cos \phi - (\dot{\theta}^2 + \dot{\phi}^2) \tan \theta \sin \phi + 2\dot{\theta}\dot{\phi} \cos \phi]) \end{aligned} \quad (44)$$

Substituting the added mass forces (equation (44)) into the generalized moment equations (8) and (9), and integrating, result in the generalized moments due to fluid added mass,

$$\begin{aligned} M_{ad}^\theta &= \frac{1}{12} C_A \rho \pi \frac{D^2}{4} L^3 (\ddot{\theta} (1 + \tan^2 \theta) + \dot{\phi}^2 \tan \theta) \\ M_{ad}^\phi &= \frac{1}{12} C_A \rho \pi \frac{D^2}{4} L^3 (\ddot{\phi} \tan^2 \theta + 2\dot{\theta}\dot{\phi} \tan \theta) \end{aligned} \quad (45)$$

3.4.4 Friction Moment

Dissipation in the tower hinge is assumed to be modeled as coulomb friction. In this section this friction/damping moment is evaluated. The damping force is equal to the product of the normal force N and the coefficient of friction μ . It is assumed to be independent of the velocity, once the motion is initiated. Since the sign of the damping force is always opposite to that of the velocity, the differential equation of motion for each sign is valid only for half cycle intervals. The friction force is

$$\begin{aligned} F_{fr}^\theta &= N\mu[\text{sgn}(\dot{\theta})] \\ F_{fr}^\phi &= N\mu[\text{sgn}(\dot{\phi})]. \end{aligned} \quad (46)$$

The normal force is

$$N = \sum F_x \cos \theta + \sum F_y \cos \phi \sin \theta + \sum F_z \sin \phi \sin \theta, \quad (47)$$

where $\sum F_x$, $\sum F_y$ and $\sum F_z$ are the total forces due to gravity, buoyancy and tower acceleration in the x , y and z directions respectively. The fluid forces; drag, inertia and vortex shedding, do not influence the friction force since they are perpendicular to the tower. Thus,

$$\sum F_x = T_0 - F_g + F_{ac}^x$$

$$\sum F_y = F_{ac}^y \quad (48)$$

$$\sum F_z = F_{ac}^z,$$

where T_0 is the buoyancy force given in equation (33), F_g is the gravitational force,

$$F_g = (\bar{m}l + M)g, \quad (49)$$

and the forces due to the tower acceleration $F_{ac}^x, F_{ac}^y, F_{ac}^z$ are

$$\begin{aligned} F_{ac}^x &= \left[\frac{1}{8} C_A \rho \pi D^2 L^2 + \frac{1}{2} \left(\frac{1}{2} \bar{m}l + M \right) \bar{l} \right] \frac{1}{\cos \theta} (\ddot{\theta} \tan \theta + \dot{\theta}^2) \quad (50) \\ F_{ac}^y &= \left[\frac{1}{8} C_A \rho \pi D^2 L^2 + \frac{1}{2} \left(\frac{1}{2} \bar{m}l + M \right) \bar{l} \right] \frac{1}{\cos \theta} \cdot \\ &\quad \cdot (-\ddot{\theta} \cos \phi + \ddot{\phi} \tan \theta \sin \phi + (\dot{\theta}^2 + \dot{\phi}^2) \tan \theta \cos \phi + 2\dot{\theta}\dot{\phi} \sin \phi) \\ F_{ac}^z &= \left[\frac{1}{8} C_A \rho \pi D^2 L^2 + \frac{1}{2} \left(\frac{1}{2} \bar{m}l + M \right) \bar{l} \right] \frac{1}{\cos \theta} \cdot \\ &\quad \cdot (\ddot{\theta} \cos \phi - \ddot{\phi} \tan \theta \sin \phi - (\dot{\theta}^2 + \dot{\phi}^2) \tan \theta \cos \phi - 2\dot{\theta}\dot{\phi} \sin \phi). \end{aligned}$$

where \bar{l} is the projection of the tower's length l in the x direction,

i.e., $\bar{l} = l \cos \theta$. Assuming a hinge radius R_h , and rearranging

$$\begin{aligned} M_{f_r}^\theta &= R_h N \mu [\text{sgn}(\dot{\theta})] \\ M_{f_r}^\phi &= R_h \sin \theta N \mu [\text{sgn}(\dot{\phi})], \quad (51) \end{aligned}$$

where N , the normal force is

$$N = \left[\frac{1}{8} C_A \rho \pi D^2 \frac{L^2}{\cos^2 \theta} + \frac{1}{2} \left(\frac{1}{2} \bar{m} l + M \right) l \right] (\dot{\theta}^2 + \frac{1}{2} \dot{\phi}^2) - \left[\frac{1}{8} C_A \rho \pi D^2 L^2 + \frac{1}{2} \left(\frac{1}{2} \bar{m} l + M \right) l \cos 2\theta \right] \frac{1}{2} \dot{\phi}^2 + (T_0 - F_g) \cos \theta. \quad (52)$$

We can see that the only terms remaining in the acceleration forces are the centrifugal ones which are along the normal, that is, $l\dot{\theta}^2$.

3.5 Dynamic moments

The dynamic moments M_{dy}^θ , and M_{dy}^ϕ , those which are evaluated in the left hand side of Lagrange's equation (1), are found using expressions for the kinetic, potential, and dissipative energies

$$\begin{aligned} K_E &= \frac{1}{2} (I_x \Omega_x^2 + I_y \Omega_y^2 + I_z \Omega_z^2) \\ P_E &= \left(\frac{1}{2} \bar{m} l + M \right) g l \cos \theta \\ D_E &= \frac{1}{2} C (\Omega_x^2 + \Omega_y^2 + \Omega_z^2), \end{aligned} \quad (53)$$

where C is the structural damping constant and I_x , I_y , I_z are the moments of inertia of the tower, given by

$$I_x = \left(\frac{1}{3} \bar{m} l + M \right) l^2 \sin^2 \theta + \frac{1}{2} (\bar{m} l + M) \frac{D^2}{2} \cos^2 \theta$$

$$\begin{aligned}
I_y &= \left(\frac{1}{3}\bar{m}l + M\right)l^2 \cos^2 \theta + \frac{1}{2}(\bar{m}l + M)\frac{D^2}{2} \sin^2 \theta \\
I_z &= \left(\frac{1}{3}\bar{m}l + M\right)l^2.
\end{aligned} \tag{54}$$

Substituting equations (54) and (16) into (53) leads to the expression for the kinetic and dissipative energies,

$$\begin{aligned}
\mathbf{K_E} &= \frac{1}{2} \left(\left(\frac{1}{3}\bar{m}l + M\right)l^2 \sin^2 \theta + \frac{1}{2}(\bar{m}l + M)\frac{D^2}{2} \cos^2 \theta \right) \dot{\phi}^2 \\
&\quad + \frac{1}{2} \left(\frac{1}{3}\bar{m}l + M\right)l^2 \dot{\theta}^2 \\
\mathbf{D_E} &= \frac{1}{2}C (\dot{\phi}^2 + \dot{\theta}^2).
\end{aligned} \tag{55}$$

Substituting the kinetic, potential and dissipative energies into equation (1) leads, after some mathematical manipulations and rearranging, to M_{dy}^θ , M_{dy}^ϕ

$$\begin{aligned}
M_{dy}^\theta &= \left(\frac{1}{3}\bar{m}l + M\right)l^2 \ddot{\theta} + C\dot{\theta} - \left(\frac{1}{2}\bar{m}l + M\right)gl \sin \theta + \\
&\quad \left(\frac{l^2}{2} \left(\frac{1}{3}\bar{m}l + M\right) - \frac{D^2}{8}(\bar{m}l + M) \right) \dot{\phi}^2 \sin 2\theta \\
M_{dy}^\phi &= \left(\left(\frac{1}{3}\bar{m}l + M\right)l^2 \sin^2 \theta + \frac{1}{4}(\bar{m}l + M)D^2 \cos^2 \theta \right) \ddot{\phi} + C\dot{\phi} + \\
&\quad \left(\frac{l^2}{2} \left(\frac{1}{3}\bar{m}l + M\right) - \frac{D^2}{8}(\bar{m}l + M) \right) \dot{\phi} \dot{\theta} \sin 2\theta.
\end{aligned} \tag{56}$$

3.6 Governing Equations of Motion

The governing nonlinear differential equations of motion are found by equating the dynamic moments to the applied external moments

$$\begin{aligned}M_{dy}^{\theta} &= M_{ap}^{\theta} \\M_{dy}^{\phi} &= M_{ap}^{\phi}.\end{aligned}\quad (57)$$

The applied moments are found by adding equations (33),(42),(45) and (51)

$$\begin{aligned}M_{ap}^{\theta} &= M_b^{\theta} + M_{fl}^{\theta} + M_{fr}^{\theta} - M_{ad}^{\theta} \\M_{ap}^{\phi} &= M_b^{\phi} + M_{fl}^{\phi} + M_{fr}^{\phi} - M_{ad}^{\phi}\end{aligned}\quad (58)$$

Substituting equations (58) and (56) into (57) and rearranging terms leads to the governing nonlinear differential equations of motion for the tower;

$$\begin{aligned}&J_{eff}^{\theta} \ddot{\theta} + C\dot{\theta} + I_g \dot{\phi}^2 + M_{gb}^{\theta} \\&= \int_0^L (-F_{fl_x} \tan \theta + F_{fl_y} \cos \phi + F_{fl_z} \sin \phi) x dx - M_{fr}^{\theta}\end{aligned}$$

(59)

$$\begin{aligned}
& J_{eff}^{\phi} \ddot{\phi} + C \dot{\phi} + I_g \dot{\phi} \dot{\theta} \\
& = \int_0^L \left(-F_{f_{lv}} \tan \theta \sin \phi + F_{f_{lz}} \tan \theta \cos \phi \right) x dx - M_{fr}^{\phi},
\end{aligned}$$

where J_{eff}^{θ} and J_{eff}^{ϕ} are the effective position dependent moments of inertia about z and x axis, respectively

$$\begin{aligned}
J_{eff}^{\theta} & = \left(\frac{1}{3} \bar{m} l + M \right) l^2 + \frac{1}{12} C_A \rho \pi D^2 L^3 (1 + \tan^2 \theta) \\
J_{eff}^{\phi} & = \left(\frac{1}{3} \bar{m} l + M \right) l^2 \sin^2 \theta + \frac{1}{4} (\bar{m} l + M) D^2 \cos^2 \theta + \\
& \quad \frac{1}{12} C_A \rho \pi D^2 L^3 \tan^2 \theta
\end{aligned} \tag{60}$$

I_g is a constant depending on the system parameters,

$$I_g = \left(\frac{l^2}{2} \left(\frac{1}{3} \bar{m} l + M \right) - \frac{D^2}{8} (\bar{m} l + M) \right) \sin 2\theta \tag{61}$$

and M_{gb}^{θ} is the moment due to gravity and buoyancy

$$\begin{aligned}
M_{gb}^{\theta} & = \rho g \pi \frac{D^2}{4} \left[\frac{D^2}{32} \tan^2 \theta (2 \cos \theta + \sin \theta) + \frac{1}{2} \left(\frac{d + \eta(y, t)}{\cos \theta} \right)^2 \sin \theta \right] \\
& \quad - \left(\frac{1}{2} \bar{m} l + M \right) g l \sin \theta.
\end{aligned} \tag{62}$$

4 Monte-Carlo Simulations

In this section, the stochastic response of the tower due to uniformly distributed random parameters, is evaluated utilizing Monte-Carlo simulations. The governing nonlinear differential equation of motion (59) is repeatedly solved using 'ACSL'. At each run different values are assigned to the parameters and the average response is calculated until a convergence is achieved, i.e., the change in the averages between the current and previous runs is less than 1%. The analysis is performed using a PC with a Pentium processor (unbugged). About 20 cycles are needed for the average to converge and each run takes about one hour. The results are then analyzed using 'MATLAB'. The fluid's coefficients, the wave height, and the wave frequency used in the simulations are taken from Hogben et al. 1977 [15]. The following physical parameters are used in the simulation:

Deterministic Physical Parameters

- l - Length of tower = 400 m

- D - Tower diameter = 15 m
- M - End mass = 2.5×10^5 Kg
- m - Tower mass per unit length = 20×10^3 Kg/m
- R_h - Pivot radius = 3 m
- d - Mean water level = 350 m
- ρ - Water density = 1025 Kg/m^3
- ζ - Structural damping = 0.02
- U_c^t, U_c^w - Current velocities = 0.5, 1.5 m/s respectively

Random Parameters

- C_D - Drag coefficient = 0.6 to 2.0
- C_M - Inertia coefficient = 1.4 to 2.0
- C_L - Lift coefficient = 0.6 to 2.0
- H - Significant wave height = 1 to 3 m
- α - Angle between current and wave propagation = $0^\circ \pm 10^\circ$
and $90^\circ \pm 10^\circ$

- μ - Friction coefficient = 0.05 to 0.2

All random parameters are assumed to be uniformly distributed between the limits above. In our study the wave height H is much smaller than the mean water level d , i.e. $H \ll d$. Therefore, the relation between the wave height and the wave frequency, given in Hooft (1981) [16] is used. This relation with the deep water simplification $\tanh kd = 1$, leads to

$$\omega = \sqrt{\frac{\pi}{2H}}, \quad (63)$$

where ω is the wave frequency. The tower's average deflection angles θ_{av} and ϕ_{av} , and their bounds, $\theta_{av} \pm \sigma$ and $\phi_{av} \pm \sigma$, where σ is the standard deviation, are calculated and plotted, for different parameters.

4.1 Random Fluid Parameters

In this run all parameters are kept constant except for the fluid constants C_D, C_M, C_L that were set to be random. First we looked at free vibrations. The wave height is set to zero, and a velocity initial condition on the deflection angle is given, $\dot{\theta}(t = 0) = 0.001$

rad/s. Fig. 5 shows the deflection angle in the time domain (a) and in the frequency domain (b). The parameter that causes a change in the natural frequency is C_M because it is related to the tower's moment of inertia through $C_A = C_M - 1$. The average fundamental frequency is about $\omega_n = 0.026$ Hz.

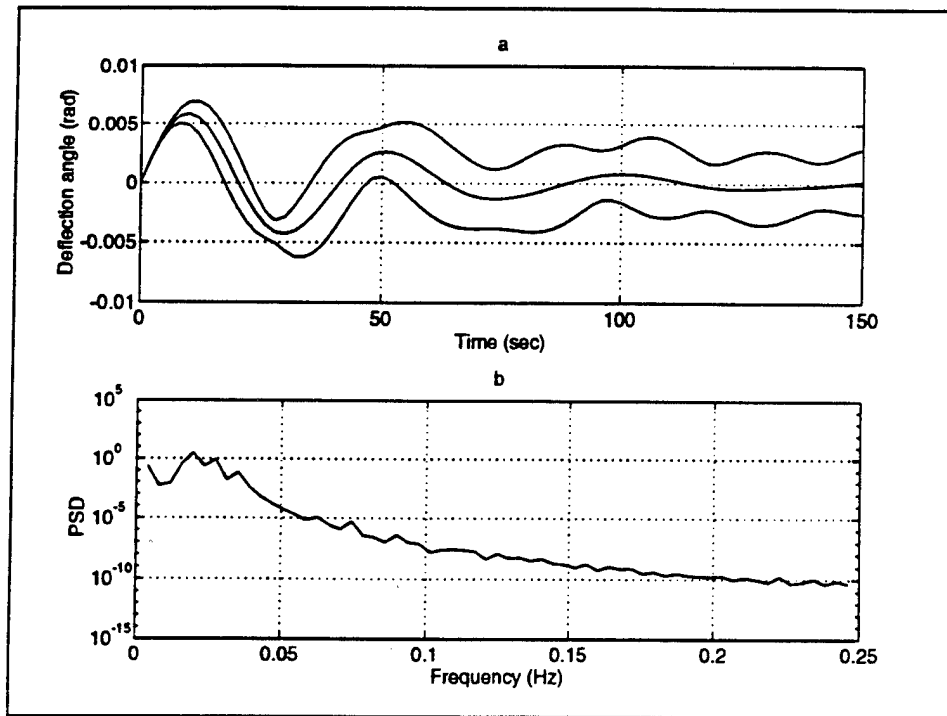


Figure 5: Damped Free Vibration Response. (a) Time Domain, (b) Frequency Domain

Next, waves are included. The wave height is $H = 2$ m, the wave frequency $\omega = 0.5$ rad/s, the coulomb friction coefficient $\mu = 0$, and the current velocity $U_c = 0$. Fig. 6 (a) depicts the average deflection θ_{av} of the tower and its bounds of $\theta_{av} \pm \sigma$, and Fig. 6 (b) depicts the average rotation angle ϕ_{av} and $\phi_{av} \pm \sigma$. From the figure we see that the average steady state deflection θ_{av} is about zero since the current velocity is zero, and it is bounded -0.005 rad $< \theta_{av} < 0.005$ rad. The rotation average angle ϕ_{av} is much larger and grows continuously with time.

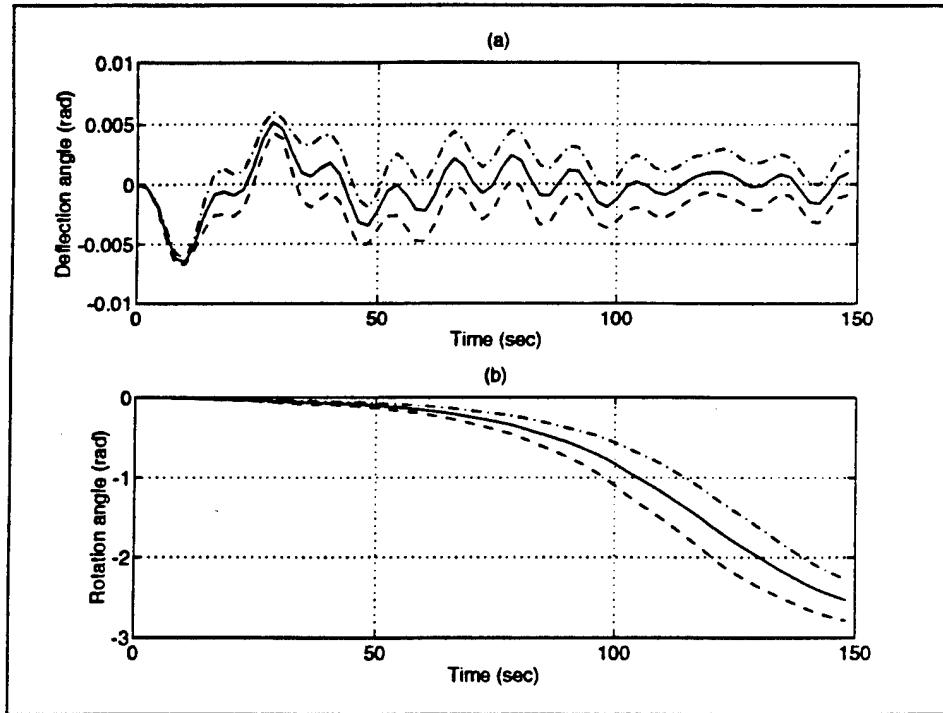


Figure 6: Tower Response to Random Fluid Parameters.(a) Deflection Angle θ_{av} (solid line), $\theta_{av} \pm \sigma$ (dashed line). (b) Rotation Angle ϕ_{av} (solid line), $\phi_{av} \pm \sigma$ (dashed line).

The tower's end displacements in the z and y directions is described in Fig. 7 (a). It can be seen that the displacement in the y direction is larger than the one in the z direction since the wave propagates in this direction. Also we see that the motion is oscillatory about zero position. Fig. 7 (b) shows the displacements (y, z) in the frequency domain.

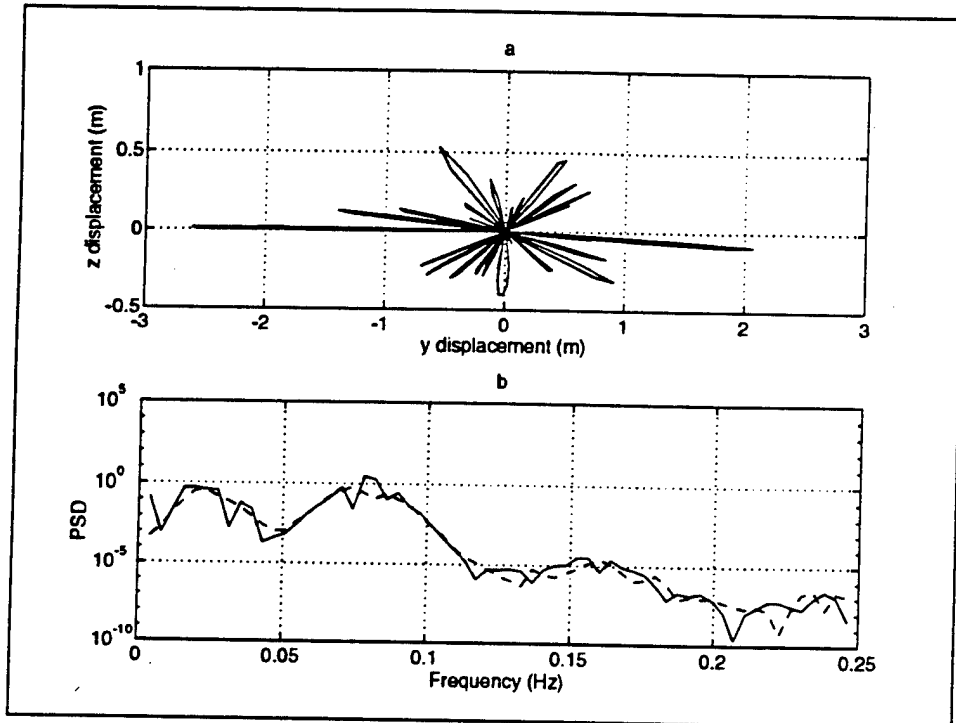


Figure 7: Tower Response to Random Fluid Parameters. (a) Tower's end Displacements. (b) Tower's Response in the frequency Domain; *y*-solid line, *z*-dashed line.

4.2 Influence of Current Direction

The influence of current direction is next investigated. The fluid parameter are constant $C_D = 1.2$, $C_M = 1.5$ and $C_L = 1.0$. All other parameters are the same as in the previous run. Fig. 8 shows the tower's response for current direction is $\alpha = 0^\circ \pm 10^\circ$. It can be seen that both angles oscillate about an equilibrium position which is not zero. The standard deviation of the average rotation angle ϕ_{av} is larger than the average deflection angle θ_{av} , primarily due to the fact that the rotation angle ϕ_{av} can be much larger than the deflection angle.

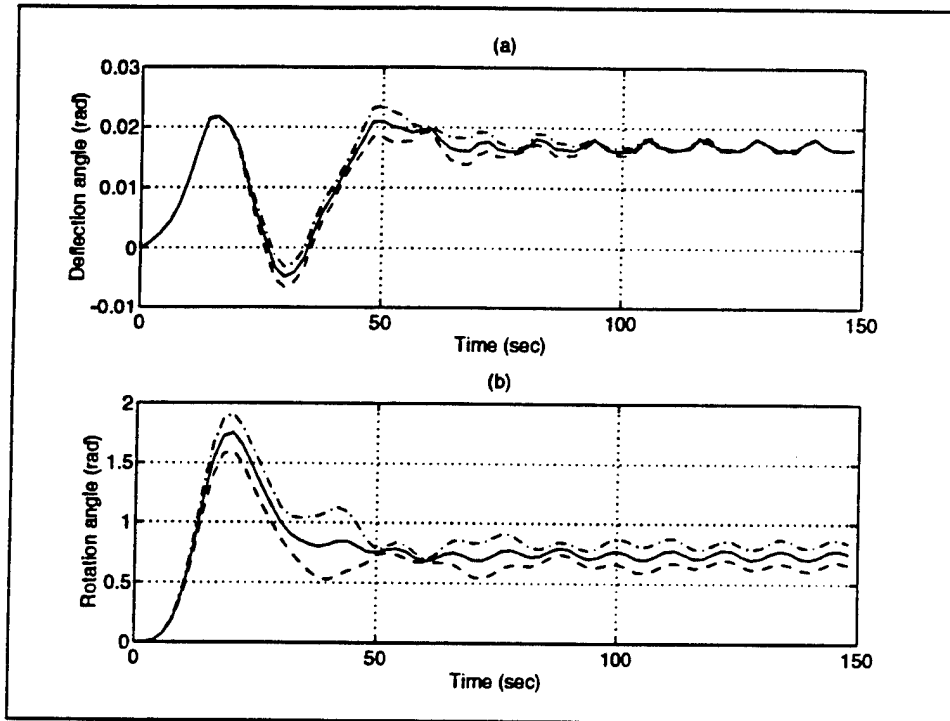


Figure 8: Influence of Current Direction - $\alpha = 0^0 \pm 10^0$. (a) Deflection Angle θ_{av} (solid line), $\theta_{av} \pm \sigma$ (dashed line). (b) Rotation Angle ϕ_{av} (solid line), $\phi_{av} \pm \sigma$ (dashed line).

Fig 9 (a) describes the tower's end displacements, and its frequency response (b). We see the tower's steady state (after the transient decays) motion oscillates about an equilibrium position $(y, z) = (5 \pm 0.5, 4.6 \pm 0.1)$ m. The shift of the equilibrium position is due to current. From the frequency response (b), the wave frequency $\omega = 0.08$ Hz and the vortex-shedding frequency which is $2\omega = 0.16$ Hz are clearly seen.

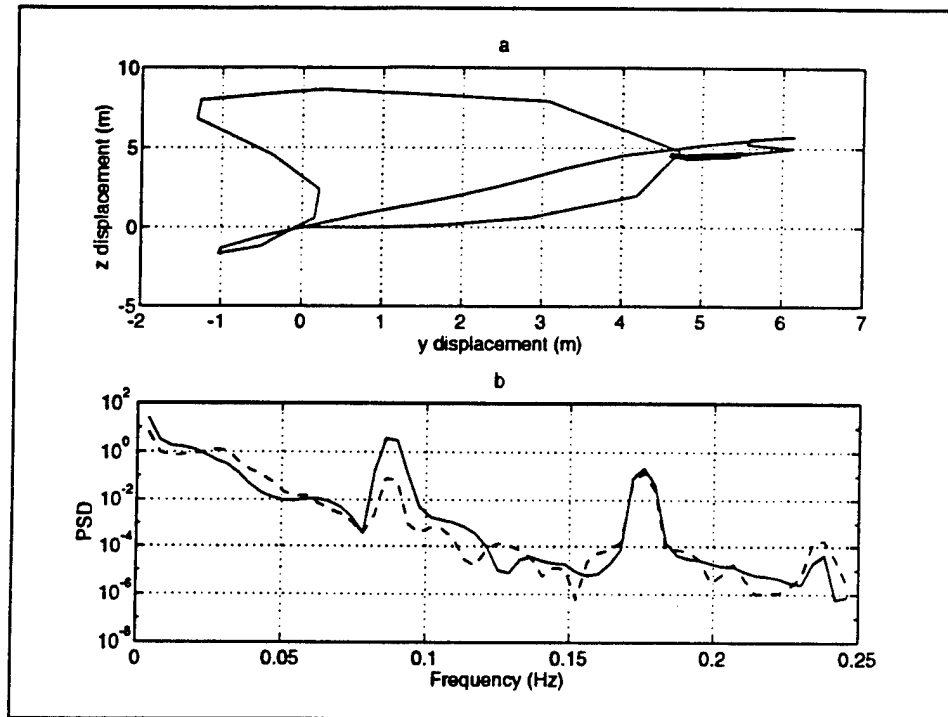


Figure 9: Influence of Current Direction - $\alpha = 0^\circ \pm 10^\circ$. (a) Tower's End Displacements. (b) Tower's Response in the Frequency Domain; *y*-solid line, *z*-dashed line.

The response for $\alpha = 90^\circ \pm 10^\circ$ is shown in Figs. 10 and 11. We see that the tower's steady state response oscillates about an equilibrium position $(y, z) = (-4.5 \pm 0.5, 5.5 \pm 0.2)$ m. The change in the equilibrium position is due to current direction.

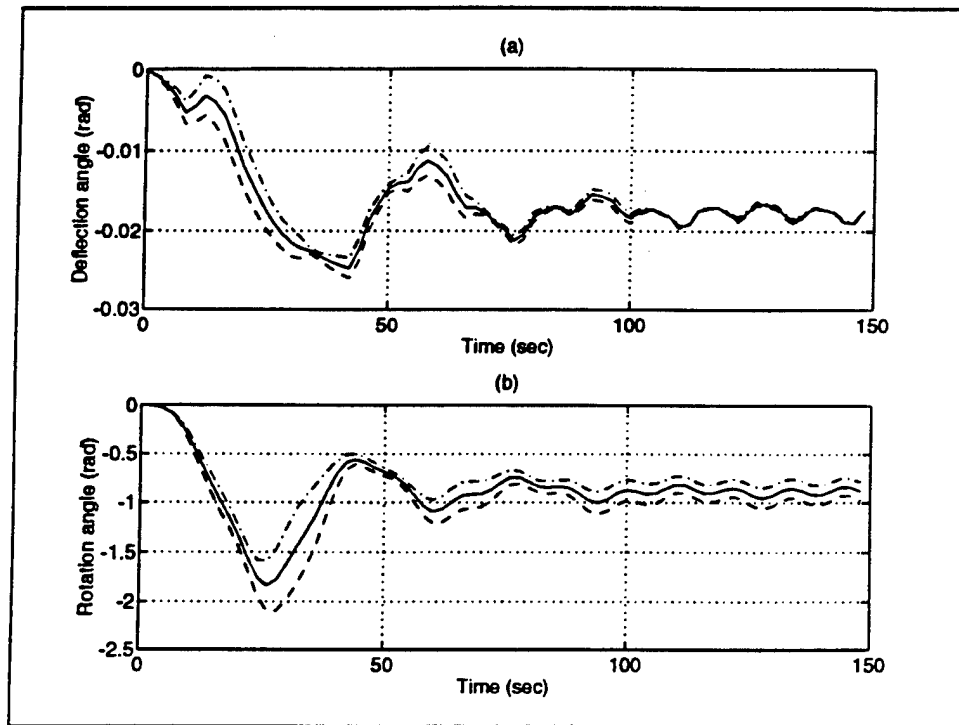


Figure 10: Influence of Current Direction - $\alpha = 90^\circ \pm 10^\circ$. (a) Deflection Angle θ_{av} (solid line), $\theta_{av} \pm \sigma$ (dashed line). (b) Rotation Angle ϕ_{av} (solid line), $\phi_{av} \pm \sigma$ (dashed line).

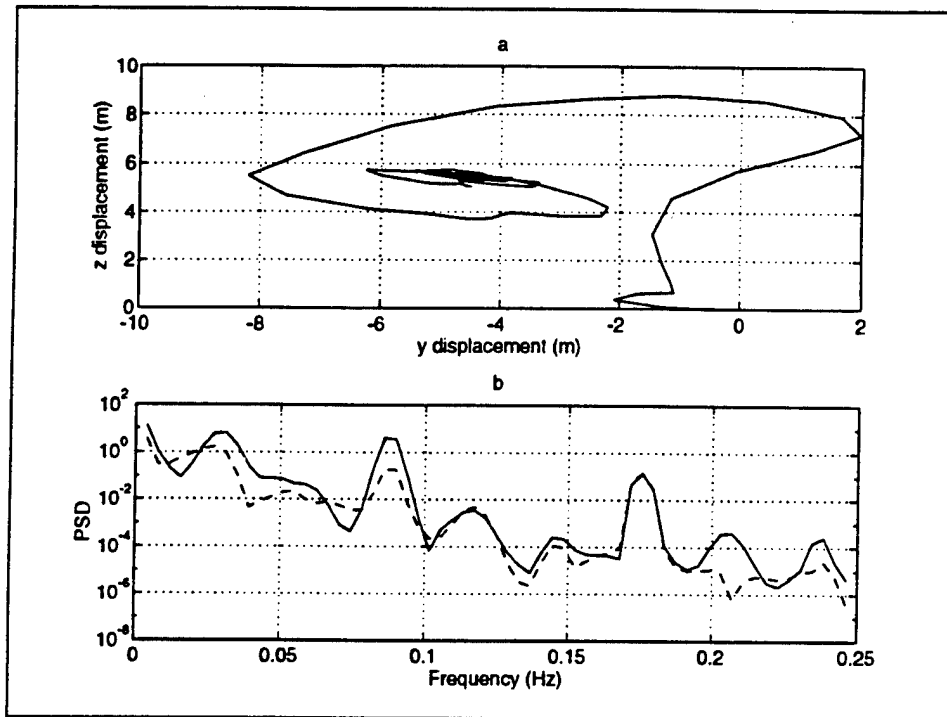


Figure 11: Influence of Current Direction - $\alpha = 90^\circ \pm 10^\circ$. (a) Tower's End Displacements. (b) Tower's Response in the Frequency Domain; *y*-solid line, *z*-dashed line.

Reducing the drag coefficient to $C_D = 0.6$ changes the tower's response as can be observed from Fig. 12. The equilibrium position is different than with $C_D = 1.2$ due to the fact that it depends on $C_D |U_c \cos \alpha| U_c \cos \alpha$ as explained in the paper by Bar-Avi and Benaroya [1].

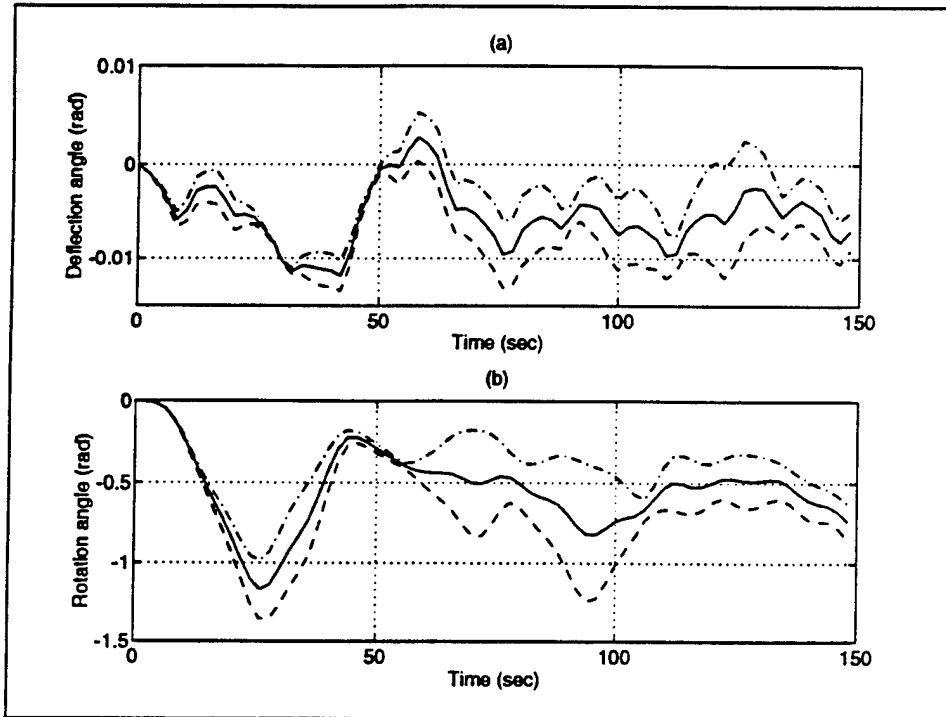


Figure 12: Influence of Current Direction - $\alpha = 0^\circ \pm 10^\circ$. (a) Deflection Angle θ_{av} (solid line), $\theta_{av} \pm \sigma$ (dashed line). (b) Rotation Angle ϕ_{av} (solid line), $\phi_{av} \pm \sigma$ (dashed line).

The influence of current and drag coefficients on the average response is summarized in the next two figures. Fig. 13 (a) depicts the average deflection θ_{av} and Fig. 13 (b) shows the average rotation angle ϕ_{av} for $\alpha = 0^0, 90^0$ with constant drag coefficient $C_D = 1.2$. It can be seen that for $\alpha = 0^0$, the average response $\theta_{av} = 0.02$ rad, and $\phi_{av} = 0.77$, while with $\alpha = 90^0$, $\theta_{av} = -0.02$ rad and $\phi_{av} = -0.85$ rad. The direction of the current velocity causes a change in the direction of the lift force, which results in different equilibrium positions.

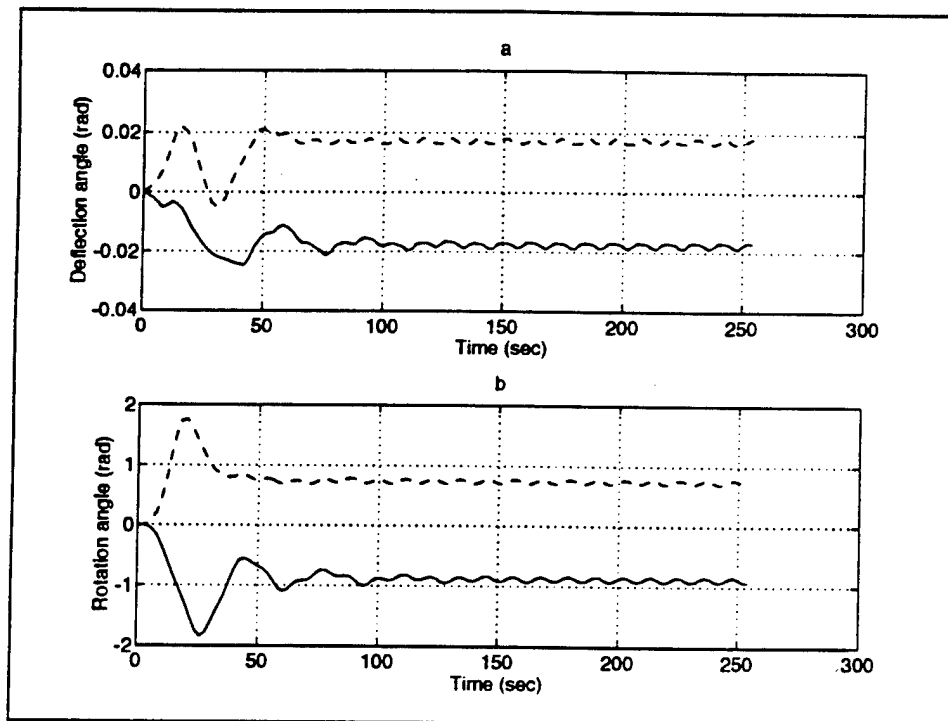


Figure 13: Tower's Average Response for $\alpha = 0^\circ, 90^\circ$ and $C_D = 1.2$. (a) θ_{av} and
 (b) ϕ_{av} with $\alpha = 0^\circ \pm 10^\circ$ dashed line and $\alpha = 90^\circ \pm 10^\circ$ solid line

Fig. 14 (a) depicts the average deflection θ_{av} and Fig. 13 (b) shows the average rotation angle ϕ_{av} for $C_D = 1.2, 0.6$ with $\alpha = 90^\circ$.

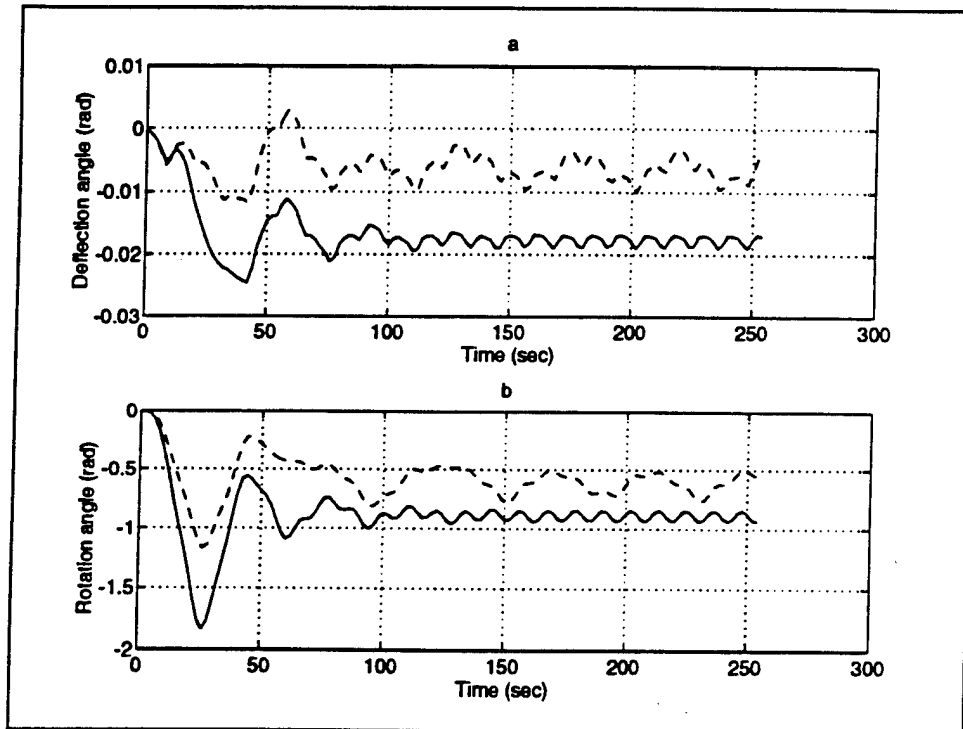


Figure 14: Tower's Average Response for $C_D = 0.6, 1.2$ with $\alpha = 90^\circ$. (a) θ_{av} and (b) ϕ_{av} with $C_D = 0.6$ dashed line and $C_D = 1.2$ solid line

4.3 Coulomb Friction and Wave Height

The influence of coulomb friction on the average steady state response θ_{av} and ϕ_{av} is very small. As can be seen from Fig. 15 the transient response is smaller with friction, but the steady state is the same.

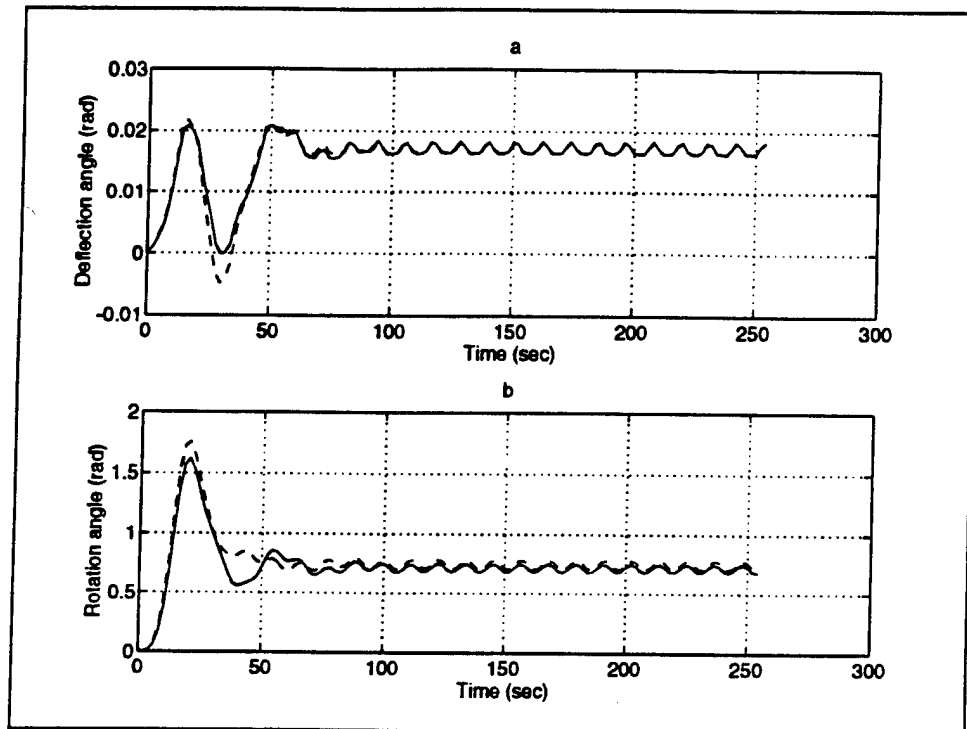


Figure 15: Influence of Coulomb Friction on the Tower's Average Response.

$\mu = 0$ solid line, $\mu = 0.05$ to 0.2 dashed line

Fig. 16 describes the tower's average response θ_{av} and ϕ_{av} due to random wave height in the presence of current. The results are similar to those with constant wave height $H = 2$ m which is the average height in this run.

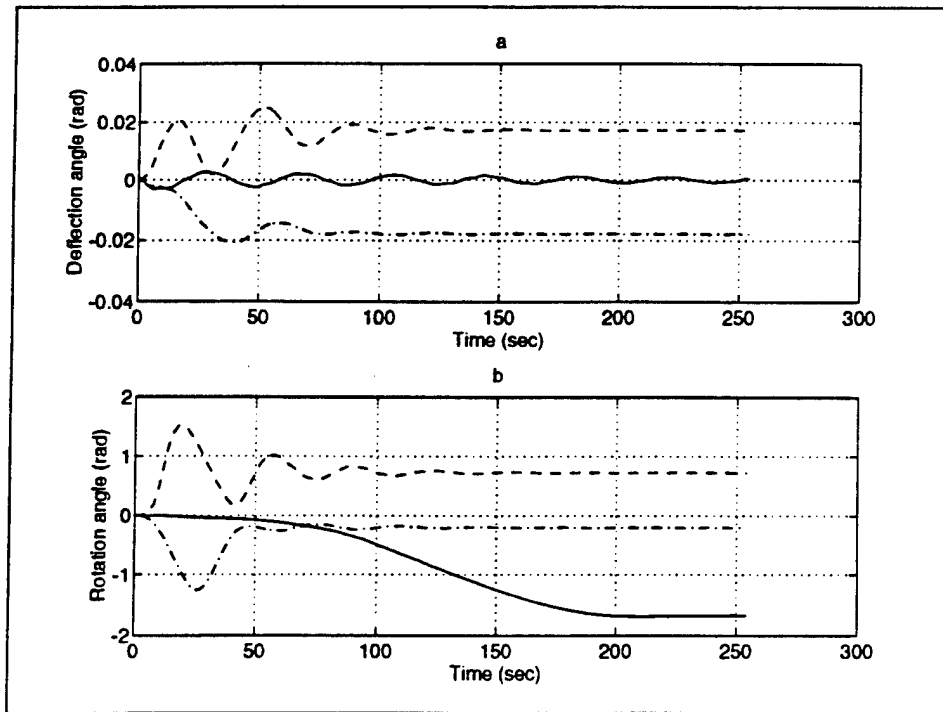


Figure 16: Response (a) θ_{av} and (b) ϕ_{av} in the Presence of Current. $U_c = 0$
 solid line, $\alpha = 0^\circ \pm 10^\circ$ dashed line, and $\alpha = 90^\circ \pm 10^\circ$ dashed-dotted line

Finally, Figs. 17 and 18 describe the tower's response with parameters H, C_D, C_M, C_L, μ modeled as random variables with zero current velocity. Fig. 17 shows θ_{av} and $\theta_{av} \pm \sigma$, and ϕ_{av} and $\phi_{av} \pm \sigma$, while Fig. 18 (a) depicts the tower's end average displacement and Fig. 18 (b) shows the average response in the frequency domain.

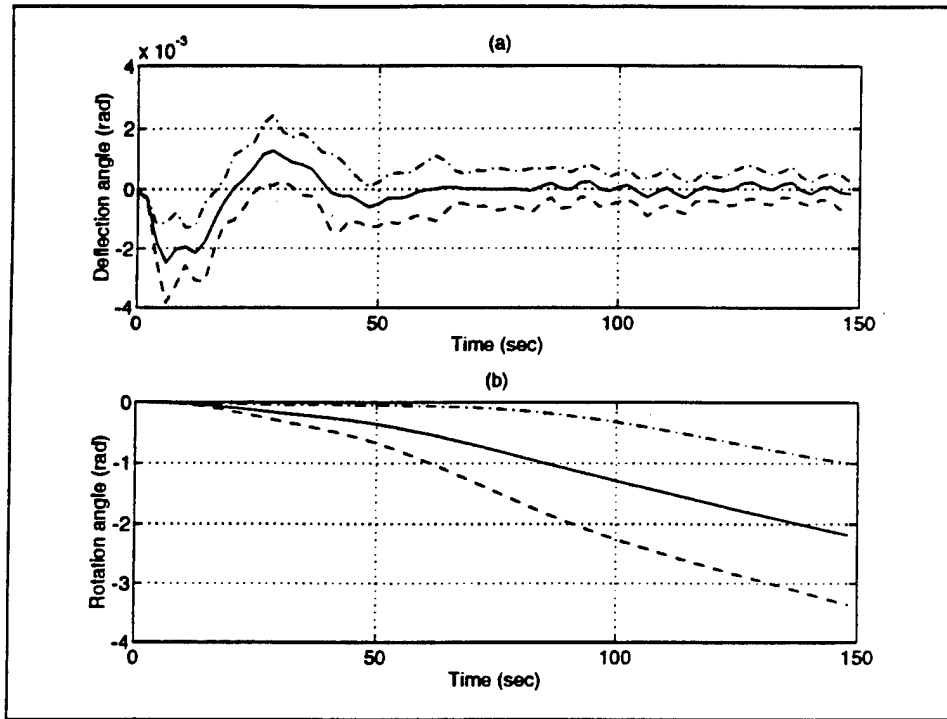


Figure 17: Tower Response to Random Parameters. (a) Deflection Angle θ_{av} (solid line) $\theta_{av} \pm \sigma$ (dashed line). (b) Rotation Angle ϕ_{av} (solid line) $\phi_{av} \pm \sigma$ (dashed line).

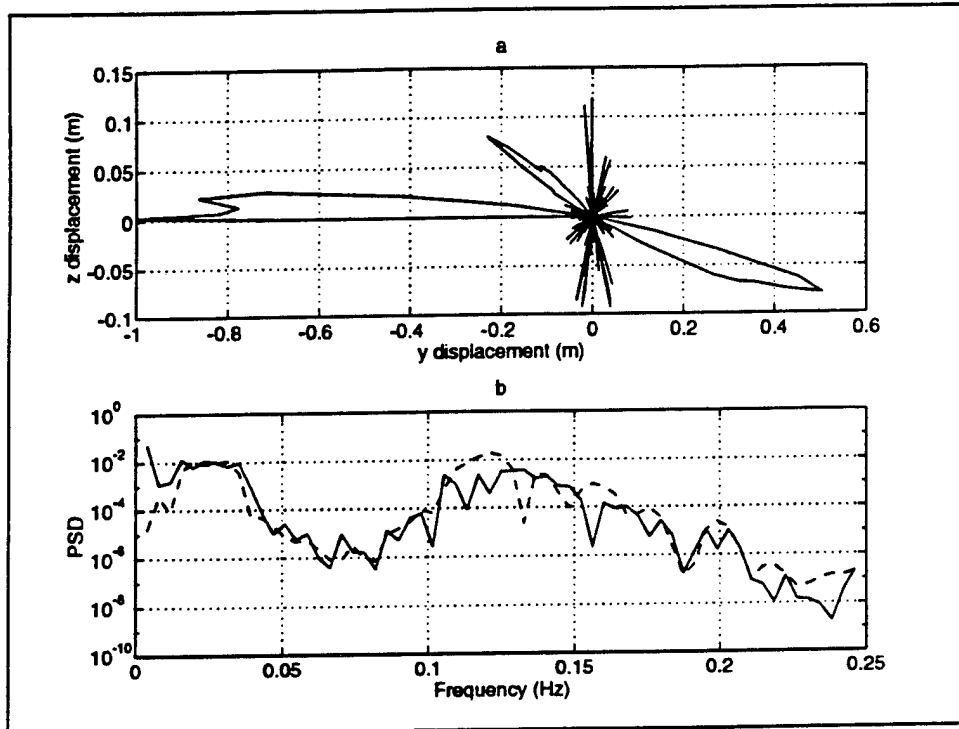


Figure 18: Tower Response to Random Parameters. (a) Tower's End Displacements. (b) Tower's Response in the Frequency Domain; *y*-solid line, *z*-dashed line.

5 Discussion and Summary

The nonlinear differential equations of motion for a two degree of freedom articulated tower submerged in the ocean are derived including coulomb and viscous damping. Geometric and force nonlinearities are included in the derivation. The fluid forces, drag, inertia and lift due to waves and current, are determined at the instantaneous position of the tower. The equations are solved numerically for uniformly distributed random parameters such as, wave height, current direction, fluid coefficients and coulomb friction coefficient. Monte-Carlo simulations are performed, using 'ACSL', to determine the tower's average response and standard deviation.

From the analysis it is found that the standard deviation of the rotation angle ϕ_{av} is larger than that of the deflection angle θ_{av} . The average equilibrium position (θ_{av}, ϕ_{av}) depends on the drag coefficient, and current velocity and direction, $C_D U_c \cos \alpha | U_c \cos \alpha |$. Coulomb friction is found to have a very small effect on the average steady state response, but a larger one on the transient response.

The motion of the tower (sway) oscillates about the equilibrium position.

At the present time the two degree of freedom model with vortex-shedding loads and wave slamming forces coupled to the structure is being analyzed. The response due to wave, current (colinear and otherwise), impact and earth rotation is investigated and results will be published in the near future. Work is also proceeding on an elastic articulated tower.

Acknowledgment

This work is supported by the Office of Naval Research Grant no. N00014 - 93 - 1 - 0763. The authors are grateful for this support from ONR and Program Manager Dr. T. Swain for his interest in our work.

References

- [1] P. Bar-Avi and H. Benaroya. Nonlinear dynamics of an articulated tower submerged in the ocean. *Journal of Sound and Vibration (submitted for publication)*, 1994.

- [2] S.K. Chakrabarti and D.C. Cotter. Motion analysis of articulated tower. *Journal of the Waterway, Port, Coastal and Ocean Division, ASCE*, 105:281 - 292, 1979.
- [3] S.K. Chakrabarti and D.C. Cotter. Transverse motion of articulated tower. *Journal of the Waterway, Port, Coastal and Ocean Division, ASCE*, 107:65 - 77, 1980.
- [4] R.K. Jain and C.L. Kirk. Dynamic response of a double articulated offshore loading structure to noncollinear waves and current. *Journal of Energy Resources Technology*, 103:41 - 47, 1981.
- [5] Y. Dong and J.Y.K. Lou. Vortex-induced nonlinear oscillation of tension leg platform tethers. *Ocean Engineering*, 18(5):451 -464, 1991.
- [6] Y. Dong, G. Xie, and J.Y.K. Lou. Stability of vortex-induced oscillations of tension leg platform tethers. *Ocean Engineering*, 19(6):555 -571, 1992.
- [7] O. Gottlieb, C.S. Yim, and R.T. Hudspeth. Analysis of nonlinear response of an articulated tower. *International Journal of Offshore and Polar Engineering*, 2(1):61 - 66, 1992.
- [8] P.K. Muhuri and A.S. Gupta. Stochastic stability of tethered buoyant platforms. *Ocean Engineering*, 10(6):471 - 479, 1983.
- [9] K. Jain and T.K. Datta. Stochastic response of articulated towers. In *Deep Offshore Technology 4th International Conference and Exhibit*, 1987.

- [10] T.K. Datta and A.K. Jain. Response of articulated tower platforms to random wind and wave forces. *Computers and Structures*, 34(1):137 - 144, 1990.
- [11] A.K. Jain and T.K. Datta. Nonlinear behavior of articulated tower in random sea. *Journal of Engineering for Industry*, 113:238 - 240, 1991.
- [12] J.F. Wilson. *Dynamics of Offshore Structures*. John Wiley and Sons, 1984.
- [13] M. Issacson. Wave and current forces on fixed offshore structure. *Canadian Journal Civil Engineering*, 15:937 - 947, 1988.
- [14] K.Y.R. Billah. *A Study of Vortex-Induced Vibration*. PhD thesis, Princeton University, 1989.
- [15] N. Hogben, B.L. Miller, J.W. Searle, and G. Ward. Estimation of fluid loading on offshore structures. *Proceeding of Civil Engineering*, pages 515-562, 1977.
- [16] J.P. Hooft. *Advanced Dynamics of Marine Structures*. John Wiley and Sons, 1982.
- [17] S.K. Chakrabarti. *Hydrodynamics of Offshore Structures*. Computational Mechanics Publications, 1987.
- [18] M.H. Patel. *Dynamics of Offshore Structures*. Butterworths, 1988.

Dynamic Response of an Articulated Tower to Random Wave and Current Loads

P. Bar-Avi and H. Benaroya
Department of Mechanical and Aerospace Engineering, Rutgers University
Piscataway, N.J. 08855

January 22, 1995

ABSTRACT

In a previous paper [1], the response of an articulated tower in the ocean subjected to deterministic and random wave loading was investigated. The tower was modeled as an upright rigid pendulum with a concentrated mass at the top and having one angular degree of freedom about a hinge with coulomb damping. In this paper, which is an extension of the previous one, the tower is modeled as a spherical pendulum having two angular degrees of freedom. The tower is subjected to wave, current, and vortex shedding loads. Geometrical nonlinearities as well as nonlinearities due to wave drag force, which is assumed be proportional to the square of the relative velocity between the tower and the waves, were considered. The governing coupled differential equations of motion are highly nonlinear, and have time-dependent coefficients. The tower's average response is evaluated for uniformly distributed random fluid constants C_D, C_M, C_L , friction coefficient μ and current direction α . This is accomplished computationally via Monte-Carlo simulations with the use of 'ACSL' software. The influence on the tower's response of different parameter values is investigated.

Key words : Articulated tower, Dynamics, Random

I. INTRODUCTION

Compliant platforms such as articulated towers are economically attractive for deep water conditions because of their reduced structural weight compared to conventional platforms. The foundation of the tower does not resist lateral forces due to wind, waves and currents; instead, restoring moments are provided by a large buoyancy force, a set of guylines or a combination of both. These structures have a fundamental frequency well below the wave lower-bound frequency. As a result of the relatively large displacements, geometric nonlinearity is an important consideration in the analysis of such a structure. The analysis and investigation of these kinds of problems can be divided into two major groups: deterministic and random wave and/or current loading. Most workers have considered the tower to be an upright rigid pendulum attached to the sea floor via a pivot having one or two degrees of freedom.

Bar-Avi and Benaroya (1994) [1] investigated the nonlinear response of a single degree of freedom articulated tower. The equation of motion was derived via Lagrange's equation. Nonlinearities due to geometry and wave drag force are considered. A combined wave and current field, coulomb friction force, and vortex shedding force are included in the analysis. The influences on the response by current velocity and direction, significant wave height and frequency, and damping mechanism were analyzed. The response to sub/superharmonics and harmonic excitation demonstrate beating, and for certain excitation frequencies a chaotic behavior was observed. Current has a large influence on the response and on the equilibrium position of the tower.

Other studies of the response of a single degree of freedom were performed by Chakrabarti and Cotter [2], Gottlieb et al. [3], Muhuri [4], Datta and Jain [5], [6], [7]. Two degree of freedom models were analyzed by Chakrabarti and Cotter [8] and Jain and Kirk (1981) [9]. A detailed description of these studies is given in [1].

In this paper, the stochastic response of a two degree of freedom articulated tower submerged in the ocean is analyzed. The nonlinear differential equations of motion are derived, including nonlinearities due to geometry, coulomb damping, drag force, added mass, and buoyancy. All forces/moments are evaluated at the instantaneous position of the tower and, therefore, they are not only time-dependent, but also highly nonlinear. The equations are then numerically integrated and Monte-Carlo simulations are performed to evaluate the tower's average response and scatter. Effects of various parameters such as the fluid constants, significant wave height, coulomb and structural damping coefficient, and current direction are then investigated.

II. EQUATIONS OF MOTION

A. Problem Description

A schematic of the structure under consideration is shown in Fig. 1. It consists of a tower submerged in the ocean having a concentrated mass at the top and two degrees of freedom; θ about the z axis and ϕ about the x axis. The tower is subjected to wave, current, and vortex shedding loads. As can be seen from Fig. 1, two coordinate systems are used: one fixed x, y, z and the second attached to the tower x', y', z' . All forces/moments, velocities, and accelerations are derived in the fixed coordinate system.

The equations of motion are derived using Lagrange's equation for large displacements. To do so, the kinetic, dissipative, and potential energies need to be evaluated, as well as the generalized forces. A full and detailed derivation can be found in a paper by Bar-Avi and Benaroya [10]. The two generalized moments are derived using the virtual work concept and are given by,

$$M_\theta = \int_0^L (-F_x \tan \theta + F_y \cos \phi + F_z \sin \phi) x dx, \quad (1)$$

and

$$M_\phi = \int_0^L (-F_y \tan \theta \sin \phi + F_z \tan \theta \cos \phi) x dx, \quad (2)$$

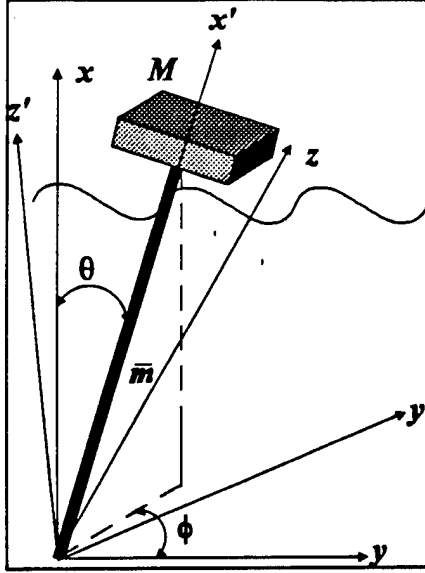


Figure 1: Model and Coordinate Systems

where F_x, F_y, F_z are the external forces in the x, y, z direction and L is the projection in the x direction of the submerged part of the tower. In this study, linear waves combined with uniform current U_c is assumed. The current propagates in a direction α relative to the direction of the wave propagation. Thus, the velocity and acceleration field is expressed at the instantaneous position of the tower (see Wilson [11] pp. 84):

$$\begin{aligned}
 w &= \frac{1}{2} H \omega \frac{\sinh kx}{\sinh kd} \sin(kx \tan \theta \cos \phi - \omega t) \\
 u &= \frac{1}{2} H \omega \frac{\cosh kx}{\sinh kd} \cos(kx \tan \theta \cos \phi - \omega t) + U_c \cos \alpha \\
 v &= U_c \sin \alpha,
 \end{aligned} \tag{3}$$

$$\begin{aligned}
 \dot{w} &= \frac{1}{2} H \omega \left(-\omega + \dot{\theta} \frac{kx \cos \phi}{\cos^2 \theta} - \dot{\phi} kx \tan \theta \sin \phi \right) \frac{\sinh kx}{\sinh kd} \cos(kx \tan \theta \cos \phi - \omega t) \\
 \dot{u} &= -\frac{1}{2} H \omega \left(-\omega + \dot{\theta} \frac{kx \cos \phi}{\cos^2 \theta} - \dot{\phi} kx \tan \theta \sin \phi \right) \frac{\cosh kx}{\sinh kd} \sin(kx \tan \theta \cos \phi - \omega t) \\
 \dot{v} &= 0,
 \end{aligned} \tag{4}$$

where u, v and w are the total velocities in x, y and z directions, respectively. H is the significant wave height, ω the wave frequency, k the wave number, and d the mean water level.

B. External Fluid Forces and Moments Acting on the Tower

The external forces acting on the tower are; buoyancy, fluid force due to drag, inertia, added mass, vortex shedding, gravity and friction.

1. Fluid Forces

In general, the fluid forces acting on a slender smooth tower submerged in the ocean are of four types: drag, inertia, vortex-shedding and wave slamming. The drag and inertia forces per unit length are approximated by Morison's equation. The drag force is proportional to the square of the relative velocity between the fluid and the tower, and the inertia force is proportional to the fluid acceleration,

$$\mathbf{F}_{fl} = C_M \rho \pi \frac{D^2}{4} \mathbf{l} \times \dot{\mathbf{U}}_{\mathbf{w}} \times \mathbf{l} + C_D \rho \frac{D}{2} |\mathbf{l} \times (\mathbf{U}_{\mathbf{w}} - \mathbf{V}) \times \mathbf{l}| (\mathbf{l} \times (\mathbf{U}_{\mathbf{w}} - \mathbf{V}) \times \mathbf{l}), \quad (5)$$

where \mathbf{F}_{fl} is the fluid force per unit length normal to the tower. $\mathbf{U}_{\mathbf{w}}$ is the wave velocity vector, \mathbf{V} is the tower's velocity vector, and $\dot{\mathbf{U}}_{\mathbf{w}}$ is the fluid acceleration vector. C_D and C_M are the drag and inertia coefficients, respectively, D is the tower diameter, ρ is the water density, and \mathbf{l} is a unit vector of the directional cosines along which the tower is oriented. The lift force \mathbf{F}_L due to vortex shedding is acting in a direction normal to the wave velocity vector and normal to the tower. Different models of lift force exist in the literature; see especially Billah [12]. We will initially use a simple model given in a paper by Dong (1991) [13], and Issacson (1988) [14],

$$\mathbf{F}_L = C_L \rho \frac{D}{2} \cos 2\omega t |\mathbf{l} \times \mathbf{U}_T| (\mathbf{l} \times \mathbf{U}_T), \quad (6)$$

where \mathbf{U}_T is the vector of the maximum velocity, along the tower, C_L is the lift coefficient, and ω is the gravity wave frequency.

The moment due to fluid forces due to drag, inertia, and lift M_{fl}^{θ} , M_{fl}^{ϕ} are evaluated via the virtual work principle to be

$$\begin{aligned} M_{fl}^{\theta} &= \int_0^L (-F_{fl_x} \tan \theta + F_{fl_y} \cos \phi + F_{fl_z} \sin \phi) x dx \\ M_{fl}^{\phi} &= \int_0^L (-F_{fl_y} \tan \theta \sin \phi + F_{fl_x} \tan \theta \cos \phi) x dx, \end{aligned} \quad (7)$$

where L is the projection in the x direction of the submerged part of the tower.

2. Additional External Moments

There are three additional moments acting on the tower, these are: buoyancy, added mass, and friction moment. The buoyancy moment is

$$M_b^{\theta} = \rho g \pi \frac{D^2}{4} \left[\frac{D^2}{32} \tan^2 \theta (2 \cos \theta + \sin \theta) + \frac{1}{2} \left(\frac{d + \eta(y, t)}{\cos \theta} \right)^2 \sin \theta \right], \quad (8)$$

where η is the wave height elevation. The added mass moments are

$$\begin{aligned} M_{ad}^{\theta} &= \frac{1}{12} C_A \rho \pi \frac{D^2}{4} L^3 (\ddot{\theta} (1 + \tan^2 \theta) + \dot{\phi}^2 \tan \theta) \\ M_{ad}^{\phi} &= \frac{1}{12} C_A \rho \pi \frac{D^2}{4} L^3 (\ddot{\phi} \tan^2 \theta + 2\dot{\theta} \dot{\phi} \tan \theta), \end{aligned} \quad (9)$$

where $C_A = C_M - 1$ is the added mass coefficient. Finally the coulomb friction moments is

$$\begin{aligned} M_{fr}^{\theta} &= R_h N \mu [\text{sgn}(\dot{\theta})] \\ M_{fr}^{\phi} &= R_h \sin \theta N \mu [\text{sgn}(\dot{\phi})], \end{aligned} \quad (10)$$

where R_h is the hinge radius, and N the normal force given by,

$$N = \left[\frac{1}{8} C_A \rho \pi D^2 \frac{L^2}{\cos^2 \theta} + \frac{1}{2} \left(\frac{1}{2} \bar{m} l + M \right) l \right] (\dot{\theta}^2 + \frac{1}{2} \dot{\phi}^2) - \left[\frac{1}{8} C_A \rho \pi D^2 L^2 + \frac{1}{2} \left(\frac{1}{2} \bar{m} l + M \right) l \cos 2\theta \right] \frac{1}{2} \dot{\phi}^2 + (T_0 - F_g) \cos \theta. \quad (11)$$

C. Governing Equations of Motion

The governing nonlinear differential equations of motion are found by equating the dynamic moments to the applied external moments,

$$J_{eff}^{\theta} \ddot{\theta} + C \dot{\theta} + I_g \dot{\phi}^2 + M_{gb}^{\theta} = \int_0^L (-F_{flz} \tan \theta + F_{flv} \cos \phi + F_{flx} \sin \phi) x dx - M_{fr}^{\theta} \quad (12)$$

$$J_{eff}^{\phi} \ddot{\phi} + C \dot{\phi} + I_g \dot{\phi} \dot{\theta} = \int_0^L (-F_{flv} \tan \theta \sin \phi + F_{flx} \tan \theta \cos \phi) x dx - M_{fr}^{\phi},$$

where J_{eff}^{θ} and J_{eff}^{ϕ} are the effective moments of inertia which are position dependent, I_g is a constant depending on the system parameters, and M_{gb}^{θ} is the moment due to gravity and buoyancy.

III. MONTE-CARLO SIMULATIONS

In this section, the stochastic response of the tower due to uniformly distributed random parameters is evaluated utilizing Monte-Carlo simulations. The governing nonlinear differential equation of motion (13) is repeatedly solved using 'ACSL'. At each run different values are assigned to the parameters and the average response is calculated until a convergence is achieved, i.e., the change in the averages between the current and previous runs is less than 1%. The analysis is performed using a PC with a Pentium processor (unbugged). About 20 cycles are needed for the average to converge and each run takes about one hour. The results are then analyzed using 'MATLAB'. The fluid's coefficients, the wave height, and the wave frequency used in the simulations are taken from Hogben et al. 1977 [15]. The following physical random parameters are used in the simulation: $C_D = 0.6$ to 2.0, $C_M = 1.4$ to 2.0, $C_L = 0.6$ to 2.0, $H = 1$ to 3 m, and $\alpha = 0^\circ \pm 10^\circ$ and $90^\circ \pm 10^\circ$, where at each instance, the random variable is uniformly distributed within the range given. The tower's average deflection angles θ_{av} and ϕ_{av} , and their bounds, $\theta_{av} \pm \sigma$ and $\phi_{av} \pm \sigma$, where σ is the standard deviation, are calculated and plotted, for different parameters.

A. Random Fluid Parameters

In this run all parameters are kept constant except for the fluid constants C_D, C_M, C_L that were set to be random. The wave height is $H = 2$ m, the wave frequency $\omega = 0.5$ rad/s, and the current velocity $U_c = 0$. Fig. 2 (a) depicts the average deflection θ_{av} of the tower and its bounds of $\theta_{av} \pm \sigma$, and Fig. 2 (b) depicts the average rotation angle ϕ_{av} and $\phi_{av} \pm \sigma$. From the figure we see that the average steady state deflection θ_{av} is about zero since the current velocity is zero, and it is bounded $-0.005 \text{ rad} < \theta_{av} < 0.005 \text{ rad}$. The rotation average angle ϕ_{av} is much larger and grows continuously with time, as expected.

The tower's end displacements in the z and y directions are described in Fig. 3 (a). It can be seen that the displacement in the y direction is larger than the one in the z direction since the wave propagates in this direction. Also we see that the motion is oscillatory about zero position. Fig. 3

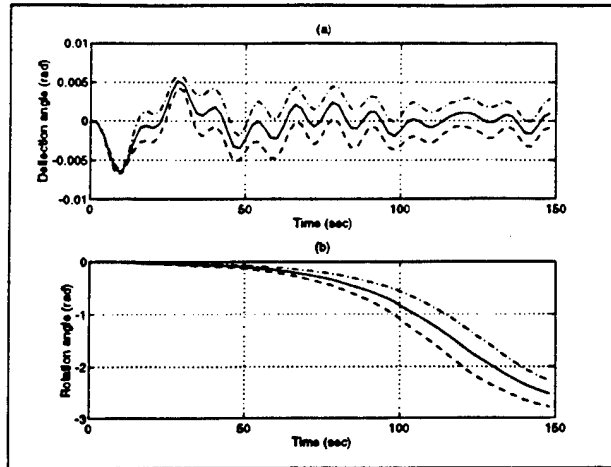


Figure 2: Tower Response to Random Fluid Parameters. (a) Deflection Angle θ_{av} (solid line), $\theta_{av} \pm \sigma$ (dashed line). (b) Rotation Angle ϕ_{av} (solid line), $\phi_{av} \pm \sigma$ (dashed line).

(b) shows the displacements (y, z) in the frequency domain from which the average fundamental frequency $\omega_n = 0.026$ Hz and the excitation frequency $\omega = 0.08$ are seen.

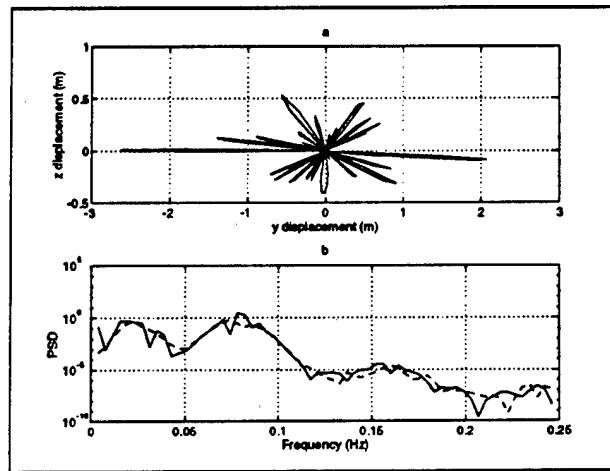


Figure 3: Tower Response to Random Fluid Parameters. (a) Tower's end Displacements. (b) Tower's Response in the frequency Domain; y -solid line, z -dashed line.

B. Influence of Current Direction

The influence of current direction is next investigated. The fluid parameter are constant $C_D = 1.2$, $C_M = 1.5$ and $C_L = 1.0$. All other parameters are the same as in the previous run. Fig. 4 shows the tower's response for current direction $\alpha = 0^\circ \pm 10^\circ$. It can be seen that both angles oscillate about an equilibrium position which is not zero. The standard deviation of the average rotation angle ϕ_{av} is larger than the average deflection angle θ_{av} , primarily due to the fact that the rotation

angle ϕ_{av} can be much larger than the deflection angle.

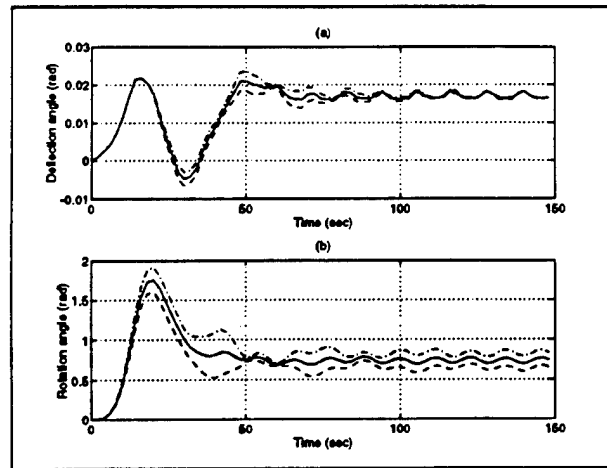


Figure 4: Influence of Current Direction - $\alpha = 0^{\circ} \pm 10^{\circ}$. (a) Deflection Angle θ_{av} (solid line), $\theta_{av} \pm \sigma$ (dashed line). (b) Rotation Angle ϕ_{av} (solid line), $\phi_{av} \pm \sigma$ (dashed line).

The response for $\alpha = 90^{\circ} \pm 10^{\circ}$ is shown in Figs. 5 and 6. We see that the tower's steady state response oscillates about an equilibrium position $(y, z) = (-4.5 \pm 0.5, 5.5 \pm 0.2)$ m. The change in the equilibrium position is due to current direction.

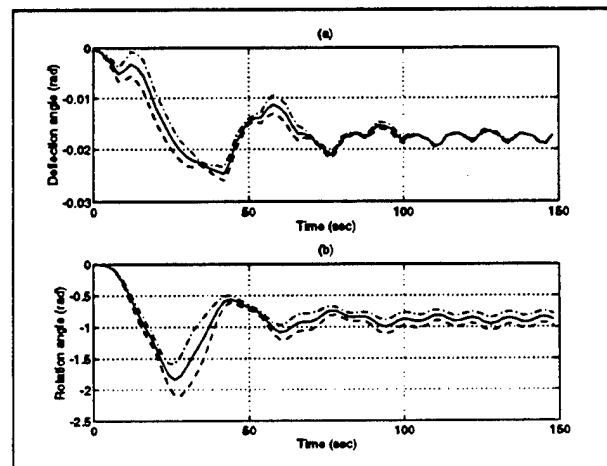


Figure 5: Influence of Current Direction - $\alpha = 90^{\circ} \pm 10^{\circ}$. (a) Deflection Angle θ_{av} (solid line), $\theta_{av} \pm \sigma$ (dashed line). (b) Rotation Angle ϕ_{av} (solid line), $\phi_{av} \pm \sigma$ (dashed line).

The influence of current direction on the average response is summarized in the next figure. Fig. 7 (a) depicts the average deflection θ_{av} and Fig. 7 (b) shows the average rotation angle ϕ_{av} for $\alpha = 0^{\circ}, 90^{\circ}$ with constant drag coefficient $C_D = 1.2$. It can be seen that for $\alpha = 0^{\circ}$, the average response $\theta_{av} = 0.02$ rad, and $\phi_{av} = 0.77$, while with $\alpha = 90^{\circ}$, $\theta_{av} = -0.02$ rad and $\phi_{av} = -0.85$ rad. The direction of the current velocity causes a change in the direction of the lift force, which results in different equilibrium positions.

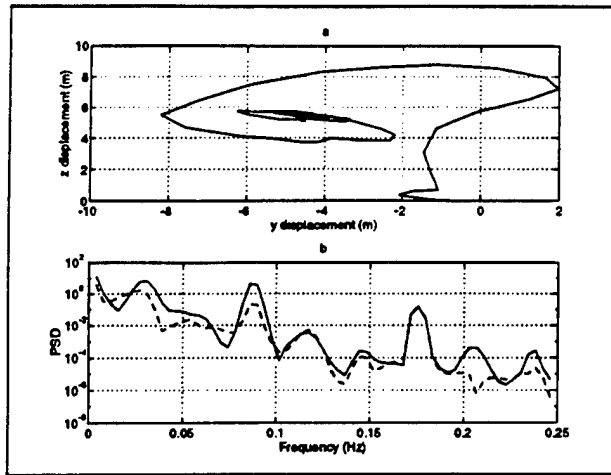


Figure 6: Influence of Current Direction - $\alpha = 90^0 \pm 10^0$. (a) Tower's End Displacements. (b) Tower's Response in the Frequency Domain; y -solid line, z -dashed line.

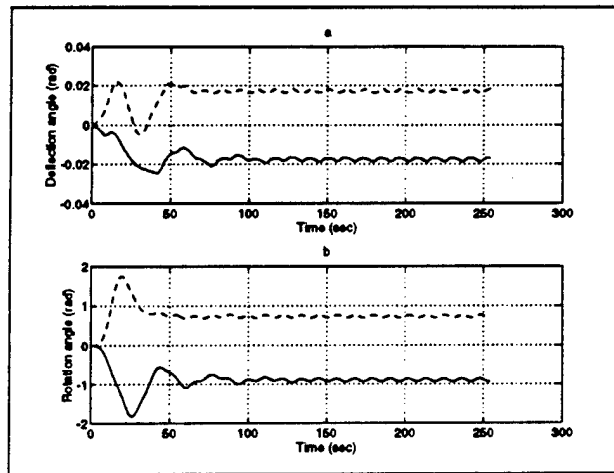


Figure 7: Tower's Average Response for $\alpha = 0^0, 90^0$ and $C_D = 1.2$. (a) θ_{av} and (b) ϕ_{av} with $\alpha = 0^0 \pm 10^0$ dashed line and $\alpha = 90^0 \pm 10^0$ solid line

C. Wave Height

Fig. 8 describes the tower's average response θ_{av} and ϕ_{av} due to random wave height in the presence of current. The results are similar to those with constant wave height $H = 2$ m which is the average height in this run.

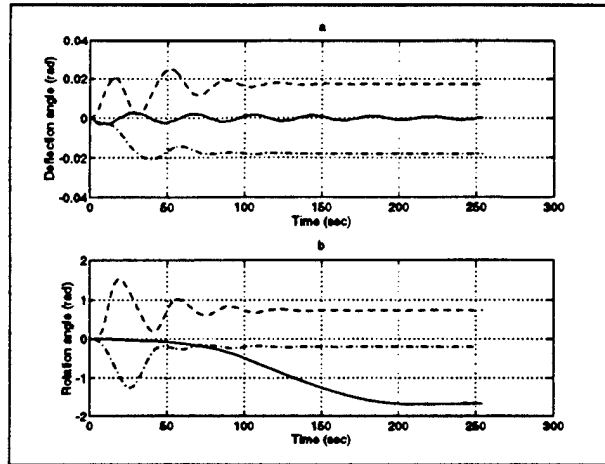


Figure 8: Response (a) θ_{av} and (b) ϕ_{av} in the Presence of Current. $U_c = 0$ solid line, $\alpha = 0^\circ \pm 10^\circ$ dashed line, and $\alpha = 90^\circ \pm 10^\circ$ dashed-dotted line

IV. DISCUSSION AND SUMMARY

The nonlinear differential equations of motion for a two degree of freedom articulated tower submerged in the ocean are derived including coulomb and viscous damping. Geometric and force nonlinearities are included in the derivation. The fluid forces, drag, inertia and lift due to waves and current, are determined at the instantaneous position of the tower. The equations are solved numerically for uniformly distributed random parameters such as wave height, current direction, fluid coefficients and coulomb friction coefficient. Monte-Carlo simulations are performed, using 'ACSL', to determine the tower's average response and standard deviation.

From the analysis it is found that the standard deviation of the rotation angle ϕ_{av} is larger than that of the deflection angle θ_{av} . The average equilibrium position (θ_{av}, ϕ_{av}) depends on the drag coefficient, and current velocity and direction, $C_D U_c \cos \alpha$ or $|U_c \cos \alpha|$. Coulomb friction is found to have a very small effect on the average steady state response, but a larger one on the transient response. The motion of the tower (sway) oscillates about the equilibrium position.

At the present time the two degree of freedom model with vortex-shedding loads and wave slamming forces coupled to the structure is being analyzed. The response due to wave, current (colinear and otherwise), impact and earth rotation is investigated and results will be published in the near future. Work is also proceeding on an elastic articulated tower.

Acknowledgment

This work is supported by the Office of Naval Research Grant no. N00014 - 93 - 1 - 0763. The authors are grateful for this support from ONR and Program Manager Dr. T. Swain for his

interest in our work. This work is part of a research effort which will be submitted by the first author in partial fulfillment of the requirements for a Doctorate.

REFERENCES

- [1] P. Bar-Avi and H. Benaroya. Nonlinear dynamics of an articulated tower submerged in the ocean. *Journal of Sound and Vibration (submitted for publication)*, 1994.
- [2] S.K. Chakrabarti and D.C. Cotter. Motion analysis of articulated tower. *Journal of the Waterway, Port, Coastal and Ocean Division, ASCE*, 105:281 – 292, 1979.
- [3] O. Gottlieb, C.S. Yim, and R.T. Hudspeth. Analysis of nonlinear response of an articulated tower. *International Journal of Offshore and Polar Engineering*, 2(1):61 – 66, 1992.
- [4] P.K. Muhuri and A.S. Gupta. Stochastic stability of tethered buoyant platforms. *Ocean Engineering*, 10(6):471 – 479, 1983.
- [5] K. Jain and T.K. Datta. Stochastic response of articulated towers. In *Deep Offshore Technology 4th International Conference and Exhibit*, 1987.
- [6] T.K. Datta and A.K. Jain. Response of articulated tower platforms to random wind and wave forces. *Computers and Structures*, 34(1):137 – 144, 1990.
- [7] A.K. Jain and T.K. Datta. Nonlinear behavior of articulated tower in random sea. *Journal of Engineering for Industry*, 113:238 – 240, 1991.
- [8] S.K. Chakrabarti and D.C. Cotter. Transverse motion of articulated tower. *Journal of the Waterway, Port, Coastal and Ocean Division, ASCE*, 107:65 – 77, 1980.
- [9] R.K. Jain and C.L. Kirk. Dynamic response of a double articulated offshore loading structure to noncollinear waves and current. *Journal of Energy Resources Technology*, 103:41 – 47, 1981.
- [10] P. Bar-Avi and H. Benaroya. Stochastic response of a two dof articulated tower. *International Journal of Non-linear Mechanics*, 1995 (submitted for publication).
- [11] J.F. Wilson. *Dynamics of Offshore Structures*. John Wiley and Sons, 1984.
- [12] K.Y.R. Billah. *A Study of Vortex-Induced Vibration*. PhD thesis, Princeton University, 1989.
- [13] Y. Dong and J.Y.K. Lou. Vortex-induced nonlinear oscillation of tension leg platform tethers. *Ocean Engineering*, 18(5):451 – 464, 1991.
- [14] M. Issacson. Wave and current forces on fixed offshore structure. *Canadian Journal Civil Engineering*, 15:937 – 947, 1988.
- [15] N. Hogben, B.L. Miller, J.W. Searle, and G. Ward. Estimation of fluid loading on offshore structures. *Proceeding of Civil Engineering*, pages 515–562, 1977.
- [16] S.K. Chakrabarti. *Hydrodynamics of Offshore Structures*. Computational Mechanics Publications, 1987.
- [17] M.H. Patel. *Dynamics of Offshore Structures*. Butterworths, 1988.

Dynamic Response of Offshore Articulated Towers

P. Bar-Avi and H. Benaroya

March, 1995

ABSTRACT

Offshore compliant structures such as guyed platforms, tension leg platforms and articulated towers are economically attractive for deep water conditions because of their reduced structural weight compared to conventional platforms. The foundations of these kinds of structures do not resist lateral environmental loads forces; instead, restoring moments are provided by a large buoyancy force, a set of guylines or a combination of both. These structures have a fundamental frequency well below the ocean wave's lower frequency-bound. As a result of the relatively large displacements, geometric nonlinearity is an important consideration in the analysis of such a structure.

This paper presents a literature review on offshore articulated towers. The review focuses on the static and dynamic response of the tower due to various environmental conditions, such as wind, waves and current. Emphasis is placed on modeling techniques and methods of solution.

I. INTRODUCTION

During the past 15 to 20 years, a need for deep water structures that would exploit energy resources such as oil and carbon has arisen. When deep water combined with hostile weather conditions are considered, conventional fixed offshore structures require excessive dimensions to obtain the stiffness and strength needed, and therefore are very costly. Thus, special deep water platforms called *compliant offshore structures* had to be considered. This kind of structure is flexibly linked to the sea-floor and is free to move with the waves. Since the foundation of the structure cannot resist lateral forces due to waves, current and/or wind, the restoring moment is provided by a large buoyancy force, a set of guylines or a combination of both. The structure's natural frequency is designed to be well below the wave lower frequency-bound in order to avoid resonances. That results in relatively large displacements, and thus geometric nonlinearity is an important consideration in the analysis of such structures. Three types of platforms fall into the category of compliant structures: *guyed tower*, *tension leg platform* and *articulated tower*.

S. Fjeld and S. Flogeland (1980) [1] discussed the feasible applications for each of the different types of structures, and their conclusions are summarized in Table 1.

	Guyed	Tension leg	Articulated
Predrilling	Possible	Possible	Possible
Drilling and production	Possible	Possible	Not feasible
Subsea installation	Feasible	Feasible	Feasible

Table 1: Platform Concepts, Areas of Feasibility

The first type of compliant structure is the guyed tower which is shown in Fig. 1. It consists of a tower connected to the sea-floor via a universal joint. An array of cables restrain the tower to the ocean floor and provides a restoring lateral force to overcome the environmental forces. Many studies have been done on these kind of structures. Among them, Hanna et al. (1983) [2] analyzed the nonlinear dynamics of a guyed tower using a lumped parameter model. Wilson and Orgill (1984) [3] presented a study which deals with the methodology for selecting the parameters for the best cable mooring array. The idea was to find a cable configuration so that the tower's root mean square deflection is minimized. Kanegaonkar and Haldar (1988) [4] investigated the nonlinear random vibration of a guyed tower.

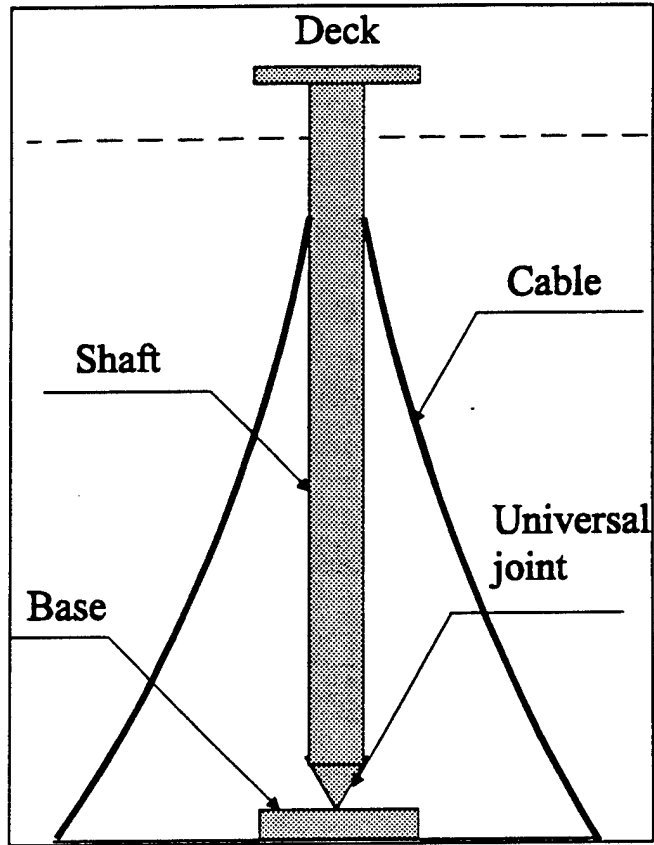


Figure 1: Schematic of a Guyed Tower

The second type of compliant structure is the tension leg platform depicted in Fig. 2. It consists of a platform (deck), which is connected to the sea-floor via several tethers/cables. The cables are pretensioned, and kept in tension through buoyancy that is part of the deck. This structure, as opposed to the guyed tower, cannot be assumed to be a rigid body, and continuous elastic models have to be considered. Many researchers investigated the response of the tension leg platform (TLP). Haritos (1992) [5] studied the response of the TLP, modeled as a lumped mass, to random wave, wind and current. Kareem and Li, (1990) [6] and (1993) [7], investigated the response to wind, wave and current, using the frequency-domain approach. Dong (1992) [8] investigated the response due to vortex shedding. Patel and Park, (1991) [9] and (1992) [10], investigated the dynamic response and stability of a TLP where the cables are in low tension.

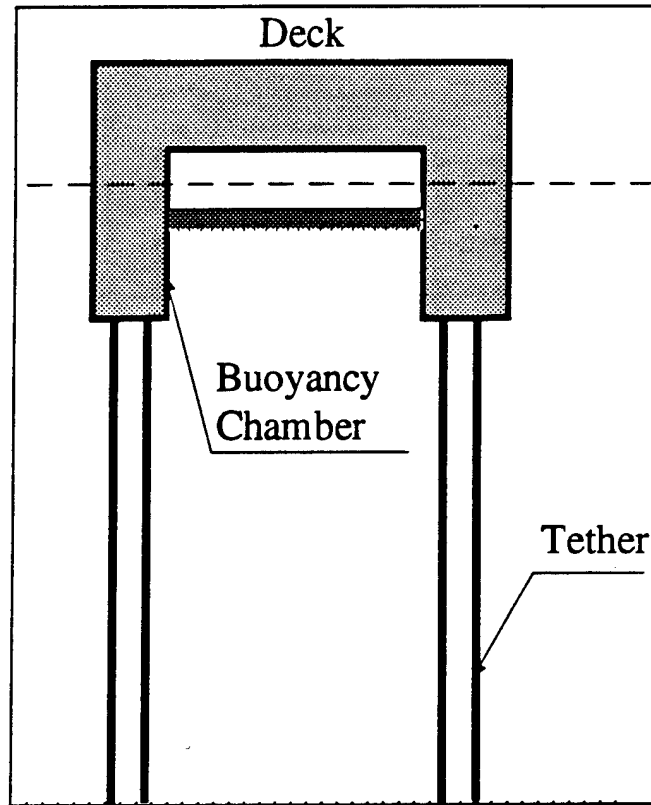


Figure 2: Schematic of a Tension Leg Platform (TLP)

II. ARTICULATED TOWER

This review focuses on the third kind of compliant structure, the *articulated tower*. The articulated tower consists of a vertical column to which a buoyancy chamber is attached near the water surface and to which a ballast is usually added near the bottom. The tower is connected to the sea-floor through a universal joint connected to a base. The tower itself may be either a tubular column or a trussed steel latticework. The structure's fundamental frequency is designed to be well below those wave frequencies with high amplitudes. Articulated towers are typically designed for water depths of 100 to 500 m and are used as single point mooring or as loading terminals, control towers and early and/or full production facilities.

This review is divided into two main sections, one describes the design and construction, and the other discusses the dynamic response.

A. Design and construction

Very few papers discussing the design and construction aspects of articulated towers are found. The first articulated tower ever built was designed in response to an industry call, in 1963, for innovative offshore structures. A full scale experimental structure, for a water depth of 330 feet, was constructed and installed in 1968. The tower remained on site for three years during which time many measurements were done for a wide variety of weather conditions. This experiment demonstrated that the articulated tower concept can be utilized in the offshore industry.

Burns and D'Amorim (1977) [11] discussed the development, design and construction of two articulated towers that provide mooring facilities and house flow lines from subsea equipment to surface facilities. The towers were designed for a water depth of 420 feet. Environmental loads due to waves, current and wind were considered in the evaluation of the tower's dynamic response and the reaction forces in the base. The tower is constructed of the following major parts (see Fig. 3). *Base* - connects the tower to the sea-floor and keeps it from lifting or sliding. *Universal joint* - has two degrees of freedom, one can tilt 30° and the other 90° , so that the tower can be constructed horizontally. It is designed to withstand horizontal loads of 1000 kips, and downward loads of 2000 kips. *Ballast chamber* - it is located above the joint and is 32 feet in diameter. During towing it is pressurized to give buoyancy, but it is flooded when installed. *Shaft* - its diameter is 18 feet. It connects the ballast and the buoyancy chamber and it is full of water during service. *Buoyancy chamber* - the 32 feet in diameter chamber provides the vertical force that keeps the tower upright.

Hays et al. (1979) [12] discussed the operation of an articulated oil loading tower in the North Sea at a water depth of 400 feet. The reasons for selecting the articulated tower concept were simplicity of design, that it could remain as an unmanned facility during loading operations, its superior underwater reliability and motion characteristics. The structure consists of a steel body which oscillates about a universal joint connected to the sea-floor via a concrete ballast. The head of the tower rotates, so when a tanker is moored to the tower, the orientation of the head is determined by the weather conditions. The tower was built and tested and, according to the authors, it fulfilled their expectations.

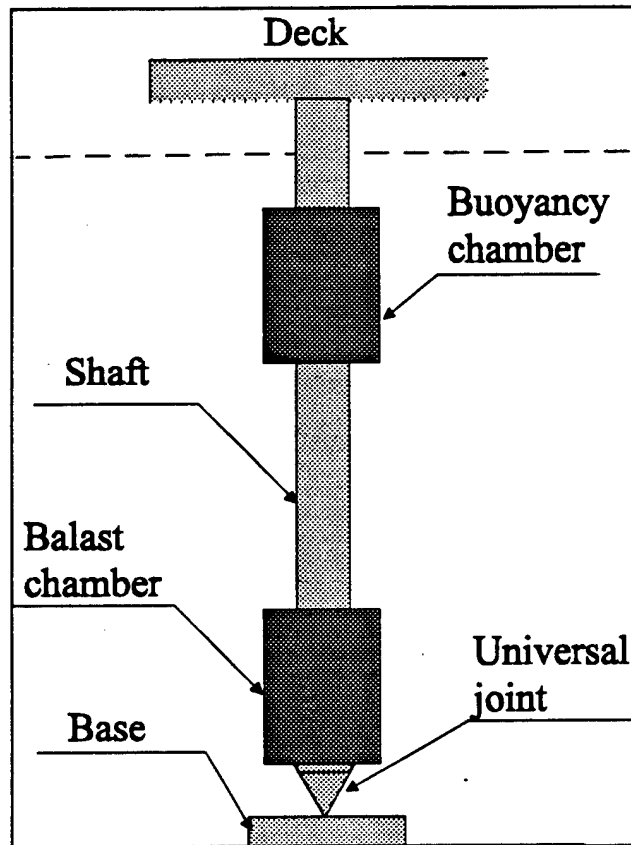


Figure 3: Schematic of an Articulated Tower

In two papers by Smith (1979) [13] and Smith and Taylor (1980) [14], the applicability, function and performance of an articulated tower was examined. The construction program covered the following aspects; hydrodynamics, materials, economic assessments and interaction between the structure and the fluid. The tower was designed for a water depth of 250 m, and its predicted cost was approximately \$700 million, while a conventional fixed structure would have cost on the order of \$1.5 billion. An analysis of the response due to waves and wind was performed and the results were compared to a 1:64 scale model. A fairly good correlation between the analytical model and the experimental one was found. From the analysis and testing, the authors concluded the following;

- Articulated towers can perform in a range of functions in offshore production.
- A good analytical model to predict the tower's response is important.
- A close collaboration with the oil industry, in order to address real problems, is needed.

In a paper by Butt et al. (1980) [15], a large-scale test program for a concrete articulated tower was presented. The tests were planned to be performed in the vicinity of a research platform called 'Nordsee'. The aim of the test program was to demonstrate the technical feasibility of the CONAT (Concrete Articulated Tower) concept. The special features of this concept are the bottle-shaped concrete tower and the ball joint which creates the articulated connection. The problems of oscillating platforms and basic design steps were discussed. And finally the scheduled program tests was briefly discussed.

Naess (1980) [16] presented the results of an extensive scale 1:70 model test of an articulated tower. The model, 20 m in length, was built of steel and aluminium to give the

necessary strength and polyurethane foam to give the correct outer dimensions. The tests were done with and without a tanker moored to it. The tests included the following measurements; wave elevation, pitch and roll of the tower were measured with accelerometers, axial and lateral (shear) forces were measured at the universal joint by strain gauges, bending moment near the buoyancy chamber and tension force at the mooring cable were also measured by strain gauges. The system was tested under wind of 24 m/s, waves with significant wave height of 5.5 m and frequency 0.12 Hz, and current velocity 0.5 m/s. From the tests they found the natural period to be 58.6 s and the damping ratio $\zeta = 0.46$. The pitch angle was about 10 deg. An attempt to measure the natural period in the presence of current failed because the free oscillations were immediately damped out, a phenomenon which is explained in Bar-Avi and Benaroya [17].

The paper (1990) [18], describes the world's largest single-point-mooring (SPM) terminal. It was hooked up in December 1989, in the Timor Sea off Australia's northwest coast. The tower was designed to survive conditions of significant wave height up to 9 m, wind velocity of 47 m/s and current velocity of 2 m/s. The operational environmental conditions were; a significant wave height of 3 m, wind velocity of 14.5 m/s and current velocity of 1 m/s. The main components of the SPM are the same as in any other articulated tower; a ballast, a universal joint, a tower and a mooring yoke.

B. Dynamic Response

Since articulated towers comply with the environmental forces, they can undergo large displacements. Therefore, the dynamic response of these kinds of structures is very important. Most of the studies considered the tower as a rigid body having a one or two angular degrees

of freedom about a universal joint. Structures having multiple articulations in planar or 3D motion were also analyzed. Very few studies considered the tower as a flexible structure and those that did, used lumped mass or finite element methods and not the classical methods of continuum mechanics. The external forces considered by most studies were due to waves, current and wind. Linear wave theory was applied, and the forces were approximated by Morison's equation (1950) [19]. This subsection summarizes the literature on the dynamic response of articulated towers. It is divided to three sections;

- Single degree of freedom systems - The tower is assumed rigid and only planar motion was considered.
- Two degrees of freedom system - Rigid body and 3D analysis of motion and loads.
- Multiple articulation and flexible systems - Planar or 3D motion of multi-articulated towers or towers that were considered flexible.

1. Single Degree of Freedom Systems

Chakrabarti and Cotter (1978) [20] developed a mathematical model to analyze the dynamic response of a tower-tanker system. The tower was assumed rigid, connected to the tanker via a spring with stiffness K . Forces due waves, current and wind are considered collinear. First the static equilibrium state due to only current and wind was found. Then small perturbations about the equilibrium position were assumed in the formulation of the equation of motion. The tanker was assumed to have two degrees of freedom; one linear (surge), and the other angular (pitch). The equations for the tower and the ship were derived and coupled through the spring connecting the tower to the tanker,

$$I_t \ddot{\psi} + F_{Dt} + C_B \psi + F_r l \cos(\theta + \phi) = M_t e^{i(\varepsilon_1 - \sigma t)}$$

$$m \ddot{x} + F_{D1s} - F_r \cos \theta = F_t e^{i(\varepsilon_2 - \sigma t)} \quad (1)$$

$$I_s \ddot{\mu} + F_{D2s} + C_B \mu - F_r (H_s \cos \theta + \frac{L}{2} \sin \theta) = M_s e^{i(\varepsilon_3 - \sigma t)},$$

where ψ, x, μ are the tower's deflection angle, the ship's surge and pitch, respectively. F_r is the spring force which couples the tower to the ship, C_B is buoyancy term, F_{Dt}, F_{D1s}, F_{D2s} are the drag forces proportional to the square of the relative velocity between the fluid and the structure, and σ is the wave frequency. The equations were solved numerically and the solution was compared to experimental results obtained from a model that was built with a scale of 1:48. Good correlation between the test results and theoretical predictions for small displacements was found. When soft spring-mass systems are considered, irregular waves produce a drift (static) force that the model did not predict.

In a later paper, Chakrabarti and Cotter (1979) [21] investigated the motion of an articulated tower fixed by a universal joint having a single degree of freedom. They assumed linear waves, small perturbations about an equilibrium position, and that the wind, current and wave are collinear. Their resulting equation of motion is

$$I \ddot{\psi} + B(\dot{\psi}) + D\dot{\psi} + C\psi = M_0 e^{i(\alpha - \beta t)}, \quad (2)$$

where I is the total moment of inertia including added mass, $B(\dot{\psi})$ is the nonlinear drag term, $D\dot{\psi}$ is the structural damping, $C\psi$ is the restoring moment due to buoyancy and M_0 is the magnitude of the wave moment. A linear equation was obtained by assuming a linear drag force and an analytical solution was obtained. The solution was then compared to

experimental results, showing good agreement as long as the system is inertia dominant, and not drag dominant.

Kim and Lau (1981) [22] evaluated the response of an articulated loading platform in regular waves. The objective of the study was to develop a reliable technique to predict the loads and motion of the tower. The following assumptions have been made; rigid single degree of freedom body, linear drag force, small deflection angle, and deep water. In the derivation of the equation of motion, the tower was assumed to be in its upright position so that geometrical nonlinearities were not included. The analytical solution of the linear equation of motion was obtained,

$$\psi_0 \cos(\omega t + \varepsilon_\psi) = \frac{M_{0\psi}}{B_\psi - \omega^2 I_v} \cos(\omega t + \varepsilon_M), \quad (3)$$

where ψ_0 represents the displacement angle, with phase shift ε_ψ . $M_{0\psi}$ is the total moment acting on the tower due to inertia and linear drag forces, and its phase shift is ε_M . B_ψ, I_v are the moments of inertia of the tower and added mass. The equation was then solved numerically and the solutions were compared to the experimental results presented by Naess [16] to show only qualitatively similarity, although using the same physical parameters. The authors concluded that a better model for the fluid forces, as well as not assuming deep water, will result in better predictions.

Muhuri and Gupta (1983) [23] investigated the stochastic stability of a buoyant platform. They used a linear single degree of freedom model as follows

$$\ddot{x} + 2c\dot{x} + (1 + G(t))x = 0, \quad (4)$$

where x is the displacement, c is the damping coefficient and $G(t)$ is a stochastic time-

dependent function due to buoyancy. It is assumed that $G(t)$ is a narrow-band random process with zero-mean. A criterion for the mean square stability is obtained from which the following results are found: for $c > 1$ the system is always stable, and for $0 < c < 1$ there are regions of stability and instability.

Thompson et al. (1984) [24] investigated the motions of an articulated mooring tower. They modeled the structure as a bilinear oscillator which consists of two linear oscillators having different stiffnesses for each half cycle,

$$m\ddot{x} + c\dot{x} + (k_1, k_2)x = F_0 \sin \omega t, \quad (5)$$

where k_1, k_2 are the stiffnesses for $x > 0$ and $x < 0$, respectively. The equation is solved numerically for different spring ratios and, as expected, harmonic and subharmonic resonances appeared in the response. A comparison between the response and experimental results of a reduced-scale model showed good agreement in the main phenomenon.

Chantrel and Marol (1987) [25] presented a study on a tanker moored to a single degree of freedom articulated tower. The objective of the study was to identify the relative importance of the different nonlinear terms in the equation of motion, especially the terms that cause subharmonic response. A few assumptions were made in deriving the equation of motion;

- In the restoring moment due to buoyancy quadratic terms were neglected.
- The drag force due water velocity was neglected.
- Forces/moments were evaluated at the upright position of the tower.
- The force in the mooring cable was assumed to have a cubic form.

Applying these assumptions resulted in the equation of motion

$$I\ddot{\theta} + C_1\dot{\theta} + C_2\dot{\theta}|\dot{\theta}| + K_{HYD}\theta - p(\theta_0 - \theta)^3 = M_0 \cos(\omega t + \varepsilon), \quad (6)$$

where I is the moment of inertia that includes the added mass, C_1, C_2 are the linear and quadratic damping coefficients, K_{HYD} is the hydrodynamic restoring stiffness, $p(\theta_0 - \theta)^3$ is the moment due to the mooring cable which is set to zero for $\theta_0 \geq \theta$ and finally $M_0 \cos(\omega t + \varepsilon)$ is the external wave moment that includes only inertia terms. Linearization of the equation by assuming small perturbations about an equilibrium position resulted in

$$\ddot{u} + 2\gamma\omega_n\dot{u} + \omega_n(1 + f_v \cos(\omega t + \varepsilon))u = \frac{M_0}{I} \cos(\omega t + \varepsilon). \quad (7)$$

This equation is actually the Mathieu equation, and stability analysis was performed to show an unstable region around the first natural frequency of the system. This region, as expected, gets smaller when linear damping is added to the system. Equation 6 was then solved numerically for regular and irregular waves having the Pierson-Moskowitz spectra and the following conclusions were drawn,

- The subharmonic response is due to the nonlinear characteristic of the mooring cable's stiffness.
- The subharmonic response occurs for very precise environmental conditions.
- A region of parametric instability that depends on the system's damping was found.

Datta and Jain (1987) [26], and (1990) [27] investigated the response of an articulated tower to random wave and wind forces. In the derivation of the single degree of freedom

equation of motion the tower is discretized into n elements having appropriate masses, volumes and areas lumped at the nodes, and there is viscous damping. The equation of motion is

$$I(1 + \beta(t))\ddot{\theta} + c\dot{\theta} + R(1 + \nu(t))\theta = F(t), \quad (8)$$

where $I\beta(t)$ is the time varying added mass term, $R\nu(t)$ is the time varying buoyancy moment and $F(t)$ is the random force due to wave and wind. The Pierson-Moskowitz spectrum is assumed for the wave height and Davenport's spectrum is assumed for the wind velocity. The equation is solved in the frequency domain using an iterative method, which requires that the deflection angle $\theta(t)$ and the forcing function $F(t)$ be decomposed into Fourier series. The coefficients of the *sin* and *cos* are then found iteratively. From their parametric study, they concluded the following;

- Nonlinearities such as large displacements and drag force do not influence the response when only wind force is considered.
- The random wind forces result in higher responses than do only wave forces.
- The root mean square response due only to wind forces varies in a linear fashion with the mean wind velocity.

In a later paper, Jain and Datta (1991) [28] used the same equation and the same method of solution to investigate the response due to random wave and current loading. The wave loadings (drag, inertia and buoyancy) are evaluated via numerical integration. The following results were obtained from the parametric study;

- The dynamic response is very small since its fundamental frequency is well below the wave's fundamental frequency.
- Nonlinear effects (drag force, variable buoyancy) have considerable influence on the response.
- Current velocity has a large influence on the response.

Virgin and Bishop (1990) [29] studied the domains of attraction (catchment regions) for a single degree of freedom articulated tower connected to a tanker. This was done using numerical techniques based on Poincaré mapping ideas. A basic bi-linear oscillator model was assumed, the equation of motion was the same as equation (11). This equation can exhibit multiple solutions, but in the example solved, the coefficients (stiffness and mass) were chosen so that only two solutions may coexist, depending on initial conditions; harmonic and 4th order subharmonic. The equation was solved numerically and it was shown that a domain of attraction could be found.

Choi and Lou (1991) [30] have investigated the behavior of an articulated offshore platform. They modeled it as an upright pendulum having one degree of freedom, with linear springs at the top having different stiffnesses for positive and negative displacements (bilinear oscillator). The equation of motion is simplified by expanding nonlinear terms into a power series and retaining only the first two terms. They assumed that the combined drag and inertia moment is a harmonic function. The discontinuity in the stiffness is assumed to be small, and thus replaced by an equivalent continuous function using a least-squares method to get the following Duffing equation

$$I\ddot{\theta} + c\dot{\theta} + k_1\theta + k_2\theta^2 + k_3\theta^3 = M_0 \cos \omega t, \quad (9)$$

where k_1, k_2, k_3 are spring constants depending on buoyancy, gravity and the mooring lines. The equation of motion is solved analytically and numerically, and stability analysis is performed. The analytical solution agrees very well with the numerical solution. The main results of their analyses are that as damping decreases, jump phenomena and higher subharmonics occur, and chaotic motion occurs only for large waves and near the first subharmonic (excitation frequency equals twice the fundamental frequency); the system is very sensitive to initial conditions.

Gottlieb et al. (1992) [31] analyzed the nonlinear response of a single degree of freedom articulated tower. In the derivation of the equation, the expressions for the buoyancy moment arm, added mass term, and drag and inertia moments are evaluated along the stationary upright tower position and not at the instantaneous position of the tower. The governing equation is of the form

$$\ddot{\theta} + \gamma\dot{\theta} + R(\theta) = M(\dot{\theta}, t), \quad (10)$$

where $R(\theta) = \alpha \sin \theta$ and α is linear function of buoyancy and gravity, $M(\dot{\theta}, t)$ is the drag moment. Approximate harmonic and subharmonic solutions are derived using a finite Fourier series expansion, and stability analysis is performed by a Lyapunov function approach. The solution shows a jump phenomenon in the primary and secondary resonances.

Gerber and Engelbrecht (1993) investigated the response of an articulated mooring tower to irregular seas. It is an extension of earlier work done by Thompson et al. (1984) [24]. The tower is modeled as a bilinear oscillator

$$m\ddot{x} + c\dot{x} + (k_1, k_2)x = F(t). \quad (11)$$

The random forcing function $F(t)$ is assumed to be the sum of a large number of harmonic

components, each at different frequencies, a procedure similar to that proposed by Borgman (1969) [32]. The equation is then solved analytically since it is linear for each half cycle. The solution is obtained for different cases; linear oscillator (both stiffnesses are the same), bilinear oscillator, and for the case of impact oscillator (a rigid cable) in which oscillation can occur only in one half of the cycle. For future study they suggest including of nonlinear stiffness and/or using a different spectrum to describe the wave height.

Bar-Avi and Benaroya (1994) [33] investigated the nonlinear response of a single degree of freedom articulated tower. The equation of motion was derived via Lagrange's equation. Nonlinearities due to geometry and wave drag force are considered. A combined wave and current field, coulomb friction force, and vortex shedding force are included in the analysis. The governing equation of motion is,

$$J(\theta)\ddot{\theta} + C\dot{\theta} + M_{gb}(\theta, t) = M_{fl}(\theta, t) - M_{fr}(\theta), \quad (12)$$

where $J(\theta)$ is a position-dependent moment of inertia that includes added mass terms, C is the structural damping coefficient, $M_{gb}(\theta, t)$ is a time and position-dependent moment due to buoyancy and gravity, $M_{fl}(\theta, t)$ is the fluid moment due to inertia, drag and vortex shedding force, and $M_{fr}(\theta)$ is the friction moment. The influence on the response of current velocity and direction, significant wave height and frequency, and damping mechanism was analyzed.

The following observations were made;

- The equilibrium position is proportional to the product of the current velocity squared and the drag coefficient.
- The highest response is when the current direction is perpendicular to the wave.

- The response to sub/superharmonics and harmonic excitation demonstrate beating.
- For most excitation frequencies, the response is quasiperiodic, but for certain frequencies chaotic behavior was observed.
- Damping (friction, structural) has a stabilizing effect.

A simplified equation for a single degree of freedom articulated tower was presented in Bar-Avi and Benaroya [34]. The equation was derived using the Taylor expansion of the fully nonlinear equation derived in [33]. Terms of second power or less were kept and the solutions of both, the fully nonlinear and the simplified equations were compared. From the comparison it was found that the simplified equation predicts the tower's response very well over a broad regime of behavior. Analytical expressions for the natural frequency and equilibrium position due to current were presented. It was also shown that current causes an additional damping mechanism in the system that can be expressed as $\frac{1}{3}C_D\rho Dd^3U_c\dot{\theta}$. This result agrees with the experimental results presented by Naess (1980) [16].

2. Two Degree of Freedom Systems

Kirk and Jain (1977) [35] investigated the dynamic response of a two degree of freedom articulated tower to noncolinear waves and current. The two equations of motion were obtained via Lagrange's equation. The waves were assumed linear with current modification of the frequency and amplitude. Forces due to buoyancy, wave drag and inertia, and added mass were considered. The equations were solved numerically, and the influence of drag coefficient and wave direction was analyzed. From the solution they concluded that;

- Higher drag coefficients result in lower response.

- The maximum deflection occurs when the current and the waves are in the same direction.

When vortex shedding forces are included the last conclusion is not correct as shown in Bar-Avi and Benaroya [33].

Olsen et al. (1978) [36] evaluated the motion and loads acting on a single-point mooring system. The tower was modeled as a rigid body connected to the sea-floor via a universal joint. The equation for the tower and the tanker were derived separately. To derive the equations of motion for the tower, it was divided into N elements having two degrees of freedom each; a horizontal and vertical displacement and the forces due to wave, current and wind were evaluated at each element. Hence, $2N$ nonlinear differential equations were found

$$\sum_{i=1}^N \left\{ (\bar{r}_{iV} - z_0 \cdot \hat{k}) \times \bar{F}_{iV} + \bar{r}_{iH} \times \bar{F}_{iH} \right\} = 0, \quad (13)$$

where \bar{r}_{iV} , \bar{r}_{iH} are the displacements of element i in the vertical and horizontal directions, \bar{F}_{iV} , \bar{F}_{iH} are the environmental loads acting on element i in the vertical and horizontal direction, $z_0 \cdot \hat{k}$ is the motion of the universal joint in the z direction. The tanker was modeled as a rigid body having three transverse degrees of freedom. The equations are derived in the tanker coordinate system and then transformed into the tower's coordinate system to yield

$$[M] \{\ddot{x}\} + [C] \{\dot{x}\} + [K] \{x\} = [F], \quad (14)$$

where $[M]$, $[C]$, $[K]$ are the mass (including added mass terms), damping and stiffness matrices of the tanker, $[F]$ is the force vector acting on the tanker and $\{\ddot{x}\}$, $\{\dot{x}\}$, $\{x\}$ are the acceleration, velocity and position vectors of the tanker. The tanker's and tower's equations

are coupled by applying a constant mooring force $[F_M]$ at each time step of the integration. The solution gives the low frequency motion of the tanker as well as the tower's response. The high frequency motion of the tanker was assumed to be unaffected by the fact that the tanker is moored. Therefore the tanker's high-frequency amplitudes were calculated independently from the low frequency, and then the responses were added together. The equations were solved numerically and compared to test results to show a reasonably good correlation, but according to the authors, a more accurate model should be developed. The effect of the tanker on the surrounding wave field was also investigated to find a 0-10% change in the wave velocity and acceleration. The effect of these changes on the response was not investigated.

Chakrabarti and Cotter (1980) [37] investigated transverse motion, the motion perpendicular to the horizontal velocity. The tower pivot is assumed to have two angular degrees of freedom and is taken to be frictionless. It is also assumed that the motion is not coupled, so the in-line solution is obtained (the same as in the previous paper), from which the relative velocity between the tower and the wave is obtained. The lift force (in the transverse direction) can then be obtained and the linear equation of motion is solved analytically and compared to experimental results. The comparison shows good agreement, especially when the drag terms are small.

Schellin and Koch [38] calculated the dynamic response due to waves and compared results with model tests. The calculation of the response was done for three different sets of fluid coefficients; coefficients that depend on the wave period, coefficients selected from experimental data and coefficients that are calculated using diffraction theory. The tower was assumed rigid and connected to the sea-floor via a two degree of freedom universal joint.

Forces due to wind, wave and current as well as nonlinearities due to geometry and wave drag force are considered. The tower was divided into N elements for which the following force was found;

$$\mathbf{F}_i = C_{Mi}\dot{\mathbf{u}}_{wi} + C_{Di}\mathbf{u}_{wi}|\mathbf{u}_{rel}| + \mathbf{F}_{Bi} + \mathbf{F}_{Gi} + \mathbf{F}_{Wi} - \mathbf{m}_i\ddot{\mathbf{r}}_i - C_{Di}\dot{\mathbf{r}}_i|\mathbf{u}_{rel}|, \quad (15)$$

where \mathbf{F}_i is the vector of the total force acting on the element due fluid inertia force $C_{Mi}\dot{\mathbf{u}}_{wi}$, fluid drag force $C_{Di}\mathbf{u}_{wi}|\mathbf{u}_{rel}|$, buoyancy, gravity and wind forces; \mathbf{F}_{Bi} , \mathbf{F}_{Gi} , \mathbf{F}_{Wi} , inertia force due to tower's acceleration $\mathbf{m}_i\ddot{\mathbf{r}}_i$, and drag force due to tower velocity $C_{Di}\dot{\mathbf{r}}_i|\mathbf{u}_{rel}|$. Summing all forces on each element and multiplying by the moment arm leads to the equations of motion

$$\sum_{i=1}^N \{(\mathbf{r}_i - H\hat{z}) \times \mathbf{F}_i\} = 0, \quad (16)$$

where H is the distance in the z direction between the universal joint and the mean water level. The equations of motion were solved numerically for an idealized tower that consists of a series of circular cylinders. The numerical solutions were compared to experimental results of a model which has been built to a scale of 1:32.75 and the following conclusions have been drawn;

- Proper choices of the drag and the added mass coefficients results in good correlation between the theoretical and test results, for the tower's deflection and horizontal reaction force on the universal joint.
- The correlation of the vertical reaction force is not good.

- The added mass coefficient has a predominant effect on the dynamic response and the drag coefficient almost none.
- The theoretical results for waves having small period (high frequency) do not correlate as well as results for waves with large period.

Liaw et al. (1989) [39] formulated the equations of motion for a two degree of freedom articulated tower using Lagrange's equations, and then solved and analyzed the large motion of the structure. This was done using Euler's theorem, which states that 'if a body has one point O fixed, then any displacement of the body from one given position to another is equivalent to a rotation about a unique axis through O '. The equation was solved for three cases. First, the static equilibrium inclination of the tower due to current was obtained. Next, the response due to linear waves with height of 3 m and period of 17 s was evaluated. Finally, the previous waves along with orthogonal current were applied and the solution was found. All three cases were compared to the solution obtained by Leonard and Young (1985) [40], who used a finite element method, and the results matched quite well.

In a paper from 1992, Liaw et al. [41] showed that the subharmonic phenomenon, which occurs in articulated towers, is due to the coupling between the wave force and the structure. They used the equations that were developed in their previous paper [39], but reduced from 2 degrees of freedom to a single degree of freedom system. The equation was solved them numerically and harmonic and subharmonic responses were obtained. The following observations were made;

- The amplitude of the response in the subharmonic region can be as high as the one in the harmonic region.

- The initial conditions determine the final steady state response.

Similar results for a single degree of freedom model were obtained in a study presented by Bar-Avi and Benaroya [33], although, for a two degree of freedom system (see [42]) it was found that the subharmonic response is not as pronounced as in the single degree of freedom model.

Bar-Avi and Benaroya [17],[42], investigated the response of a two degree of freedom articulated tower to deterministic loading. The nonlinear differential equations of motion were derived using Lagrange's equations. The tower was assumed to have the same dynamic properties as an upright spherical pendulum with additional effects and forces;

- Coulomb friction in the pivot (hinge)
- Structural viscous damping
- Drag fluid force due to waves and current, and wind coupled to the structure
- Inertia, buoyancy and added mass fluid forces
- Vortex shedding loads due to waves and wind
- Wave slamming that was modeled as a periodic impulsive force
- Gyroscopic moments due to the rotation of the earth (Coriolis acceleration).

All fluid forces due to waves, current, and wind are determined at the instantaneous position of the tower, resulting in two, highly nonlinear, coupled, ordinary differential equations with time-dependent coefficients, with rotation angle ϕ , and deflection angle θ

$$J_{eff}^{\theta}(\theta)\ddot{\theta} + C\dot{\theta} + I_g(\theta)\dot{\phi}^2 + M_{gb}^{\theta}(\theta) = M_{fl}^{\theta}(\theta, t) + M_{sm}^{\theta}(\theta, t) + M_w^{\theta}(\theta) - M_{fr}^{\theta}(\theta, t) \quad (17)$$

$$J_{eff}^{\phi}(\theta)\ddot{\phi} + C\dot{\phi} + I_g(\theta)\dot{\phi}\dot{\theta} = M_{fl}^{\phi}(\theta, t) + M_{sm}^{\phi}(\theta, t) + M_w^{\phi}(\theta) - M_{fr}^{\phi}(\theta, t),$$

The equations of motion were numerically solved and the following observations were made;

- An analytical expression for the equilibrium position due to current and wind was found.
- The response due to wave slamming is very small since an impulsive force is attenuated when the pulse duration is shorter than the system's fundamental duration, which is the case here.
- Wind loads and current loads affect the equilibrium position of the tower.
- The Coriolis acceleration force has a small but important influence on the response, since it causes a coupling so that planar motion is not possible under real conditions.
- The regions in which the beating phenomenon occurs are very small and it is not as pronounced as in a single degree of freedom system.
- Due to the system nonlinear behavior chaotic regions exist.

Later, Bar-Avi and Benaroya [43], [44] analyzed the response of a two degree of freedom tower, where key parameters were taken to be random variables. The wave height, drag,

inertia and lift coefficients, and coulomb friction coefficient were assumed to be random uniformly distributed variables. The nonlinear differential equations of motion (18) were numerically solved and Monte-Carlo simulations were performed to evaluate the average response and the standard deviation. It was found that the standard deviation for the rotation angle is larger than that of the deflection angle. The value of the friction coefficient has a very small influence on the average response, unlike the wave height and the drag coefficient.

3. Multiple Articulations and Flexible Systems

In a paper by Jain and Kirk (1981) [45], a double articulated offshore structure subjected to waves and current loading was analyzed. They assumed four degrees of freedom, two angular degrees for each link. The equations of motion were derived using Lagrange's equations. In deriving the equations of motion the following assumptions were made: drag and inertia forces tangent to the tower are negligible, and the wave and current velocities are evaluated at the upright position (small angles assumption). The linearized equations were solved to find the natural frequencies of the system and then numerically solved to find the response due to colinear and non-colinear current and wave velocities. They found that when the wave and the current velocities are colinear, the response of the top is sinusoidal, while for noncolinear velocities the response is a complex three dimensional whirling oscillation.

Seller and Niedzwecki (1992) [46] investigated the response of a multi-articulated tower in planar motion (upright multi-pendulum) to account for the tower flexibility. The restoring moments (buoyancy and gravity) were taken as linear rotational springs between each link, although the authors state that nonlinear springs are more adequate for this model. Each

link is assumed to have a different cross section and density. The equations of motion are derived using Lagrange's equations, in which the generalized coordinates are the angular deflections of each link. The equations in matrix form are

$$[M]\{\ddot{\theta}\} + [K]\{\theta\} = \{Q\}, \quad (18)$$

where $[M]$ is a mass matrix that includes the actual mass of the link and added mass terms, while the stiffness matrix $[K]$ includes buoyancy and gravity effects. Damping and drag forces are not included in the model. The homogeneous equations for a tri-articulated tower are numerically solved to study the effects of different parameters, such as link length, material density and spring stiffness, on the natural frequency of the system.

In two papers, one by Havery et al. (1982) [47], and by McNamara and Lane (1984) [48], a finite element method is used to calculate the response of a planar flexible multi-articulated tower. Examples of the response of single point mooring, bi-articulated and multi-articulated towers were presented. In order to derive the equation of motion, the displacement was decomposed into a rigid body motion and a deformed motion. Two coordinate systems were used. One fixed and the other attached to the tower's rigid body motion. The deformation were first expressed in the rotating system and then transformed into the fixed coordinate system in which the equation of motion was expressed for each element, to find

$$M\ddot{w} + Kw = Kw^{rb} + F, \quad (19)$$

where M is the mass matrix, K is the stiffness matrix, w, w^{rb} are the total and rigid body displacements, respectively, and F is the force due to wave and current, calculated by the Morison's equation. For random wave, the Pierson-Moskowitz spectrum was transformed

into the time domain using Borgman's method [32]. The equations were solved numerically using a finite difference method in which artificial damping was introduced which, according to the authors, does not significantly influence the response. It was found that the finite element solution using 21 elements was stable up to a time step of 0.7 s. A solution for the same problem, based on numerical integration of the Lagrange's equations (not presented), was compared to the finite element solution and the results agreed exactly except for a few initial cycles. The method presented can be extended to more realistic problems such as two degree of freedom universal joints.

The objective of the paper by Leonard and Young (1985) [40] was to develop a solution method to evaluate the dynamic response of an articulated tower. The method is based on three dimensional finite elements. The tower was subjected to wave and current and nonlinearities due to geometry and drag force were included. The equations of motion are

$$[M] \{\ddot{q}\} + [C] \{\dot{q}\} + [K] \{q\} = \{F(t)\}, \quad (20)$$

where $[M]$, $[C]$, $[K]$ are the mass, damping and stiffness matrices, $\{\ddot{q}\}$, $\{\dot{q}\}$, $\{q\}$ are the generalized acceleration, velocity and displacement vectors and $\{F(t)\}$ is the generalized force vector due to wave and current. The response was evaluated numerically for steady current only and then for waves. The results were compared to those presented by Jain and Kirk (1981) [45]. From this comparison it was concluded that the three dimensional finite element method is adequate. For linear analysis it requires more time than other linear computer schemes, but when nonlinearities are included the method actually requires less time.

Hanna et al. (1988) [49] investigated the dynamic response of tri-articulated tower subjected to wave, wind and current. The tower geometry and dynamic characteristics were optimized such that: tower periods fall outside the 5 to 20 s range, and reaction forces and weight are minimized. The model consisted of three rigid segments with different lengths and mass, with total length of 3000 feet. Each segment had a single degree of freedom and they were connected via a rotational spring. Thus three linear ordinary nonlinear differential equations were obtained for small angles

$$[M] \{\ddot{x}\} + [K] \{x\} = \{F\}, \quad (21)$$

where $[M]$, $[K]$ are 3×3 mass and stiffness matrices, respectively, $\{F\}$ is the forcing vector due to wave, wind and current, and $\{x\}$ is the displacement vector. Equations (21) were used to determine the static stability due offsets of the deck weight. Values for segment length, weight and joint stiffness were found for the highest critical load. To analyze the dynamic response and the stresses, large angular deflections were considered. The tower was divided into N elements each having a single degree of freedom. Nonlinearities due to geometry and drag forces were included resulting in

$$[M] \{\ddot{u}\} + [C] \{\dot{u}\} + [K] \{u\} = \{P(t, u, \dot{u})\}, \quad (22)$$

where $[M]$, $[C]$, $[K]$ are the mass, damping and stiffness matrices, and $\{P(t, u, \dot{u})\}$ is the vector of the forces due to waves and colinear current approximated by the Morison's equation, and due to static wind loads. Numerical solutions were obtained for deterministic and irregular waves having the Pierson-Moskowitz spectra. From the analysis it was concluded

that compliant towers with multiple articulations provide an attractive concept to optimize the dynamic response without penalizing the structure's weight. Furthermore, the method of analysis can be utilized for 3D structures and also other similar compliant towers with multiple articulations.

Helvacioğlu and Incecik (1988) [50] described analytical models to predict the dynamic response of a single and bi-articulated tower subjected to waves and wind. The analytical solutions were compared to test measurements. The effects of changes in the buoyancy position, joint location and deck weight on the bi-articulated tower response were studied. In both models planar motion was assumed, and although it wasn't mentioned in the paper, fluid drag forces were not included, and therefore simple equations were derived that resulted in simple analytical solutions. In both models the equations were simple oscillators with damping subjected to harmonic forces,

$$[M] \{\ddot{\theta}\} + [C] \{\dot{\theta}\} + [K] \{u\} = \{M_F\} \sin \omega t, \quad (23)$$

where $[M]$, $[C]$, $[K]$ are scalars for a single articulation or 2×2 matrices for the bi-articulated system. From the parametric study it was found that the buoyancy tank position has a significant effect on the natural frequencies. According to the authors, the mathematical model for the bi-articulated tower correlated reasonably with the test results.

Active control of offshore articulated towers was discussed in a paper by Yoshida et al. (1988) [51]. A preliminary attempt was to control the dynamic response of an articulated tower subjected to regular waves. Two models were used; one was a rigid body having a single degree of freedom, and the other was a flexible tower fixed at the bottom. The control

scheme was expressed as a combination of feedforward control based on the disturbance and a feedback control. The feedback control copes with the higher order noise remaining after the compensation of the feedforward control. Two feedforward control schemes were discussed. One is to compensate for the whole wave force acting on the structure, while the other was on-off control to compensate for the principle Fourier components of the wave force. The simulation results for both models showed that the response of the controlled structure was reduced to about 30% of those of the uncontrolled system.

In a later paper, Yoshida and Suzuki (1989) [52] discussed the experimental results of the response of an actively controlled tri-articulated tower. The application of active control to offshore structures is advantageous, increasing strength (stiffness) and reducing weight. The structure can be artificially stiffened and damped by means of active control according to the environmental conditions. Ultrasonic sensing systems were used to measure the deflection of each segment of the tower. The data from the measuring system was processed and the signals for the controllers were obtained. The control force was generated by thrusters which were built into each segment. Optimal control was applied to several cases;

- A neutral model, in which the buoyancy and gravity forces are equal, was controlled. The response of the model against an imposed displacement was controlled. The thrusters had a phase delay, and therefore vibrations in high frequency could not be controlled.
- An unstable model, in which the buoyancy force was less than the gravity force was controlled. In this case the structure was stabilized but again high frequency vibrations could not be controlled.

- Static deflection due to current was controlled successfully, but with large deflection angle the high gain necessary to control the structure caused some instability.

Ganapathy et al. 1990 [53] developed a general finite element program for the analysis of the nonlinear statics and dynamics of articulated towers. The tower was modeled as a three-dimensional beam element, which includes axial shear and bending deformations. The equations of motion have the standard finite element formulation

$$[M] \{\ddot{u}\} + [C] \{\dot{u}\} + [K] \{u\} = \{F(t)\}. \quad (24)$$

Linear wave theory was assumed and the wave force was evaluated via Morison's equation. The equations were numerically solved and the effects of the water depth, buoyancy force magnitude and position, and wave and current loads were investigated and the following conclusions were drawn;

- For moderate water depth (100 m), the maximum bending moment occurs at the position of the chamber, while for deep water (300 m), the maximum bending moment can occur at the mid span or at the buoyancy chamber, depending on the chamber's position.
- Larger buoyancy forces cause a decrease in the tower's deflection and an increase in the bending moment.
- Current load has a significant effect on the deflection and the bending moment.
- There is a nonlinear relation between the total force and the deflection.

Mathisen and Bergan (1991) [54] outline a general approach to large displacement static and dynamic analysis of an interconnected rigid and deformable multibody system submerged or floating in water. The system's equations of motion were generated by combining the equation of motion derived for each subsystem, which can be either rigid or deformable. The investigation is based on the Lagrangian description of motion in which the current coordinate of a material point is described in terms of its initial material point and time. The equation of motion of each part was derived using variational methods, and then combined with a nonlinear finite element displacement formulation. The formulation was applied to a bi-articulated tower, and the purpose was to find the response of the top of the platform, as well as to evaluate the distribution of the axial force and bending moment along the tower. The equations were solved for deterministic wave height of 30 m with a period of 30 s, and irregular (random) waves having the Jonswap spectrum.

III. SUMMARY AND CONCLUDING THOUGHTS

The important class of offshore structures known as articulated towers has been studied over the past two decades. Such structures have found primary offshore application in the oil industry, but also for cases where a stable ocean platform is needed for communication and mooring.

This paper summarizes the literature focused on articulated towers. Forces on these structures due to ocean and atmosphere include ocean waves and current, wind, buoyancy, and friction at the base. Various models have been developed for these forces, with a spectrum of sophistication. Similarly, the complex equations of motion governing structural response

find numerous methods for their solution.

The interested worker will find here the necessary background on this problem, and will be able then to proceed with the research literature.

IV. ACKNOWLEDGMENT

This work is supported by the Office of Naval Research Grant no. N00014 - 93 - 1 - 0763.

The first author is grateful for the ONR sponsored Fellowship, and the second author for additional support.

REFERENCES

- [1] S. Fjeld and S. Flogeland. Deepwater platforms problem areas. In *European Offshore Petroleum Conference and Exhibition*, pages 223-234, 1980.
- [2] S.Y. Hanna, A. Mangiavacchi, and R. Suhendra. Nonlinear dynamic analysis of guyed tower platforms. *Journal of Energy Resources Technology*, 105:205 - 211, 1983.
- [3] J.F. Wilson and G. Orgill. Optimal cable configuration for passive dynamic control of compliant tower. *Journal of Dynamic Systems, Measurement, and Control*, pages 311-318, 1984.
- [4] H.B. Kanegaonkar and A. Haldar. Nonlinear random vibrations of compliant offshore platforms. *Symposium of Nonlinear Stochastic Dynamic Engineering Systems*, pages 351 - 360, 1987.

- [5] N. Haritos. Modeling the response of TLP structures to environmental loading. *Journal of Wind Engineering and Industrial Aerodynamics*, pages 2475–2485, 1992.
- [6] A. Kareem and Y. Li. Response of tension leg platform to wind, waves and currents: A frequency domain approach. In *The 22nd Annual Offshore Technology Conference*, pages 1023–1037, 1990.
- [7] A. Kareem and Y. Li. Wind-excited surge response of tension-leg platform: Frequency-domain approach. *Journal of Engineering Mechanics*, pages 161–171, 1993.
- [8] Y. Dong and J.Y.K. Lou. Vortex-induced nonlinear oscillation of tension leg platform tethers. *Ocean Engineering*, 18(5):451–464, 1991.
- [9] M.H. Patel and H.I. Park. Dynamics of tension leg platform tether at low tension. Part 1 - Mathieu stability at large parameters. In *Proceeding of the 10th International Conference on Offshore Mechanics and Arctic Engineering*, pages 257–273, 1991.
- [10] H.I. Park and M.H. Patel. Dynamics of tension leg platform tethers at low tension: Part 2 - combined excitation. In *Proceedings of the 11th International Conference on Offshore Mechanics and Arctic Engineering*, pages 265–274, 1992.
- [11] G.E. Burnd and G.C. D'Amorim. Buoyant tower for phase one development of Garoupa field. In *9th Annual Offshore Technology Conference*, pages 177–184, 1977.
- [12] D.L. Hays, M. McSwiggan, and R. Vilain. Operation of an articulated oil loading column at the Beryl field in the North Sea. In *11th Annual Offshore Technology Conference*, pages 1805–1815, 1979.

- [13] J.R. Smith. The application of a concrete articulating buoyant column to offshore drilling and production systems. In *Proceedings Symposium on New Technology for Exploration and Exploitation of Oil and Gas Resources*, pages 377-389, 1979.
- [14] J.R. Smith and R.S. Taylor. The development of articulated buoyant system column system as an aid to economic offshore production. In *European Offshore Petroleum Conference and Exhibition*, pages 545-557, 1980.
- [15] H.G. Butt, J. Salewski, and P. Wagner. A large-scale test with the concrete articulated tower conat in the vicinity of the research platform 'nordsee'. In *International Conference on Marine Science and Ocean Engineering*, pages 31-47, 1980.
- [16] A. Naess. Loads and motions of an articulated loading platform with moored tanker. In *12th Annual Offshore Technology Conference*, pages 409-417, 1980.
- [17] P. Bar-Avi and H. Benaroya. Response of an articulated tower to loads due to wave slamming, wind and coriolis acceleration. In *The 36th AIAA/ASME/ASCE/AHS/ASC Structures, Structural Dynamics, And Materials Conference*, 1995.
- [18] Anonymous. BHP brings Challis onstream with world's largest SALRAM. *Ocean Industry*, pages 53-56, 1990.
- [19] J.R. Morison, M.P. O'Brien, J.W. Johnson, and S.A. Schaaf. The force by surface waves on piles. *Petroleum Transactions, AIME*, 189:149-154, 1950.
- [20] S.K. Chakrabarti and D.C. Cotter. Analysis of a tower-tanker system. In *Proceedings of the 10th Annual Offshore Technology Conference*, pages 1301-1310, 1978.

- [21] S.K. Chakrabarti and D.C. Cotter. Motion analysis of articulated tower. *Journal of the Waterway, Port, Coastal and Ocean Division, ASCE*, 105:281 – 292, 1979.
- [22] C.H. Kim and P.A. Luh. Motions and loads of an articulated loading platform in waves. *IEEE, Ocean Engineering*, pages 956–961, 1981.
- [23] P.K. Muhuri and A.S. Gupta. Stochastic stability of tethered buoyant platforms. *Ocean Engineering*, 10(6):471 – 479, 1983.
- [24] J.M.T. Thompson, A.R. Bokaian, and R. Ghaffai. Stochastic and chaotic motions of compliant offshore structures and articulated mooring towers. *Journal of Energy Resources Technology*, 106:191 – 198, 1984.
- [25] J. Chantrel and P. Marol. Subharmonic response of articulated loading platform. In *Proceedings of the 6th Conference on Offshore Mechanics and Arctic Engineering*, pages 35–45, 1987.
- [26] K. Jain and T.K. Datta. Stochastic response of articulated towers. In *Deep Offshore Technology 4th International Conference and Exhibit*, pages 191–208, 1987.
- [27] T.K. Datta and A.K. Jain. Response of articulated tower platforms to random wind and wave forces. *Computers and Structures*, 34(1):137 – 144, 1990.
- [28] A.K. Jain and T.K. Datta. Nonlinear behavior of articulated tower in random sea. *Journal of Engineering for Industry*, 113:238 – 240, 1991.

- [29] L.N. Virgin and S.R. Bishop. Catchment regions of multiple dynamic responses in nonlinear problems of offshore mechanics. *Journal of Offshore Mechanics and Arctic Engineering*, pages 127–133, 1990.
- [30] H.S. Choi and J.Y.K. Lou. Nonlinear behaviour of an articulated offshore loading platform. *Applied Ocean Research*, 12(2):63 – 74, 1991.
- [31] O. Gottlieb, C.S. Yim, and R.T. Hudspeth. Analysis of nonlinear response of an articulated tower. *International Journal of Offshore and Polar Engineering*, 2(1):61 – 66, 1992.
- [32] L.E. Borgman. Ocean wave simulation for engineering design. *Journal of the Waterways and Harbors Division, ASCE*, 95:557–583, 1969.
- [33] P. Bar-Avi and H. Benaroya. Nonlinear dynamics of an articulated tower submerged in the ocean. *Journal of Sound and Vibration*, in press 1995.
- [34] P. Bar-Avi and H. Benaroya. Simplified equation for a SDOF articulated tower. *Journal of Engineering Mechanics (submitted for publication)*, 1995.
- [35] C.L. Kirk and R.K. Jain. Response of articulated tower to waves and current. *The 9th Annual Offshore Technology Conference*, pages 545 – 552, 1977.
- [36] O.A. Olsen, A. Braathen, and A.E. Loken. Slow and high frequency motions and loads of articulated single point mooring system for large tanker. *Norwegian Marin Research*, pages 14–28, 1978.

- [37] S.K. Chakrabarti and D.C. Cotter. Transverse motion of articulated tower. *Journal of the Waterway, Port, Coastal and Ocean Division, ASCE*, 107:65 – 77, 1980.
- [38] T.E. Schellin and T. Koch. Calculated response of an articulated tower in eaves comparison with model tests. In *Proceedings of the Forth Offshore Mechanics and Arctic Engineering Symposium, ASME, Vol. 1*, 1985.
- [39] C.W. Liaw, N.J. Shankar, and K.S. Chua. Large motion analysis of compliant structures using Euler parameters. *Ocean Engineering*, 16(6):545–557, 1989.
- [40] J.W. Leonard and R.A. Young. Coupled response of compliant offshore platforms. *Engineering Structures*, 7:74 – 84, 1985.
- [41] C.Y. Liaw, N.J. Shankar, and K.S. Chua. Subharmonic motions and wave force-structure interaction. *Marine Structures*, 5:281–295, 1992.
- [42] P. Bar-Avi and H. Benaroya. Deterministic response of articulated tower to different environmental conditions. *International Journal of Nonlinear Mechanics (submitted for publication)*, 1995.
- [43] P. Bar-Avi and H. Benaroya. Dynamic response of an articulated tower to random waves and current loads. In *Third International Conference on Stochastic Structural Dynamics*, 1995.
- [44] P. Bar-Avi and H. Benaroya. Stochastic response of an articulated tower. *International Journal of Nonlinear Mechanics*, Submitted for publication 1995.

- [45] R.K. Jain and C.L. Kirk. Dynamic response of a double articulated offshore loading structure to noncollinear waves and current. *Journal of Energy Resources Technology*, 103:41 – 47, 1981.
- [46] L.L. Sellar and J.M. Niedzwecki. Response characteristics of multi-articulated offshore towers. *Ocean Engineering*, 19(1):1 – 20, 1992.
- [47] K.F. Haverty, J.F. McNamara, and B. Moran. Finite dynamics motions of articulated offshore loading towers. In *Proceedings of the International Conference of Marine Research Ship Technology and Ocean Engineering*, 1982.
- [48] J.F. McNamara and M. Lane. Practice modeling for articulated risers and loading columns. *Journal of Energy Resources Technology*, pages 444–450, 1984.
- [49] S.Y. Hanna, D.I. Karsen, and J.Y. Yeung. Dynamic response of a compliant tower with multiple articulations. In *Seventh International Conference on Offshore Mechanics and Arctic Engineering*, pages 257–269, 1988.
- [50] I.H. Hevacioglu and A. Incecik. Dynamic analysis of coupled articulated tower and floating production system. In *The 7th International Conference on Offshore Mechanics and Arctic Engineering*, pages 279–287, 1988.
- [51] K. Yoshida, H. Suzuki, and N. Ona. Control of dynamic response of tower-like offshore structures in waves. In *7th International Conference on Offshore Mechanics and Arctic Engineering*, ASME, volume 1, pages 249–256, 1988.

- [52] K. Yoshida, H. Suzuki, and S. Mishima. Response control of articulated compliant tower. In *Eighth International Conference on Offshore Mechanics and Arctic Engineering*, pages 199–207, 1989.
- [53] C. Ganapathy, B.P. Samantaray, and K. Nagamani. Truss type articulated towers for deep water applications. In *The 9th International Conference on Offshore Mechanics and Arctic Engineering*, pages 477–484, 1990.
- [54] K.M. Mathisen and P.G. Bergan. Large displacement analysis of submerged multibody systems. *Engineering Computations*, 9:609–634, 1992.

Patrick Bar-Avi
Haym Benaroya
Rutgers, The State University of New Jersey
Piscataway, New Jersey

Abstract

In a previous paper [1], the stochastic response of a two degree of freedom articulated tower in the ocean was investigated. The governing coupled differential equations of motion are highly nonlinear, and have time-dependent coefficients due to fluid forces and geometrical nonlinearities. The tower's average response was evaluated for uniformly distributed random fluid constants, friction coefficient, and current direction. In this paper additional terms due to wave slamming loads and earth angular velocity (Coriolis force) are added to the equations of motion. The equations are then solved numerically.

Introduction

Compliant platforms such as articulated towers are economically attractive for deep water conditions because of their reduced structural weight compared to conventional platforms. The foundation of the tower does not resist lateral forces due to wind, waves and currents; instead, restoring moments are generated by a large buoyancy force, a set of guy-lines or a combination of both. These structures have a fundamental frequency well below the wave lower-bound frequency. As a result of the relatively large displacements, geometric nonlinearity is an important consideration in the analysis of such a structure. The analysis and investigation of these kinds of problems can be divided into two major groups: deterministic and random wave and/or current loading. Most works consider the tower as an upright rigid pendulum attached to the sea floor via a pivot having one or two degrees of freedom.

Bar-Avi and Benaroya (1994) [2] investigated the nonlinear response of a single degree of freedom articulated tower. The equation of motion was derived via Lagrange's equation. Nonlinearities due to geometry and wave drag force are considered. A combined wave and current field, coulomb friction force, and vortex shedding force are included in the analysis. The influences on the response of current velocity and direction, significant wave height and frequency, and damping mechanism were analyzed. The response to sub/superharmonics and harmonic excitation demonstrate beating, and for certain excitation frequencies a chaotic behavior was observed. Current has a large influence on the response and on the equilibrium position of the tower.

In later papers, Bar-Avi and Benaroya (1995) [3],[1] investigated the stochastic response of a two degree of freedom articulated tower submerged in the ocean. The nonlinear differential equations of motion were derived, including nonlinearities due to geometry, coulomb damping, drag force, added mass, and buoyancy. All forces/moments were evaluated at the instantaneous position of the tower and, therefore, they are not only time-dependent, but also highly nonlinear. The equations were then numerically integrated and Monte-Carlo simulations performed to evaluate the tower's average response and scatter. Effects of various parameters such as the fluid constants, significant wave height, coulomb and structural damping coefficient, and current direction were then investigated.

Other studies on single degree of freedom models were performed by Chakrabarti and Cotter [4], Gottlieb et al. [5], Muhuri [6], Datta and Jain [7], [8], [9]. Two degree of freedom models were analyzed by Chakrabarti and Cotter [10] and Jain and Kirk (1981) [11]. A detailed description of these

studies is given in [2].

New Study

In this paper the response of a two degree of freedom articulated tower to deterministic loads is investigated. The nonlinear differential equations of motion are derived using Lagrange's equation. They are similar to those discussed in the previous paper by Bar-Avi and Benaroya [1] but with additional terms due to wave slamming loads, wind loads and Coriolis forces generated by the rotation of the earth. The equations are then solved numerically using ACSL software to determine the influence of these forces on the tower's dynamic response.

Equations of Motion

Problem description

The structure is modeled as a tower submerged in the ocean having a concentrated mass at the top and two degrees of freedom; θ about the z axis and ϕ about the x axis. The tower is subjected to wave, current, vortex shedding, wind force, and wave slamming loads. This problem has similarities to that of an inverted spherical pendulum with additional considerations,

- additional fluid and buoyancy forces
- earth angular velocity is included.

The equations of motion are derived using Lagrange's equation. The equations are derived for large displacements. Only key terms are shown here. A full derivation of the equations of motion without the earth rotation effect and wave slamming force can be found in Bar-Avi and Benaroya (1994) [1]. Only the additional terms will be derived here.

The derivation of the equations of motion using Lagrange's equations requires that the kinetic, dissipative and potential energies be evaluated, as

well as the generalized forces. In this subsection, the tower absolute velocities, linear and angular, and accelerations are determined in the fixed coordinate system x, y, z attached to earth. Fig. 1 describes the earth coordinate system from which the tower's absolute angular velocity can be evaluated.

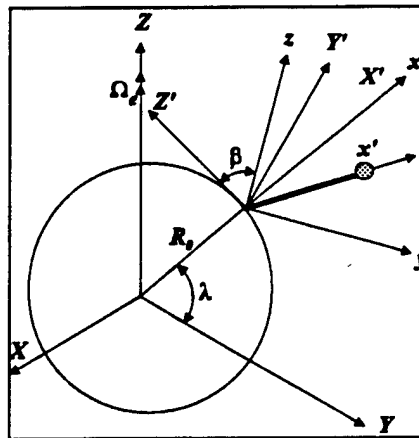


Figure 1: Earth and Tower Coordinate Systems

The system X, Y, Z is an inertial coordinate system, X', Y', Z' is attached to earth, where X' is normal to earth, Y' is directed to east and Z' is directed to the north. The coordinate system x, y, z is attached to earth. Its origin is at the tower's pivot, and it is rotated with an angle β about the X' direction with its y coordinate in the direction of the wave propagation. Therefore the tower's absolute angular velocity is,

$$\Omega_T = (\Omega \sin \lambda + \dot{\phi})\hat{x} + (\Omega \cos \lambda \sin \beta)\hat{y} + (\Omega \cos \lambda \cos \beta + \dot{\theta})\hat{z}, \quad (1)$$

where λ is the altitude angle and Ω is the angular velocity of earth.

External Fluid Forces and Moments

Fig. 2 depicts the external forces (except for gravity) acting on the tower. Those are; buoyancy, fluid forces due to drag, inertia, added mass and vortex shedding, wave slamming force and wind loads.

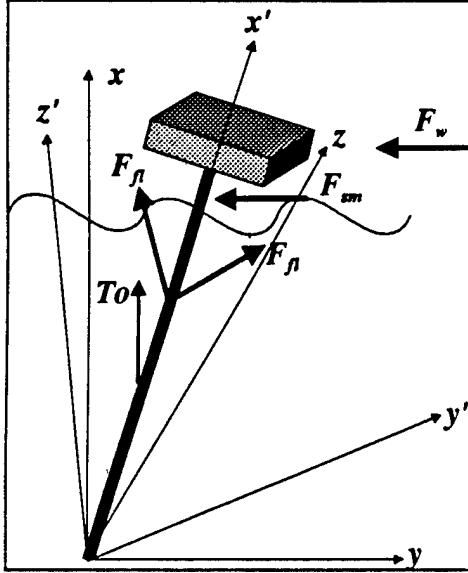


Figure 2: External Forces Acting on the Tower
Fluid Forces

In general, the fluid forces acting on a slender smooth tower submerged in the ocean are of four types: drag, inertia, vortex-shedding and wave slamming. The drag and inertia forces per unit length are approximated by Morison's equation. The drag force is proportional to the square of the relative velocity between the fluid and the tower, and the inertia force is proportional to the fluid acceleration,

$$\begin{aligned} F_{fl} = & C_M \rho \pi \frac{D^2}{4} \mathbf{l} \times \dot{\mathbf{U}}_w \times \mathbf{l} + \\ & C_D \rho \frac{D}{2} |\mathbf{l} \times (\mathbf{U}_w - \mathbf{V}) \times \mathbf{l}| \cdot \\ & \cdot (\mathbf{l} \times (\mathbf{U}_w - \mathbf{V}) \times \mathbf{l}), \end{aligned} \quad (2)$$

where F_{fl} is the fluid force per unit length normal to the tower, \mathbf{U}_w is the wave velocity vector, \mathbf{V}

is the tower's velocity vector, and $\dot{\mathbf{U}}_w$ is the fluid acceleration vector. C_D and C_M are the drag and inertia coefficients, respectively, D is the tower diameter, ρ is the water density, and \mathbf{l} is a unit vector of the directional cosines along which the tower is oriented.

The lift force F_L due to vortex shedding is acting in a direction normal to the wave velocity vector and normal to the tower. Different models of the lift force exist in the literature; see especially Billah [12]. We will initially use a simple model given in a paper by Dong (1991) [13], and Issacson (1988) [14],

$$\mathbf{F}_L = C_L \rho \frac{D}{2} \cos 2\omega t |\mathbf{l} \times \mathbf{U}_T| (\mathbf{l} \times \mathbf{U}_T), \quad (3)$$

where \mathbf{U}_T is the vector of the maximum velocity, along the tower, and C_L is the lift coefficient, and ω is the gravity wave frequency.

The parts of a structural member that are above the mean water level are exposed an impulsive force caused by wave slamming and wind loads. The wave slamming force per unit length has a similar form as the drag force (see Chakrabarti (1990) pp. 142-143 [15]),

$$\mathbf{F}_{sm} = C_S \rho \frac{D}{2} |\mathbf{l} \times \mathbf{U}_S \times \mathbf{l}| (\mathbf{l} \times \mathbf{U}_S \times \mathbf{l}), \quad (4)$$

where C_S , the slamming coefficient, has a theoretical value of π , but a typical mean value may be taken as 3.5 even though considerable scatter in this coefficient has been found in laboratory experiments. \mathbf{U}_S is the relative velocity between the fluid and the tower on the wave front at the point of impact. This force is assumed to be a periodic impulse with the wave period, and duration of $\tau_s = 0.01$ s, as described in Faltinsen pp. 282-285 [16].

The fluid moments due to drag, inertia, and lift, M_{fl}^θ , M_{fl}^ϕ , are evaluated via the virtual work principle to be

$$M_{fl}^\theta = \int_0^L \begin{pmatrix} -F_{flz} \tan \theta + F_{fl_y} \cos \phi + \\ F_{fl_x} \sin \phi \end{pmatrix} x dx$$

$$M_{fi}^\phi = \int_0^L \begin{pmatrix} -F_{fi_v} \tan \theta \sin \phi + \\ F_{fi_x} \tan \theta \cos \phi \end{pmatrix} x dx, \quad (5)$$

where L is the projection in the x direction of the submerged part of the tower. The moments due to wave slamming is evaluated by integrating the slamming force along the exposed part of the tower, from the mean water level d to the wave height $d + \frac{1}{2}H$,

$$M_{sm}^\theta = \int_d^{d+\frac{1}{2}H} \begin{pmatrix} -F_{sm_x} \tan \theta + F_{sm_v} \cos \phi + \\ F_{sm_x} \sin \phi \end{pmatrix} x dx$$

$$M_{sm}^\phi = \int_d^{d+\frac{1}{2}H} \begin{pmatrix} -F_{sm_v} \tan \theta \sin \phi + \\ F_{sm_x} \tan \theta \cos \phi \end{pmatrix} x dx. \quad (6)$$

Wind Loads

Wind loads are similar to current forces, i.e., drag and lift (vortex shedding). Both, the drag and lift force expressions are similar to those of the fluid. The drag force is,

$$\mathbf{F}_D^w = C_D^a \rho^a \frac{D}{2} \begin{bmatrix} |\mathbf{l} \times (\mathbf{u}_w - \mathbf{V}) \times \mathbf{l}| \cdot \\ (\mathbf{l} \times (\mathbf{u}_w - \mathbf{V}) \times \mathbf{l}) \end{bmatrix} \quad (7)$$

where C_D^a is the air drag coefficient, ρ^a is the air density and \mathbf{u}_w is the wind velocity vector given by

$$\mathbf{u}_w = u_w \cos \nu \hat{y} + u_w \sin \nu \hat{z}, \quad (8)$$

where ν is the direction between the wind propagation and the y axis. The lift force is,

$$\mathbf{F}_L^w = C_L^a \rho^a \frac{D}{2} \omega_w \cos t |\mathbf{l} \times \mathbf{u}_w| (\mathbf{l} \times \mathbf{u}_w), \quad (9)$$

where C_L^a is the air lift coefficient. The vortex shedding frequency ω_w is

$$\omega_w = \frac{0.2u_w}{D}. \quad (10)$$

The moments due to wind loads M_w^θ, M_w^ϕ are found in a similar way as the fluid moments (eqn. (5)), but with the integral going from d to $l \cos \theta$.

Additional External Moments

There are three additional moments acting on the tower, these are: buoyancy, added mass, and friction moment. The buoyancy moment is

$$M_b^\theta = \rho g \pi \frac{D^2}{4} \left[\frac{D^2}{32} \tan^2 \theta (2 \cos \theta + \sin \theta) + \frac{1}{2} \left(\frac{d + \eta(y,t)}{\cos \theta} \right)^2 \sin \theta \right], \quad (11)$$

where η is the wave height elevation. The added mass moments are

$$M_{ad}^\theta = \frac{1}{12} C_A \rho \pi \frac{D^2}{4} L^3 \left(\ddot{\theta} (1 + \tan^2 \theta) + \dot{\theta}^2 \tan \theta \right)$$

$$M_{ad}^\phi = \frac{1}{12} C_A \rho \pi \frac{D^2}{4} L^3 \left(\ddot{\phi} \tan^2 \theta + 2\dot{\theta}\dot{\phi} \tan \theta \right) \quad (12)$$

where $C_A = C_M - 1$ is the added mass coefficient. Finally the coulomb friction moments are,

$$M_{fr}^\theta = R_h N \mu [\text{sgn}(\dot{\theta})]$$

$$M_{fr}^\phi = R_h \sin \theta N \mu [\text{sgn}(\dot{\phi})], \quad (13)$$

where R_h is the hinge radius, and N the normal force.

Governing Equations of Motion

The governing nonlinear differential equations of motion are found by equating the dynamic moments, M_{dy}^θ and M_{dy}^ϕ , that are evaluated in the left hand side of Lagrange's equations, to the applied external moments, that are found by adding equations (11),(5),(12), and (13),

$$J_{eff}^\theta \ddot{\theta} + C\dot{\theta} + I_g \sin 2\theta \left(\frac{(\Omega \sin \lambda + \dot{\phi})^2}{(\Omega \cos \lambda \sin \beta)^2} - \right)$$

$$= M_{fi}^\theta + M_{sm}^\theta - M_{gb}^\theta - M_{fr}^\theta \quad (14)$$

$$J_{eff}^\phi \ddot{\phi} + C\dot{\phi} + I_g (\Omega \sin \lambda + \dot{\phi}) \dot{\theta} \sin 2\theta$$

$$= M_{fi}^\phi + M_{sm}^\phi - M_{fr}^\phi,$$

where J_{eff}^θ and J_{eff}^ϕ are the effective moments of inertia which are position dependent, I_g is a constant depending on the system parameters, and M_{gb}^θ is the moment due to gravity and buoyancy.

Numerical Solution

In this section, the influence of the rotation of the earth, wind loads, and wave slamming loads, on response of the tower is determined. The governing nonlinear differential equations of motion (17) are solved using 'ACSL' and the results are then analyzed using 'MATLAB'. The fluid's coefficients, the wave height, and the wave frequency used in the simulations are taken from Hogben et al. 1977 [17] and the wind drag and lift coefficients are taken from Van Nunen et al. [18]. The following physical parameters are used in the simulation: C_D^α - Air drag coefficient = 0.8, C_L^α - Lift coefficient = 0.4, u_w - Wind velocity = 20 (m/s), C_s - Wave slamming coefficient = 3.5. All other parameters can be found in the previous paper by Bar-Avi and Benaroya [2]. In our study the wave height H is much smaller the mean water level d , i.e., $\frac{H}{d} < 0.01$. Therefore, the relation between the wave height and the wave frequency, given in Hooft (1981) [19] is used. This relation with the deep water simplification $\tanh kd = 1$, leads to

$$\omega = \sqrt{\frac{\pi}{2H}} \quad (15)$$

where ω is the wave frequency.

Wave Slamming

As mentioned earlier, the wave slamming force is a periodic impulsive force. The pulse duration is set to be $\tau_s = 0.01$ s and the period is the same as the wave's period. The response due to an impulsive load depends on the pulse duration, and it can be twice as high as a quasistatic load having the same magnitude. In this study the wave period is much higher than the impulse duration, $\frac{\tau_s}{\tau_n} = 0.0026$, ($\tau_n = \frac{2\pi}{\omega_n}$), hence the deflection angle response due to wave slamming is attenuated and expected to

be 100 times lower than if the load was quasistatic (see Shock [20]). For an articulated tower modeled as an elastic beam that has high frequencies, wave slamming can cause higher deflections especially if its period coincides with one of the tower's modes.

Fig. 3 shows the response in the time domain due to wave slamming only; (a) is the deflection angle response θ and (b) is the rotation angle response ϕ . In this run the fluid coefficient C_D, C_M, C_L , are set to zero. The deflection angle θ is very small, on the order of 10^{-5} , as expected.

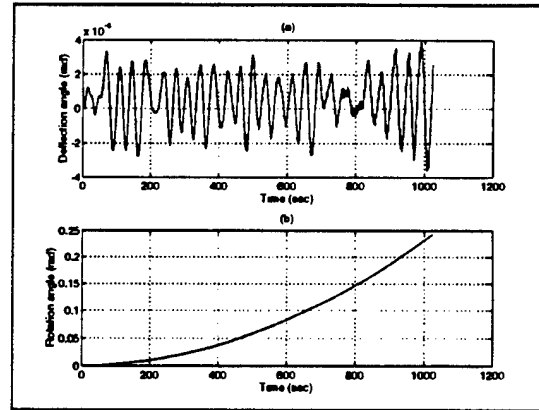


Figure 3: Tower's Response due to Wave Slamming. (a) Deflection Angle θ . (b) Rotation Angle ϕ .

Fig. 4 depicts the tower's end motion (a) and the frequency response (b). The tower oscillates about $(y, z) = (0, 0)$ since there are not any constant moments that cause a shift in the equilibrium position. From the frequency response two frequencies are seen; one is the natural frequency $\omega_n = 0.026$ Hz, and the wave frequency $\omega = 0.11$ Hz that correspond the one calculated by eq. 15 for $H = 3$ m.

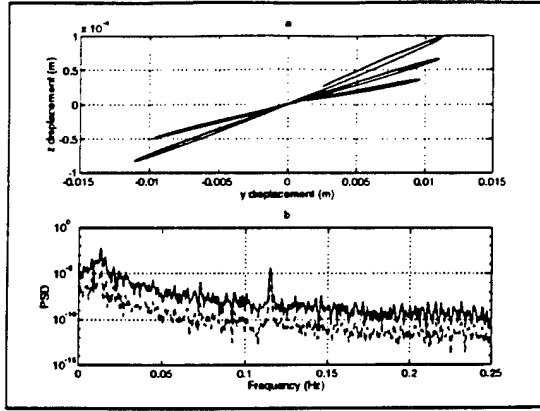


Figure 4: Tower's Response due to Wave Slamming. (a) Tower's End Motion. (b) Tower's Frequency Response.

Coriolis Force

The rotation of the earth causes an additional moment, due to the Coriolis force. Hence it affects the response of tower. These maximum moments are

$$\begin{aligned} M_{co}^{\theta} &= I_g \sin 2\theta (\Omega + \dot{\phi})^2 \\ M_{co}^{\phi} &= I_g \sin 2\theta (\Omega + \dot{\phi}) \dot{\theta} \end{aligned} \quad (16)$$

where $M_{co}^{\theta}, M_{co}^{\phi}$ are the generalized gyroscopic moments for θ and ϕ coordinates, respectively. These moments are small ($\sim 10^4$ N-m) and their effect on the response is expected to be small, but the uniqueness of this load is that it couples the two generalized coordinates, so that a motion in one direction will cause a response in the other. Fig. 5 describes the tower's response due to Coriolis force only. Fig. 5 (a) shows the deflection angle θ , (b) is the rotation angle and (c) its motion in the y, z plane. It is clearly seen that the response is not planar ($\phi \neq 0$), due to the gyroscopic moments.

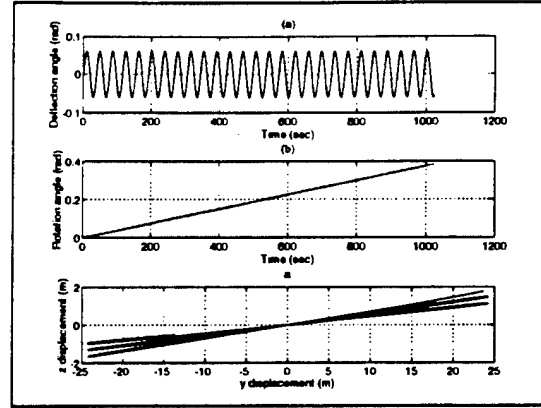


Figure 5: Tower's Response Due to Coriolis Force. (a) Deflection Angle θ . (b) Rotation Angle ϕ . (c) Tower's End Motion.

Wind Loads

Out of the three different types of loading discussed in this paper, wind loads have the largest effect on the tower's response. Although the magnitude of this load is close to wave slamming (both are $\sim 5 \times 10^7$ N-m), its influence is much higher because of its quasistatic nature while the other is impulsive with a very short duration relative to the tower's natural period. Figs.6 shows the tower's response due to wind propagating in the y direction, i.e., $\nu = 0$ deg. The deflection angle θ (a,c) oscillates at the natural frequency, $\omega_n = 0.026$ Hz, about a nonzero position caused by the wind drag force, while the rotation angle ϕ oscillates at the natural frequency and the vortex shedding frequency given by eq. 10, which in this case is $\omega_w = 0.042$ Hz, as can be seen from Fig. 6 (b,d).

When $\nu = 90$ deg, the situation is reversed, as shown in Fig. 7 (a,b,c,d). The deflection angle θ oscillates in both, the natural and vortex shedding frequencies and the rotation angle ϕ undergoes a DC motion with a low amplitude oscillations in the natural frequency.

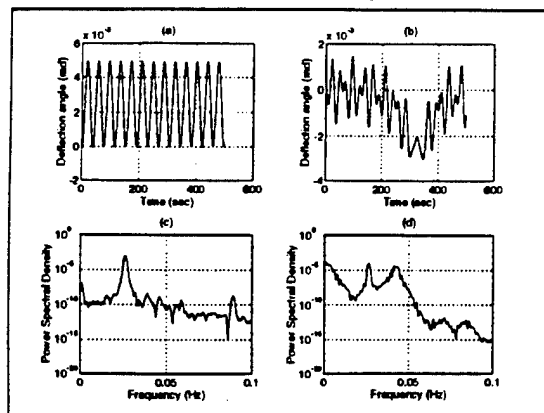


Figure 6: Tower's Response Due to Wind Load, $\nu = 0$. (a,c) - Deflection angle θ in Time and Frequency Domain. (b,d) - Rotation angle ϕ in Time and Frequency Domain.

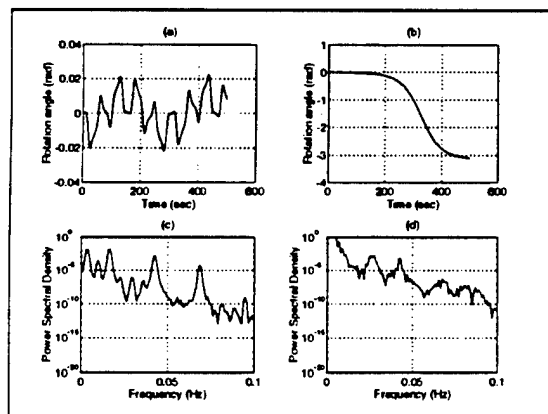


Figure 7: Tower's Response Due to Wind Load, $\nu = 0$. (a,c) - Deflection angle θ in Time and Frequency Domain. (b,d) - Rotation angle ϕ in Time and Frequency Domain.

Fig. 8 describes the tower's end motion for $\nu = 0$ deg (a), and for $\nu = 90$ deg (b). The difference between the responses is seen.

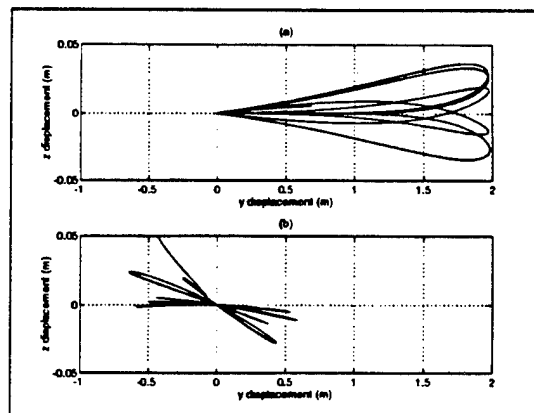


Figure 8: Tower's End Motion. (a) For $\nu = 0$ deg. (b) For $\nu = 90$ deg.

Discussion and Summary

The nonlinear differential equations of motion for a two degree of freedom articulated tower submerged in the ocean are derived. Coriolis force, due to earth rotation, wave slamming, and wind loads are included in the derivation. All forces are evaluated at the instantaneous position of the tower. The equations are solved numerically using 'ACSL' to determine the tower's response to wave slamming, Coriolis and wind loads.

Although the magnitude of the wave slamming load is almost the same as the wind load, the later has a larger effect on the tower's response. The reason is that the impulse duration of the wave slamming force is very short compared to the natural period of the structure. Hence the response is attenuated.

The Coriolis force due the earth rotation, although of small influence on the response, is important since it causes a coupling between the two angles; that means that pure planar motion is not possible under real conditions.

At the present time, a parametric study is being performed on the two degree of freedom model. The response due to combination of forces such as wave, current (colinear and otherwise), impact, wind and earth rotation is investigated and results will be published in the near future. Work is also proceeding on an elastic articulated tower.

Acknowledgment

This work is supported by the Office of Naval Research Grant no. N00014 - 93 - 1 - 0763. The first author is grateful for the ONR sponsored Fellowship, and the second author for additional support.

References

- 1 P. Bar-Avi and H. Benaroya. Stochastic response of an articulated tower. *International Journal of Nonlinear Mechanics*, Submitted for publication 1995.
- 2 P. Bar-Avi and H. Benaroya. Nonlinear dynamics of an articulated tower submerged in the ocean. *Journal of Sound and Vibration (send for publication)*, 1994.
- 3 P. Bar-Avi and H. Benaroya. Dynamic response of an articulated tower to random waves and current loads. In *Third International Conference on Stochastic Structural Dynamics*, 1995.
- 4 S.K. Chakrabarti and D.C. Cotter. Motion analysis of articulated tower. *Journal of the Waterway, Port, Coastal and Ocean Division, ASCE*, 105:281 - 292, 1979.
- 5 O. Gottlieb, C.S. Yim, and R.T. Hudspeth. Analysis of nonlinear response of an articulated tower. *International Journal of Offshore and Polar Engineering*, 2(1):61 - 66, 1992.
- 6 P.K. Muhuri and A.S. Gupta. Stochastic stability of tethered buoyant platforms. *Ocean Engineering*, 10(6):471 - 479, 1983.
- 7 K. Jain and T.K. Datta. Stochastic response of articulated towers. In *Deep Offshore Technology 4th International Conference and Exhibit*, 1987.
- 8 T.K. Datta and A.K. Jain. Response of articulated tower platforms to random wind and wave forces. *Computers and Structures*, 34(1):137 - 144, 1990.
- 9 A.K. Jain and T.K. Datta. Nonlinear behavior of articulated tower in random sea. *Journal of Engineering for Industry*, 113:238 - 240, 1991.
- 10 S.K. Chakrabarti and D.C. Cotter. Transverse motion of articulated tower. *Journal of the Waterway, Port, Coastal and Ocean Division, ASCE*, 107:65 - 77, 1980.
- 11 R.K. Jain and C.L. Kirk. Dynamic response of a double articulated offshore loading structure to noncollinear waves and current. *Journal of Energy Resources Technology*, 103:41 - 47, 1981.
- 12 K.Y.R. Billah. *A Study of Vortex-Induced Vibration*. PhD thesis, Princeton University, 1989.
- 13 Y. Dong Y and J.Y.K. Lou. Vortex-induced nonlinear oscillation of tension leg platform tethers. *Ocean Engineering*, 18(5):451 - 464, 1991.
- 14 M. Issacson. Wave and current forces on fixed offshore structure. *Canadian Journal Civil Engineering*, 15:937 - 947, 1988.
- 15 S.K. Chakrabarti. *Nonlinear Methods in Offshore Engineering*. Elsevier Science Publishing Company Inc., 1990.
- 16 O.M. Faltinsen. *Sea Loads on Ships and Offshore Structures*. Cambridge University Press, 1994.
- 17 N. Hogben, B.L. Miller, J.W. Searle, and G. Ward. Estimation of fluid loading on off-

shore structures. *proceeding of civil Engineering*, pages 515-562, 1977.

- 18 J.W.G. Van Nunen, A.J. Person, and H. Tijde-
man. Analysis of steady and unsteady pressure
and force measurements on... Technical report,
National Aerospace Laboratory - The Nether-
lands, 1971.
- 19 J.P. Hooft. *Advanced Dynamics of Marine
Structures*. John Wiley and Sons, 1982.
- 20 C. M. Harris. *Shock and Vibration Handbook*.
McGraw-Hill, 1987.
- 21 S.K. Chakrabarti. *Hydrodynamics of Offshore
Structures*. Computational Mechanics Publica-
tions, 1987.
- 22 M.H. Patel. *Dynamics of Offshore Structures*.
Butterworths, 1988.

Response of an Articulated Tower to Wave Slamming, Wind and Coriolis Acceleration

P. Bar-Avi and H. Benaroya

Department of Mechanical and Aerospace Engineering

RUTGERS University

The 36th AIAA/ASME/ASCE/AHS/ASC

SDM Conference, April 10, 1995

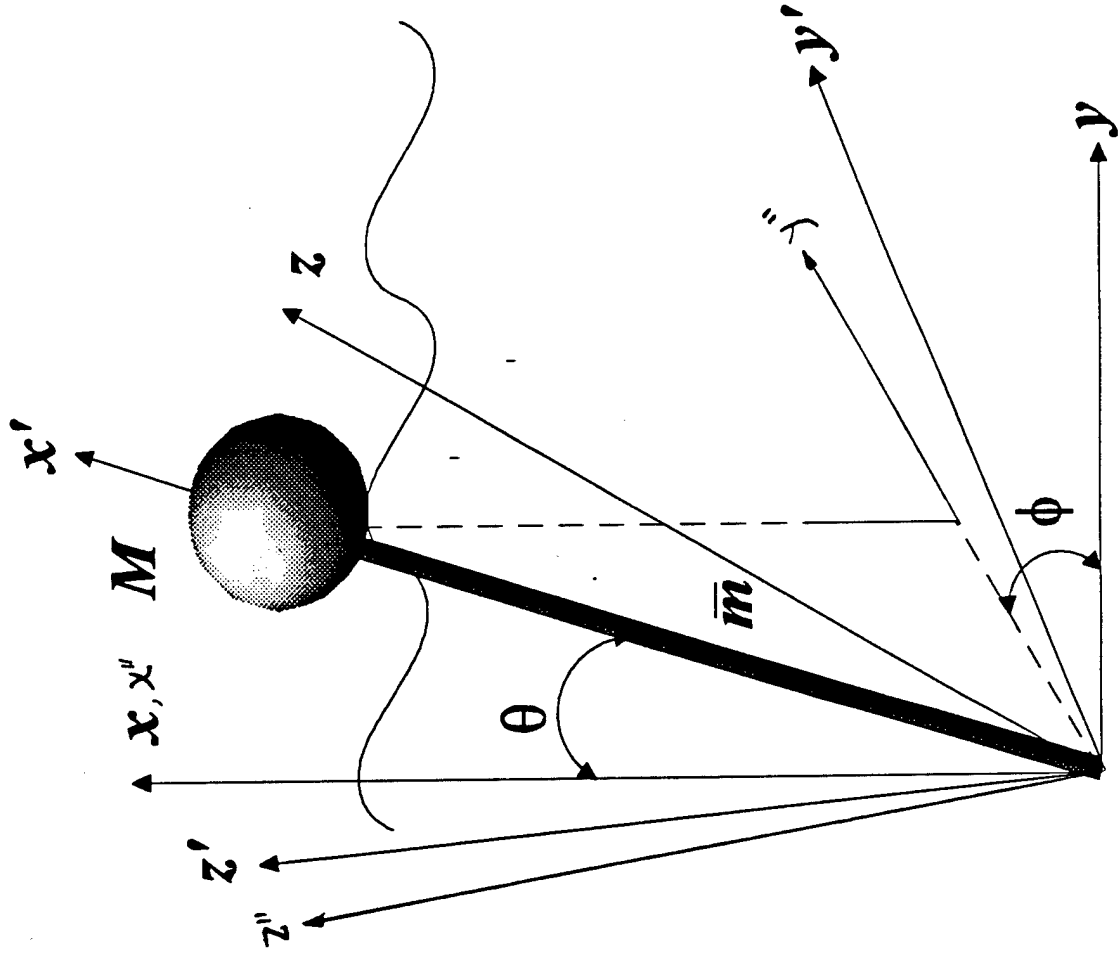
This work is sponsored by the Office of Naval Research



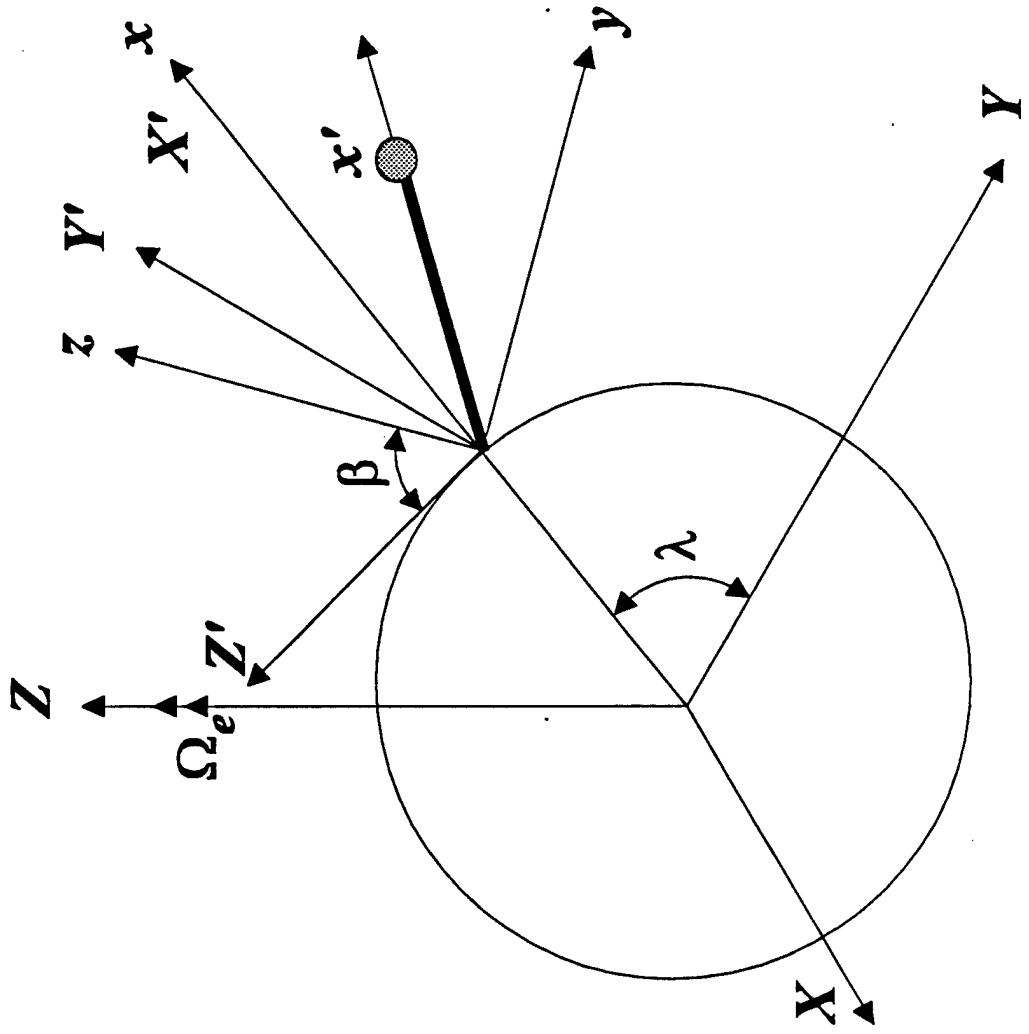
Outline

- Problem Description
- Equations of Motion - Assumptions and Derivation
- Results
- Summary
- Current Study

Problem Description



Coordinate Systems



Equations of Motion

Assumptions

- Linear wave theory.
- Deterministic Fluid Constants.
- The end mass has no volume.
- Rigid body, EI infinitely large.
- Smooth and slender tower.

Lagrange's Equation

$$\frac{d}{dt} \left(\frac{\partial K_E}{\partial \dot{q}_i} \right) - \frac{\partial K_E}{\partial q_i} + \frac{\partial P_E}{\partial q_i} + \frac{\partial D_E}{\partial \dot{q}_i} = Q_{q_i}$$

Kinematics

Wave and Current

Current velocity

$$U_c(x) = U_c^t \left(\frac{x}{d} \right)^{\frac{1}{7}} + U_c^w \left(\frac{x}{d} \right).$$

Total velocities

$$w = \frac{1}{2} H \omega \frac{\sinh kx}{\sinh kd} \sin(kx \tan \theta \cos \phi - \omega t)$$

$$u = \frac{1}{2} H \omega \frac{\cosh kx}{\sinh kd} \cos(kx \tan \theta \cos \phi - \omega t) + U_c \cos \alpha$$

$$v = U_c \sin \alpha,$$

Total accelerations

$$\dot{w} = \frac{1}{2} H \omega \left(-\omega + \dot{\theta} \frac{kx \cos \phi}{\cos^2 \theta} - \dot{\phi} kx \tan \theta \sin \phi \right) \frac{\sinh kx}{\sinh kd} \cos(kx \tan \theta \cos \phi - \omega t)$$

$$\dot{u} = -\frac{1}{2} H \omega \left(-\omega + \dot{\theta} \frac{kx \cos \phi}{\cos^2 \theta} - \dot{\phi} kx \tan \theta \sin \phi \right) \frac{\cosh kx}{\sinh kd} \sin(kx \tan \theta \cos \phi - \omega t)$$

$$\dot{v} = 0.$$

Kinematics

Position, velocity, acceleration

$$\mathbf{R} = x\hat{x} + x \tan \theta \cos \phi \hat{y} + x \tan \theta \sin \phi \hat{z}$$

$$\mathbf{V} = -x\dot{\theta} \tan \theta \hat{x} + x(\dot{\theta} \cos \phi - \dot{\phi} \tan \theta \sin \phi) \hat{y} + x(\dot{\theta} \sin \phi + \dot{\phi} \tan \theta \cos \phi) \hat{z}$$

$$\dot{\mathbf{V}} = -x(\ddot{\theta} \tan \theta + \dot{\theta}^2) \hat{x} +$$

$$x[\ddot{\theta} \cos \phi - \ddot{\phi} \tan \theta \sin \phi - (\dot{\theta}^2 + \dot{\phi}^2) \tan \theta \cos \phi - 2\dot{\theta}\dot{\phi} \sin \phi] \hat{y} +$$

$$x[\ddot{\theta} \sin \phi + \ddot{\phi} \tan \theta \cos \phi - (\dot{\theta}^2 + \dot{\phi}^2) \tan \theta \sin \phi + 2\dot{\theta}\dot{\phi} \cos \phi] \hat{z}.$$

Angular velocity

$$\Omega_T = (\Omega \sin \lambda + \dot{\phi}) \hat{x}'' + (\Omega \cos \lambda \sin \beta \cos \phi) \hat{y}'' + (\Omega \cos \lambda \cos \beta \sin \phi + \dot{\theta}) \hat{z}''$$



Energies

$$\begin{aligned} K_E &= \frac{1}{2} \left(\left(\frac{1}{3} \bar{m} l + M \right) l^2 \sin^2 \theta + \frac{1}{2} (\bar{m} l + M) \frac{D^2}{4} \cos^2 \theta \right) (\Omega \sin \lambda + \dot{\phi})^2 + \\ &\frac{1}{2} \left(\left(\frac{1}{3} \bar{m} l + M \right) l^2 \cos^2 \theta + \frac{1}{2} (\bar{m} l + M) \frac{D^2}{4} \sin^2 \theta \right) (\Omega \cos \lambda \sin \beta \cos \phi)^2 + \\ &\frac{1}{2} \left(\frac{1}{3} \bar{m} l + M \right) l^2 (\Omega \cos \lambda \cos \beta \sin \phi + \dot{\theta})^2 \end{aligned}$$

$$P_E = \left(\frac{1}{2} \bar{m} l + M \right) g l \cos \theta$$

$$D_E = \frac{1}{2} C (\dot{\phi}^2 + \dot{\theta}^2)$$

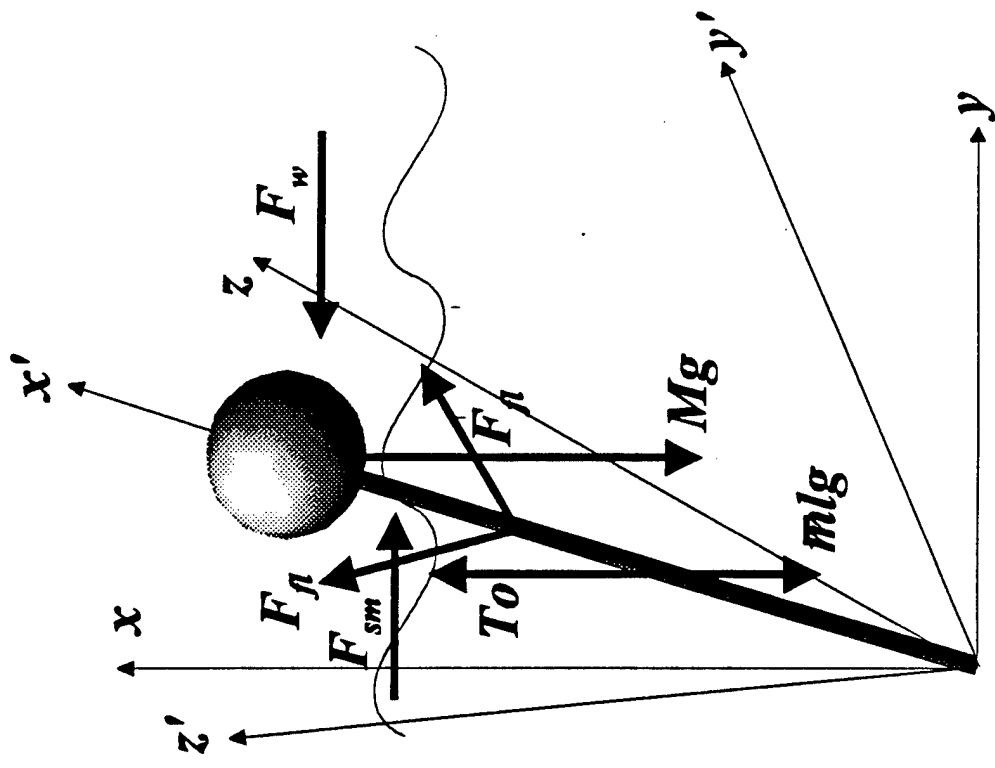
Dynamic Moments

$$M_{dy}^{\theta} = \left(\frac{1}{3}\bar{m}l + M\right)l^2\ddot{\theta} + C\dot{\theta} - \left(\frac{1}{2}\bar{m}l + M\right)gl \sin \theta + \left[\frac{l^2}{2}\left(\frac{1}{3}\bar{m}l + M\right) - \frac{D^2}{16}(\bar{m}l + M)\right] \sin 2\theta \left[(\Omega \sin \lambda + \dot{\phi})^2 + (\Omega \cos \lambda \sin \beta \cos \phi)^2\right]$$

$$M_{dy}^{\phi} = \left(\frac{1}{3}\bar{m}l + M\right)l^2 \sin^2 \theta + \frac{1}{8}(\bar{m}l + M)D^2 \cos^2 \theta \ddot{\phi} + C\dot{\phi} + \left[\frac{l^2}{2}\left(\frac{1}{3}\bar{m}l + M\right) - \frac{D^2}{8}(\bar{m}l + M)\right] \sin 2\theta \left[\Omega \sin \lambda + \dot{\phi}\right] \dot{\theta} - \frac{1}{2}I_{y'} (\Omega \cos \lambda \sin \beta)^2 \sin 2\phi + I_{z'} \left(\frac{1}{2}\Omega \cos \lambda \cos \beta \sin 2\phi + \dot{\theta}\Omega \cos \lambda \cos \beta \cos \phi\right)$$

Applied Forces

- Fluid forces: Drag, Inertia, Added mass
- Wave Slamming
- Wind force
- Coriolis force due to earth rotation
- Buoyancy



External Moments

Buoyancy

$$M_b^\theta = \rho g \pi \frac{D^2}{4} \left[\frac{D^2}{32} \tan^2 \theta (2 \cos \theta + \sin \theta) + \frac{1}{2} \left(\frac{d + \eta(y, t)}{\cos \theta} \right)^2 \sin \theta \right]$$

Added Mass

$$M_{ad}^\theta = \frac{1}{12} C_{A\rho\pi} \frac{D^2}{4} L^3 (\ddot{\theta} (1 + \tan^2 \theta) + \dot{\phi}^2 \tan \theta)$$

$$M_{ad}^\phi = \frac{1}{12} C_{A\rho\pi} \frac{D^2}{4} L^3 (\ddot{\phi} \tan^2 \theta + 2\dot{\theta}\dot{\phi} \tan \theta)$$

Friction

$$M_{fr}^\theta = R_h N \mu [\text{sgn}(\dot{\theta})] \quad M_{fr}^\phi = R_h \sin \theta N \mu [\text{sgn}(\dot{\phi})]$$

$$N = \left[\frac{1}{8} C_{A\rho\pi} D^2 \frac{L^2}{\cos^2 \theta} + \frac{1}{2} \left(\frac{1}{2} \bar{m} l + M \right) l \right] (\dot{\theta}^2 + \frac{1}{2} \dot{\phi}^2) - \left[\frac{1}{8} C_{A\rho\pi} D^2 L^2 + \frac{1}{2} \left(\frac{1}{2} \bar{m} l + M \right) l \cos 2\theta \right] \frac{1}{2} \dot{\phi}^2 + (T_0 - F_g) \cos \theta$$

Fluid Forces

Drag Force

$$\mathbf{F}_{fl}^D = C_D \rho \frac{D}{2} |\mathbf{1} \times (\mathbf{U}_w - \mathbf{V}) \times \mathbf{1}| |(\mathbf{1} \times (\mathbf{U}_w - \mathbf{V}) \times \mathbf{1})|$$

Inertia Force

$$\mathbf{F}_{fl}^M = C_M \rho \pi \frac{D^2}{4} \mathbf{1} \times \dot{\mathbf{U}}_w \times \mathbf{1}$$

Vortex-Shedding (Lift) Force

$$\mathbf{F}_L = C_L \rho \frac{D}{2} \cos \omega_s t |\mathbf{1} \times \mathbf{U}_T| |(\mathbf{1} \times \mathbf{U}_T)|$$

Wave Slamming Force

$$\mathbf{F}_{sm} = C_{sp} \rho \frac{D}{2} |\mathbf{1} \times \mathbf{U}_s \times \mathbf{1}| |(\mathbf{1} \times \mathbf{U}_s \times \mathbf{1})|$$

Fluid Moments

$$M_{fl}^{\theta} = \int_0^L \left(-F_x^{fl} \tan \theta + F_y^{fl} \cos \phi + F_z^{fl} \sin \phi \right) x dx$$

$$M_{fl}^{\phi} = \int_0^L \left(-F_y^{fl} \tan \theta \sin \phi + F_z^{fl} \tan \theta \cos \phi \right) x dx$$

$$M_{sm}^{\theta} = \int_d^{d+\frac{1}{2}H} \left(-F_x^{sm} \tan \theta + F_y^{sm} \cos \phi + F_z^{sm} \sin \phi \right) x dx$$

$$M_{sm}^{\phi} = \int_d^{d+\frac{1}{2}H} \left(-F_y^{sm} \tan \theta \sin \phi + F_z^{sm} \tan \theta \cos \phi \right) x dx$$



Wind Moments

$$\mathbf{F}_D^w = C_D^a \rho^a \frac{D}{2} [|\mathbf{1} \times (\mathbf{u}_w - \mathbf{V}) \times \mathbf{1}| (\mathbf{1} \times (\mathbf{u}_w - \mathbf{V}) \times \mathbf{1})]$$

$$\mathbf{F}_L^w = C_L^a \rho^a \frac{D}{2} \cos \omega_w t |\mathbf{1} \times (\mathbf{u}_w - \mathbf{V})| (\mathbf{1} \times (\mathbf{u}_w - \mathbf{V}))$$

$$\omega_w = \frac{St u_w}{D}$$

$$M_w^\theta = \int_d^{l \cos \theta} (-F_x^w \tan \theta + F_y^w \cos \phi + F_z^w \sin \phi) x dx$$

$$M_w^\phi = \int_d^{l \cos \theta} (-F_y^w \tan \theta \sin \phi + F_z^w \tan \theta \cos \phi) x dx$$

Nonlinear Equations of Motion

$$\begin{aligned}
 & J_{eff}^{\theta} \ddot{\theta} + C \dot{\theta} + I_g \left[(\Omega \sin \lambda + \dot{\phi})^2 + (\Omega \cos \lambda \sin \beta \cos \phi)^2 \right] + M_{gb}^{\theta} \\
 & = M_{fl}^{\theta} + M_{sm}^{\theta} + M_w^{\theta} - M_{fr}^{\theta}
 \end{aligned}$$

$$\begin{aligned}
 & J_{eff}^{\phi} \ddot{\phi} + C \dot{\phi} + I_g \left[\Omega \sin \lambda + \dot{\phi} \right] \dot{\theta} + \frac{1}{2} I_{y'} (\Omega \cos \lambda \sin \beta)^2 \sin 2\phi + \\
 & I_{z'} \left(\frac{1}{2} \Omega \cos \lambda \cos \beta \sin 2\phi + \dot{\theta} \Omega \cos \lambda \cos \beta \cos \phi \right) \\
 & = M_{fl}^{\phi} + M_{sm}^{\phi} + M_w^{\phi} - M_{fr}^{\phi}
 \end{aligned}$$

where

$$J_{eff}^{\theta} = \left(\frac{1}{3} \bar{m}l + M \right) l^2 + \frac{1}{12} C_A \rho \pi D^2 L^3 (1 + \tan^2 \theta)$$

$$J_{eff}^{\phi} = \left(\frac{1}{3} \bar{m}l + M \right) l^2 \sin^2 \theta + \frac{1}{4} (\bar{m}l + M) D^2 \cos^2 \theta + \frac{1}{12} C_A \rho \pi D^2 L^3 \tan^2 \theta$$

$$I_g = \left(l^2 \frac{1}{2} \left(\frac{1}{3} \bar{m}l + M \right) - \frac{D^2}{8} (\bar{m}l + M) \right) \sin 2\theta$$

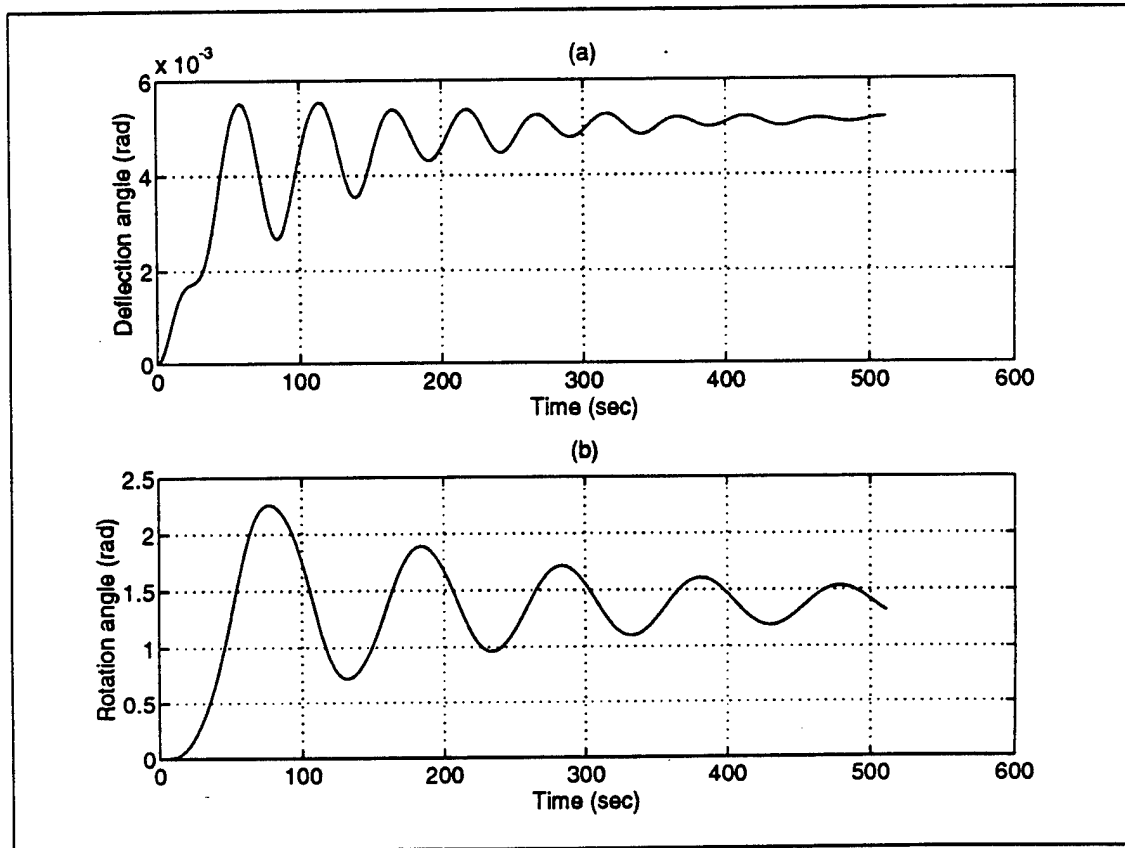
$$M_{gb}^{\theta} = \rho g \pi \frac{D^2}{4} \left[\frac{D^2}{32} \tan^2 \theta (2 \cos \theta + \sin \theta) + \frac{1}{2} \left(\frac{d + \eta(y, t)}{\cos \theta} \right)^2 \sin \theta \right] - \left(\frac{1}{2} \bar{m}l + M \right) gl \sin \theta$$

Results

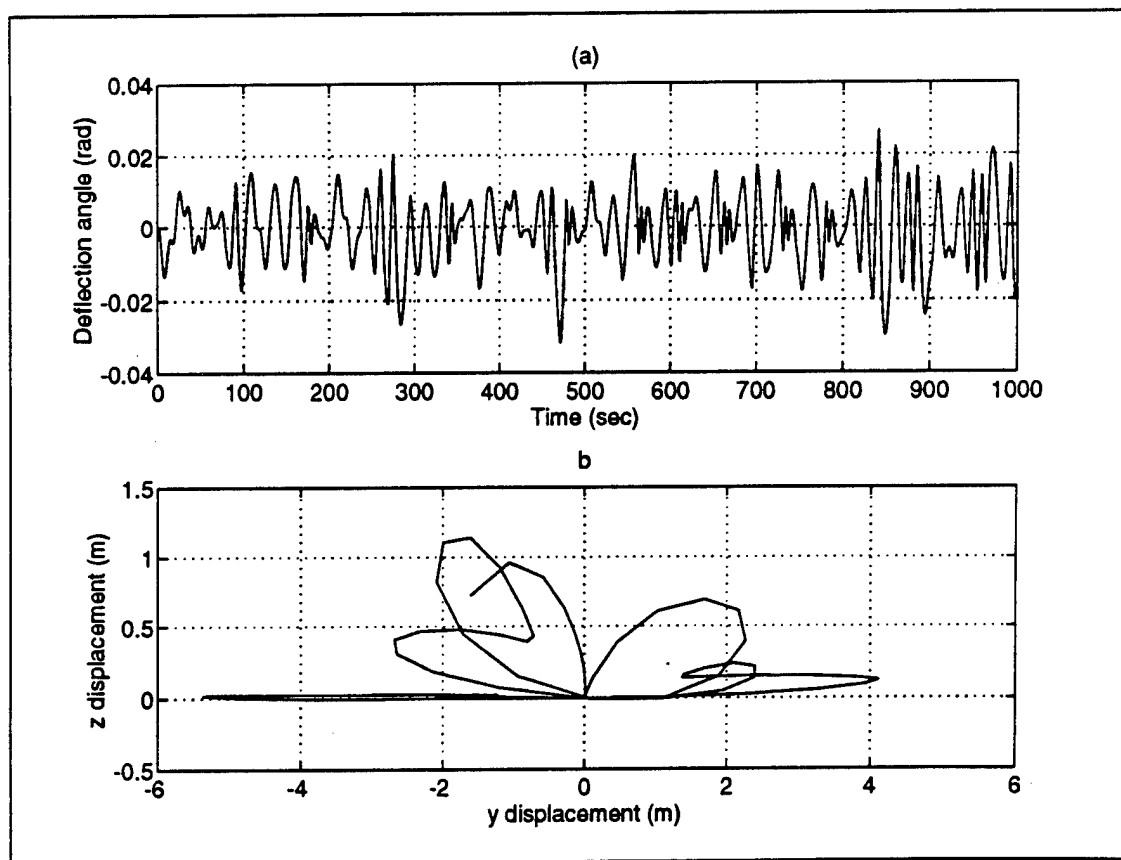
Physical Parameters

- Length = 400 m
- Diameter = 15 m
- Water level = 350 m
- End mass = 250 ton
- Tower's mass = 20 ton/m
- Current velocity = 0-2 m/s
- Wind velocity = 20 m/s
- $C_D = 1.0$
- $C_M = 1.5$
- $C_L = 1.0$
- $C_s = 3.5$
- $H = 5$ m
- $v = 0^\circ$ or 90°

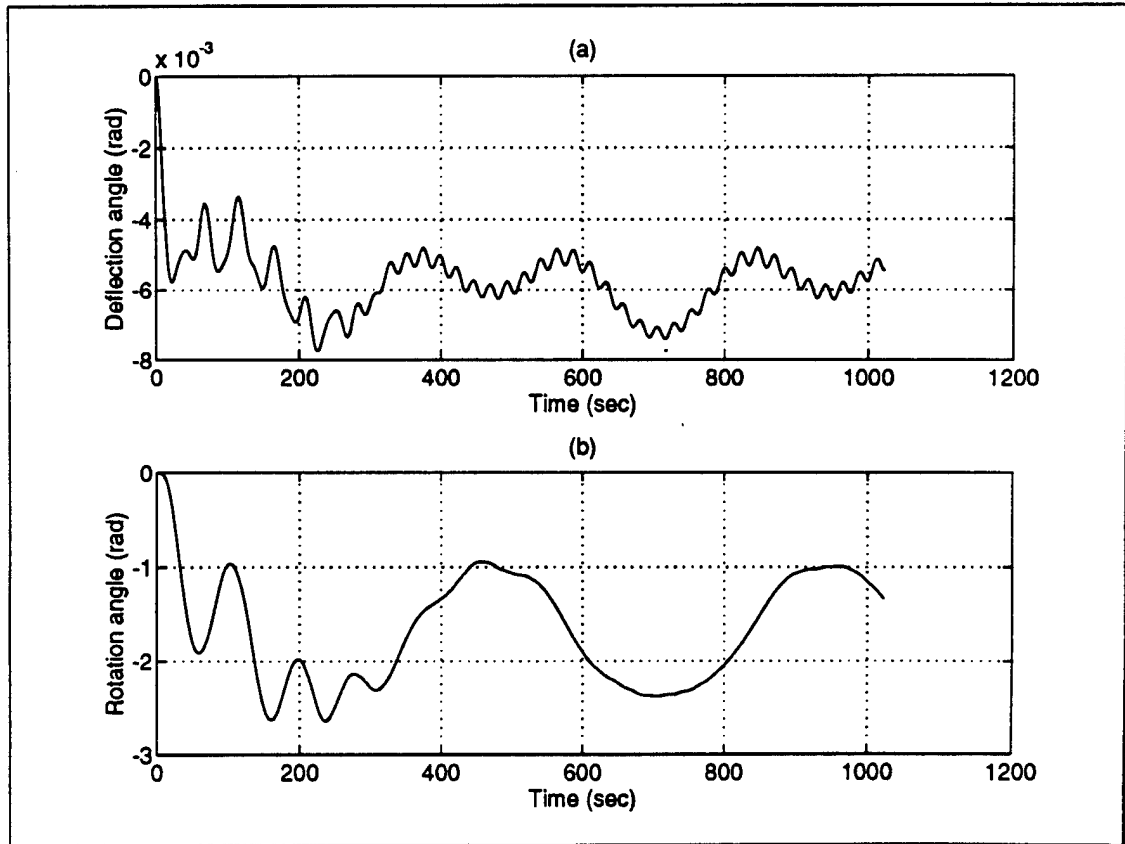
Equilibrium position due to wind and current $C_L = 0$



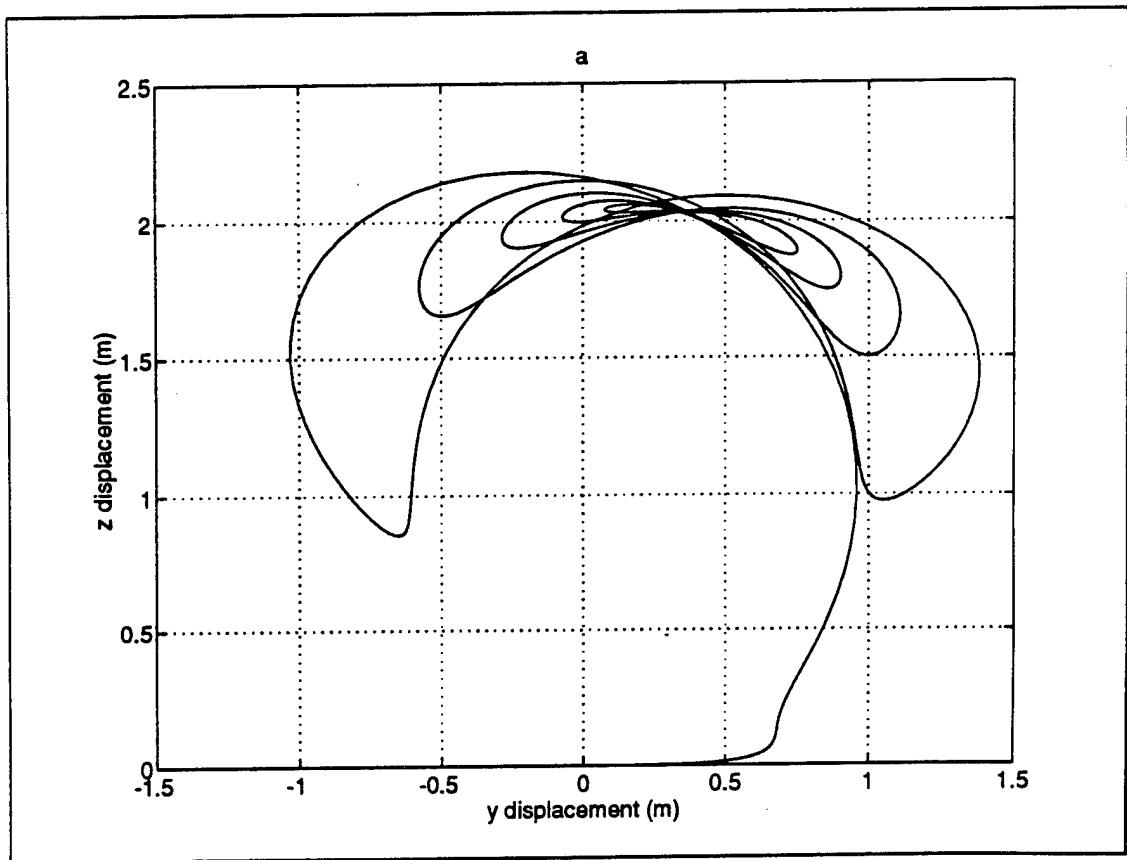
Response to wave load - $H = 5$ m



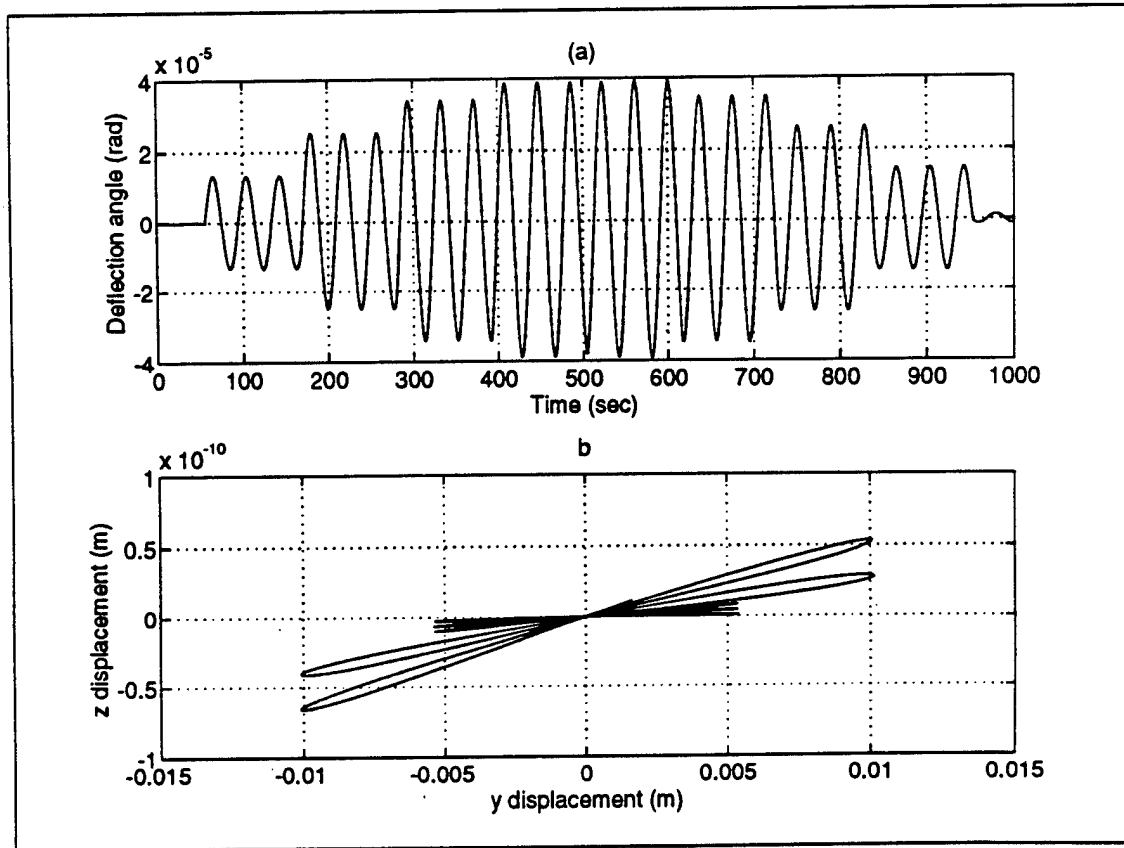
Equilibrium position due to wind and current $C_L = 1$



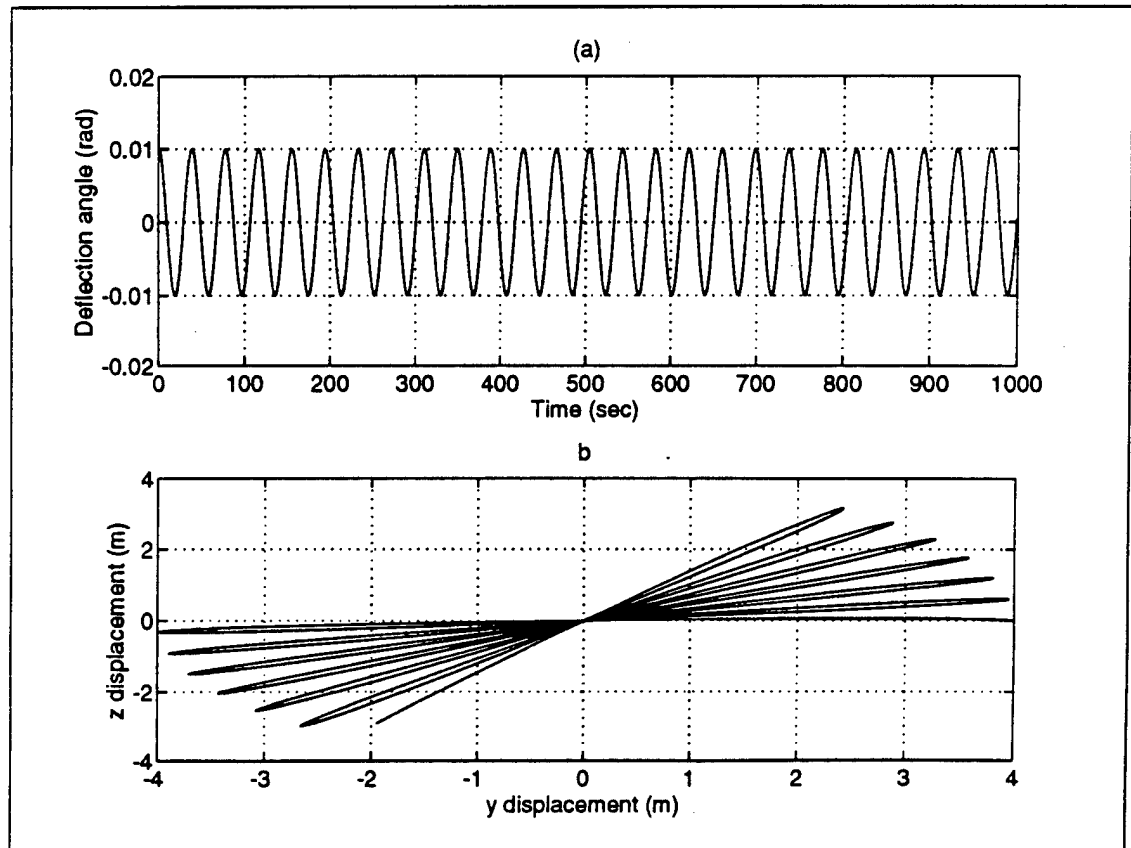
Equilibrium position due to wind and current $C_L = 0$



Response to earth rotation and wave slamming

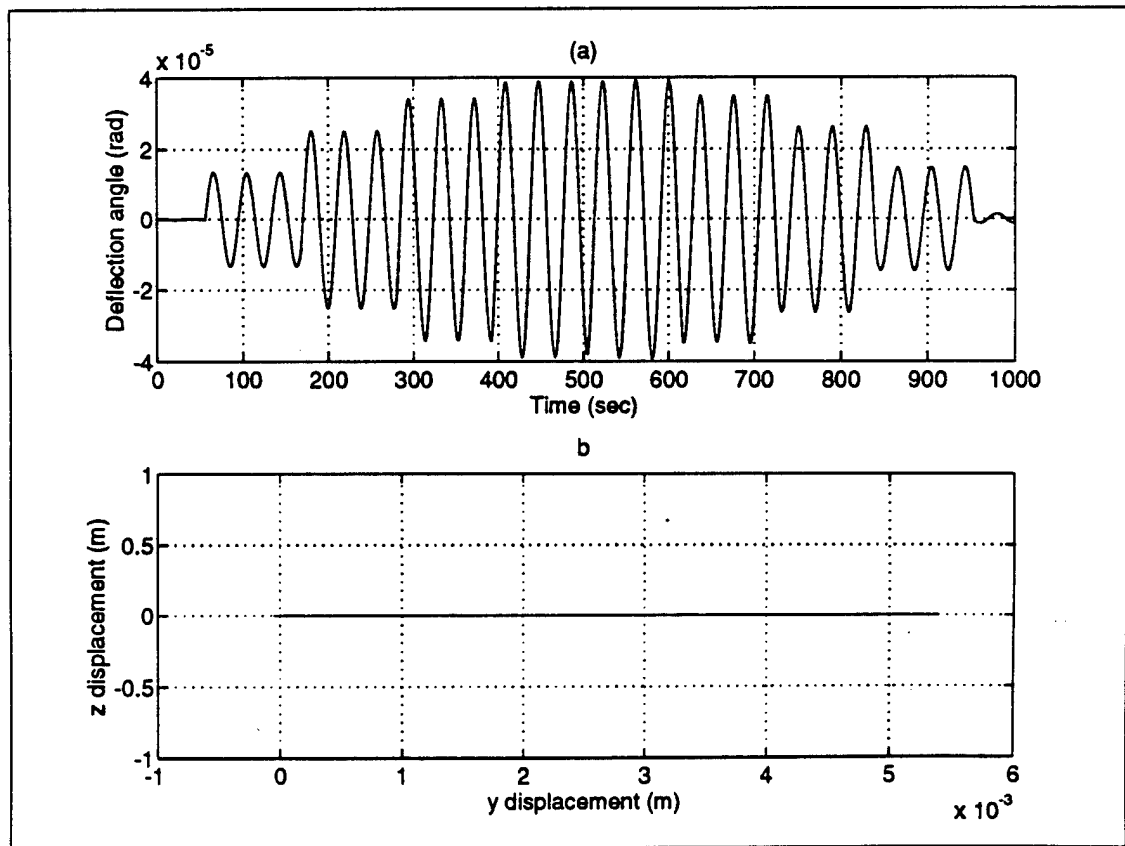


Response to earth rotation only



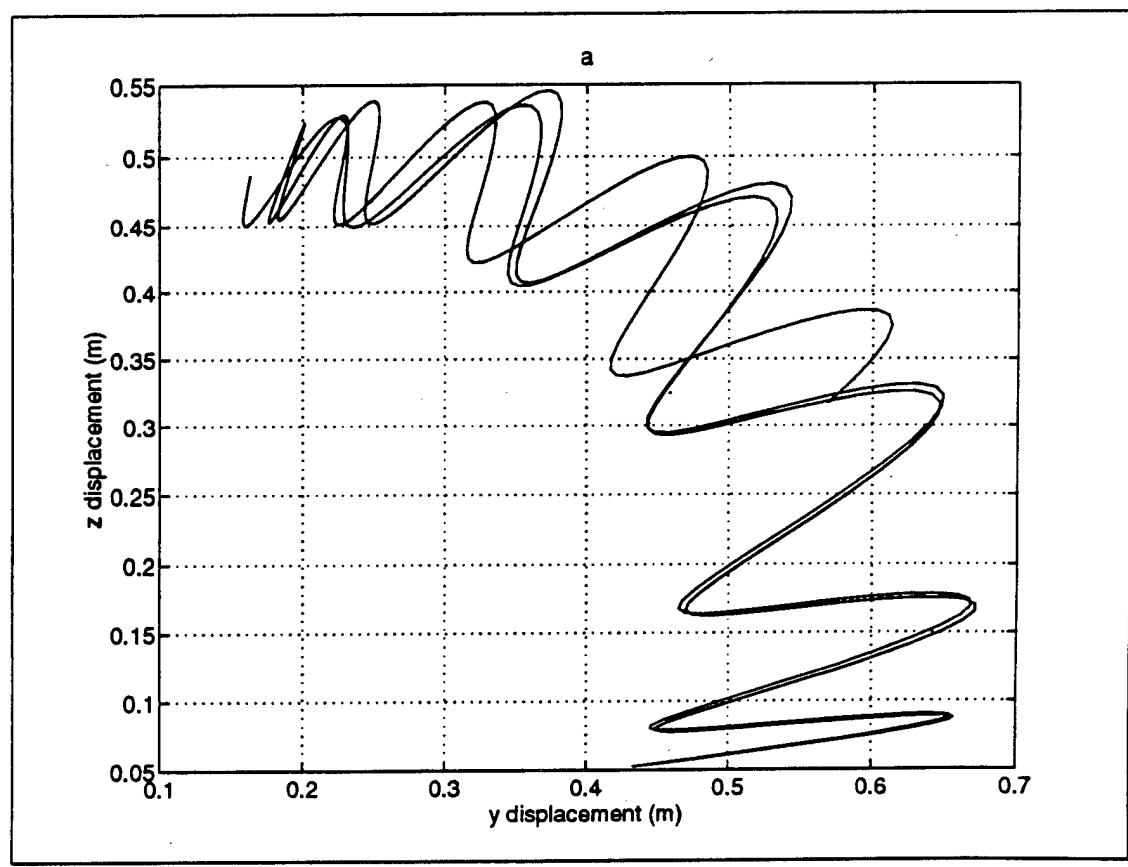
Response to wave slamming load

$$C_L = C_D = C_M = 0$$



Response to wind and current loads

$$\nu = 90^0, \alpha = 0^0, U_c = 0.5 \text{ m/s}$$



Response to wind and current loads

$$\nu = 90^0, \alpha = 0^0, U_c = 0.5 \text{ m/s}$$

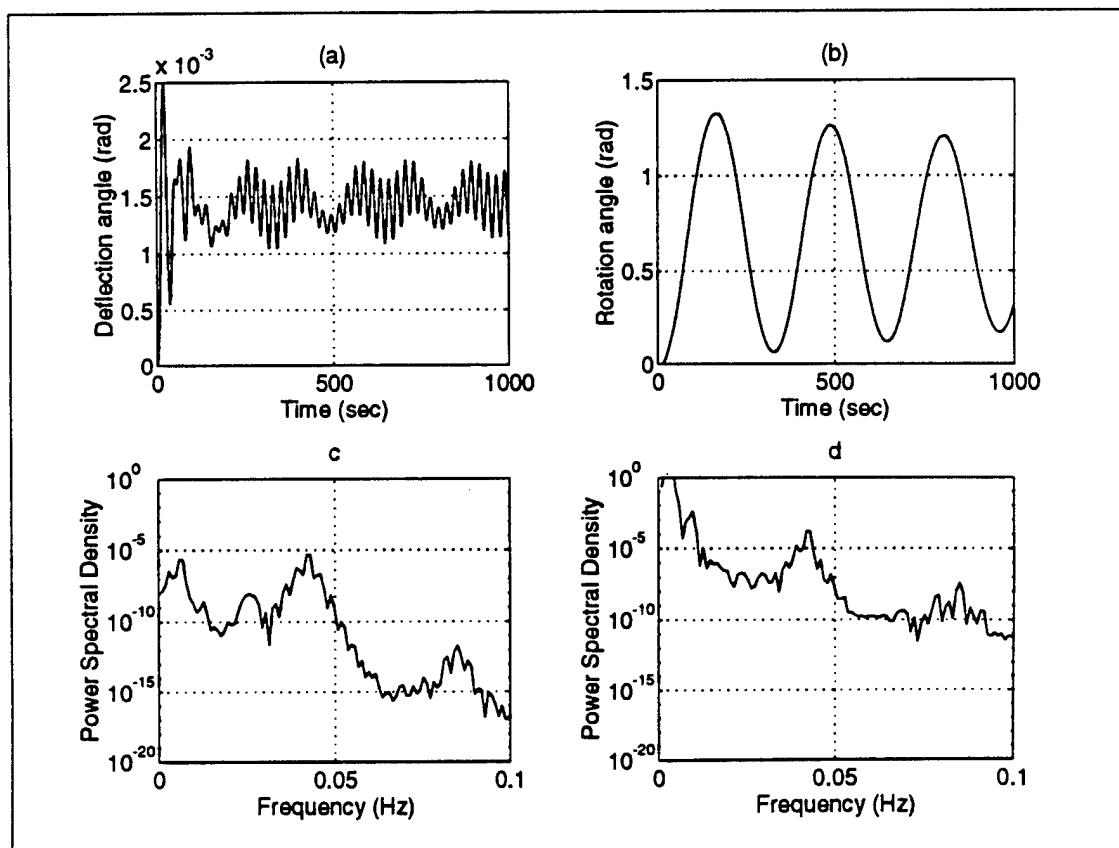
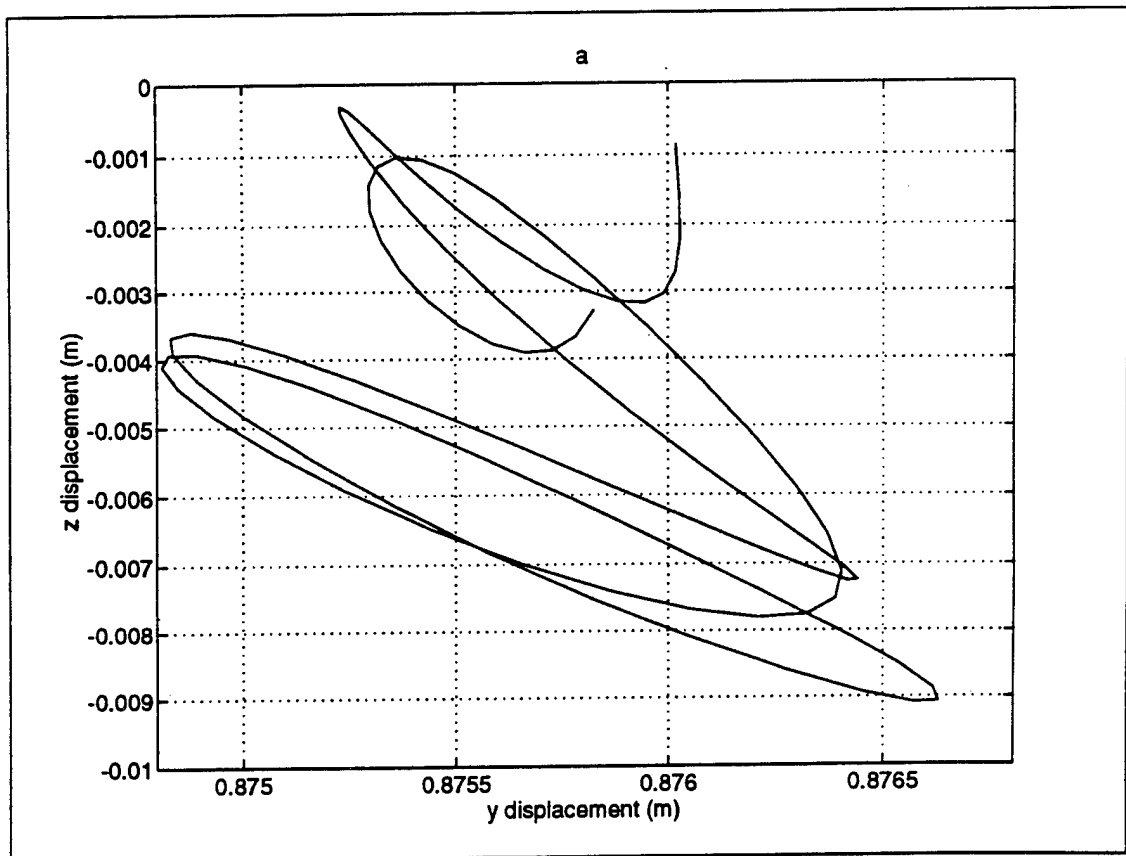


Figure 11.2.11

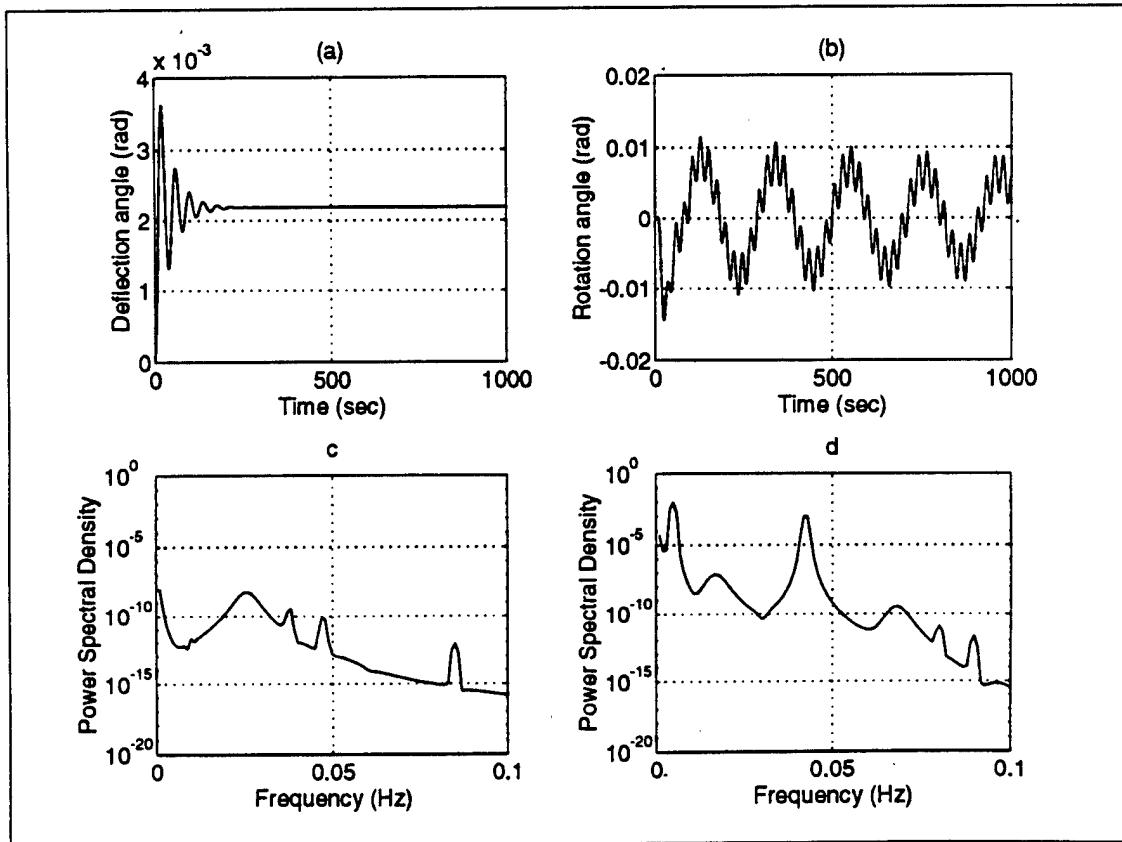
Response to wind and current loads

$$\nu = 0^0, \alpha = 0^0, U_c = 0.5 \text{ m/s}$$



Response to wind and current loads

$$\nu = 0^0, \alpha = 0^0, U_c = 0.5 \text{ m/s}$$



Response to wind and fluid loads

$$\nu = 90^0$$

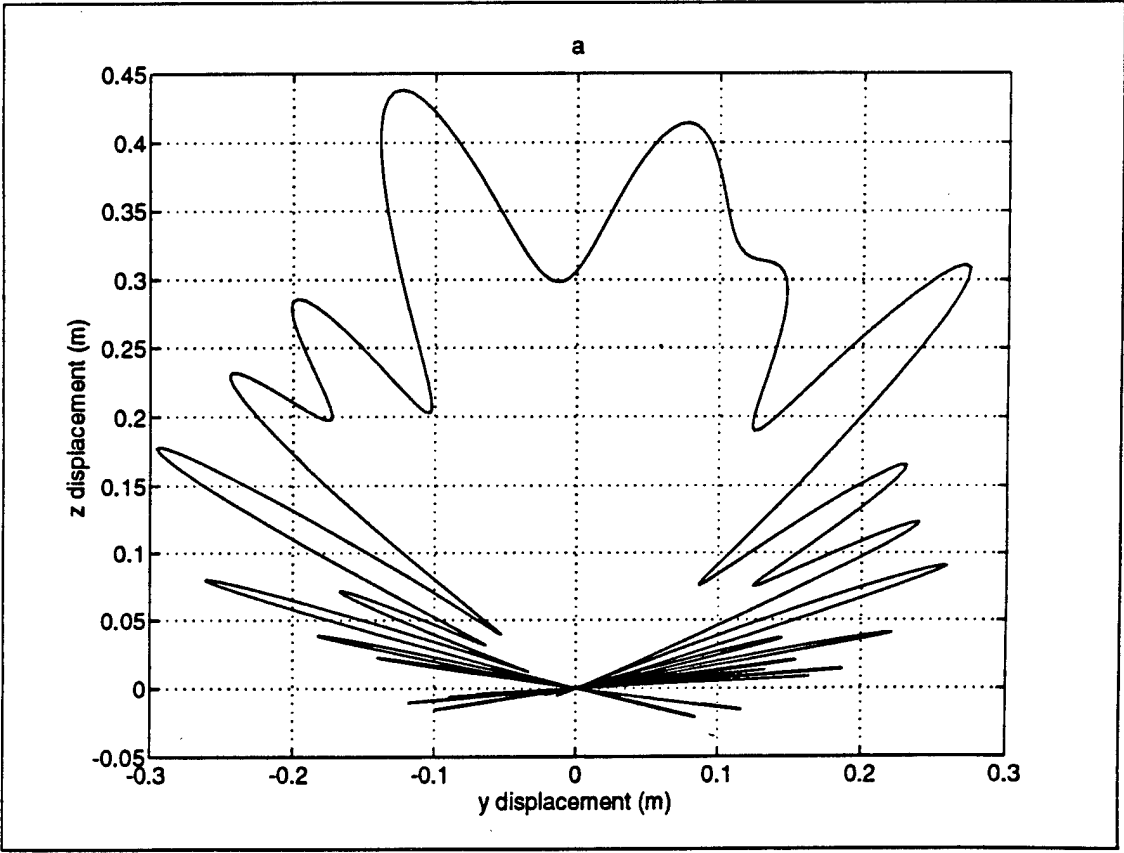


Figure 8: g100

Response to wind and fluid loads

$$\nu = 0^0$$

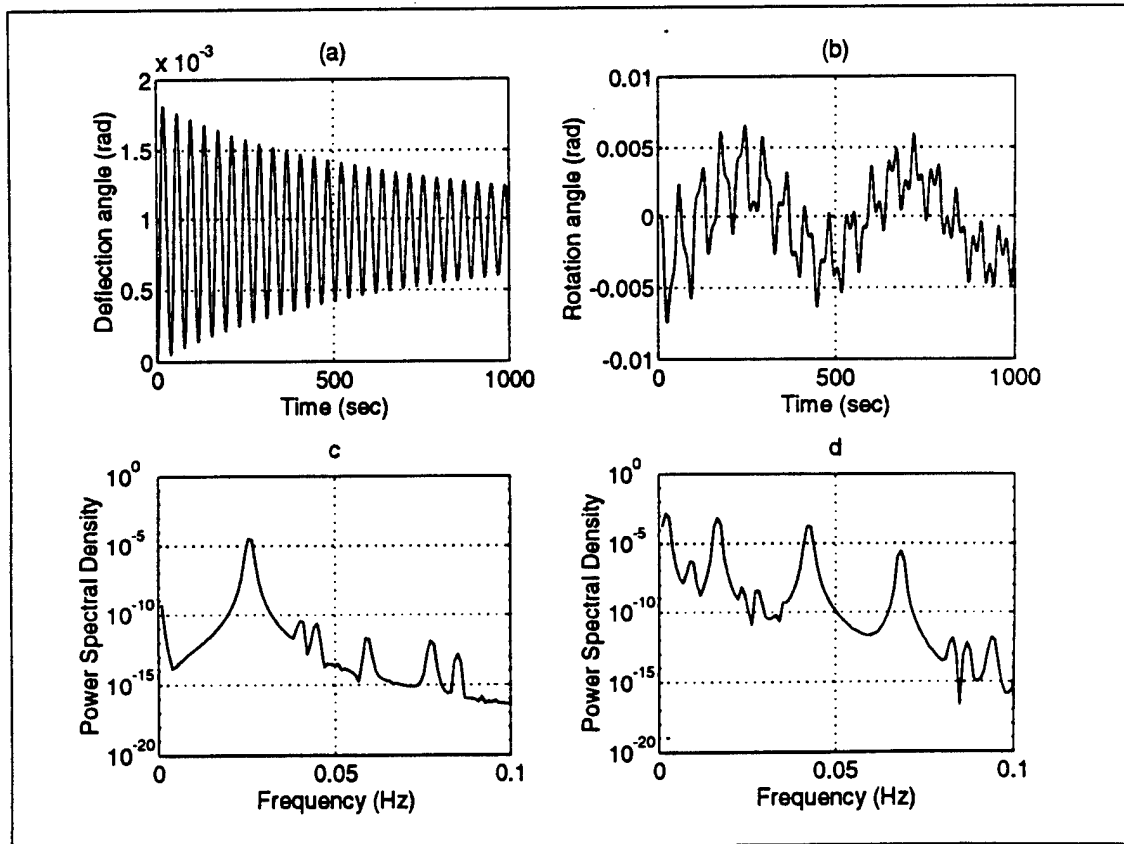
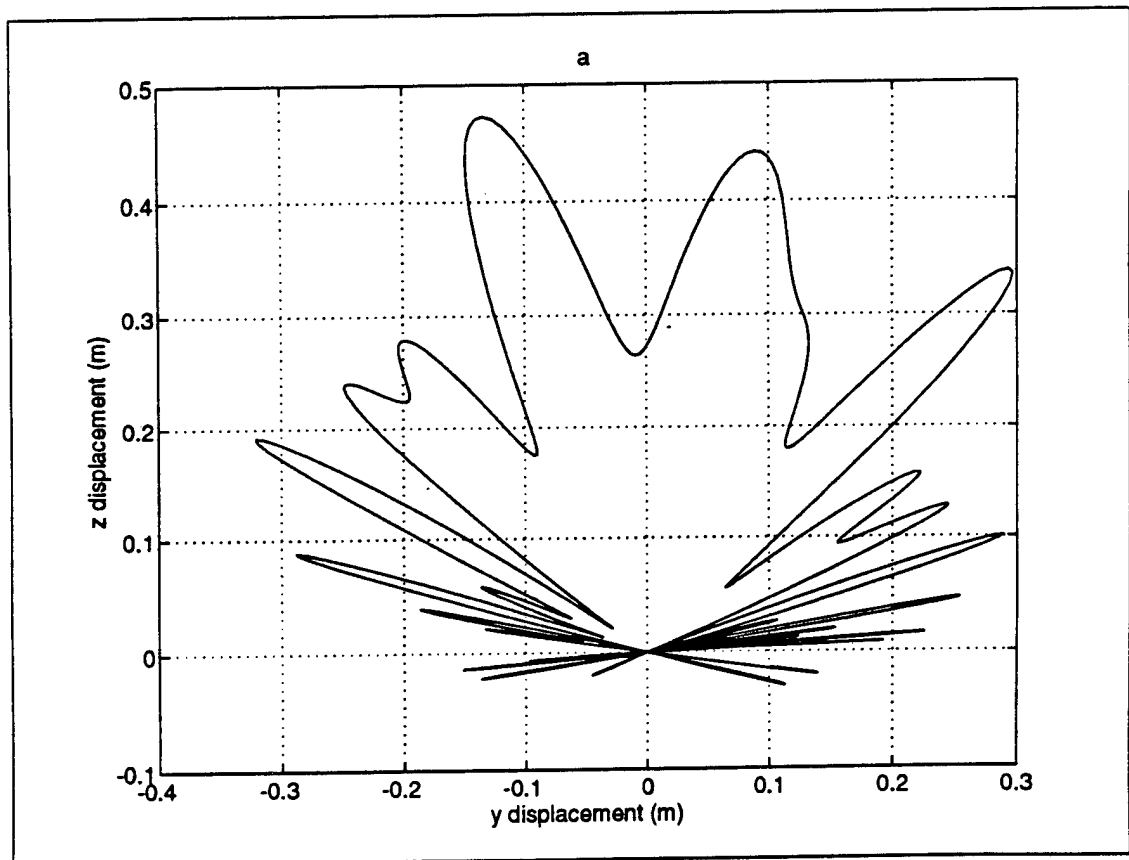


Figure 5: g12

Response to wind load only

$$\nu = 90^{\circ}$$



Response to wind and fluid loads

$$\nu = 90^0$$

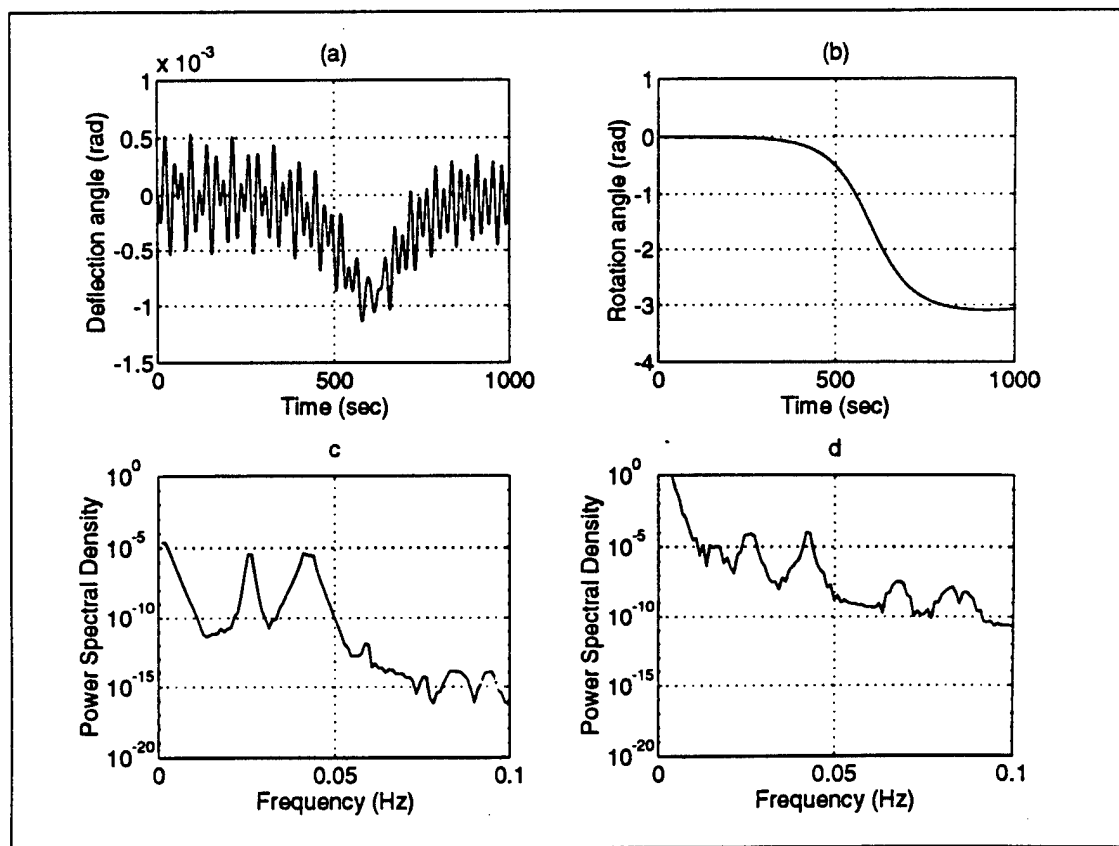


Figure 7: g13a

Response to wind and fluid loads

$$\nu = 0^0$$

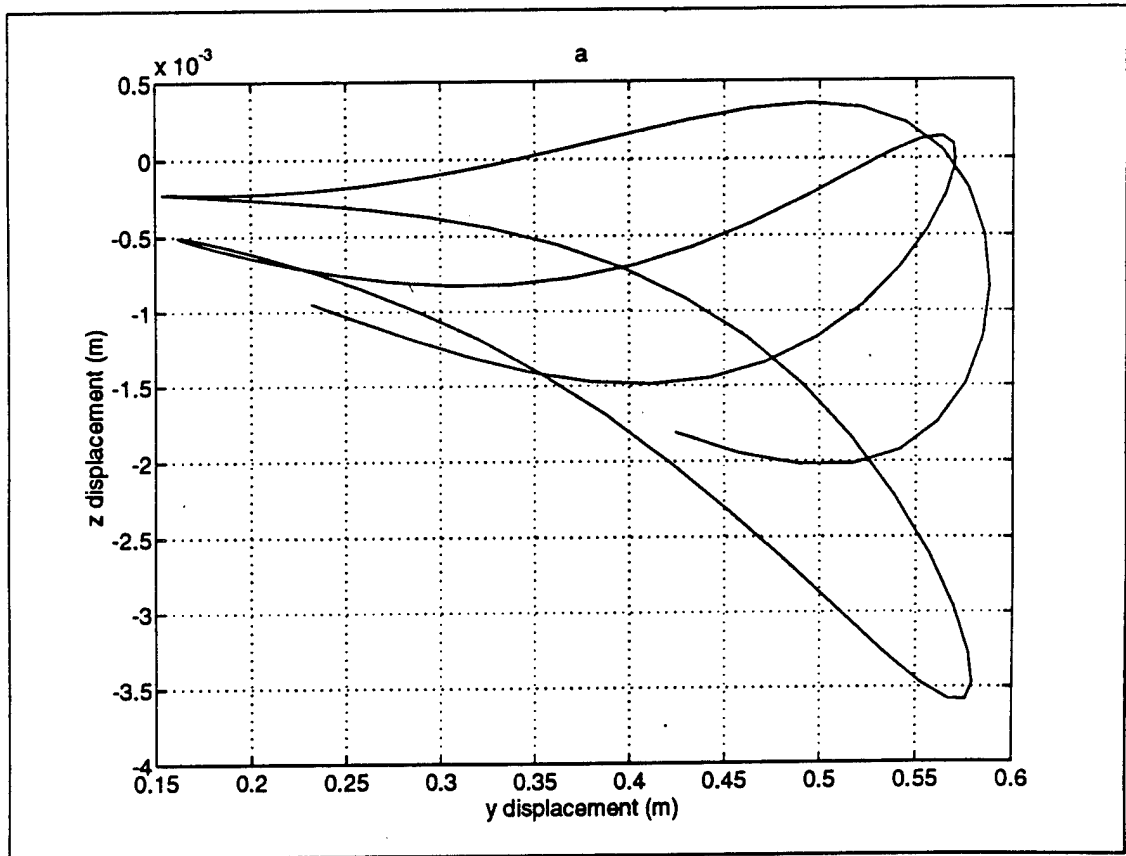
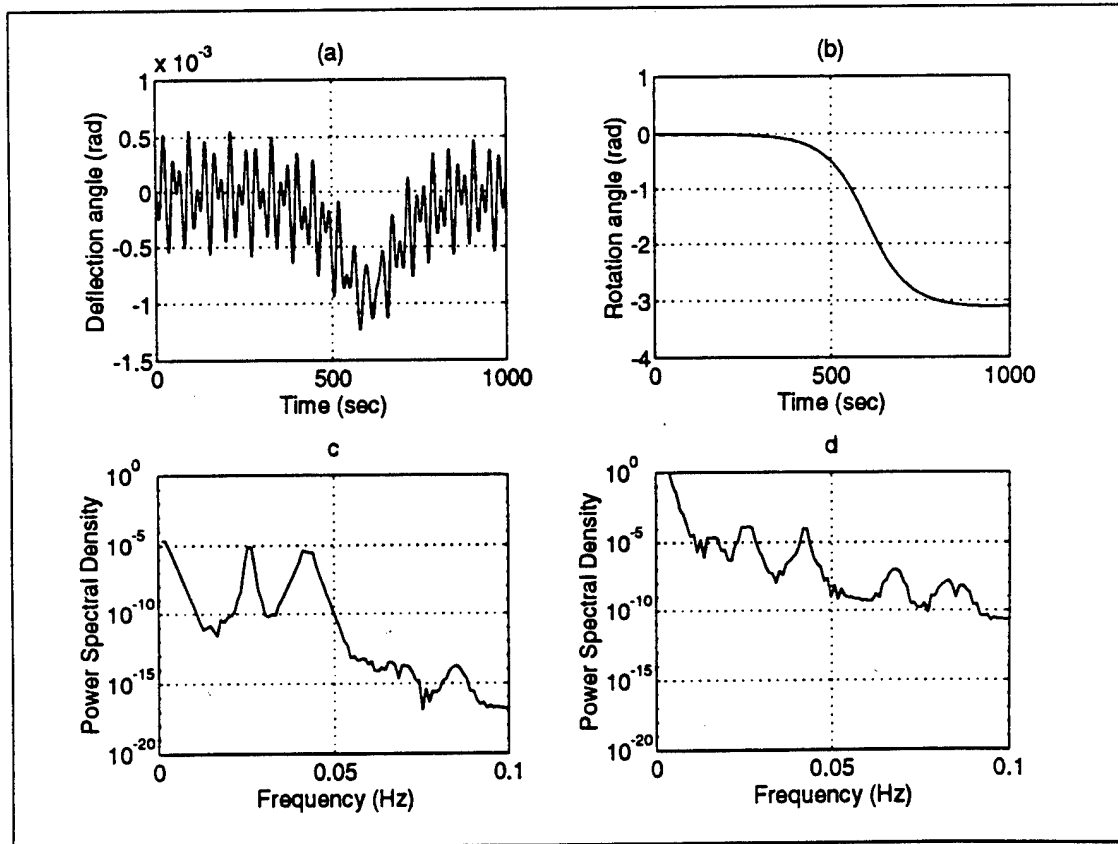


Figure 6: g12b

Response to wind load only

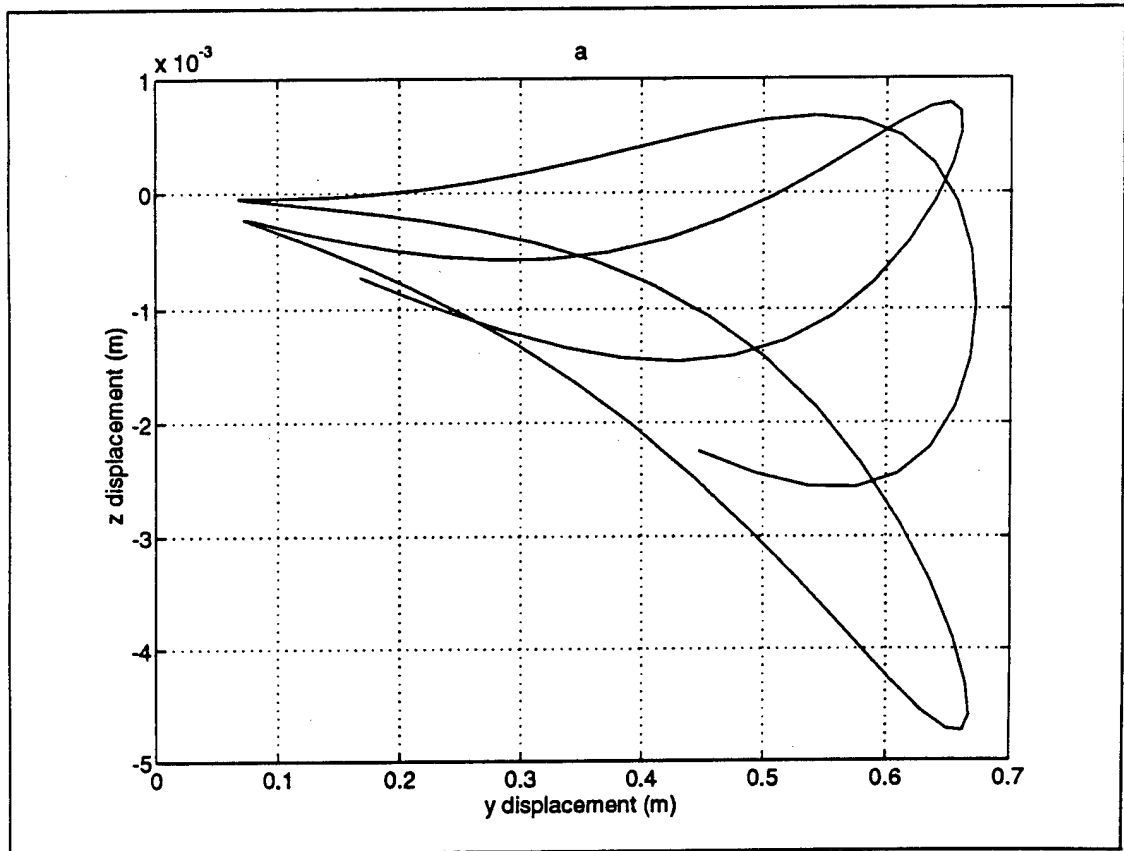
$$\nu = 90^0$$



Continued

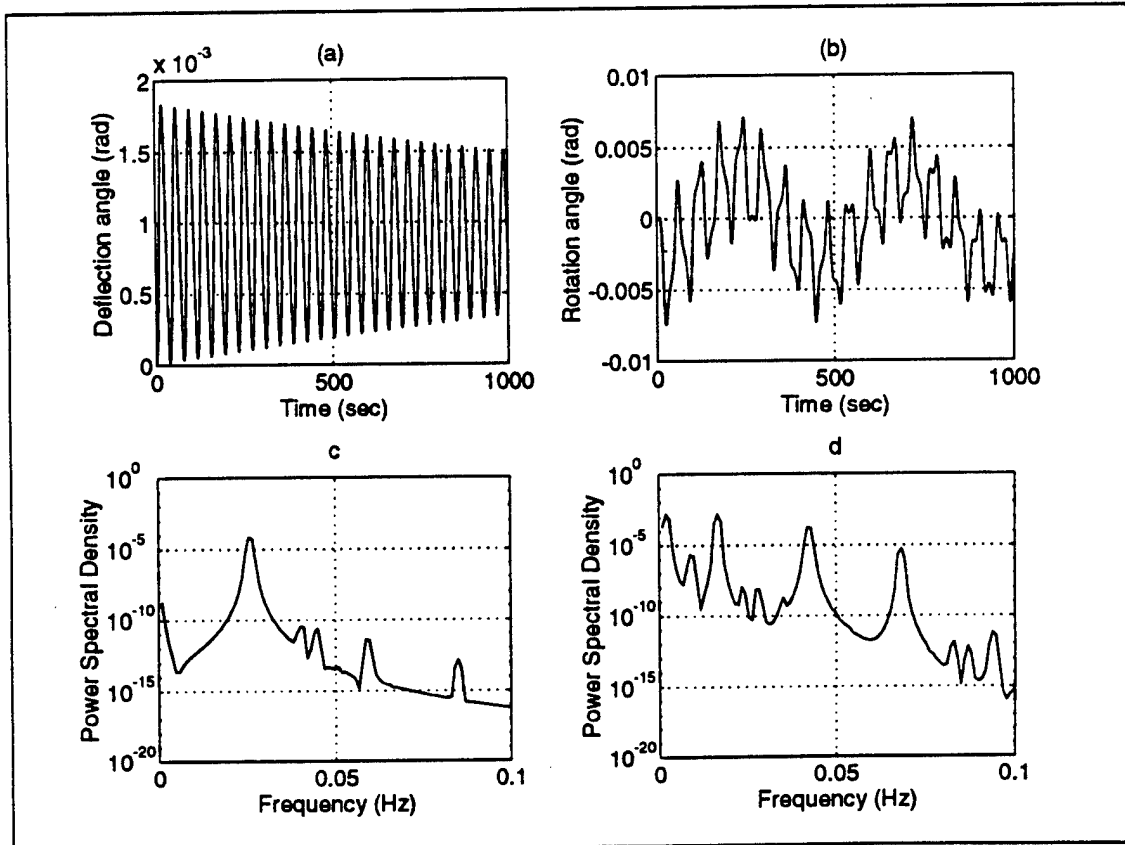
Response to wind load only

$$\nu = 0^0$$

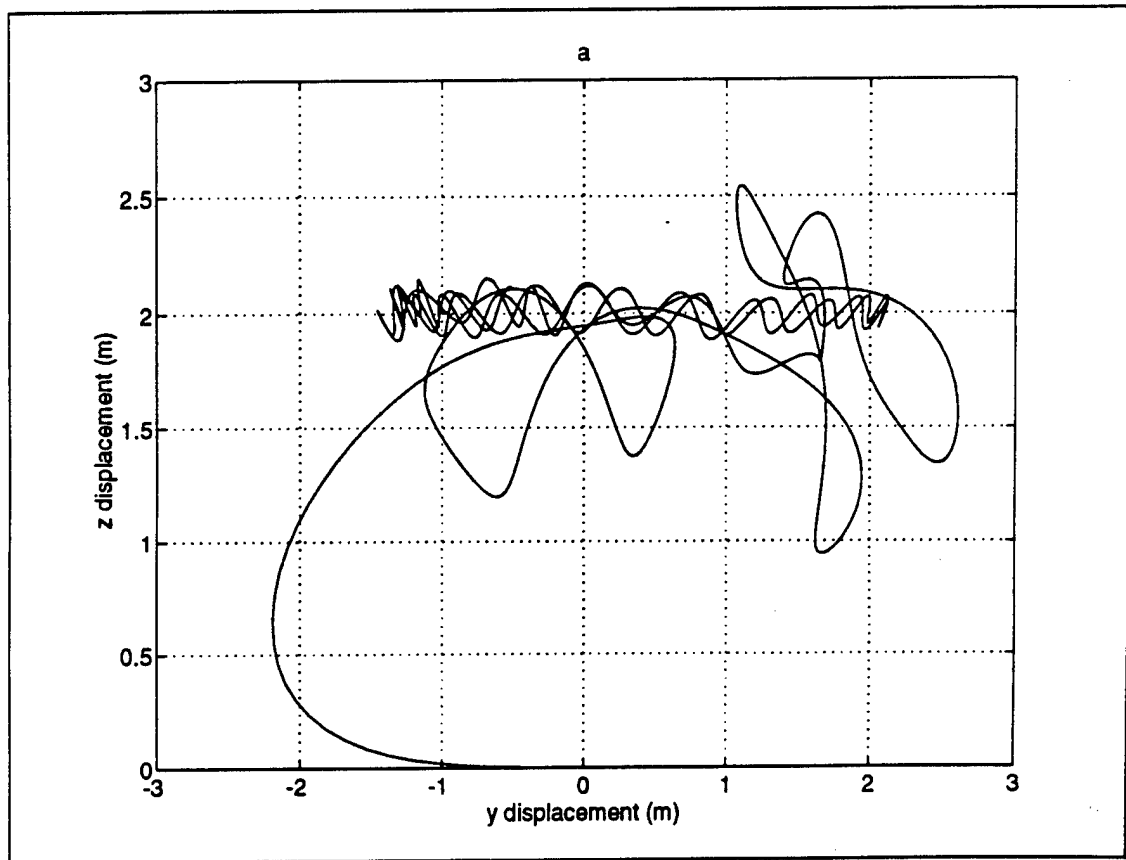


Response to wind load only

$$\nu = 0^0$$



Equilibrium position due to wind and current $C_L = 1$



Summary

- The nonlinear coupled differential equations were derived.
- Wind force has a significant effect on the response.
- Coriolis force due to earth rotation has a small influence on the response, but its importance is the coupling it causes.
- Wave slamming also has a small effect on the tower's response. The reason is the short duration of the pulse compared to the wave period.

Current and Future Study

- Parametric study on this model
- Including elasticity in the tower
- Effect of earthquake (base excitation)



Response of a Two DOF Articulated Tower to Different Environmental Conditions

P. Bar-Avi and H. Benaroya

Department of Mechanical and Aerospace Engineering, Rutgers University

Piscataway, N.J. 08855

April, 1995

ABSTRACT

In a previous paper [1], the response of an articulated tower in the ocean subjected to deterministic and random wave loading was investigated. The tower was modeled as an upright rigid pendulum with a concentrated mass at the top and having one angular degree of freedom about a hinge with coulomb damping. In this paper, which is an extension of the previous one, the tower is modeled as a spherical pendulum having two angular degrees of freedom. The tower is subjected to wave, current, vortex shedding, wind and Coriolis acceleration loads. Geometrical nonlinearities as well as nonlinearities due to wave drag force, which is assumed be proportional to the square of the relative velocity between the tower and the waves, were considered. The governing coupled differential

equations of motion are highly nonlinear, and have time-dependent coefficients. The tower's response to the external forces is found, that is equilibrium position due to wind and current and response to wave excitation. Resonances (harmonic and subharmonic) and also chaotic response are investigated.

Key words : Articulated tower, Dynamics, Resonance

I. INTRODUCTION

Compliant platforms such as articulated towers are economically attractive for deep water conditions because of their reduced structural weight compared to conventional platforms. The foundation of the tower does not resist lateral forces due to wind, waves and currents; instead, restoring moments are provided by a large buoyancy force, a set of guylines or a combination of both. These structures have a fundamental frequency well below the wave lower-bound frequency. As a result of the relatively large displacements, geometric nonlinearity is an important consideration in the analysis of such a structure. The analysis and investigation of these kinds of problems can be divided into two major groups: deterministic and random wave and/or current loading. Most workers have considered the tower to be an upright rigid pendulum attached to the sea floor via a pivot having one or two degrees of freedom.

Bar-Avi and Benaroya (1994) [1] investigated the nonlinear response of a single degree of freedom articulated tower. The equation of motion was derived via Lagrange's equation. Nonlinearities due to geometry and wave drag force are considered. A combined wave and current field, coulomb friction force, and vortex shedding force are included in the analysis. The influences on the response of current velocity and direction, significant wave height and frequency, and damping mechanism were analyzed. The response to sub/superharmonics and harmonic excitation demonstrate beating, and for certain excitation frequencies a chaotic behavior was observed. Current has a large influence on the response and on the equilibrium position of the tower.

Other studies of the response of a single degree of freedom were performed by Chakrabarti

and Cotter [2], Gottlieb et al. [3], Muhuri [4], Datta and Jain [5], [6], [7].

Two degree of freedom models were also studied by several researchers. Kirk and Jain [8], [9] investigated the dynamic response of a two degree of freedom articulated tower to noncolinear waves and current. The two equations of motion were obtained via Lagrange's equation. The waves were assumed linear with current modification of the frequency and amplitude. Forces due to buoyancy, wave drag and inertia, and added mass were considered. The equations were solved numerically, and the influence of drag coefficient and wave direction was analyzed. From the analysis they concluded that;

- Higher drag coefficient results in lower response.
- The maximum deflection occurs when the current and the waves are in the same direction.

Olsen et al. (1978) [10] evaluated the loads acting on a single-point mooring system and the resulting response. The tower was modeled as a rigid body connected to the sea-floor via a universal joint. The equation for the tower and the tanker were derived separately. To derive the equations of motion for the tower, it was divided into N elements having two degrees of freedom each; a horizontal and vertical displacement and the forces due to wave, current and wind were evaluated at each element. The tanker was modeled as a rigid body having three transverse degrees of freedom. The solution gives the low frequency motion of the tanker as well as the tower's response. The high frequency motion of the tanker was assumed to be unaffected by the fact that the tanker is moored. Therefore the tanker's high-frequency amplitudes were calculated independently from the low frequency, and then the responses were added together. The equations were solved numerically and compared

to test results to show a reasonably good correlation, but according to the authors, a more accurate model should be developed. The effect of the tanker on the surrounding wave field was also investigated to find a 0-10% change in the wave velocity and acceleration. The effect of these changes on the response was not investigated.

Chakrabarti and Cotter (1980) [11] investigated transverse motion, the motion perpendicular to the horizontal velocity. The tower pivot is assumed to have two angular degrees of freedom and is taken to be frictionless. It is also assumed that the motion is not coupled, so the in-line solution is obtained (the same as in the previous paper), from which the relative velocity between the tower and the wave is obtained. The lift force (in the transverse direction) can then be obtained and the linear equation of motion is solved analytically and compared to experimental results. The comparison shows good agreement, especially when the drag terms are small.

Vortex induced oscillation of tension leg platform tethers was analyzed by Dong and Lou 1991 [12], and Dong et al. 1992 [13]. The tether was modeled as a uniform tension beam under combined action of wave and current. Only the response normal to the direction of the wave and current was considered. A numerical solution was obtained to find the response and to perform a stability analysis. They found out that for small drag and lift coefficients the system may become unstable. For moderate drag and lift coefficients multiple equilibrium positions occur, one of them is unstable. The region of multiple solutions, where the response can jump from one branch to the other, is reduced as the drag and/or lift coefficients are increased. When the frequency of excitation was not exactly the fundamental frequency, a beating phenomenon was observed. However chaotic motion was not detected. A detailed

description of these studies and other is given in [14].

A. Current Study

This paper is the second part of a comprehensive study on the nonlinear dynamic response of a two degree of freedom articulated tower submerged in the ocean. In the previous study the stochastic response was investigated (see Bar-Avi and Benaroya [15]), and here the deterministic response is analyzed. The nonlinear differential equations of motion are derived, including nonlinearities due to geometry, coulomb damping, drag force (waves, current and wind), added mass, Coriolis acceleration, wave slamming and buoyancy. All forces/moments are evaluated at the instantaneous position of the tower and, therefore, they are not only time-dependent, but also highly nonlinear. The equations are then numerically solved using 'ACSL' software. The effects on the response of the various forces and parameters such as the fluid constants, wave height, coulomb friction, and current and wind magnitude and direction are investigated.

II. PROBLEM DESCRIPTION

A schematic of the structure under study is shown in Fig. 1. It consists of a tower submerged in the ocean having a concentrated mass at the top and two degrees of freedom; θ about the z'' axis and ϕ about the x'' axis. The tower is subjected to wave, current, wind and vortex shedding loads. As can be seen from Fig. 1, three coordinate systems are used; one fixed (x, y, z) , the second attached to the tower (x', y', z') and the third is rotating about x at $\dot{\phi}$ (x'', y'', z'') . All forces/moment velocities and acceleration are derived in the fixed coordinate system.

This problem has similarities to that of an inverted spherical pendulum with additional considerations,

- Buoyancy force is included
- Drag force proportional to the square of the relative velocity between the fluid and the tower needs to be considered
- Fluid inertia and added mass forces due to fluid and tower acceleration are part of the loading environment
- Vortex shedding and wave slamming forces are considered
- Current and wind forces are included
- Earth angular velocity is included.

III. EQUATIONS OF MOTION

The equations of motion are derived using Lagrange's equation for large displacements. Certain assumptions have been made and they are listed below.

A. Assumptions

- The tower stiffness is infinite: $EI = \infty$.
- The hinge consists of coulomb friction.
- The tower has a uniform mass per unit length, \bar{m} and is of length l and diameter D .
- The tower diameter is much smaller than its length, $D \ll l$.

- The tower is a slender smooth structure with uniform cross section.
- The structure is at static stable position due to the buoyancy force.
- The waves are linear having random height.
- Wave forces are approximated via Morison's equation.

B. Lagrange's Equations

The general form of Lagrange's equations is

$$\frac{d}{dt} \left(\frac{\partial K_E}{\partial \dot{q}_i} \right) - \frac{\partial K_E}{\partial q_i} + \frac{\partial P_E}{\partial q_i} + \frac{\partial D_E}{\partial \dot{q}_i} = Q_{q_i}, \quad (1)$$

where K_E is the kinetic energy, P_E is the potential energy, D_E is the dissipative energy and Q_{q_i} is the generalized force related to the q_i generalized coordinate.

The model consists of two degrees of freedom, thus, two generalized coordinates are used; θ and ϕ . The generalized forces in the relevant direction are derived using the principle of virtual work. First the general form for the forces is derived assuming an external force per unit length having three components,

$$\mathbf{F}_e = F_x \hat{x} + F_y \hat{y} + F_z \hat{z}. \quad (2)$$

From Fig. 2 the virtual work done by \mathbf{F}_e due to a virtual displacement $\delta\theta$ is found to be

$$\begin{aligned} F_\theta \delta\theta &= F_x x' [\cos(\theta + \delta\theta) - \cos \theta] + \\ &F_y x' \cos \phi [\sin(\theta + \delta\theta) - \sin \theta] + \\ &F_z x' \sin \phi [\sin(\theta + \delta\theta) - \sin \theta], \end{aligned} \quad (3)$$

and using appropriate trigonometric identities

$$\begin{aligned} F_\theta \delta\theta &= F_x x' [\cos \theta \cos \delta\theta - \sin \theta \sin \delta\theta - \cos \theta] + \\ &F_y x' \cos \phi [\sin \theta \cos \delta\theta + \cos \theta \sin \delta\theta - \sin \theta] + \\ &F_z x' \sin \phi [\sin \theta \cos \delta\theta + \cos \theta \sin \delta\theta - \sin \theta]. \end{aligned} \quad (4)$$

By setting the virtual displacement to $\delta\theta \ll 1$, and replacing $x' = \frac{x}{\cos\theta}$, the generalized force per unit length for the θ coordinate is formed

$$F_\theta = -F_x x \tan\theta + F_y x \cos\phi + F_z x \sin\phi. \quad (5)$$

From Fig. 3 the virtual work done by F_e due to a virtual displacement $\delta\phi$ is derived,

$$\begin{aligned} F_\phi \delta\phi = & F_y x' \sin\theta [\cos(\phi + \delta\phi) - \cos\phi] + \\ & F_z x' \sin\theta [\sin(\phi + \delta\phi) - \sin\phi], \end{aligned} \quad (6)$$

and going through the same procedure described for F_θ , the generalized force per unit length is found to be

$$F_\phi = -F_y x \tan\theta \sin\phi + F_z x \tan\theta \cos\phi. \quad (7)$$

Finally, the generalized moments are evaluated by integrating F_θ and F_ϕ ,

$$M_\theta = \int_0^L (-F_x \tan\theta + F_y \cos\phi + F_z \sin\phi) x dx, \quad (8)$$

and

$$M_\phi = \int_0^L (-F_y \tan\theta \sin\phi + F_z \tan\theta \cos\phi) x dx, \quad (9)$$

where L is the projection in the x direction of the submerged part of the tower. L is a function of the deflection angle θ as follows :

$$L = \begin{cases} l \cos\theta & \text{if } d > l \cos\theta \\ d + \eta(y, t) & \text{if } d < l \cos\theta, \end{cases} \quad (10)$$

and $\eta(y, t)$ is the wave height elevation to be defined later.

C. Tower, Wave and Current Kinematics

To derive the equations of motion using Lagrange's equations, the kinetic, dissipative, and potential energies need to be evaluated, as well as the generalized forces. In this subsection, the tower's linear and angular absolute velocities and accelerations are determined in the fixed coordinate system x, y, z .

1. Tower Kinematics

The tower is assumed to be oriented along a unit vector \mathbf{l} with the following directional cosines (see Fig. (1))

$$\mathbf{l} = \cos \theta \hat{x} + \sin \theta \cos \phi \hat{y} + \sin \theta \sin \phi \hat{z} \quad (11)$$

so that the tower's radius vector \mathbf{R} , velocity \mathbf{V} , and acceleration $\dot{\mathbf{V}}$ are

$$\begin{aligned} \mathbf{R} &= x\hat{x} + x \tan \theta \cos \phi \hat{y} + x \tan \theta \sin \phi \hat{z} \\ \mathbf{V} &= -x\dot{\theta} \tan \theta \hat{x} + x(\dot{\theta} \cos \phi - \dot{\phi} \tan \theta \sin \phi) \hat{y} + x(\dot{\theta} \sin \phi + \dot{\phi} \tan \theta \cos \phi) \hat{z} \\ \dot{\mathbf{V}} &= -x(\ddot{\theta} \tan \theta + \dot{\theta}^2) \hat{x} + \\ &\quad x[\ddot{\theta} \cos \phi - \ddot{\phi} \tan \theta \sin \phi - (\dot{\theta}^2 + \dot{\phi}^2) \tan \theta \cos \phi - 2\dot{\theta}\dot{\phi} \sin \phi] \hat{y} + \\ &\quad x[\ddot{\theta} \sin \phi + \ddot{\phi} \tan \theta \cos \phi - (\dot{\theta}^2 + \dot{\phi}^2) \tan \theta \sin \phi + 2\dot{\theta}\dot{\phi} \cos \phi] \hat{z}. \end{aligned} \quad (12)$$

Fig. 4 describes the earth coordinate system from which the tower's absolute angular velocity can be evaluated.

The system X, Y, Z is an inertial coordinate system, X', Y', Z' is attached to earth, where X' is normal to earth, Y' is directed to east and Z' is directed to the north. The

coordinate system x, y, z is attached to earth with origin at the tower's pivot. It is rotated with an angle β about the X' direction, and its y coordinate is in the direction of the wave propagation. To simplify the calculations, the earth angular velocity is expressed in a coordinate system, x'', y'', z'' , that rotates about x with the tower's angular rotation velocity $\dot{\phi}$. The earth angular velocity is

$$\Omega_e = \Omega \hat{Z} = \Omega \sin \lambda \hat{X}' + \Omega \cos \lambda \hat{Z}', \quad (13)$$

where λ is the altitude angle. Transforming the earth angular velocity to the rotating coordinate system yields,

$$\Omega_e = \Omega \sin \lambda \hat{x}'' + \Omega \cos \lambda \sin \beta \cos \phi \hat{y}'' + \Omega \cos \lambda \cos \beta \sin \phi \hat{z}'' . \quad (14)$$

The tower's angular velocity relative to the earth rotation is

$$\Omega_t = \dot{\phi} \hat{x}'' + \dot{\theta} \hat{z}'' . \quad (15)$$

Finally the absolute angular velocity of the tower is,

$$\Omega_T = \Omega_t + \Omega_e = (\Omega \sin \lambda + \dot{\phi}) \hat{x}'' + (\Omega \cos \lambda \sin \beta \cos \phi) \hat{y}'' + (\Omega \cos \lambda \cos \beta \sin \phi + \dot{\theta}) \hat{z}'' . \quad (16)$$

2. Wave and Current Kinematics

In this study linear wave theory is assumed, and therefore, the wave vertical and horizontal velocities are (Wilson [16] pp. 84):

$$\begin{aligned} w_w &= \frac{1}{2} H \omega \frac{\sinh kx}{\sinh kd} \sin(ky - \omega t) \\ u_w &= \frac{1}{2} H \omega \frac{\cosh kx}{\sinh kd} \cos(ky - \omega t), \end{aligned} \quad (17)$$

and the respective accelerations:

$$\begin{aligned}\dot{w}_w &= -\frac{1}{2}H\omega^2\frac{\sinh kx}{\sinh kd}\cos(ky - \omega t) \\ \dot{u}_w &= \frac{1}{2}H\omega^2\frac{\cosh kx}{\sinh kd}\sin(ky - \omega t),\end{aligned}\quad (18)$$

where H is the significant wave height, ω the wave frequency, k the wave number, and d the mean water level, which are related by

$$\omega^2 = gk \tanh(kd). \quad (19)$$

Without losing generality we assume that the wave propagates in the y direction so that the horizontal velocity u is in that direction, and w is in the x direction. We are aware of the fact that random waves are not unidirectional, but this consideration is beyond the scope of this study.

Current velocity magnitude is calculated assuming that the current is made up of two different components (Issacson (1988) [17]): the tidal component, U_c^t , and the wind-induced current U_c^w . If both components are known at the water surface, the vertical distribution of the current velocity $U_c(x)$ may be taken as

$$U_c(x) = U_c^t \left(\frac{x}{d}\right)^{\frac{1}{7}} + U_c^w \left(\frac{x}{d}\right). \quad (20)$$

The tidal current U_c^t at the surface can be obtained directly from the tide table, and the wind-driven current U_c^w at the surface is generally taken as 1 to 5 % of the mean wind speed at 10 m above the surface.

When current and wave coexist, the combined flow field should be used to determine the wave loads. The influence of an assumed uniform current on the wave field is treated

by applying wave theory in a reference frame which is fixed relative to the current. For a current of magnitude U_c propagating in a direction α relative to the direction of the wave propagation, the wave velocity, $c_0 = \frac{\omega_0}{k}$ for no current, is modified and becomes

$$\begin{aligned} c &= c_0 + U_c \cos \alpha, \\ \omega &= ck. \end{aligned} \quad (21)$$

The velocities then used to determine the wave loads are the vectorial sum of the wave and current velocities

$$\begin{aligned} w &= w_w \\ u &= u_w + U_c \cos \alpha \\ v &= U_c \sin \alpha, \end{aligned} \quad (22)$$

where u , v and w are the total velocities in x , y and z directions, respectively.

To consider geometric nonlinearities, the velocities and accelerations are evaluated at the instantaneous position of the tower. Replacing $y = x \tan \theta \cos \phi$ in the velocity and acceleration expressions (equations (22) and (18)) yields velocities,

$$\begin{aligned} w &= \frac{1}{2} H \omega \frac{\sinh kx}{\sinh kd} \sin(kx \tan \theta \cos \phi - \omega t) \\ u &= \frac{1}{2} H \omega \frac{\cosh kx}{\sinh kd} \cos(kx \tan \theta \cos \phi - \omega t) + U_c \cos \alpha \\ v &= U_c \sin \alpha, \end{aligned} \quad (23)$$

and accelerations

$$\dot{w} = \frac{1}{2} H \omega \left(-\omega + \dot{\theta} \frac{kx \cos \phi}{\cos^2 \theta} - \dot{\phi} kx \tan \theta \sin \phi \right) \frac{\sinh kx}{\sinh kd} \cos(kx \tan \theta \cos \phi - \omega t)$$

$$\begin{aligned} \dot{u} &= -\frac{1}{2}H\omega \left(-\omega + \dot{\theta} \frac{kx \cos \phi}{\cos^2 \theta} - \dot{\phi} kx \tan \theta \sin \phi \right) \frac{\cosh kx}{\sinh kd} \sin(kx \tan \theta \cos \phi - \omega t) \\ \dot{v} &= 0. \end{aligned} \quad (24)$$

The influence of current on the significant wave height depends on the manner in which the waves propagate onto the current field. An approximation to the significant wave height in the presence of current is given by Isaacson (1988) [17],

$$H = H_0 \sqrt{\frac{2}{\gamma + \gamma^2}}, \quad (25)$$

where H_0 , H are the significant wave heights in the absence and presence of current, respectively, and γ is

$$\gamma = \sqrt{1 + \frac{4U_c}{c_0} \cos \alpha} \quad \text{for} \quad \frac{4U_c}{c_0} \cos \alpha > -1. \quad (26)$$

D. Fluid Forces and Moments Acting on the Tower

Fig. 5 depicts the external forces acting on the tower:

- T_0 is a vertical buoyancy force
- F_{fl} are the vertical and horizontal fluid forces due to drag, inertia, added mass and vortex shedding
- Mg , $\bar{m}lg$ are the forces due gravity
- F_w is the wind force
- F_{sm} is the wave slamming load.

We next describe and develop explicit expressions for these forces and moments.

1. Buoyancy Moment

The buoyancy force provides the restoring moment,

$$M_b = T_0 l_b. \quad (27)$$

T_0 is the buoyancy force, and l_b is its moment arm; both are time-dependent, where

$$T_0 = \rho g V_0 = \rho g \pi \frac{D^2}{4} L_s. \quad (28)$$

V_0 is the volume of the submerged part of the tower, ρ is the fluid density and L_s , which is the length of the submerged part of the tower, equals

$$L_s = \frac{d + \eta(y, t)}{\cos \theta}, \quad (29)$$

with wave height elevation $\eta(y, t)$ evaluated at the instantaneous position of the tower where

$$\eta(\theta, t) = \frac{1}{2} H \cos(kd \tan \theta - \omega t + \epsilon). \quad (30)$$

and at $x = d$ with $y = d \tan \theta$.

The buoyant force acts at the center of mass of the submerged part of the tower. If we consider the tower to be of cylindrical cross-section then the center of mass in the x', y', z' coordinates is

$$\begin{aligned} l_b^{y'} &= \frac{D^2}{16L_s} \tan^2 \theta \\ l_b^{x'} &= \frac{1}{2} L_s + \frac{D^2}{32L_s} \tan^2 \theta. \end{aligned} \quad (31)$$

Transforming to x, y, z coordinates, we find the moment arm l_b

$$l_b = \frac{D^2}{16L_s} \tan^2 \theta \cos \theta + \left(\frac{1}{2}L_s + \frac{D^2}{32L_s} \tan^2 \theta \right) \sin \theta, \quad (32)$$

and finally the buoyancy generalized moment is then

$$M_b^\theta = \rho g \pi \frac{D^2}{4} \left[\frac{D^2}{32} \tan^2 \theta (2 \cos \theta + \sin \theta) + \frac{1}{2} \left(\frac{d + \eta(y, t)}{\cos \theta} \right)^2 \sin \theta \right]. \quad (33)$$

2. Wave Forces/Moments

In general, the fluid forces acting on a slender smooth tower are of four types: drag, inertia, vortex-shedding, and wave slamming. In this section these forces are derived.

Drag and Inertia Forces - Morison's Equation The drag and inertia forces per unit length are approximated by Morison's equation. The drag force is proportional to the square of the relative velocity between the fluid and the tower, and the inertia force is proportional to the fluid acceleration,

$$\mathbf{F}_{fl} = C_D \rho \frac{D}{2} |\mathbf{V}_{rel}| \mathbf{V}_{rel} + C_M \rho \pi \frac{D^2}{4} \dot{\mathbf{U}}_w, \quad (34)$$

where \mathbf{F}_{fl} is the fluid force per unit length normal to the tower. \mathbf{V}_{rel} is the vector of the relative velocity between the fluid and the tower in a direction normal to the tower, and $\dot{\mathbf{U}}_w$ is the fluid acceleration normal to the tower. C_D and C_M are the drag and inertia coefficients, respectively. The relative velocity and fluid acceleration normal to the tower can be decomposed to their components as follows,

$$\begin{bmatrix} V_{rel}^x \\ V_{rel}^y \\ V_{rel}^z \end{bmatrix} = \mathbf{l} \times (\mathbf{U}_w - \mathbf{V}) \times \mathbf{l}$$

$$\begin{bmatrix} \dot{U}_w^x \\ \dot{U}_w^y \\ \dot{U}_w^z \end{bmatrix} = \mathbf{1} \times \dot{\mathbf{U}}_w \times \mathbf{1}. \quad (35)$$

Using Morison's equation (34), the tower velocity equation (12), and fluid velocity and acceleration equations (23), (24), the fluid force components are the drag force

$$\begin{bmatrix} F_{xD}^{fl} \\ F_{yD}^{fl} \\ F_{zD}^{fl} \end{bmatrix} = C_D \rho \frac{D}{2} \sqrt{(V_{rel}^x)^2 + (V_{rel}^y)^2 + (V_{rel}^z)^2} \begin{bmatrix} V_{rel}^x \\ V_{rel}^y \\ V_{rel}^z \end{bmatrix}, \quad (36)$$

and the inertia force,

$$\begin{bmatrix} F_{xI}^{fl} \\ F_{yI}^{fl} \end{bmatrix} = C_M \rho \pi \frac{D^2}{4} \begin{bmatrix} \dot{w} \\ \dot{u} \end{bmatrix}. \quad (37)$$

Vortex Shedding Force The lift force \mathbf{F}_L due to vortex shedding is acting in a direction normal to the wave velocity vector and normal to the tower. Different models of lift force exist in the literature; see especially Billah (1989) [18]. We will initially use a simple model given in a paper by Dong (1991) [12]

$$\mathbf{F}_L = C_L \rho \frac{D}{2} \cos \omega_s t |\mathbf{1} \times (\mathbf{U}_{T_w} - \mathbf{V})| (\mathbf{1} \times (\mathbf{U}_T - \mathbf{V})), \quad (38)$$

where \mathbf{U}_T , the vector of the maximum fluid velocity along the tower, is

$$\begin{bmatrix} U_T^x \\ U_T^y \\ U_T^z \end{bmatrix} = \begin{bmatrix} \frac{1}{2} H \omega \frac{\sinh kx}{\sinh kd} \\ \frac{1}{2} H \omega \frac{\cosh kx}{\sinh kd} + U_c \cos \alpha \\ U_c \sin \alpha \end{bmatrix}. \quad (39)$$

C_L is the lift coefficient, and ω_s is the vortex shedding frequency (Issacson (1988) [17]) and is given by

$$\omega_s = \begin{cases} 2\omega & H \neq 0 \\ \frac{StU_c}{D} & H = 0 \end{cases}, \quad (40)$$

where St is the Strouhal number, which varies slightly with Reynolds number but is roughly 0.2 over a wide range in Re .

Wave Slamming Force The parts of a structural member that are above the mean water level are exposed an impulsive force caused by wave slamming. The slamming force per unit length has a similar form as the drag force (see Chakrabarti (1990) pp. 142-143 [19]),

$$\mathbf{F}_{sm} = C_S \rho \frac{D}{2} |\mathbf{l} \times \mathbf{U}_S \times \mathbf{l}| (\mathbf{l} \times \mathbf{U}_S \times \mathbf{l}) \quad (41)$$

where C_S , the slamming coefficient, has a theoretical value of π , but a typical mean value may be taken as 3.5 even though considerable scatter in this coefficient has been found in laboratory experiments. \mathbf{U}_S is the relative velocity between the fluid and the tower on the wave front at the point of impact. The point of impact will be assumed to be at the mean water level. Therefore, substituting $x = d$ in the wave and tower velocity equations (23), (12) yields,

$$\begin{bmatrix} U_S^x \\ U_S^y \\ U_S^z \end{bmatrix} = \begin{bmatrix} \frac{1}{2}H\omega + d\dot{\theta} \tan \theta \\ \frac{1}{2}H\omega \frac{\cosh kd}{\sinh kd} + U_c \cos \alpha - d(\dot{\theta} \cos \phi - \dot{\phi} \tan \theta \sin \phi) \\ U_c \sin \alpha - d(\dot{\theta} \sin \phi + \dot{\phi} \tan \theta \cos \phi) \end{bmatrix}. \quad (42)$$

This force is assumed to be a periodic impulse with the period of the wave, and a duration of milliseconds as described in Flatinsen pp. 282-285 [20].

Total Fluid Moment The moment due to fluid forces (drag, inertia, and lift) is evaluated by substituting the sum of all fluid forces, defined by equation (43),

$$\begin{aligned} F_x^{fl} &= F_{xD}^{fl} + F_{xI}^{fl} + F_{xL}^{fl} \\ F_y^{fl} &= F_{yD}^{fl} + F_{yI}^{fl} + F_{yL}^{fl} \\ F_z^{fl} &= F_{zD}^{fl} + F_{zI}^{fl} + F_{zL}^{fl} \end{aligned} \quad (43)$$

into equations (8) and (9). Therefore the moments M_{fl}^θ and M_{fl}^ϕ are

$$\begin{aligned} M_{fl}^\theta &= \int_0^L \left(-F_x^{fl} \tan \theta + F_y^{fl} \cos \phi + F_z^{fl} \sin \phi \right) x dx \\ M_{fl}^\phi &= \int_0^L \left(-F_y^{fl} \tan \theta \sin \phi + F_z^{fl} \tan \theta \cos \phi \right) x dx. \end{aligned} \quad (44)$$

The wave slamming moments are evaluated by integrating the slamming force along the part of the tower onto which the waves are slamming. Since the exact length is very complicated to determine, an approximated length is used; from the mean water level d to the wave height $d + \frac{1}{2}H$, which was suggested by Chakrabarti pp. 142-143 [19], hence

$$\begin{aligned} M_{sm}^\theta &= \int_d^{d+\frac{1}{2}H} \left(-F_x^{sm} \tan \theta + F_y^{sm} \cos \phi + F_z^{sm} \sin \phi \right) x dx \\ M_{sm}^\phi &= \int_d^{d+\frac{1}{2}H} \left(-F_y^{sm} \tan \theta \sin \phi + F_z^{sm} \tan \theta \cos \phi \right) x dx, \end{aligned} \quad (45)$$

where F_x^{sm} , F_y^{sm} , F_z^{sm} are the wave slamming forces in the x, y, z direction.

3. Wind Load

Wind loads are similar to current forces, i.e., drag and lift (vortex shedding). Both, the drag and lift force expressions are similar to those of the fluid. The drag force

$$\mathbf{F}_D^w = C_D^a \rho^a \frac{D}{2} [|\mathbf{l} \times (\mathbf{u}_w - \mathbf{V}) \times \mathbf{l}| (\mathbf{l} \times (\mathbf{u}_w - \mathbf{V}) \times \mathbf{l})], \quad (46)$$

where C_D^a is the air drag coefficient, ρ^a is the air density and \mathbf{u}_w is the wind velocity which is assumed to propagate in an arbitrary direction

$$\mathbf{u}_w = u_w \cos \nu \hat{y} + u_w \sin \nu \hat{z}, \quad (47)$$

where ν is the direction between the propagating wind and the y axis. The lift force

$$\mathbf{F}_L^w = C_L^a \rho^a \frac{D}{2} \cos \omega_{Lw} t |\mathbf{l} \times (\mathbf{u}_w - \mathbf{V})| (\mathbf{l} \times (\mathbf{u}_w - \mathbf{V})), \quad (48)$$

where C_L^a is the air lift coefficient. The vortex shedding frequency ω_{Lw} is

$$\omega_{Lw} = \frac{Stu_w}{D}. \quad (49)$$

The moments due to wind loads M_w^θ, M_w^ϕ are found in a similar way as the fluid moments (eqn. (44)), but integrating along the exposed part of the tower

$$\begin{aligned} M_w^\theta &= \int_{d+\eta}^{l \cos \theta} (-F_x^w \tan \theta + F_y^w \cos \phi + F_z^w \sin \phi) x dx \\ M_w^\phi &= \int_{d+\eta}^{l \cos \theta} (-F_y^w \tan \theta \sin \phi + F_z^w \tan \theta \cos \phi) x dx, \end{aligned} \quad (50)$$

where F_x^w, F_y^w, F_z^w , are the wind forces in the x, y, z direction, due to drag and vortex shedding.

4. Added Mass Moment

The fluid added mass force per unit length \mathbf{F}_{ad} is

$$\mathbf{F}_{ad} = C_A \rho \pi \frac{D^2}{4} \dot{\mathbf{V}}, \quad (51)$$

where $C_A = C_M - 1$ is the added mass coefficient. Substituting the expression for the tower acceleration, equation (12), into equation (51) leads to the expressions for the forces in the x, y, z directions,

$$\begin{aligned} F_{ad}^x &= C_A \rho \pi \frac{D^2}{4} \left(-x(\ddot{\theta} \tan \theta + \dot{\theta}^2) \right) \\ F_{ad}^y &= C_A \rho \pi \frac{D^2}{4} \left(x[\ddot{\theta} \cos \phi - \ddot{\phi} \tan \theta \sin \phi - (\dot{\theta}^2 + \dot{\phi}^2) \tan \theta \cos \phi - 2\dot{\theta}\dot{\phi} \sin \phi] \right) \\ F_{ad}^z &= C_A \rho \pi \frac{D^2}{4} \left(x[\ddot{\theta} \sin \phi + \ddot{\phi} \tan \theta \cos \phi - (\dot{\theta}^2 + \dot{\phi}^2) \tan \theta \sin \phi + 2\dot{\theta}\dot{\phi} \cos \phi] \right). \end{aligned} \quad (52)$$

Substituting the added mass forces (equation (52)) into the generalized moment equations (8) and (9), and integrating, result in the generalized moments due to fluid added mass,

$$\begin{aligned} M_{ad}^\theta &= \frac{1}{12} C_A \rho \pi \frac{D^2}{4} L^3 \left(\ddot{\theta} (1 + \tan^2 \theta) + \dot{\phi}^2 \tan \theta \right) \\ M_{ad}^\phi &= \frac{1}{12} C_A \rho \pi \frac{D^2}{4} L^3 \left(\ddot{\phi} \tan^2 \theta + 2\dot{\theta}\dot{\phi} \tan \theta \right). \end{aligned} \quad (53)$$

5. Friction Moment

Dissipation in the tower hinge is assumed to be modeled as coulomb friction. In this section this friction/damping moment is evaluated. The damping force is equal to the product of the normal force at the hinge N and the coefficient of friction μ which is assumed to be independent of the velocity, once the motion is initiated. Since the sign of the damping force is always opposite to that of the velocity, the differential equation of motion for each sign is

valid only for half cycle intervals. The friction force is

$$\begin{aligned} F_{fr}^{\theta} &= N\mu[\text{sgn}(\dot{\theta})] \\ F_{fr}^{\phi} &= N\mu[\text{sgn}(\dot{\phi})]. \end{aligned} \quad (54)$$

The normal force is

$$N = \sum F_x \cos \theta + \sum F_y \cos \phi \sin \theta + \sum F_z \sin \phi \sin \theta, \quad (55)$$

where $\sum F_x$, $\sum F_y$ and $\sum F_z$ are the total forces due to gravity, buoyancy and tower acceleration in the x , y and z directions, respectively. The fluid forces; drag, inertia and vortex shedding, do not influence the friction force since they are perpendicular to the tower. Thus,

$$\begin{aligned} \sum F_x &= T_0 - F_g + F_{ac}^x \\ \sum F_y &= F_{ac}^y \\ \sum F_z &= F_{ac}^z, \end{aligned} \quad (56)$$

where T_0 is the buoyancy force given in equation (33), F_g is the gravitational force,

$$F_g = (\bar{m}l + M)g, \quad (57)$$

and the forces due to the tower acceleration F_{ac}^x , F_{ac}^y , F_{ac}^z are

$$\begin{aligned} F_{ac}^x &= \left[\frac{1}{8} C_A \rho \pi D^2 L^2 + \frac{1}{2} \left(\frac{1}{2} \bar{m}l + M \right) \bar{l} \right] \frac{1}{\cos \theta} (\ddot{\theta} \tan \theta + \dot{\theta}^2) \\ F_{ac}^y &= \left[\frac{1}{8} C_A \rho \pi D^2 L^2 + \frac{1}{2} \left(\frac{1}{2} \bar{m}l + M \right) \bar{l} \right] \frac{1}{\cos \theta} \cdot \\ &\quad \cdot \left(-\ddot{\theta} \cos \phi + \ddot{\phi} \tan \theta \sin \phi + (\dot{\theta}^2 + \dot{\phi}^2) \tan \theta \cos \phi + 2\dot{\theta}\dot{\phi} \sin \phi \right) \\ F_{ac}^z &= \left[\frac{1}{8} C_A \rho \pi D^2 L^2 + \frac{1}{2} \left(\frac{1}{2} \bar{m}l + M \right) \bar{l} \right] \frac{1}{\cos \theta} \cdot \\ &\quad \cdot \left(\ddot{\theta} \cos \phi - \ddot{\phi} \tan \theta \sin \phi - (\dot{\theta}^2 + \dot{\phi}^2) \tan \theta \cos \phi - 2\dot{\theta}\dot{\phi} \sin \phi \right), \end{aligned} \quad (58)$$

where \bar{l} is the projection of the tower's length l in the x direction, i.e., $\bar{l} = l \cos \theta$. Assuming a hinge radius R_h , and rearranging

$$\begin{aligned} M_{fr}^\theta &= R_h N \mu [\text{sgn}(\dot{\theta})] \\ M_{fr}^\phi &= R_h \sin \theta N \mu [\text{sgn}(\dot{\phi})], \end{aligned} \quad (59)$$

where N , the normal force is

$$\begin{aligned} N &= \left[\frac{1}{8} C_{A\rho\pi} D^2 \frac{L^2}{\cos^2 \theta} + \frac{1}{2} \left(\frac{1}{2} \bar{m} l + M \right) l \right] (\dot{\theta}^2 + \frac{1}{2} \dot{\phi}^2) - \\ &\quad \left[\frac{1}{8} C_{A\rho\pi} D^2 L^2 + \frac{1}{2} \left(\frac{1}{2} \bar{m} l + M \right) l \cos 2\theta \right] \frac{1}{2} \dot{\phi}^2 + (T_0 - F_g) \cos \theta. \end{aligned} \quad (60)$$

The only terms remaining in the acceleration forces are due to centrifugal acceleration which is along the tower, that is, $l\dot{\theta}^2$.

E. Dynamic moments

The dynamic moments M_{dy}^θ , and M_{dy}^ϕ , which are in the left hand side of Lagrange's equation (1), are found using expressions for the kinetic, potential, and dissipative energies

$$\begin{aligned} \mathbf{K}_E &= \frac{1}{2} (I_x \Omega_{Tx}^2 + I_y \Omega_{Ty}^2 + I_z \Omega_{Tz}^2) \\ \mathbf{P}_E &= \left(\frac{1}{2} \bar{m} l + M \right) g l \cos \theta \\ \mathbf{D}_E &= \frac{1}{2} C (\Omega_{ix}^2 + \Omega_{iy}^2 + \Omega_{iz}^2), \end{aligned} \quad (61)$$

where C is the structural damping constant and I_x'' , I_y'' , I_z'' are the moments of inertia of the tower, given by

$$\begin{aligned}
I_x'' &= \left(\frac{1}{3}\bar{m}l + M\right)l^2 \sin^2 \theta + \frac{1}{2}(\bar{m}l + M)\frac{D^2}{4} \cos^2 \theta \\
I_y'' &= \left(\frac{1}{3}\bar{m}l + M\right)l^2 \cos^2 \theta + \frac{1}{2}(\bar{m}l + M)\frac{D^2}{4} \sin^2 \theta \\
I_z'' &= \left(\frac{1}{3}\bar{m}l + M\right)l^2.
\end{aligned} \tag{62}$$

Substituting equations (62) and (16) into (61) leads to the expressions for the kinetic and dissipative energies,

$$\begin{aligned}
\mathbf{K}_E &= \frac{1}{2} \left(\left(\frac{1}{3}\bar{m}l + M\right)l^2 \sin^2 \theta + \frac{1}{2}(\bar{m}l + M)\frac{D^2}{4} \cos^2 \theta \right) (\Omega \sin \lambda + \dot{\phi})^2 + \\
&\quad \frac{1}{2} \left(\left(\frac{1}{3}\bar{m}l + M\right)l^2 \cos^2 \theta + \frac{1}{2}(\bar{m}l + M)\frac{D^2}{4} \sin^2 \theta \right) (\Omega \cos \lambda \sin \beta \cos \phi)^2 + \\
&\quad \frac{1}{2} \left(\frac{1}{3}\bar{m}l + M\right)l^2 (\Omega \cos \lambda \cos \beta \sin \phi + \dot{\theta})^2
\end{aligned} \tag{63}$$

$$\mathbf{D}_E = \frac{1}{2}C (\dot{\phi}^2 + \dot{\theta}^2). \tag{64}$$

Substituting the kinetic, potential and dissipative energies into equation (1) leads, after some mathematical manipulations and rearranging, to M_{dy}^θ , M_{dy}^ϕ

$$\begin{aligned}
M_{dy}^\theta &= \left(\frac{1}{3}\bar{m}l + M\right)l^2 \ddot{\theta} + C\dot{\theta} - \left(\frac{1}{2}\bar{m}l + M\right)gl \sin \theta + \\
&\quad \left[\frac{l^2}{2} \left(\frac{1}{3}\bar{m}l + M\right) - \frac{D^2}{16}(\bar{m}l + M) \right] \sin 2\theta \left[(\Omega \sin \lambda + \dot{\phi})^2 + (\Omega \cos \lambda \sin \beta \cos \phi)^2 \right] \\
M_{dy}^\phi &= \left(\left(\frac{1}{3}\bar{m}l + M\right)l^2 \sin^2 \theta + \frac{1}{8}(\bar{m}l + M)D^2 \cos^2 \theta \right) \ddot{\phi} + C\dot{\phi} + \\
&\quad \left[\frac{l^2}{2} \left(\frac{1}{3}\bar{m}l + M\right) - \frac{D^2}{8}(\bar{m}l + M) \right] \sin 2\theta \left[\Omega \sin \lambda + \dot{\phi} \right] \dot{\theta} - \\
&\quad \frac{1}{2}I_y'' (\Omega \cos \lambda \sin \beta)^2 \sin 2\phi + I_z'' \left(\frac{1}{2}\Omega \cos \lambda \cos \beta \sin 2\phi + \dot{\theta}\Omega \cos \lambda \cos \beta \cos \phi \right)
\end{aligned} \tag{65}$$

F. Governing Equations of Motion

The governing nonlinear differential equations of motion are found by equating the dynamic moments to the applied external moments

$$\begin{aligned}
M_{dy}^{\theta} &= M_{ap}^{\theta} \\
M_{dy}^{\phi} &= M_{ap}^{\phi}.
\end{aligned} \tag{67}$$

The applied moments are found by adding equations (33),(44),(53) and (59)

$$\begin{aligned}
M_{ap}^{\theta} &= M_b^{\theta} + M_{fl}^{\theta} + M_w^{\theta} + M_{sm}^{\theta} - M_{fr}^{\theta} - M_{ad}^{\theta} \\
M_{ap}^{\phi} &= M_b^{\phi} + M_{fl}^{\phi} + M_w^{\phi} + M_{sm}^{\phi} - M_{fr}^{\phi} - M_{ad}^{\phi}.
\end{aligned} \tag{68}$$

Substituting equations (68) and (65) into (67) and rearranging terms leads to the governing nonlinear differential equations of motion for the tower;

$$\begin{aligned}
&J_{eff}^{\theta} \ddot{\theta} + C\dot{\theta} + I_g \left[(\Omega \sin \lambda + \dot{\phi})^2 + (\Omega \cos \lambda \sin \beta \cos \phi)^2 \right] + M_{gb}^{\theta} \\
&= M_{fl}^{\theta} + M_{sm}^{\theta} + M_w^{\theta} - M_{fr}^{\theta}
\end{aligned} \tag{69}$$

$$\begin{aligned}
&J_{eff}^{\phi} \ddot{\phi} + C\dot{\phi} + I_g \left[\Omega \sin \lambda + \dot{\phi} \right] \dot{\theta} + \frac{1}{2} I_{y''} (\Omega \cos \lambda \sin \beta)^2 \sin 2\phi + \\
&I_{z''} \left(\frac{1}{2} \Omega \cos \lambda \cos \beta \sin 2\phi + \dot{\theta} \Omega \cos \lambda \cos \beta \cos \phi \right) \\
&= M_{fl}^{\phi} + M_{sm}^{\phi} + M_w^{\phi} - M_{fr}^{\phi},
\end{aligned} \tag{70}$$

where J_{eff}^{θ} and J_{eff}^{ϕ} are the effective position dependent moments of inertia,

$$J_{eff}^{\theta} = \left(\frac{1}{3} \bar{m}l + M \right) l^2 + \frac{1}{12} C_A \rho \pi D^2 L^3 (1 + \tan^2 \theta)$$

$$J_{eff}^{\phi} = \left(\frac{1}{3}\bar{m}l + M\right) l^2 \sin^2 \theta + \frac{1}{8}(\bar{m}l + M) D^2 \cos^2 \theta + \frac{1}{12} C_A \rho \pi D^2 L^3 \tan^2 \theta. \quad (71)$$

I_g is a constant depending on the system parameters,

$$I_g = \left(\frac{l^2}{2}\left(\frac{1}{3}\bar{m}l + M\right) - \frac{D^2}{8}(\bar{m}l + M)\right) \sin 2\theta \quad (72)$$

and M_{gb}^{θ} is the moment due to gravity and buoyancy

$$M_{gb}^{\theta} = \rho g \pi \frac{D^2}{4} \left[\frac{D^2}{32} \tan^2 \theta (2 \cos \theta + \sin \theta) + \frac{1}{2} \left(\frac{d + \eta(y, t)}{\cos \theta} \right)^2 \sin \theta \right] - \left(\frac{1}{2} \bar{m}l + M \right) gl \sin \theta. \quad (73)$$

The equations can be simplified by neglecting the Coriolis acceleration terms due to earth rotation. That results in the following equations of motion that are similar to those derived by Kirk and Jain [8],

$$J_{eff}^{\theta} \ddot{\theta} + C \dot{\theta} + I_g \dot{\phi}^2 + M_{gb}^{\theta} = M_{fl}^{\theta} + M_{sm}^{\theta} + M_w^{\theta} - M_{fr}^{\theta} \quad (74)$$

$$J_{eff}^{\phi} \ddot{\phi} + C \dot{\phi} + I_g \dot{\theta}^2 = M_{fl}^{\phi} + M_{sm}^{\phi} + M_w^{\phi} - M_{fr}^{\phi}.$$

IV. NUMERICAL SOLUTION

The governing nonlinear differential equations of motion (69), (70) are numerically solved using 'ACSL' and the results are analyzed using 'MATLAB'.

The physical parameters used in the simulations are,

- l - Length of tower = 400 m
- D - Tower diameter = 15 m
- M - End mass = 2.5×10^5 Kg
- m - Tower mass per unit length = 20×10^3 Kg/m
- R_h - Pivot radius = 3 m
- d - Mean water level = 350 m
- ρ - Water density = 1025 Kg/m^3
- ζ - Structural damping = 0.02
- C_D - Drag coefficient = 1.2
- C_M - Inertia coefficient = 1.5
- C_L - Lift coefficient = 1.0

The equations of motion are solved for the following cases:

- Free vibration and damping (drag, viscous and friction) effect
- Equilibrium position of the tower in the presence of wind and/or current
- Response to wave, wind and current
- Superharmonic, harmonic and subharmonic resonances
- Response due to wave slamming and Coriolis acceleration
- Chaotic Response.

1. Free Vibrations

To find the fundamental frequency, the wave height and current and wind velocities were set to zero. The initial condition is set to $\dot{\theta}_0 = 0.01$ rad/s. Figures 6, 7 and 8 depict the free vibration of the tower in the presence of different damping mechanisms; structural viscous damping, coulomb friction and drag force, respectively. As can be seen from the figures, the natural frequency is $\omega_n = 0.028$ Hz. The response in the presence of drag force and coulomb friction is nonlinear, and the tower vibrates in the natural frequency and its odd multiples (see Figs. 7 (b) and 8 (b)), while the response in the presence of structural damping is linear and only the natural frequency appears, see Fig. 6 (b). Figs. 6 (c), 7 (c) and 8 (c) show the phase plane of the response. The decaying characteristics of each mechanism are clearly seen from the time domain figures, i.e., exponential, hyperbolic and linear for viscous, drag and friction damping, respectively.

2. Equilibrium Position

As was shown previously by Bar-Avi and Benaroya [1] for the single degree of freedom model, the equilibrium position depends on the current velocity and the drag coefficient. In this section, the equilibrium position due to current and wind is found and also the effect of vortex shedding force on the response is investigated. The wave height is $H = 0$ m, the current velocity is $U_c = 1$ m/s and the wind velocity is $u_w = 20$ m/s. Fig. 9 shows the response due to current and wind propagating in the y direction, i.e., $\alpha = 0$, $\nu = 0$ deg. with lift coefficient $C_L = 0$. After the transient, the tower remains at a point where all forces are in equilibrium, about 2.4 m in the y direction. When the current is in the z direction, the

equilibrium position is at $y \approx 0.4$ m and $z \approx 2.0$ m as can be seen from Fig. 10. The reason is that the total force due to wind and current is a vector summation, and so the equilibrium position can be simplified to

$$\begin{aligned}\theta_{eq} &= \frac{1}{2} \sqrt{\frac{(C_D \rho D d^2 U_c^2)^2 + (C_D^a \rho^a D (l-d)^2 u_w^2)^2}{\rho g \pi D^2 d^2 - 2gl(\bar{m}l + 2M)}} \\ \phi_{eq} &= \tan^{-1} \left(\frac{C_D \rho D d^2 U_c^2 \sin \alpha + C_D^a \rho^a D (l-d)^2 u_w^2 \sin \nu}{C_D \rho D d^2 U_c^2 \cos \alpha + C_D^a \rho^a D (l-d)^2 u_w^2 \cos \nu} \right).\end{aligned}\quad (75)$$

Setting the lift coefficient to $C_L = 1$, changes the response of the tower to current and wind as can be seen from the next two figures. Fig. 11 depicts the response when both the wind and current are in the y direction. The tower's top oscillates about $y = 2.4$ m in the z direction. The oscillations are in the vortex shedding frequencies due to current $\omega_s = 0.002$ Hz and due to wind $\omega_{Lw} = 0.04$ Hz as can be seen from Fig. 11 (c). When the current is in the z direction, the tower oscillates about $y \approx 0.4$ m and $z \approx 2.0$ m, but now in the y direction as shown in Fig. 12 (b). The frequencies of oscillation are the same as those in Fig. 11.

3. Response to Waves, Current and Wind

In this study the wave height H is much smaller the mean water level d , i.e. $H \ll d$. Therefore, the relation between the wave height and the wave frequency ω , given in Hooft (1981) [21] is used. This relation with the deep water simplification $\tanh kd = 1$, leads to

$$\omega = \sqrt{\frac{\pi}{2H}}.\quad (76)$$

The fluid parameters used are $C_D = 1.2$, $C_M = 1.5$ and $C_L = 1.0$, and the wave height is $H = 3$ m. First, the response due to waves without current and wind is depicted in Fig. 13. The deflection angle θ oscillates about zero equilibrium position in the wave frequency given by equation (76), $\omega = 0.12$ Hz.

Fig. 14 shows the response due to waves, current and wind propagating in the y direction. The oscillations are now about an equilibrium position $y \approx 2.4$ m, $z = 0$, that can be calculated from equation (75). The response PSD contains several loading frequencies, as shown in 14 (c). These are; the natural frequency $\omega_n = 0.028$ Hz and its multiples, wave frequency $\omega = 0.12$ Hz, the vortex shedding frequency due to waves $\omega_s = 2\omega = 0.24$ Hz, and the vortex shedding frequency due to wind $\omega_w = 0.04$ Hz.

The effect of wind in the z direction is depicted in Fig. 15. The tower oscillates in the same frequencies as for the case of Fig. 14, but now about an equilibrium position of $y \approx 2.2$ m and $z \approx 0.04$ m.

Finally, setting the vortex shedding coefficient to zero results in a response described in Fig. 16. The vortex shedding frequencies disappeared as expected and only two main frequencies remain, the natural frequency and the wave frequency.

4. Resonance Response

Next the tower's response to harmonic, subharmonic and superharmonic excitation is investigated and compared to the response of the single degree of freedom model. Figs. 17, 18 show the tower's response to wave excitation at the natural frequency of the system $\omega \approx \omega_n$. The wave height is $H = 1$ m, the drag coefficient $C_D = 0$. From the time domain response, Fig. 17 (a) the beating phenomenon is clearly seen. Fig. 18 describes the tower response in

the phase plane (a), and the tower's top motion (b).

Superharmonic response is depicted in Figs. 19, 20. Here the excitation frequency is nearly twice the natural frequency of the system $\omega \approx 2\omega_n$. From the time domain it can be seen that the beating phenomenon is not as pronounced as in the harmonic response and the amplitude is much smaller.

From the phase plane (Fig. 20 (a)), we see that the trajectories do not repeat, but investigating this point further showed it to be a quasiperiodic response and not a chaotic one.

Superharmonic response, in which the excitation frequency is about one half of the natural frequency, i.e., $\omega \approx \frac{1}{2}\omega_n$, is depicted in Figs. 21 and 22. The amplitude of the response is small and there is no beating. The response, like in the superharmonics, is a quasiperiodic motion.

Comparing the resonance responses for the two degrees of freedom with those of the single degree of freedom (see Bar-Avi and Benaroya [1]), it is found that the regions about the resonance frequencies ($\frac{1}{2}\omega_n, \omega_n, 2\omega_n$) in which beating occurs, are much smaller and less pronounced for the two DOF system.

Finally, the harmonic response in the presence of drag force, with $C_D = 1.2$. The beating phenomenon vanishes and the trajectories in the phase plane repeat as shown in Figs. 23 and 24

5. Wave Slamming, Coriolis Acceleration and Wind Effects

The tower's response due to wave slamming, Coriolis acceleration and wind loads are investigated next. Wave slamming and Coriolis acceleration, although having a small influence

on the response, are important. The first, due to its high frequency characteristics that can cause fatigue, and the later due the coupling it causes between the two degrees of freedom.

Wave slamming response is shown in Fig. 25. The significant wave height is $H = 5$ m, the wave frequency is nearly the natural frequency of the tower, i.e., $\omega \approx \omega_n$, and all fluid parameters set to zero. The motion is in the y direction only, since there is no transverse force, and is of very small amplitude. As can be seen from the figure the response beats since the impulsive force frequency is very close to the tower's natural frequency.

When earth rotation is added to the model, a transverse (gyroscopic) moment causes a coupling between the two degrees of freedom so the response due to wave slamming is not planar any longer, as shown in Fig. 26 (c).

Fig. 27 shows the response due to waves and Coriolis effect. The vortex shedding coefficient $C_L = 0$, but as can be seen from the figure, there is a transverse force (like the vortex shedding) caused by the rotation of the earth.

Wind has a larger effect, on the response, than the previous two loads. Figs. 28 and 29 describe the tower's response due to wind in the y, z directions, respectively.

6. Chaotic Response

Due to the nonlinearity in the model, chaotic response is expected to be possible. Investigation of the chaotic response, and mapping its regions of occurrence is beyond the scope of this study. Nevertheless for completeness, a chaotic response is shown. Fig. 30 depicts the towers's response for wave height $H = 5$ m with $\omega = 0.1$ rad/s and zero initial conditions. The trajectories in the phase plane do not repeat.

Fig. 31 depicts the same response but with nonzero initial conditions. The responses are

different as can be seen by comparing the figures.

The proof that the response is chaotic is given by the Poincaré map shown in Fig. 32. For $C_D = 0$, Fig. 32 (a) the points are scattered in an erratic fashion, but for $C_D = 1.2$, Fig. 32 (b) the points are much more organized, almost as in a quasiperiodic response.

V. SUMMARY

The nonlinear differential equations of motion for a two degree of freedom articulated tower submerged in the ocean are derived using Lagrange's equations. The tower is shown to have the same dynamic properties as an upright spherical pendulum with additional effects and forces;

- Coulomb friction in the pivot (hinge)
- Structural viscous damping
- Gyroscopic moments due to the rotation of the earth
- Drag fluid force due to waves and current, coupled to the structure
- Inertia and added mass fluid forces
- Drag wind load on the exposed part of the tower
- Wave slamming force
- Vortex shedding loads due to waves and wind
- Buoyancy force.

All fluid forces mentioned above, due to waves, current, and wind, are determined at the instantaneous position of the tower, resulting in two, highly nonlinear, coupled ordinary differential equations with time-dependent coefficients. The equations are numerically solved using 'ACSL' software, and the results are analyzed with 'MATLAB'. From the simulations the following observations and conclusions are drawn;

- The equilibrium position depends on the current and wind magnitude and direction. An analytical expression that matches the numerical results is found.
- The resonance response for harmonic, subharmonic and superharmonic cases are evaluated and beating is shown. The regions in which the beating occurs are very small and are not as pronounced as in the single degree analysis performed by Bar-Avi and Benaroya [1].
- The system can exhibit chaotic behavior depending on the wave's frequency and amplitude.
- The response to wave slamming is very small since an impulsive force is attenuated when the pulse period is shorter than the system fundamental period, which is the case here.
- The Coriolis acceleration moment has a small but important influence on the response, since it causes a coupling so that planar motion is not possible under real conditions.

A. Acknowledgment

This work is supported by the Office of Naval Research Grant no. N00014 - 93 - 1 - 0763.

The authors are grateful for this support from ONR and Program Manager Dr. T. Swean for his interest in our work. This work is part of a research effort which will be submitted by the first author in partial fulfillment of the requirements for a Doctor of Philosophy.

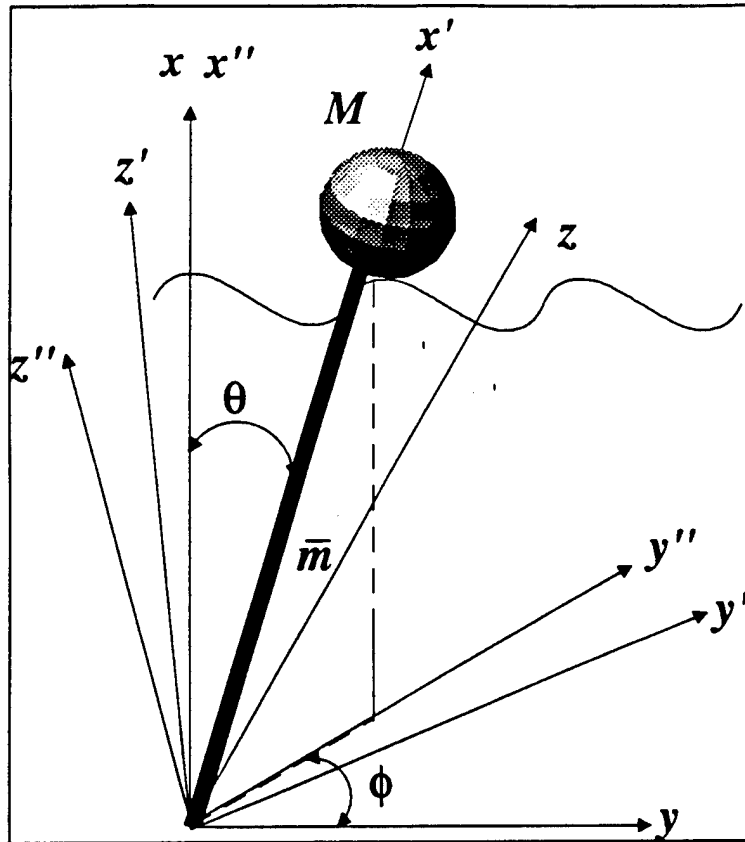


Figure 1: Model and Coordinate Systems

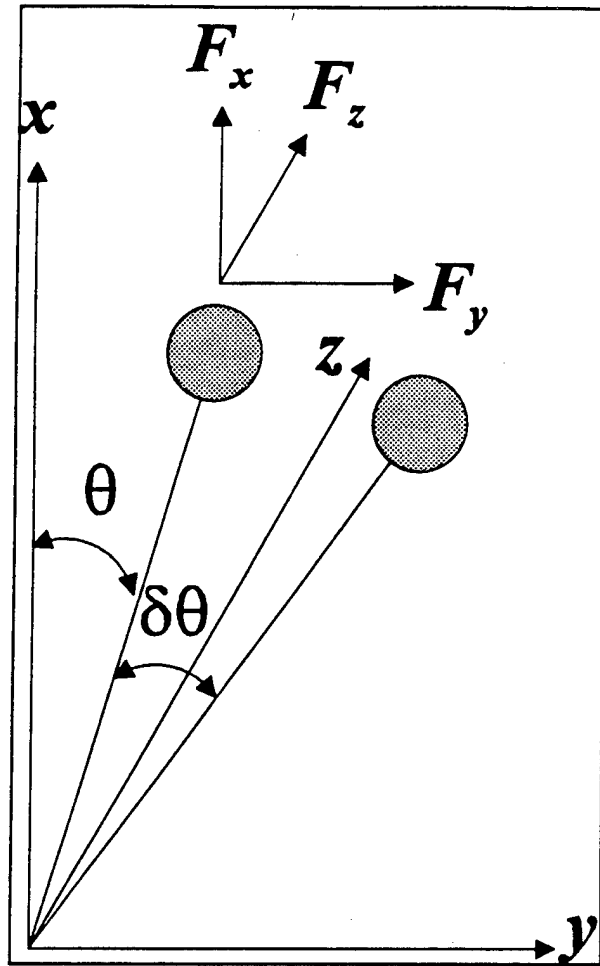


Figure 2: Generalized Force for θ

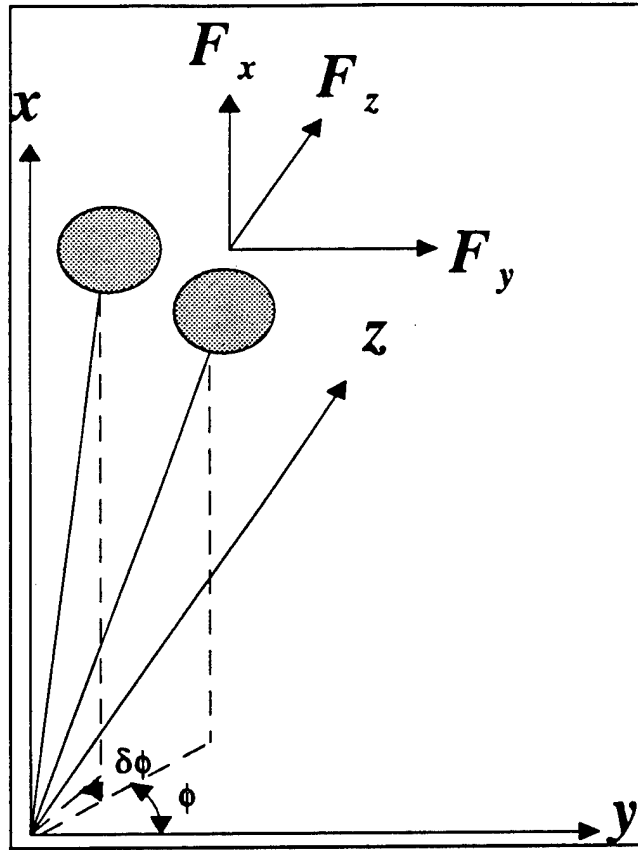


Figure 3: Generalized Force for ϕ

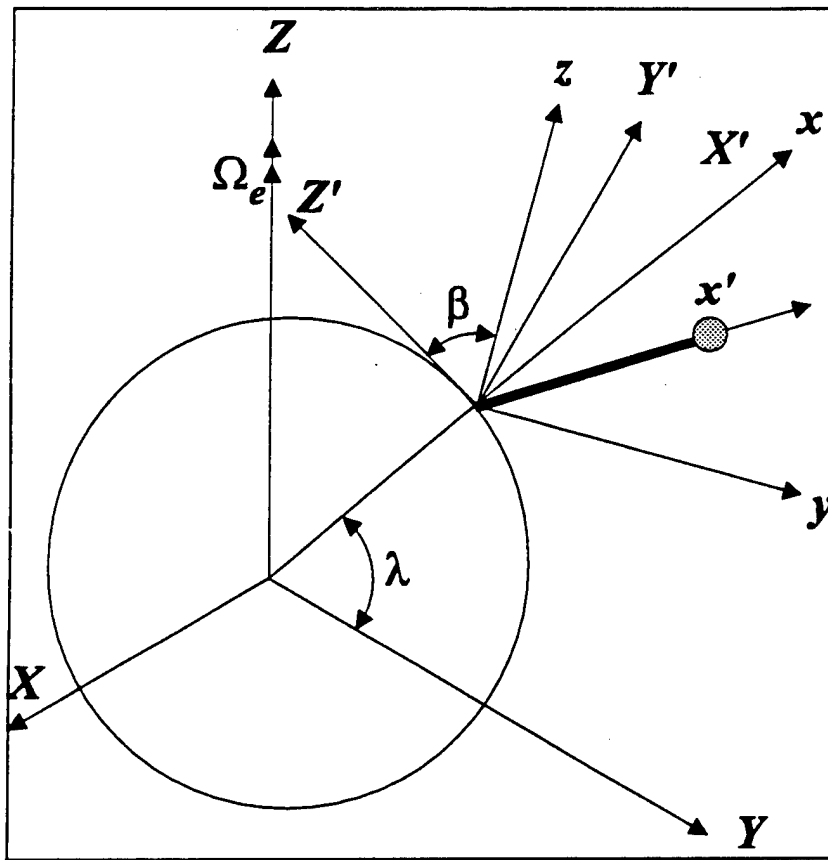


Figure 4: Earth and Tower Coordinate Systems

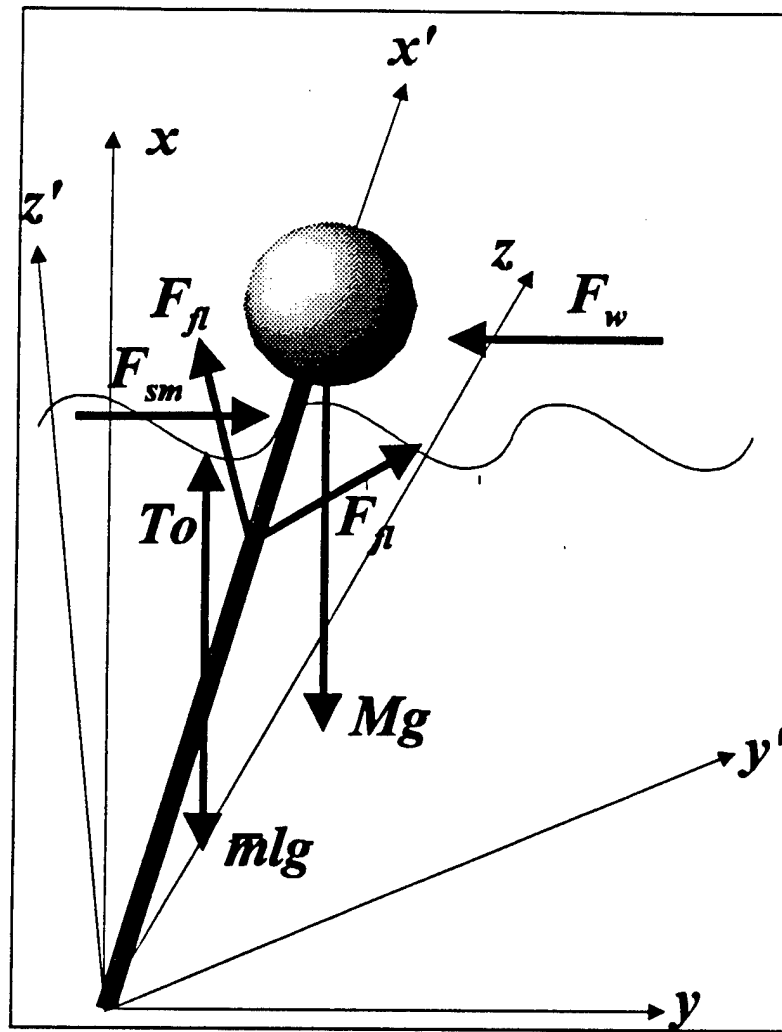


Figure 5: External Forces Acting on the Tower

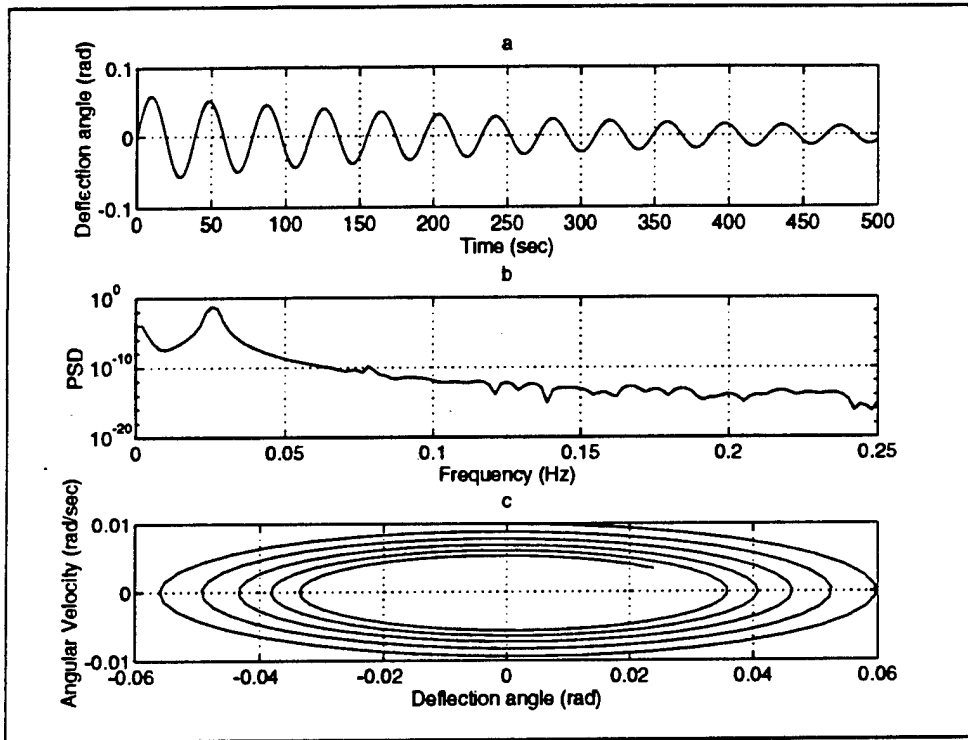


Figure 6: Damped Free-Vibration - Structural Viscous Damping, $\zeta = 0.02$

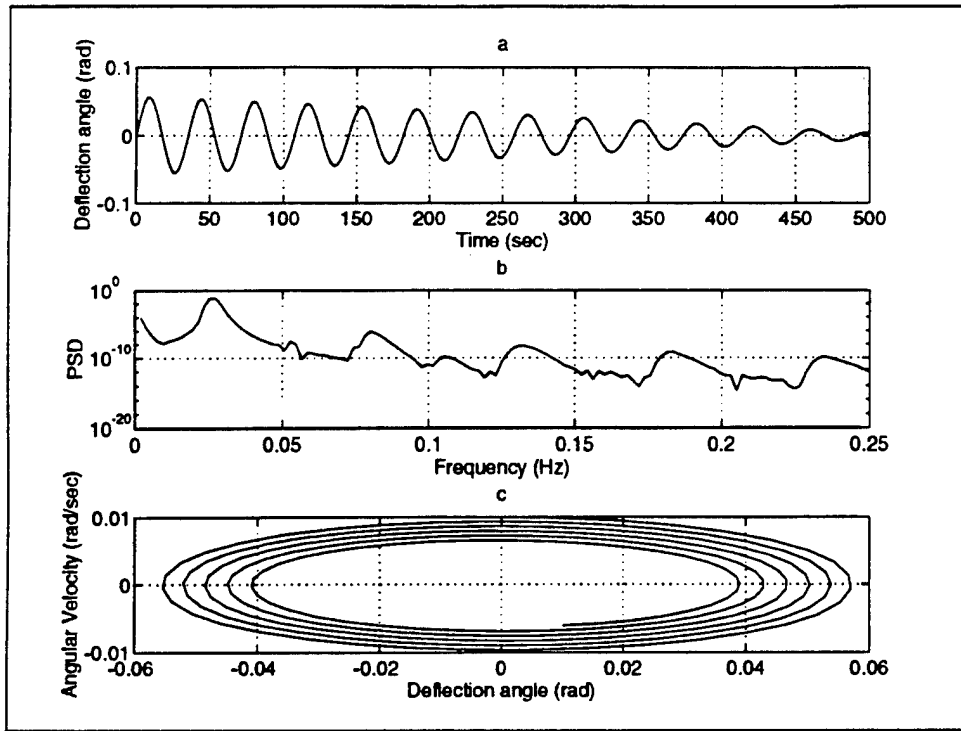


Figure 7: Damped Free-Vibration - Coulomb Friction, $\mu = 0.1$

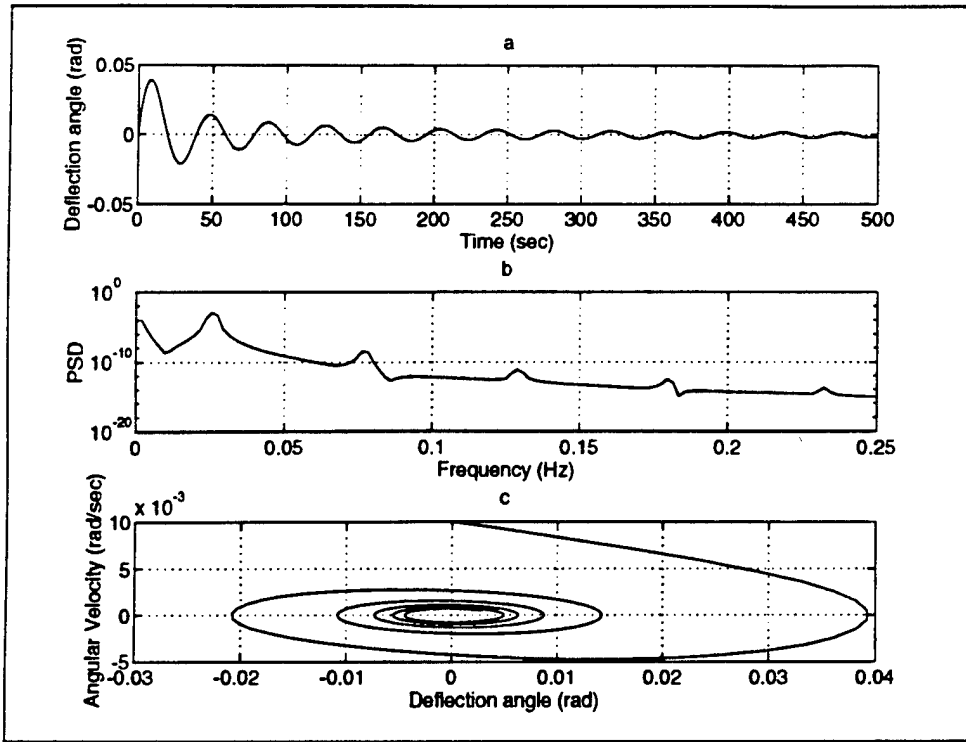


Figure 8: Damped Free-Vibration - Drag Force, $C_D = 1.2$

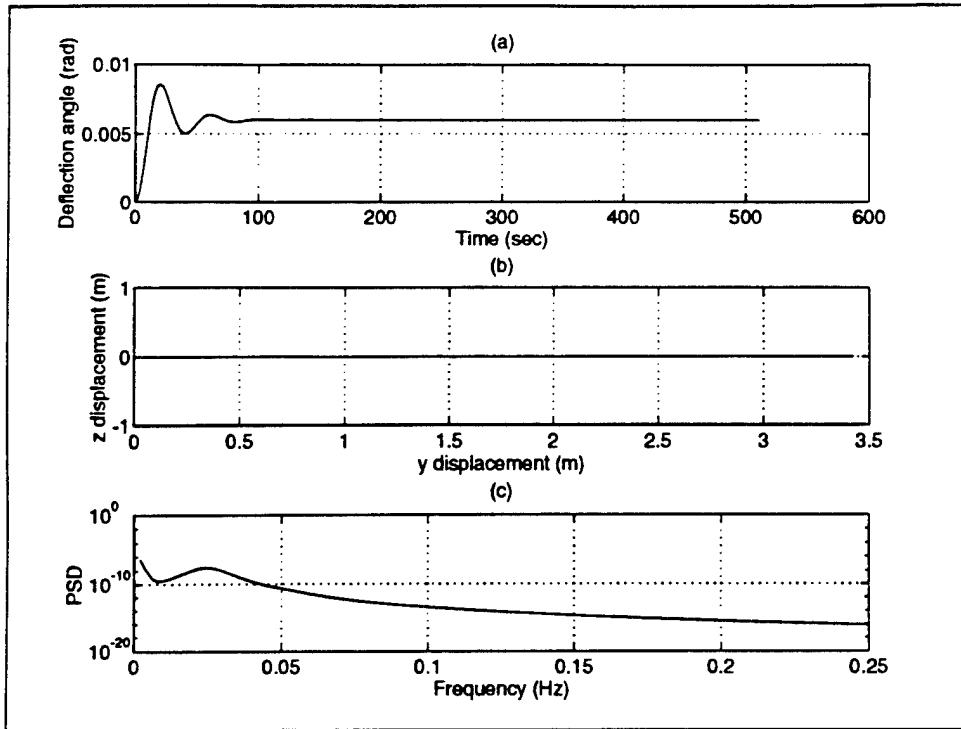


Figure 9: Equilibrium position in the Presence of Current and Wind, $C_L = 0$, $\alpha = 0$, $\nu = 0$.

(a) θ Time Domain, (b) Tower's Top Motion, (c) θ Frequency Domain

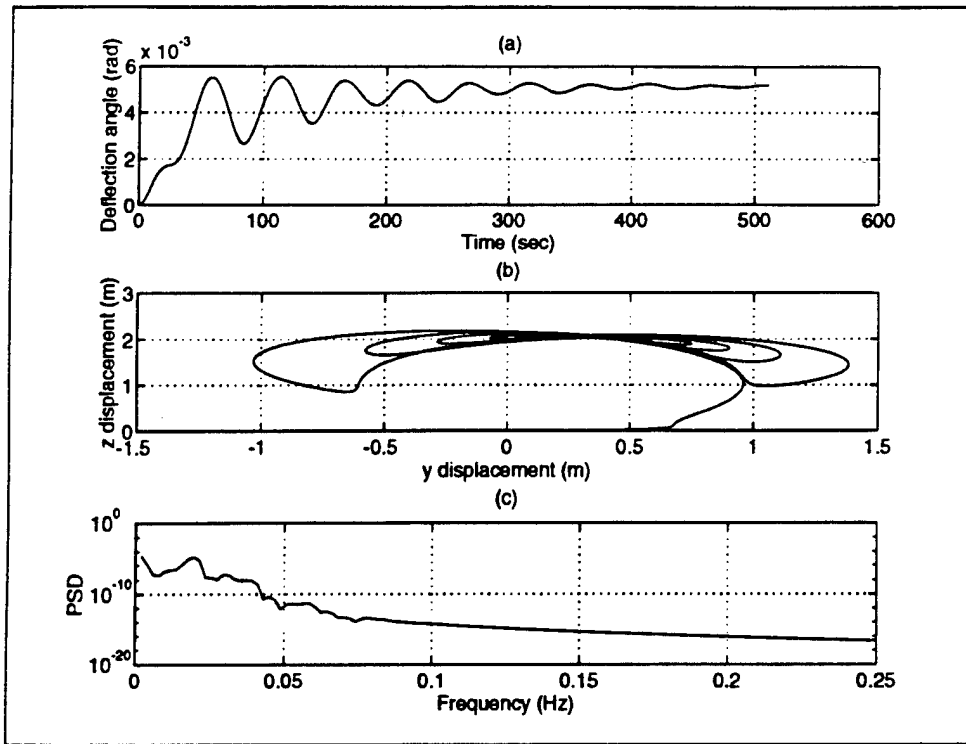


Figure 10: Equilibrium position in the Presence of Current and Wind, $C_L = 0$, $\alpha = 90$, $\nu = 0$.

(a) θ Time Domain, (b) Tower's Top Motion, (c) θ Frequency Domain

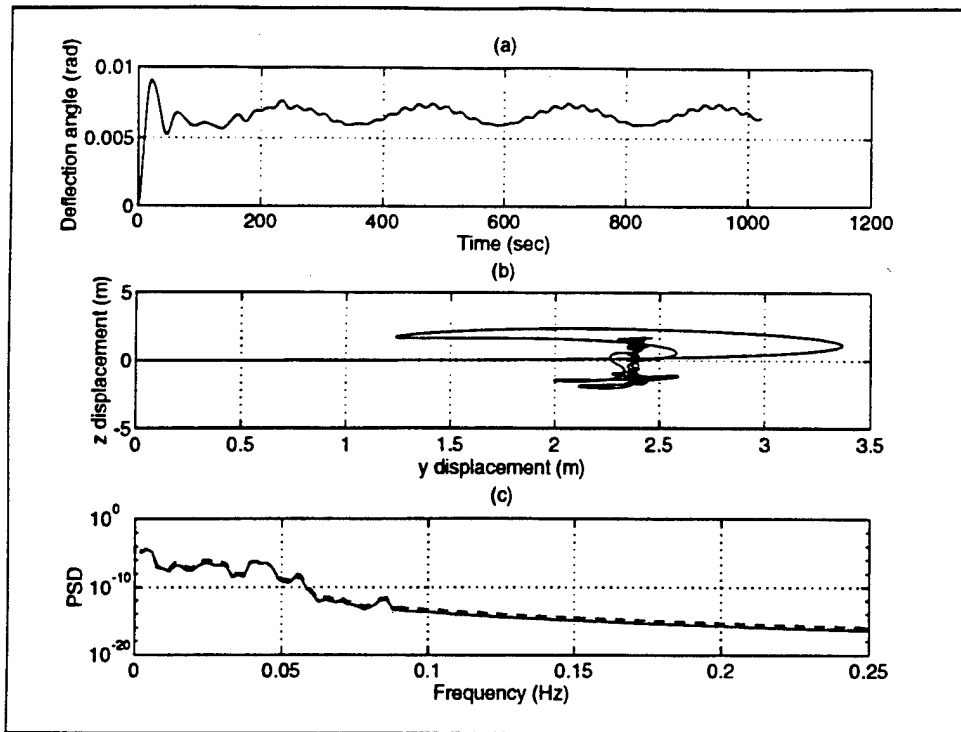


Figure 11: Equilibrium position in the Presence of Current and Wind, $C_L = 1$, $\alpha = 0$, $\nu = 0$.

(a) θ Time Domain, (b) Tower's Top Motion, (c) θ Frequency Domain

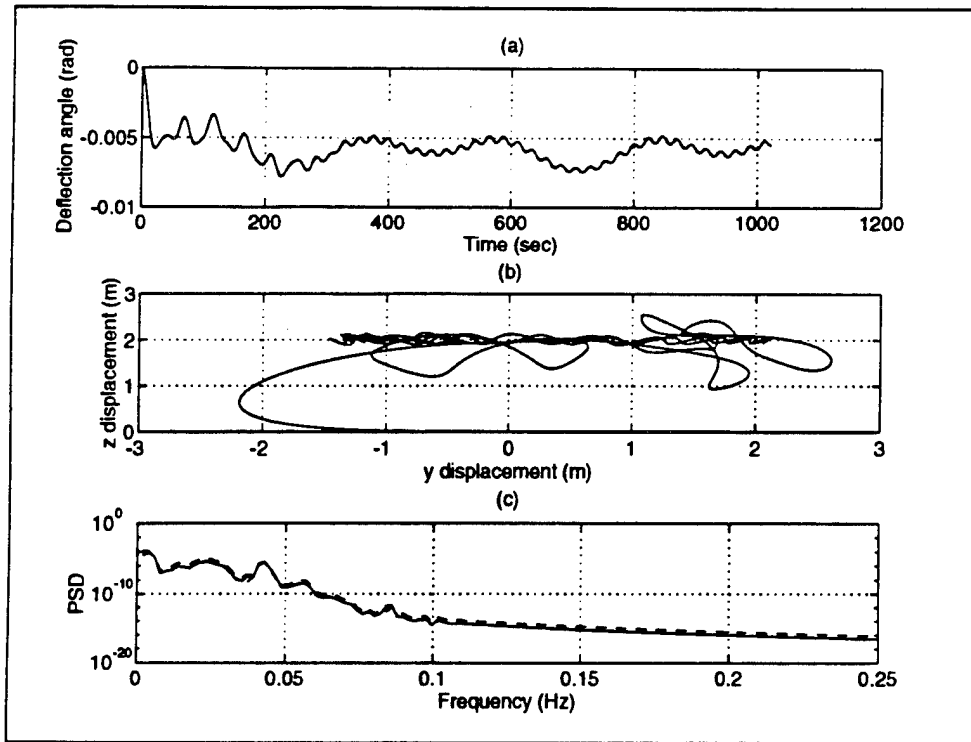


Figure 12: Equilibrium position in the Presence of Current and Wind, $C_L = 1$, $\alpha = 90$, $\nu = 0$.

(a) θ Time Domain, (b) Tower's Top Motion, (c) θ Frequency Domain

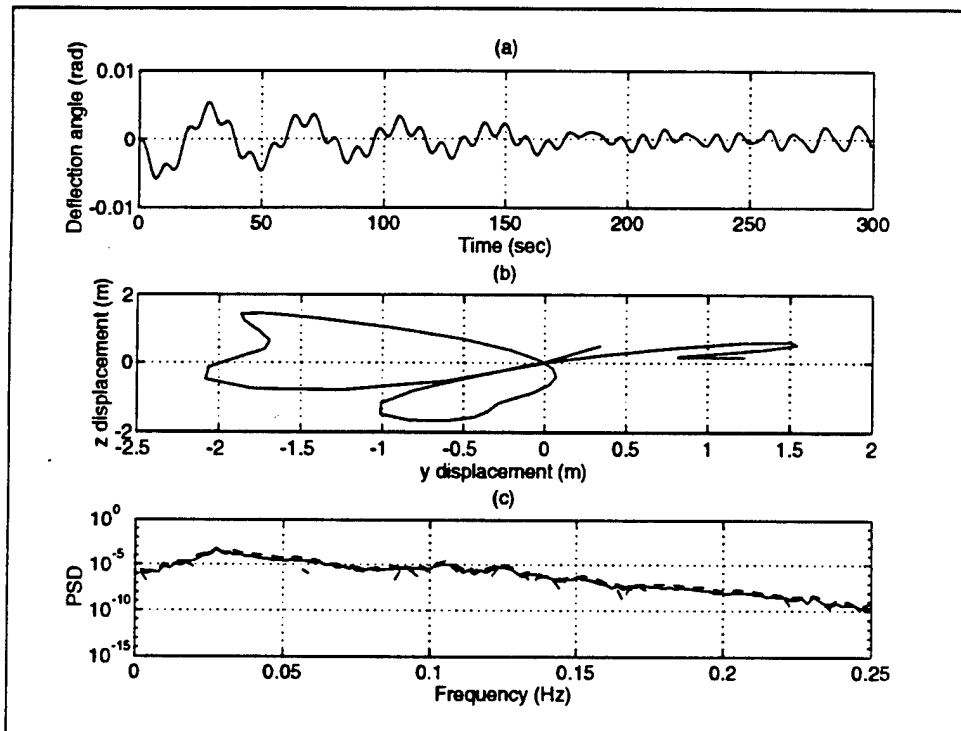


Figure 13: Response due to wave excitation, $U_c = 0$, $u_w = 0$, $\alpha = 0$, $\nu = 0$ deg.

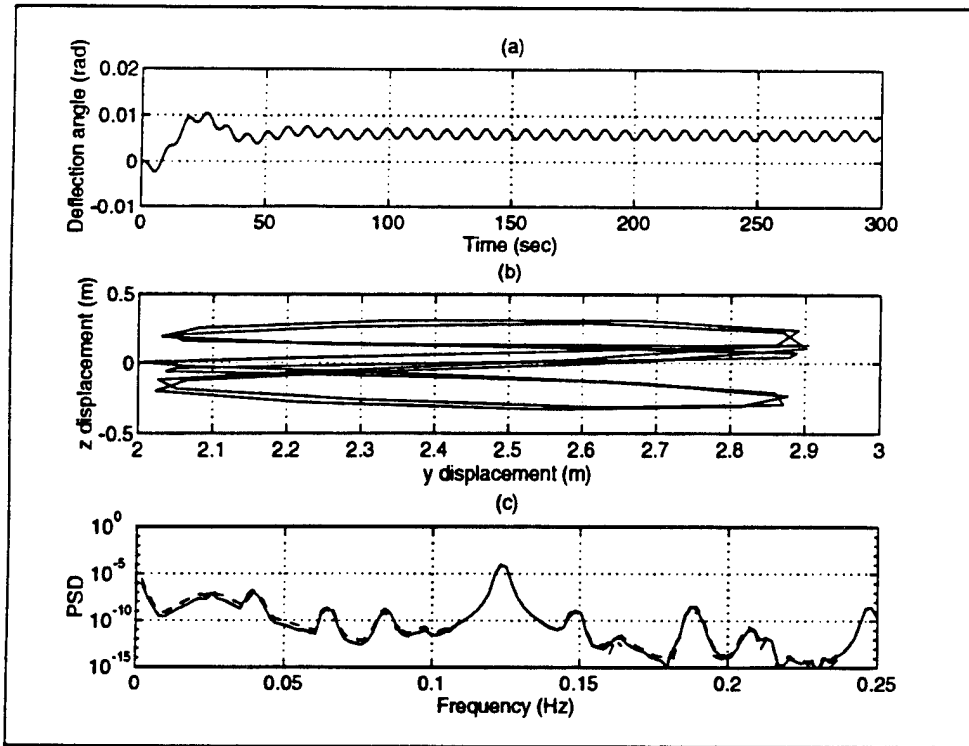


Figure 14: Response due to wave excitation, $U_c = 1$, $u_w = 20$, $\alpha = 0$, $\nu = 0$ deg.

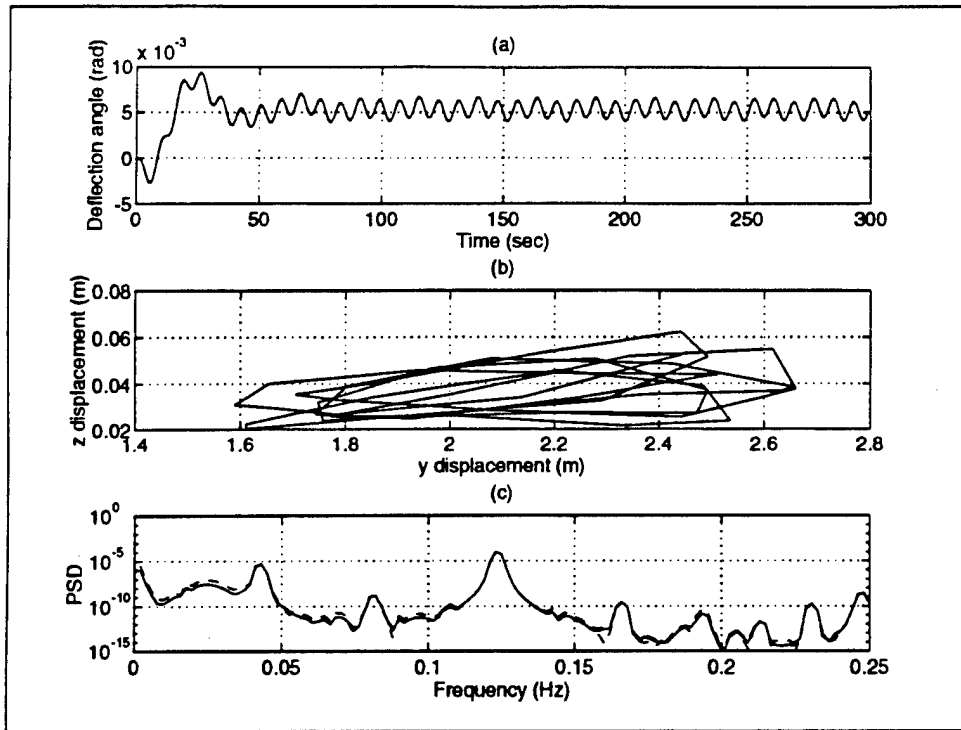


Figure 15: Response due to wave excitation, $U_c = 1$, $u_w = 20$, $\alpha = 0$, $\nu = 90$ deg.

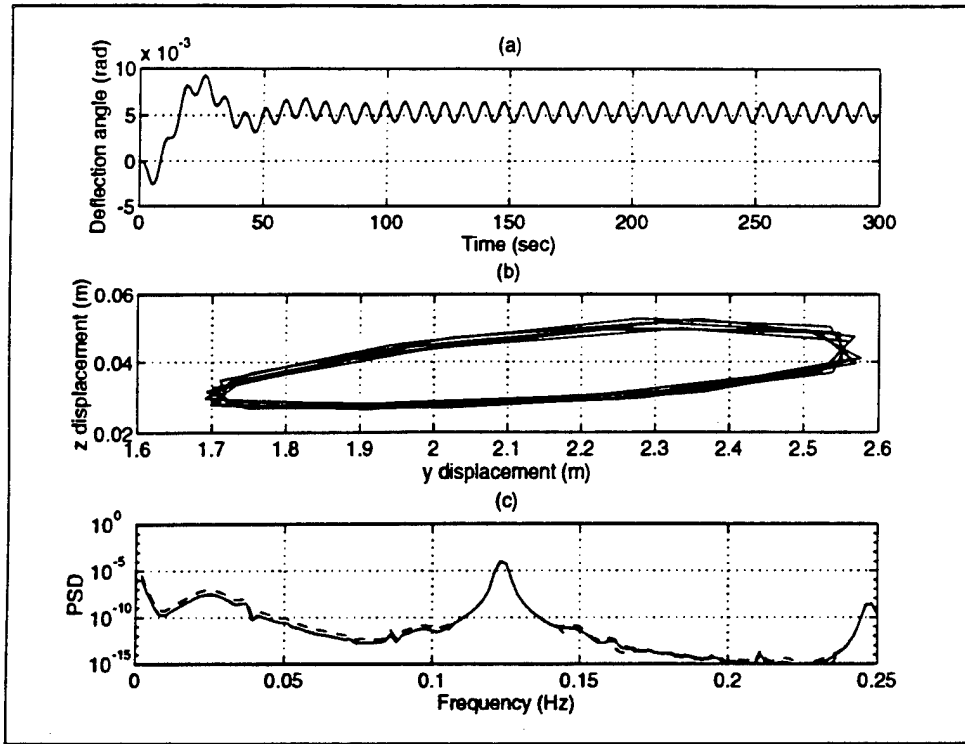


Figure 16: Response due to wave excitation with $C_L = 0$, $U_c = 1$, $u_w = 20$, $\alpha = 0$, $\nu = 0$ deg.

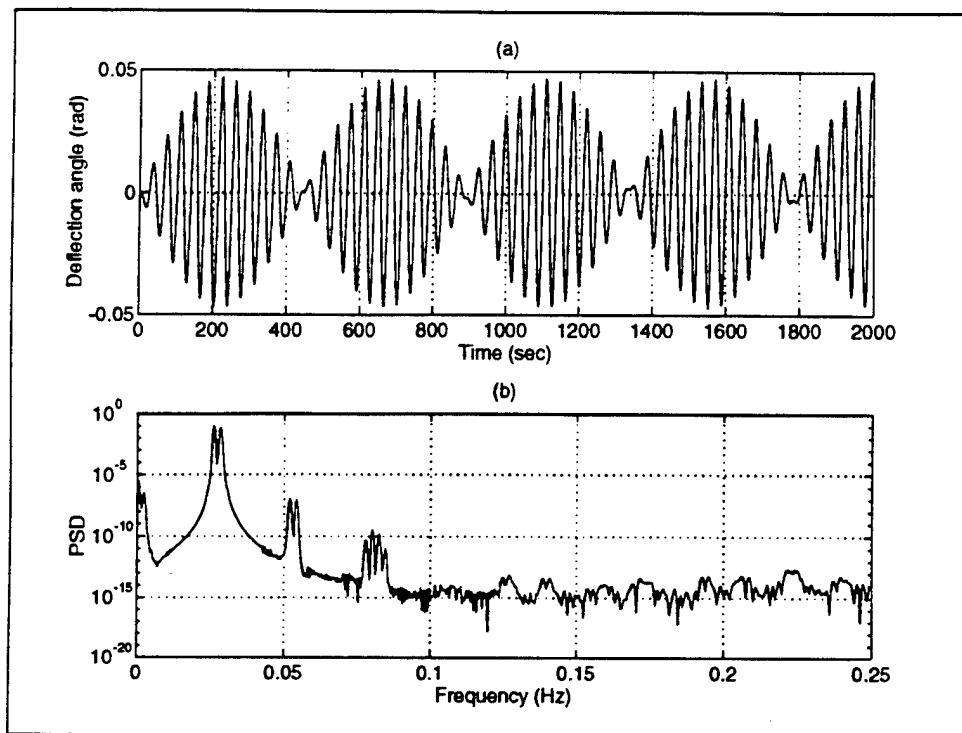


Figure 17: Undamped Response to Harmonic Excitation $\omega \approx \omega_n$, (a) Time Domain (b) Frequency Domain

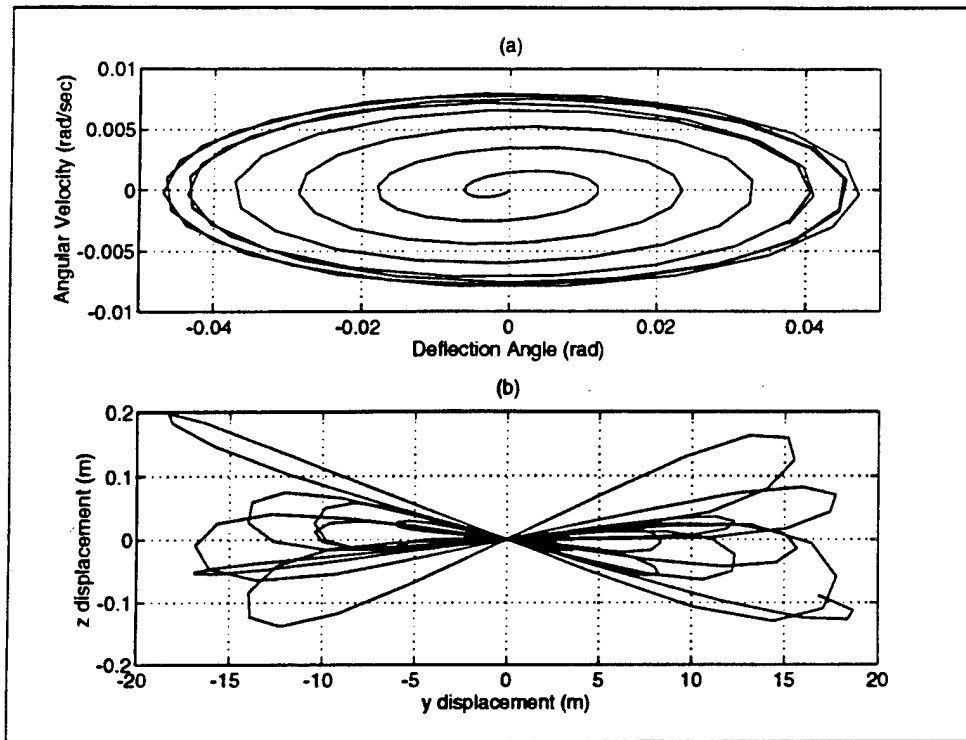


Figure 18: Undamped Response to Harmonic Excitation $\omega \approx \omega_n$, (a) Phase Plane (b) Tower's Top Motion

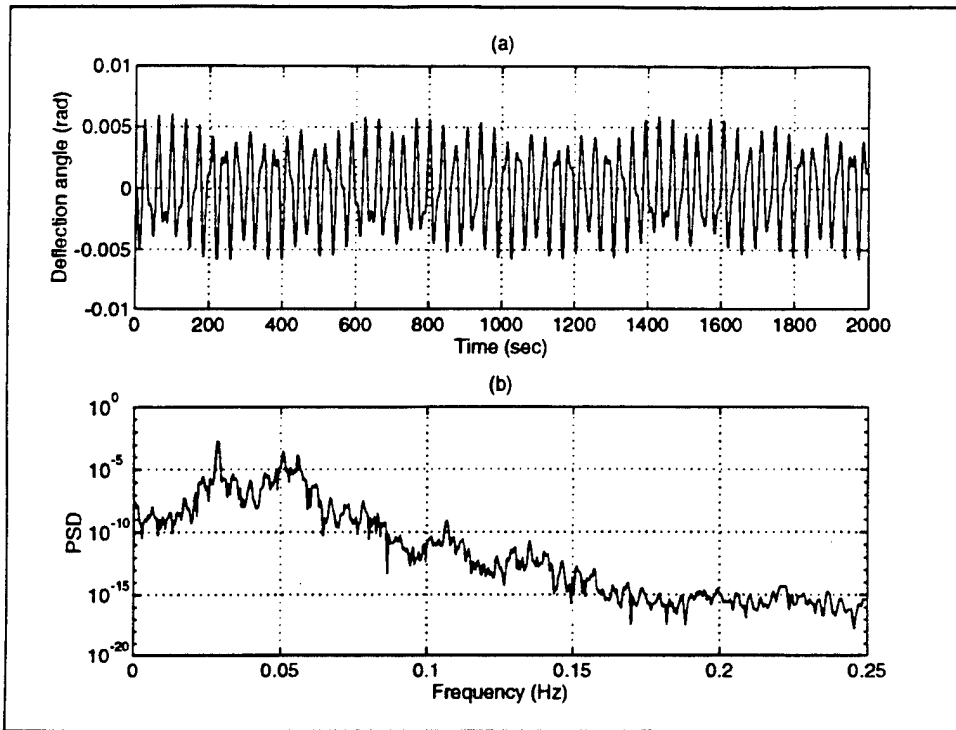


Figure 19: Undamped Response to Harmonic Excitation $\omega \approx 2\omega_n$, (a) Time Domain (b) Frequency Domain

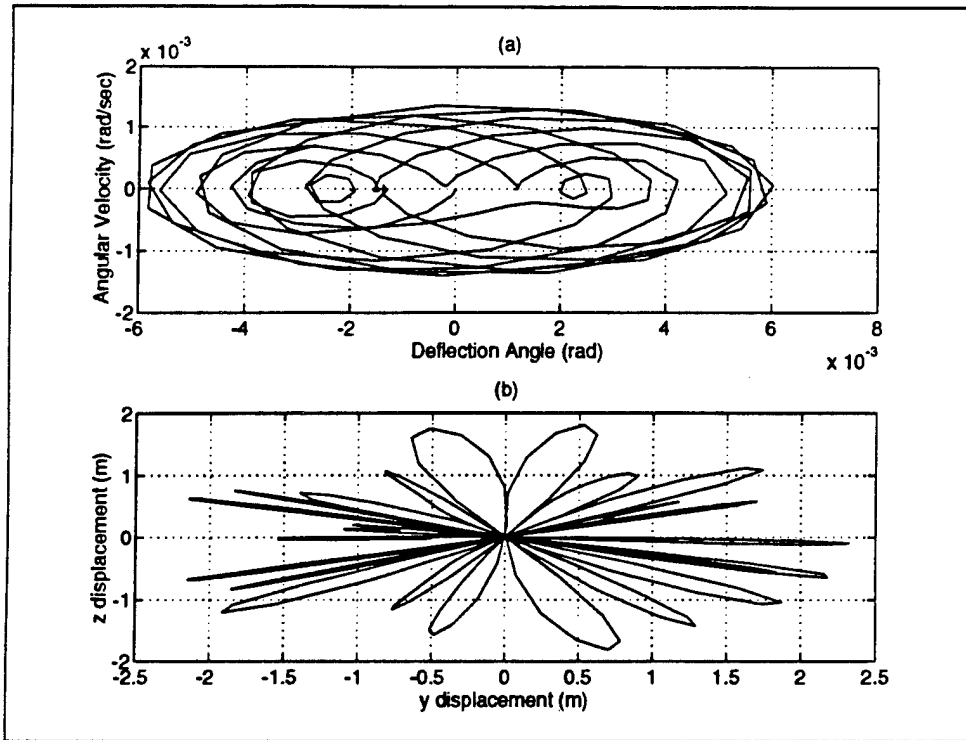


Figure 20: Undamped Response to Harmonic Excitation $\omega \approx 2\omega_n$, (a) Phase Plane (b) Tower's Top Motion

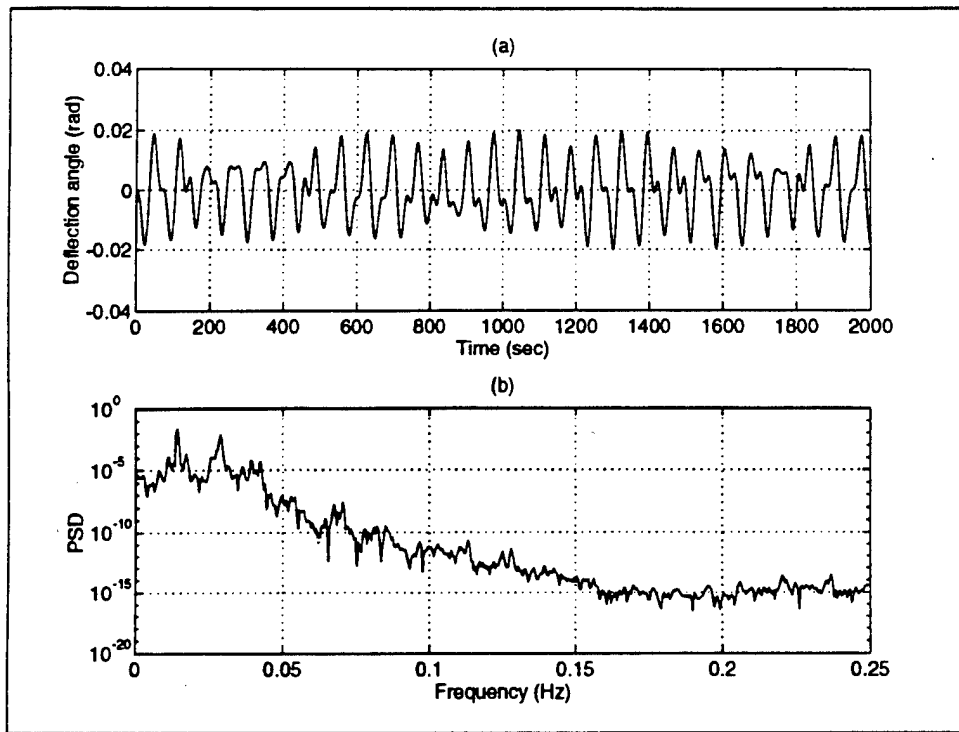


Figure 21: Undamped Response to Harmonic Excitation $\omega \approx 0.5\omega_n$, (a) Time Domain (b) Frequency Domain

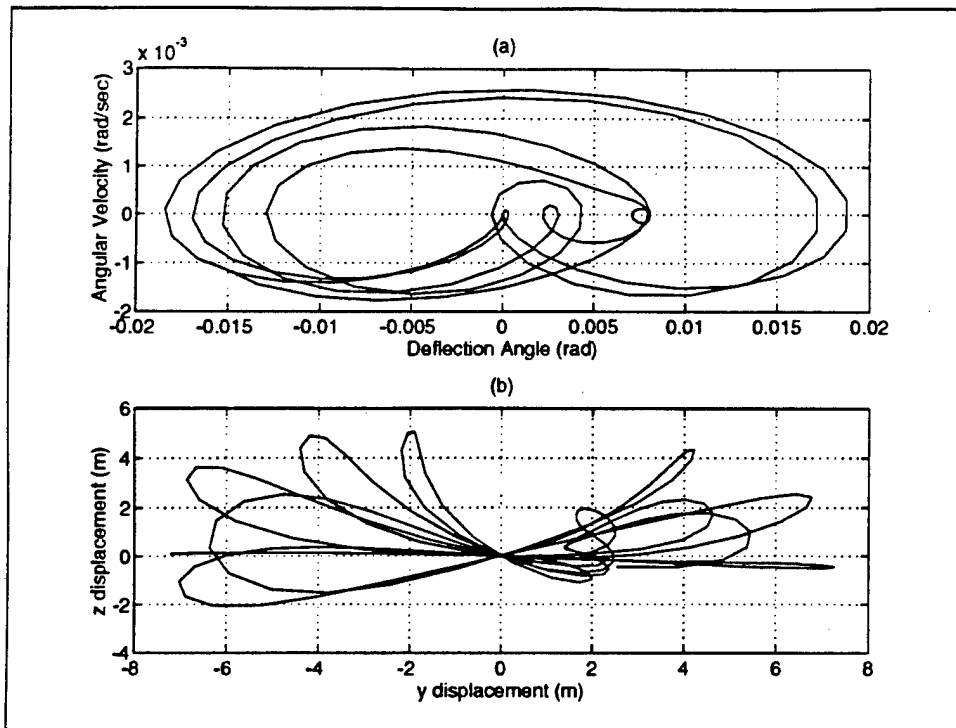


Figure 22: Undamped Response to Harmonic Excitation $\omega \approx 0.5\omega_n$, (a) Phase Plane (b) Tower's Top Motion

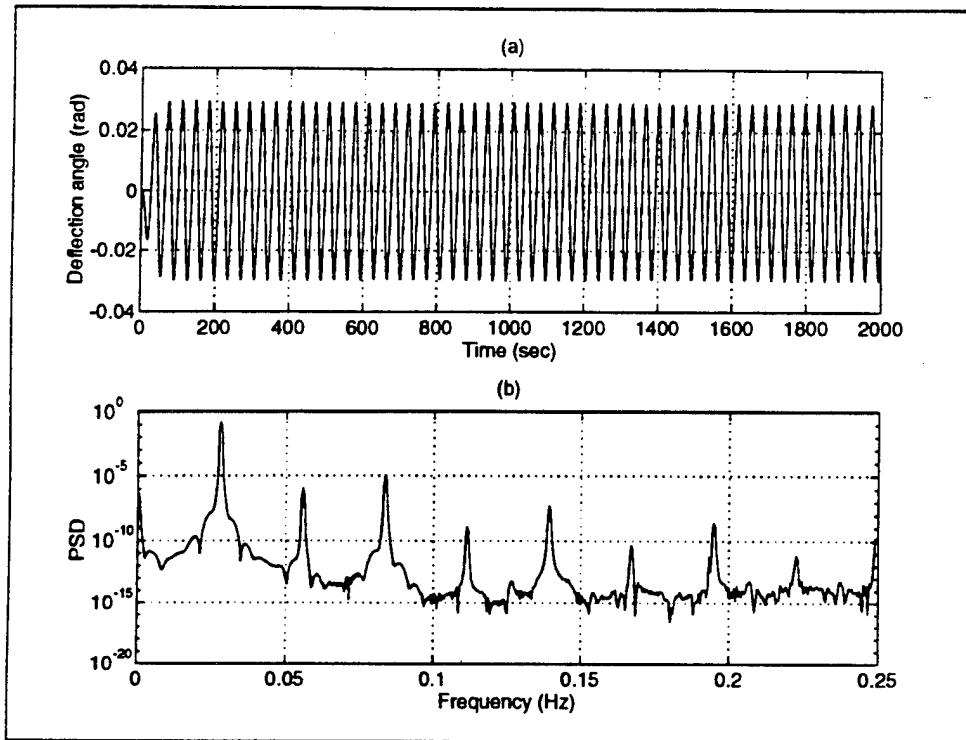


Figure 23: Undamped Response to Harmonic Excitation $\omega \approx \omega_n$, $C_D = 1.2$, (a) Time Domain

(b) Frequency Domain

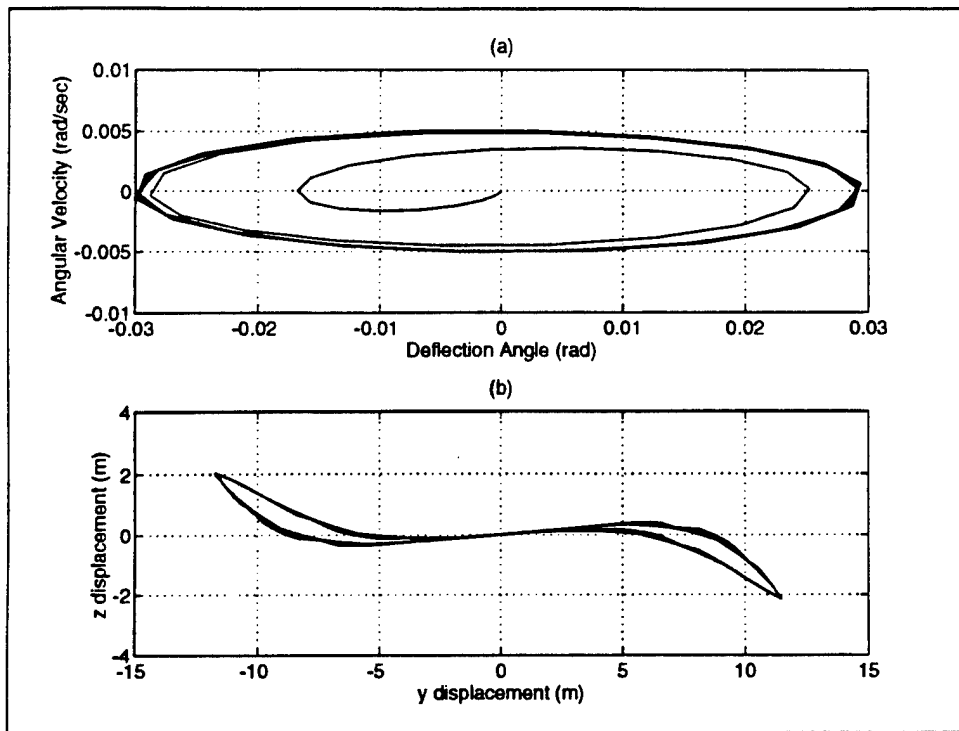


Figure 24: Undamped Response to Harmonic Excitation $\omega \approx \omega_n$, $C_D = 1.2$, (a) Phase Plane
 (b) Tower's Top Motion

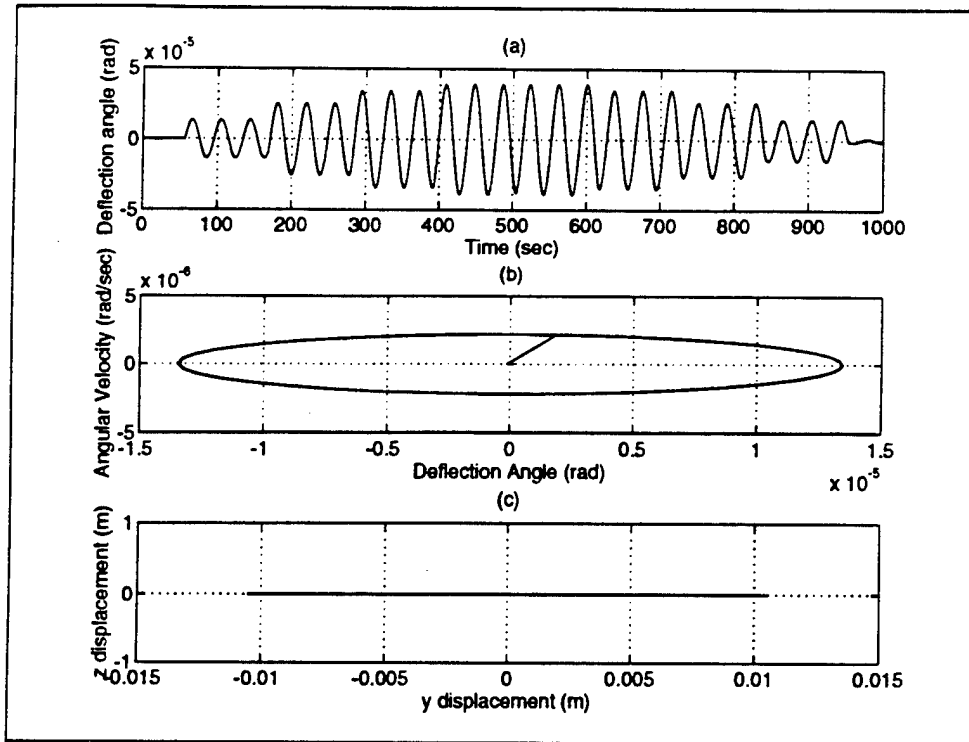


Figure 25: Response to Wave Slamming, $H = 5$ m, $C_L = C_M = C_D = 0$, (a) Time Domain
 (b) Phase Plane (c) Tower's Top Motion

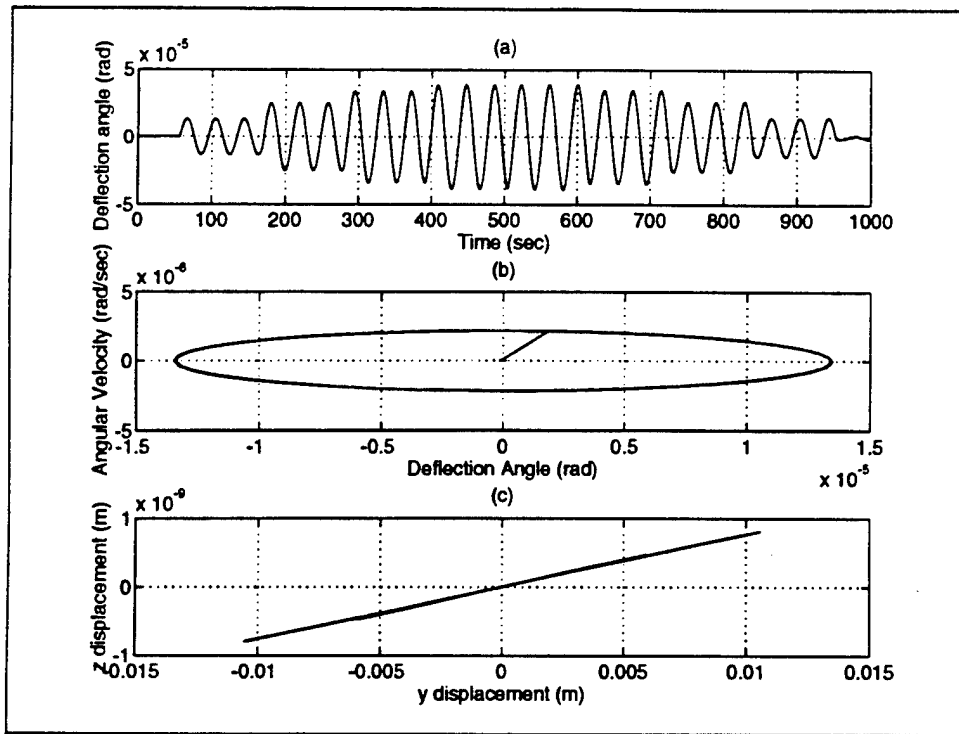


Figure 26: Response to Wave Slamming and Earth Rotation, $H = 5$ m, $C_L = C_M = C_D = 0$,

(a) Time Domain (b) Phase Plane (c) Tower's Top Motion

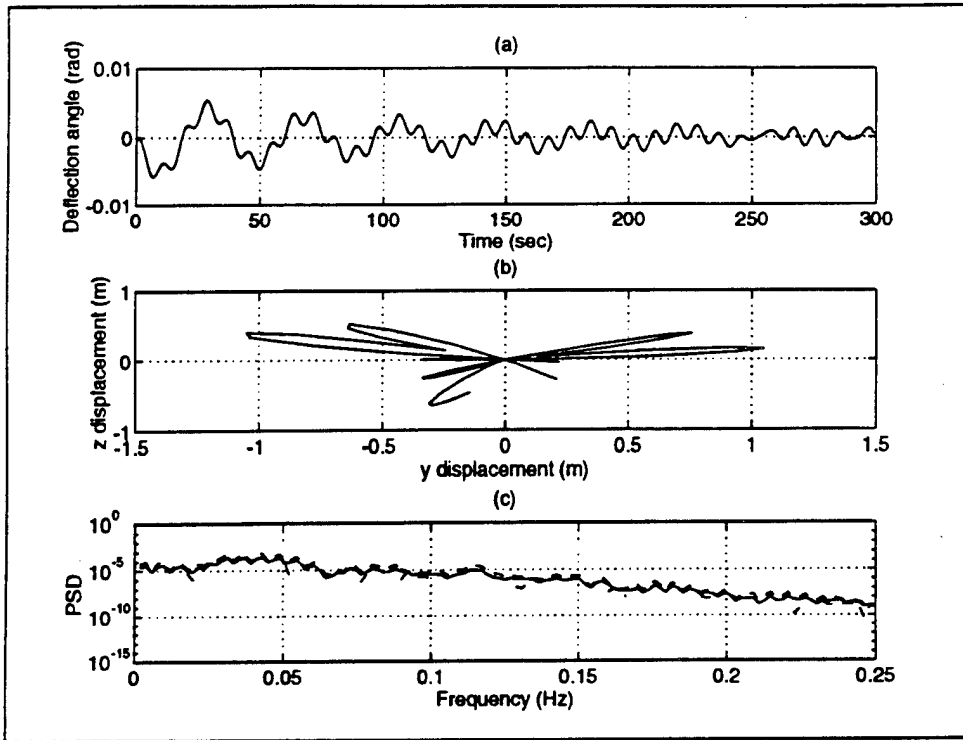


Figure 27: Response due to Waves and Coriolis Acceleration

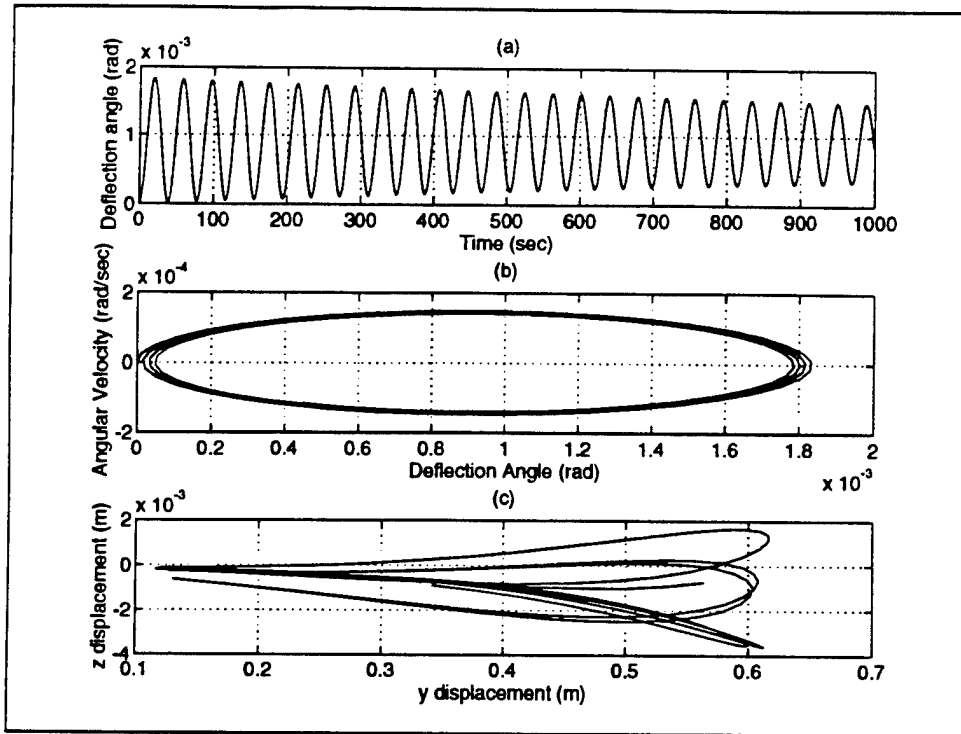


Figure 28: Influence of Wind Load, $\nu = 0$. (a) Time Domain (b) Phase Plane (c) Tower's Top Motion

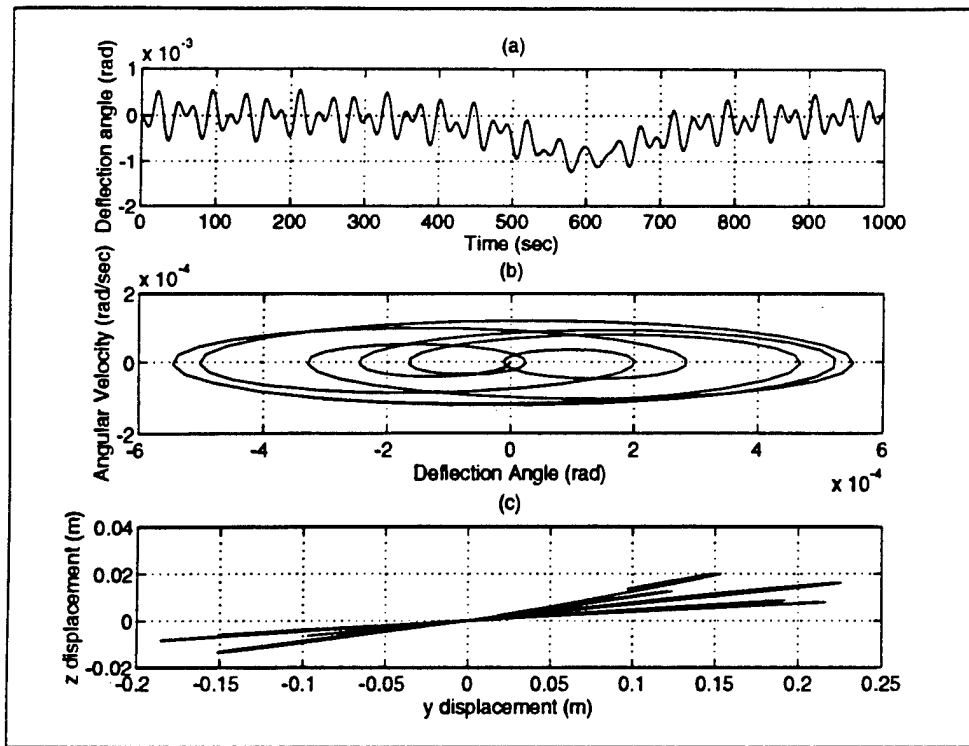


Figure 29: Influence of Wind Load, $\nu = 0$. (a) Time Domain (b) Phase Plane (c) Tower's Top Motion

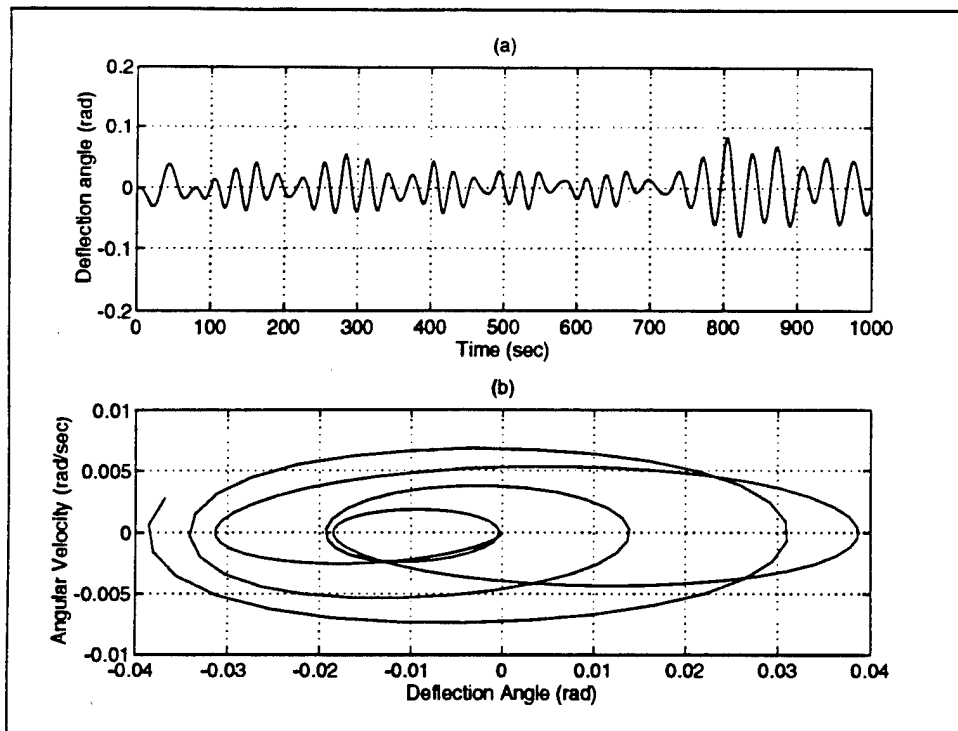


Figure 30: Chaotic Response, with Zero Initial Conditions, $\theta_0 = 0, \dot{\theta}_0 = 0$. (a) Time Domain
 (b) Phase Plane

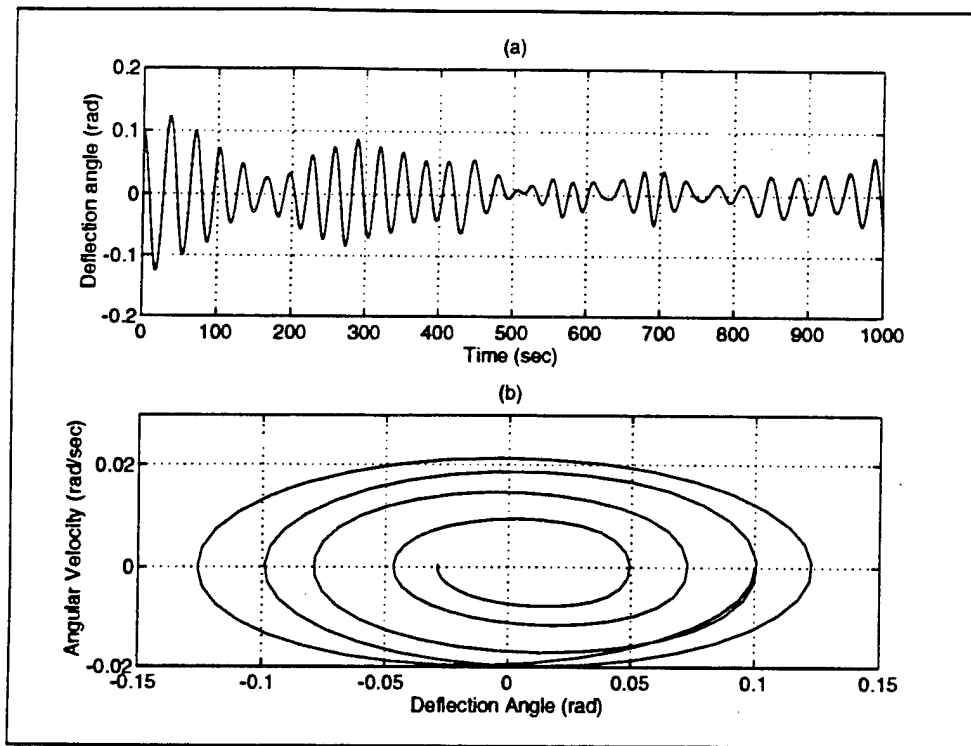


Figure 31: Chaotic Response, with Zero Initial Conditions, $\theta_0 = 0.1$ rad, $\dot{\theta}_0 = 0$. (a) Time Domain (b) Phase Plane

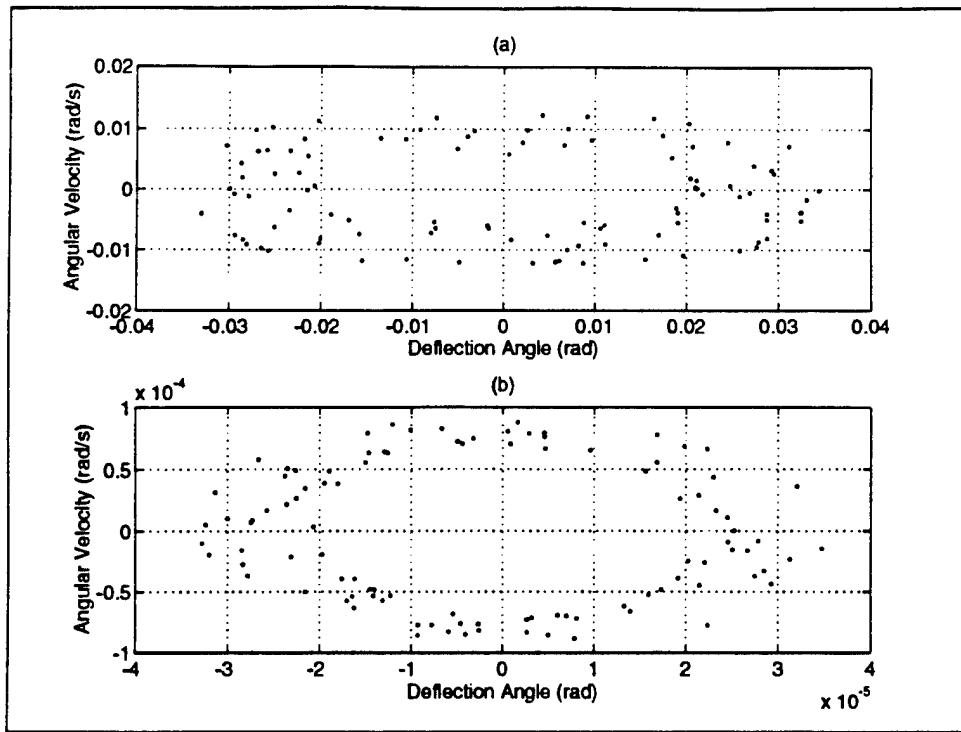


Figure 32: Poincaré Map of the Chaotic Response. (a) $C_D = 0$ (b) $C_D = 1.2$

REFERENCES

- [1] P. Bar-Avi and H. Benaroya. Nonlinear dynamics of an articulated tower submerged in the ocean. *Journal of Sound and Vibration*, in press 1995.
- [2] S.K. Chakrabarti and D.C. Cotter. Motion analysis of articulated tower. *Journal of the Waterway, Port, Coastal and Ocean Division, ASCE*, 105:281 - 292, 1979.
- [3] O. Gottlieb, C.S. Yim, and R.T. Hudspeth. Analysis of nonlinear response of an articulated tower. *International Journal of Offshore and Polar Engineering*, 2(1):61 - 66, 1992.
- [4] P.K. Muhuri and A.S. Gupta. Stochastic stability of tethered buoyant platforms. *Ocean Engineering*, 10(6):471 - 479, 1983.
- [5] K. Jain and T.K. Datta. Stochastic response of articulated towers. In *Deep Offshore Technology 4th International Conference and Exhibit*, pages 191-208, 1987.
- [6] T.K. Datta and A.K. Jain. Response of articulated tower platforms to random wind and wave forces. *Computers and Structures*, 34(1):137 - 144, 1990.
- [7] A.K. Jain and T.K. Datta. Nonlinear behavior of articulated tower in random sea. *Journal of Engineering for Industry*, 113:238 - 240, 1991.
- [8] C.L. Kirk and R.K. Jain. Response of articulated tower to waves and current. *The 9th Annual Offshore Technology Conference*, pages 545 - 552, 1977.

- [18] K.Y.R. Billah. *A Study of Vortex-Induced Vibration*. PhD thesis, Princeton University, 1989.
- [19] S.K. Chakrabarti. *Nonlinear Methods in Offshore Engineering*. Elsevier Science Publishing Company Inc., 1990.
- [20] O.M. Faltinsen. *Sea Loads on Ships and Offshore Structures*. Cambridge University Press, 1994.
- [21] J.P. Hooft. *Advanced Dynamics of Marine Structures*. John Wiley and Sons, 1982.